

*30-19*  
NASA CR-191152

PT-7452

*J. M. S.*

# A TRANSPORTRONIC SOLUTION TO THE PROBLEM OF INTERORBITAL TRANSPORTATION

by

William C. Brown

RAYTHEON COMPANY

Prepared for

NATIONAL AERONAUTICS AND SPACE ADMINISTRATION

NASA Lewis Research Center

Contract NAS3-25066

(NASA-CR-191152) A TRANSPORTRONIC  
SOLUTION TO THE PROBLEM OF  
INTERORBITAL TRANSPORTATION  
(Raytheon Co.) 178 p

N94-29355

Unclass

G3/16 0003099



NASA CR-191152

PT-7452

# A TRANSPORTRONIC SOLUTION TO THE PROBLEM OF INTERORBITAL TRANSPORTATION

by

William C. Brown

RAYTHEON COMPANY

Prepared for

NATIONAL AERONAUTICS AND SPACE ADMINISTRATION

NASA Lewis Research Center

Contract NAS3-25066



1. Report No. NASA CR-191152	2. Government Accession No.	3. Recipient's Catalog No.	
4. Title and Subtitle  A Transporttronic Solution to the Problem of Interorbital Transportation		5. Report Date July, 1992	6. Performing Organization Code
7. Author(s)  William C. Brown		8. Performing Organization Report No. PT-7452	10. Work Unit No.
9. Performing Organization Name and Address  Raytheon Company Electronic Components Division 190 Willow Street, Waltham, MA 02254		11. Contract or Grant No. NAS3-25066	13. Type of Report and Period Covered Contractor Report
12. Sponsoring Agency Name and Address  National Aeronautics and Space Administration Washington, D.C. 20546		14. Sponsoring Agency Code	
15. Supplementary Notes  Project Manager: Ronald Cull NASA Lewis Research Center, Cleveland, OH 44135			
16. Abstract  An all-electronic transportation system described by the term "TRANSPORTTRONICS" is examined as a means of solving the current problem of the high cost of transporting material from low-Earth orbit (LEO) to Geostationary orbit (GEO). In this transportation system, low cost electric energy at the surface of the Earth is efficiently converted into microwave power which is then efficiently formed into a narrow beam which is kept incident upon the orbital transfer vehicles (OTVs) by electronic tracking. The incident beam is efficiently captured and converted into DC power by a revolutionary device which has a very high ratio of DC power output to its mass. Because the mass of the electric thruster is also low, the resulting acceleration is unprecedented for electric-propelled vehicles. However, the performance of the system in terms of transit times from LEO to GEO is penalized by the short time of contact between the beam and the vehicle in low-Earth orbits. This makes it necessary to place the Earth based transmitters and the vehicles in the equatorial plane thus introducing many geopolitical factors. Technically, however, such a system as described in the report may outperform any other approach to transportation in the LEO to GEO regime.  The report describes and analyzes all portions of the beamed microwave power transmission system in considerable detail. An economic analysis of the operating and capital costs is made with the aid of a reference system capable of placing about 130,000 kilograms of payload into GEO each year. More mature states of the system are then examined, to a level in which 60,000 metric tons per year could be placed into GEO.			
17. Key Words (Suggested by Author(s))  Wireless Power Beamed Power Electric Propulsion Space Transportation		18. Distribution Statement Unclassified - unlimited	
19. Security Classif (of this report) Unclassified	20. Security Classif (of this page) Unclassified	21. No. of Pages 168	22. Price*

\*For sale by the National Technical Information Service, Springfield, Virginia 22151



## TABLE OF CONTENTS

	Page no.
<b>SUMMARY</b>	1
<b>I. INTRODUCTION</b>	3
<b>II. TEXT</b>	5
<b>1.0 Overview</b>	5
1.1 Background Information	5
1.2 Brief Description of the Overall System	8
1.3 Timeliness of the Transportronic Concept	12
1.4 Relationship of the Proposed Transportronic Transportation System to Other Applications of Beamed Microwave Power Transmission.	13
1.5 Status of the Development of Transportronic Technology	13
1.6 The Economics of the LEO to GEO Transportation System	16
1.7 Impact of Transportronic Technology upon Space Ship Design	21
1.8 Transportronics for a LEO to Moon Transportation System and as a Prime Power Source for the Moon	23
<b>2.0 Quantitative Comparison of "Transportronic" Technology With Conventional Chemical Propulsion and Solar and Nuclear Assisted Electric Propulsion.</b>	29
2.1 Comparison of Propellant Mass Needed for Electric Propulsion With Chemical Propulsion Beyond LEO	29
2.2 The Electric Power Requirements for Electric Propulsion	32
2.3 Comparison of Nuclear, Solar Photovoltaic Power Sources With the Rectenna Power Source for Ion Thrusters.	32
<b>3.0 System Analysis of the All-Electronic LEO to GEO Transportation System.</b>	35
3.1 Objectives of the System Analysis	35
3.2 General Approach to the System Analysis	36
3.3 Basic Assumptions Used in the Analysis and Rationale for Them	37
3.4 Quantification of Transit Time From One Orbital Altitude to Another, Including LEO to GEO	40
3.5 Aperture to Aperture Power Transfer Efficiency	44
3.6 System Analysis by Scenario	46
3.61 Introduction and Selection of Set of Parameters for Scenario	46
3.62 Estimation of 60 Cycle Energy Cost and Transit Time for the System Scenario	49
3.63 Initial Cost of the Microwave Power Transmission System for the System Scenario	52
3.7 The Payload and Cost Performances as Functions of Various Degrees of Maturity of the System	54

<b>4.0 Technology of the Orbital Transfer Vehicle</b>	<b>59</b>
<b>4.1 Overall Description of the Vehicle</b>	<b>59</b>
<b>4.2 The Technology of the Ion Thruster</b>	<b>60</b>
<b>4.3 Description of the Rectenna</b>	<b>66</b>
<b>4.3.1 Desirable Characteristics of the Thin-Film Rectenna Format for Space</b>	<b>66</b>
<b>4.3.2 Description and Performance of the Thin-Film Format of the Rectenna</b>	<b>67</b>
<b>4.3.3 Experimentally Measured Performance</b>	<b>70</b>
<b>4.4 The Interface Between the Ion Thruster and the Rectenna; Minimization of Power Conditioning</b>	<b>73</b>
<b>4.4.1 The Rectenna Power Source for the Ion Thruster Accelerating Grids and its Interface With the ion thrusters</b>	<b>73</b>
<b>4.4.2 The Impedance Match Between the Rectenna and the Terminals of the Ion Accelerating Grids of the Ion Thruster</b>	<b>75</b>
<b>4.4.3 Discussion of Other Dedicated Power Sources</b>	<b>77</b>
<b>4.5 Interrelationship of Rectenna Size, Mass of Bus, Electrical Loss in Bus, and Structural Considerations</b>	<b>78</b>
<b>4.6 Interaction of the Current in the Conductors With the Earth's Magnetic Field</b>	<b>81</b>
<b>5.0 The Earth Based Transmitter</b>	<b>83</b>
<b>5.1 The Overall Design of the Antenna</b>	<b>84</b>
<b>5.2 The Design of the Electronic Steering and Tracking System, Including Beam Steering, Beam Focussing, Bore Sighting, and Use of the Beam for Controlling the OTV Attitude and Position.</b>	<b>87</b>
<b>5.2.1 Beam Steering</b>	<b>87</b>
<b>5.2.2 The Reference Phase for Each Module, and the Associated Bore Sighting of the Array.</b>	<b>90</b>
<b>5.2.3 Control of the Focussing of the Beam and Compensation for Phase Shift in the Reference Phase System Caused by a change in the physical Length of the system Caused by Temperature or Other Change.</b>	<b>92</b>
<b>5.2.4 Use of the Microwave Beam as an Attitude (Roll, Pitch and Yaw) control Reference for the OTV and Also to Position the OTV in the Equatorial Plane.</b>	<b>92</b>
<b>5.3 The Design of the Radiation Module</b>	<b>94</b>
<b>5.3.1 The Requirements Placed on the Power Amplifier</b>	<b>94</b>
<b>5.3.2 The Phase Locked Magnetron Directional Amplifier as Low Cost Approach to Meeting the Requirements of the Power Amplifier in the Radiation Module.</b>	<b>94</b>
<b>5.3.3 The Use of the Buckboost Coil for Controlling the Amplitude of the Power Output</b>	<b>100</b>
<b>5.3.4 Estimated Cost of Fabricating Radiation Modules</b>	<b>103</b>

<b>5.4 Interaction of the Microwave Beam With Other Uses of the Electromagnetic Spectrum</b>	<b>103</b>
<b>6.0 An Alternative Rectenna Design</b>	<b>107</b>
<b>6.1 Introduction</b>	<b>107</b>
<b>6.2 Documentation of the Low Power Density Rectenna</b>	<b>107</b>
<b>6.2.1 Overall Description and Performance</b>	<b>107</b>
<b>6.2.2 The Impedance Changing and Rectification Cartridge</b>	<b>109</b>
<b>6.2.3 Harmonic Filter Design and Experimental Evaluation</b>	<b>107</b>
<b>6.2.4 Design and Construction of the Thin-Film, 48 Element Dipole, Broadside Antenna Array</b>	<b>119</b>
<b>6.2.5 Testing of the 48 Element Dipole Array</b>	<b>123</b>
<b>6.2.6 H-Plane and E-Plane Antenna Patterns</b>	<b>130</b>
<b>6.3 An Alternative Rectenna Design for Use in the Equatorial Plane</b>	<b>135</b>
<b>6.3.1 Introduction</b>	<b>135</b>
<b>6.3.2 The Linear Dipole Array</b>	<b>135</b>
<b>6.3.3 The Microwave Filter and Rectification Cartridge</b>	<b>139</b>
<b>6.3.4 High Diode Efficiency at High Power Levels</b>	<b>141</b>
<b>6.3.5 Experimental Data on the Radiation Cooling of Diodes in Vacuum</b>	<b>141</b>
<b>III. CONCLUDING REMARKS</b>	<b>151</b>
<b>IV. REFERENCES</b>	<b>153</b>
<b>V. APPENDICES</b>	<b>157</b>
<b>A. Payload Delivery to Geosynchronous Orbit as a Function of Electric Thruster Power Rating, Payload Fraction, and System Maturity</b>	<b>157</b>
<b>B. Mathematical Analysis of Bus Bar Mass and Electrical Losses in OTV.</b>	<b>162</b>

LIST OF ILLUSTRATIONS

	Page no.
Figure 1.1 Transportronics transportation system between LEO and GEO. Orbital transfer vehicles (OTVs) are electrically propelled and execute a circular spiral as they travel from LEO to GEO. The microwave beam generated on the Earth supplies power for electric propulsion. The microwave beam tracks the OTV's through an angular sweep of 90 degrees.	9
Figure 1.2 A mature equatorial plane power transmission system may have 24 or more ground stations on the equator. The black disks represent large aperture transmitters to beam power to electric propelled vehicles bound for geosynchronous orbit. The white disks are smaller transmitters that could assist LEO to GEO vehicles but are primarily used to supply power to orbiting industrial satellites.	9
Figure 1.3 Jarvis and Baker islands in the middle of the Pacific ocean are critically important to a mature system that needs four Earth based microwave beams. Although small in area, Jarvis Island is sufficiently large for a full scale transmitter that would be 2 square kilometers in area. Baker Island could be an ideal setting for the first experimental installation of a 40,000 square meter array to beam power to an orbiting rectenna that could first become an orbiting industrial satellite and then, after fitting with ion thrusters, become a transportation system.	10
Figure 1.4 Plan view of the three space systems shown with the aid of a mechanical model with three rings rotating at three different speeds: (1) outer ring rotating at synchronous speed with Earth contains solar power satellites, (2) middle ring shows orbital transfer vehicle tracked by beam in midflight and (3) inner ring contains fast-orbiting "Industrial Parks".	14
Figure 1.5 Photograph of a 30 cm ion thruster. Thruster consumes 10kW of power and has a mass of about 10kg. Thrust produced at a propellant velocity of 40,000 m/s is 0.37 Newtons.	14
Figure 1.6 First flight of a microwave powered aircraft occurred 1964 at the Raytheon Co. 200 watts of power was supplied to the electric motor from the rectenna that collected and rectified power from a microwave beam.	16
Figure 1.7 This beam riding helicopter self guided itself over the beam by using the microwave beam as a position reference for roll, pitch, yaw, and x and y translation.	16

- Figure 1.8** Microwave power transmission system that provided a certified demonstration of 54% overall DC to DC efficiency. Rectenna DC power output was 600 watts. Frequency was 2.45. 17
- Figure 1.9** Demonstration of beamed power over one mile distance at the JPL Goldstone facility in the Mojave Desert. Of the microwave power intercepted by the rectenna array, 82% was converted into a DC power level of over 30 kilowatts. Frequency was 2388 MHz. Power was used in matrix of illuminating lamps in front of rectenna. 17
- Figure 1.10.** Underneath surface of the successfully flown Canadian microwave powered airplane showing the use of the thin-film etched-circuit rectenna. Total rectenna weighed less than one pound and was wired directly to the electric motor without power conditioning. 19
- Figure 1.11** Schematic of orbital transfer vehicle (OTV). Rectenna collects microwave power, converts it into DC power, and transfers it to side busses which carry power to the ion thrusters. The large symbolic thrusters would be replaced with hundreds of smaller ion thrusters. 19
- Figure 1.12** The all electronic LEO to GEO transportation vehicle concept is a logical combination of the electric ion thruster and beamed microwave power to supply the thruster's electric power and energy needs. The rectenna on the bottom side of this 50,000 square meter vehicle absorbs microwave power and converts it with 85% efficiency to 20,000 kilowatts of electric power for several hundred ion thrusters. The total thrust is 750 Newtons to provide the empty vehicle with an acceleration of  $0.017 \text{ m/sec}^2$ . The corresponding specific impulse is 4000 seconds with xenon as a propellant. The orbital transfer vehicle can transport as much as 150,000 kilograms of payload to GEO. 22
- Figure 1.13** Conceptual all-electronic transportation system from LEO to the orbit of the moon. The orbit of the moon around the Earth is inclined approximately 18.5 degrees from the equatorial plane. The moon intersects the equatorial plane twice during one orbit of the moon about the Earth. 24
- Figure 3.1** Transmission efficiency through the Earth's atmosphere as related to frequency and condition of the atmosphere. 38
- Figure 3.2** Geometry that relates the approximate fraction of time that the microwave beam makes contact with the orbiting transfer vehicle to the orbital altitude  $r$  that is measured from the Earth's center. At low altitudes,  $r - R_E$ , and for values of the beam sweep angle  $\beta$  less than 45 degrees, the term  $(r-R_E)\tan\beta/2\pi r$  closely approximates the true contact time. At high orbital altitude some 38

error is introduced but the magnitude of such errors are consistent with the error magnitudes of other approximations that have been made.

43

Figure 3.3 The graph above gives the integrated value of the second major term in equation (3.7) as a function of the orbital altitude. This term depends only upon  $r$  because the diameter of the Earth,  $R_E$ , is constant. This term takes into account not only the increasing time of contact between the beam and the OTV with an increase in  $r$ , but also the decrease in the Earth's gravitational field with an increase in  $r$ .

43

Figure 3.4 The Goubau relationship between maximized aperture to aperture transfer efficiency as a function of the aperture areas  $A_t$  and  $A_r$ , the wavelength of the radiation, and the distance  $D$  between the apertures. Distribution of power over the aperture is given in Figure 3.5

45

Figure 3.5 For maximized transfer efficiency for each value of  $\Gamma$  the power distribution over the apertures must conform to the above figure.

45

Figure 3.6 To obtain representative performance of a "transporttronics" LEO to GEO transportation system, in terms of transit times to GEO and operating and capital costs, a scenario that is described in table 3.1 has been assumed. The composition of the OTV as it leaves LEO is depicted above. When the OTV reaches GEO it discharges its payload and returns to LEO in about 1/3 of the transit time for the up link.

50

Figure 3.7 The dependency of (1) overall efficiency of microwave power transmission system, and (2) rectenna incident microwave power density, upon orbital altitude that results from the parameters chosen for the system scenario.

50

Figure 3.8 The graphs show (1) accumulative 60 cycle energy, (2) accumulative delta V, and (3) total elapsed time as a function of orbital altitude with the imposed constraints given in figure 3.7.

62

Figure 4.1 Principle of the ion thruster. Positively charged gas ions are accelerated between grids with Voltage  $V$  to be ejected with velocity  $v$ .

62

Figure 4.2 Schematic diagram showing the functions performed on the foreplane of the two plane rectenna format. These functions are absorbing the microwave beam, rectifying it into DC power, harmonic filtering, and bussing of the DC power to terminals for series or parallel combining with other busses.

Figure 4.3 Simplified electrical schematic for the rectenna element.	69
Figure 4.4 Principle of the thin-film, etched-circuit rectenna. Circuit elements are etched on both sides of dielectric film. There are no interconnects between etched elements. The needed capacitors shown in figure 3 are formed with the aid of a metal patch on the back side of the dielectric film.	69
Figure 4.5 Photograph showing the flexibility of the foreplane of the thin-film etched-circuit rectenna.	71
Figure 4.6 An area of the thin-film rectenna was applied to an airplane wing and tested. Output of the rectenna was fed directly to an electric motor that was driving a propellor.	71
Figure 4.7 The efficiency of a single thin-film rectenna element as a function of DC load resistance and rectified DC power output level.	72
Figure 4.8 Theoretically derived and experimentally observed curves for normalized DC voltage output $V_L$ and normalized DC power output (denoted as "fraction of power into load resistor") as functions of the ratio $R_L/R_{LM}$ where $R_L$ is the value of the DC load resistance and $R_{LM}$ is that value that results in zero reflected power.	72
Figure 4.9 Composition of the rectenna for the orbital transfer vehicle. The requirement of the ion thrusters for potentials of the order of 1500 volts is met by placing 75 small rectenna arrays in series. Each array produces 20 volts. The power collected flows laterally to two large tapered busses that carry power directly to the ion thrusters.	74
Figure 4.10 The rectenna is connected directly to the bank of ion thrusters without power conditioning other than that shown above. Transient arcing in the thruster is accommodated by a "small mass" series inductance which lowers the voltage momentarily on the ion thruster and clears the arc. In the event of sustained arcing a fuse blows and removes the thruster from the "hard bus".	74
Figure 4.11 The interaction of the power delivered by the rectenna with the power consumed by the ion thrusters is shown above. With constant microwave power input to the rectenna, the output DC power tends to be constant over a wide variation in load resistance, leading to a voltage-current characteristic that shows a drop in voltage with an increase in current. By contrast the voltage-current characteristic of the ion thrusters shows an increase in current with an increase in voltage. As a result, the	76

overall system automatically adjusts itself as shown by the intersections of the V-I curves. The throttle in the system is the intensity of the microwave beam which can be controlled in the Earth-based transmitter.

Figure 4.12 The above chart provides information with respect to a tradeoff between bus bar electrical loss and bus bar mass, as a function of rectenna area which is proportional to power output. As an example of use of the chart assume a 50,000 square meter rectenna. Project a vertical line from the ordinate value of 50,000 square meters. It intersects the power output line of 20 megawatts. It also intersects the  $\beta$  curves. If the bus bar loss is limited to a  $\beta$  of 2% then the horizontal projection of the intersection shows that the bus bar mass is about 1.3% of the rectenna mass. For a 200,000 square meter rectenna the bus bar mass would go up to 6% of the rectenna mass, etc.

Figure 5.1 Layout of Earth-based transmitter showing folded slotted waveguide formed from thin sheet aluminum . Each radiation module is a slotted waveguide several meters long.

Figure 5.2 The electronically scanning beam generated by the transmitter of figure 5.2 can sweep as much as much as 120 degrees in the West to East direction. Scan is severely restricted in North-South direction but the application does not require it.

Figure 5.3 Proposed method for precision forming and assembly of low-cost, thin-wall, slotted waveguide arrays. Method, modified to use temporary forming tools, was used successfully to fabricate 64 slot arrays in square format that performed well on test range. Same method could be used to fabricate long slender modules for LEO to GEO transmitter as shown in figure 5.1.

Figure 5.4 Radiation module composed of a slotted waveguide antenna and a phase-locked, magnetron directional amplifier. Radiated power output of abut 600 watts.

Figure 5.5 Radiation module shown in figure 5.4 had nearly the theoretically predicted radiation pattern.

Figure 5.6 Beam steering technology that keeps beam precisely on the orbital transfer vehicle with aid of (1) a beacon in space vehicle which is tracked by interferometers on the Earth coupled to the beam steering system, and (2) sets of amplitude sensors which send error signals to Earth if beam is not precisely on target.

80

85

85

86

86

88

88

<b>Figure 5.7 Row and column steering matrix that is activated with input from interferometers on Earth and position sensors in the satellite.</b>	<b>89</b>
<b>Figure 5.8 Arrangement for boresighting the transmitting antenna to zenith position. Illustration shows (1) distribution of microwave frequency to each radiating module, and (2) arrangement for use of laser beam, modulated with microwave frequency, to be used as a reference phase and to set the phase at some integral multiple of <math>2\pi</math> at each radiating module.</b>	<b>89</b>
<b>Figure 5.9 General configuration of the five sensor elements used with a microwave beam as an attitude and position reference for roll, pitch, yaw, and x and y translation.</b>	<b>93</b>
<b>Figure 5.10 Array of sensors described in figure 5.9 as applied to the attitude and position control of a helicopter as shown in figure 1.7. Sensors are arrayed on bottom side of helicopter.</b>	<b>95</b>
<b>Figure 5.11 Schematic circuit for a radiation module consisting of the slotted waveguide antenna and a phase-locked, high-gain (30db) magnetron directional amplifier.</b>	<b>95</b>
<b>Figure 5.12 Conventional microwave oven magnetron fitted with a small buck-boost magnetic coil to increase or decrease the value of the magnetic field. This coil addition can be used either to precisely control the power output of the magnetron, even if it is connected to a common power supply with many other magnetrons, or in combination with a ferrite circulator to convert the magnetron into a phase-locked, high-gain amplifier.</b>	<b>98</b>
<b>Figure 5.13 A comparison, or contrast, of the phase versus drive frequency behavior of a magnetron directional amplifier in (1) the conventional locked mode which is characterized with much phase shift over a small change in drive frequency, and (2) the much preferred phase-locked, high-gain mode in which the input phase is compared with the output phase and the error signal used to tune the free-running frequency of the magnetron to the drive frequency.</b>	<b>99</b>
<b>Figure 5.14 The interaction of a change in the power supply voltage with the flat voltage current characteristic of the magnetron is shown. A change in magnetic field occasioned by the buck boost coil will shift the flat voltage current characteristic of the magnetron up and down, and thus will compensate for changes in the power supply voltage to keep the power output constant. The buckboost coil can be part of a feedback loop in which the power output of the magnetron is compared to the desired value and the error signal used to change the current through</b>	<b>101</b>

the buckboost coil to provide the type of data given in figure 5.15

Figure 5.15 The results of applying an error signal to the buck boost coil to keep the power output constant over a wide range of voltage applied to the magnetron is shown. For example, if the reference power output is set at 700 watts then the experimental data obtained from the control circuit indicates that the power is maintained between 687 and 716 watts while the power supply voltage is varied between 3400 and 4500 volts.

102

Figures 6.1 to 6.31 are not listed in the Table of Illustrations because of their number, their length, and the peripheral importance of section 6.0 to the previous sections.

110-151

## SUMMARY

This report is concerned with combining electric propulsion with beamed microwave power transmission to produce a new approach to large scale space transportation in the region between low-Earth orbit (LEO) and geostationary orbit (GEO), and possibly further into space. More specifically, electric energy which is abundant and inexpensive on Earth is converted into microwave power and formed into an electronically steerable microwave beam. This beam is directed toward the space vehicle, often called an Orbital Transfer Vehicle, which is equipped with a low mass device which efficiently converts the microwave energy of the beam into conventional DC power for use by the electric thrusters. The term "TRANSPORTRONICS" has been applied to the technology of this all-electronic approach to transportation.

The microwave portion of the transportation system is covered in a comprehensive manner in the report. In particular, an effort is made to evaluate the economic aspects of the microwave portion of the system. The figure of merit that is used is the cost of placing a kilogram unit of payload into geostationary orbit. Both operating costs and capital costs are considered. The technology upon which the microwave system is based is sufficiently far advanced to make this possible. It is found that costs of placing a unit of payload into geostationary orbit are strongly dependent upon the amount of payload that is being placed into orbit. Therefore a reference system designed to place 130,000 kilograms into GEO annually was defined and an economic and technology analysis of the system was made. Then costs were projected for more mature systems delivering as much as 60,000 metric tons per year into GEO.

The report begins with an overview of how the proposed system fits into the needs of the further development of space where it has been found that the cost of space transportation is a major problem. It then describes the "transportronics" approach to solving this problem and proceeds to compare it with the present paradigm of chemical propulsion, and with the proposed combination of electric propulsion with a nuclear source of power. Following this it defines the reference system and proceeds to analyze it from an economic and technical point of view. It then describes in considerable detail the orbital transfer vehicle, and in particular the technology of the rectenna which is the device that captures the microwave beam and converts its energy into DC power. It analyzes the interface with ion thrusters which were chosen as the electric thruster device. It also performs an analysis on the tradeoff between the electrical losses and mass of the electrical conductors which carry the power from the rectenna to the ion thrusters.

The report then shifts to the design of the Earth based transmitter where the technology is already well advanced in terms of what would be used for the hundreds of thousands of radiation modules that compose the transmitter. The cost of the transmitter can therefore be estimated with a high level of confidence.

The report concludes with a detailed report on other work performed under the contract that was directed toward a very low power density rectenna, followed with a discussion of how this work could apply to an improved rectenna for space use.



## I. INTRODUCTION

The major purpose of the work effort covered by this final report was to investigate the possibility of greatly improving the space transportation infrastructure in the region from low-Earth orbit (LEO) to geostationary orbit (GEO), and possibly beyond that, by employing a new engineering discipline termed "TRANSPORTRONICS". The technology of "TRANSPORTRONICS", a term derived from the words "TRANSPORT" and "electRONICS", combines the technology of high specific impulse electric propulsion with that of beamed microwave power transmission to create a new approach to space transportation in the near-Earth and cis-lunar regions.

The investigation covered by this report involves a presentation of the concept, the significance of the concept, and a large amount of technical and economic evaluation of the concept based upon the status of prior technology as well as a significant amount of new technology generated under this work effort. The conclusion, as presented in this report, is that "TRANSPORTRONICS" technology, if developed, has the potential to revolutionize space transportation in the region between low-Earth orbit and geostationary orbit .

Because of the novelty of the subject of the study and the length of this report, it has been found desirable to begin the body of the report with an Overview section that will present the concept, the significance of the concept, and some background information on the technology involved. This will be followed by other sections to give a complete outline of the report as follows:

- I. INTRODUCTION
- II. TEXT
  - I. Overview
  - 2. Quantitative Comparison of "transportronics" technology with conventional chemical propulsion and solar and nuclear assisted electric propulsion.
  - 3. System analysis of the all-electronic (transportronics) LEO to GEO transportation system
  - 4. Technology of the Orbital Transfer Vehicle (OTV)
  - 5. Technology of the Ground Array
  - 6. A new rectenna format for space use
- III. CONCLUDING REMARKS
- IV. REFERENCES
- V. APPENDICES

Attention is called to section 6, "A New Rectenna Format". A considerable portion of the total contractual effort was devoted to the design and construction of a low power density rectenna, not directly related to the all electronic transportation system. However, it was found that a spinoff of this effort was a normal power density rectenna of new design that may have a number of advantages when incorporated into a thin-film format for the all-electronic (transportronic) transportation system.

~~PRECEDING PAGE BLANK NOT FILMED~~



## II.TEXT

### 1.0 OVERVIEW

"TRANSPORTRONICS", the technology of an all-electronic propulsion and transportation system in space, in which the electric energy needed for electric propulsion is beamed from the Earth, is a new concept, barely a decade old. Although a number of papers have been given on the subject, knowledge of it is not well distributed within the space community (1,2,3,4). Further, these papers have not given the full import and implications of the new technology. The purpose of this "overview" section is to establish a better perspective on where this new technology is positioned in the unfolding development of space activities.

This "overview" section is divided into the following subsections:

- 1.1 Background Information
- 1.2 Brief Description of the Overall System
- 1.3 Timeliness of the Transportronic Concept
- 1.4 Relationship of the Proposed Transportronic Transportation System to Other Applications of Beamed Microwave Power Transmission.
- 1.5 Status of the Development of Transportronic Technology
- 1.6 The Economics of the LEO to GEO Transportronic Transportation System.
- 1.7 Impact of Transportronic Technology on Space Ship Design
- 1.8 Extension of the LEO to GEO Transportation System to a LEO to the Moon System.
- 1.9 Environmental and EMI Considerations.

#### 1.1 Background Information.

The current transportation paradigm in space depends upon conventional chemical propulsion. Chemical propulsion consumes a very large propellant mass to achieve the necessary delta V to move an interorbital vehicle from low-Earth orbit to higher orbits. The mass of the propellant becomes the largest mass in the orbital vehicle, and all of the propellant mass has to be transported from the Earth and so taxes the Earth to low-Earth orbit transportation system.

The high specific impulse of electric propulsion has always been of great interest, when compared with chemical propulsion, because it can easily reduce the amount of propellant required for a sustained thrust by a factor of ten or more (5). But electric propulsion, unlike chemical propulsion whose

propellants contain their own source of energy to accelerate the propellants to produce thrust, requires very large amounts of electric power and electric energy. And it is the very large mass of conventional power supplies that has prevented the serious consideration of the use of electric propulsion for space transportation. .

The lack of a suitable power source for electric propulsion has long been recognized. Ernst Stuhlinger, when he wrote his pioneering book, "Ion Propulsion for Space Flight", in 1964 stated, "Even a cursory look at the ion propulsion system reveals that the most critical component from the engineering standpoint is the source of electric power. The necessity of a concentrated effort to develop efficient and reliable nuclear-electric space power sources in the kilowatt and in the megawatt range cannot be over emphasized". (5).

What has happened in the intervening period since 1964 is that the ion thruster has been developed to a very high level of performance but still lacks the nuclear power source which has just recently been placed under development in the 100 kilowatt level. When this power supply is developed it may well be the source of power for a vehicle going into deep space, but its specific mass of 30 kg/kw is far too high and its power level far too low for the projected transportation tasks of an interorbital transfer service. However, very large nuclear dynamic power sources with improved specific mass are being considered for the SEI (Space Exploration Initiative) program. But finally, there is the hazard associated with any nuclear power sources operated in or near low-Earth orbit.

The other in situ sources of prime power in space are solar photovoltaic and solar thermal. Only solar photovoltaic has been developed and used in space. Although solar photovoltaic arrays would seem to be a natural source of power for the ion thrusters, they have proven to be very expensive and when power conditioning, mechanical pointing toward the sun, and shielding for going through the Van Allen belt are included, the ratio of mass to power output is in the range of 10 to 30 kilograms for each kilowatt of power. Current arrays are also limited to a maximum power output density of around 230 w/m<sup>2</sup>, and the maximum voltage developed by a single cell is under 1 volt, making it necessary either to put a very large number in series or resort to complex and mass consuming power conditioning to obtain the required voltage for an ion thruster.

Earth-based beamed microwave or laser power as a source of electric power for electric propulsion, represents a technological breakthrough because it leaves the power source on the Earth and connects it to the orbiting vehicle via a mass free microwave beam which is free of gravitational barriers. Of the possible Earth based beamed power sources the microwave one at 2.45 GHz proposed in 1982 by Brown and Glaser (2) represents the most advanced technology and will be the one focussed upon in this report. It also represents the frequency range that can best penetrate the Earth's atmosphere under all meteorological conditions.

With 2.45 Ghz technology the transducer between the microwave beam and the electric thrusters is a very low mass device termed the "rectenna", derived

from the words "rectifier" and "antenna" (6,7). The mass of the rectenna is about equal to the mass of the electric thrusters as contrasted to twenty to thirty times as much for nuclear or photovoltaic power sources. It is also very efficient (80 to 90%) in converting microwave power into DC power so that there is no problem in disposing by direct radiation into space of the small amounts of heat generated in the conversion process.

As a result of the very low specific mass of the rectenna the empty vehicle can have unprecedented accelerations for an electric propelled vehicle, and the mass of the power supply that is saved can be replaced with payload.

The transportronic solution to the transportation problem in space near the Earth has advantages over the current paradigm of chemical propulsion other than the great saving in propellant mass. One advantage is that the electric propelled vehicle would never receive an acceleration of much over  $.01 \text{ m/s}^2$  as contrasted to the two to four "G"s , or  $20\text{m/s}^2$  to  $40 \text{ m/s}^2$  for chemical propulsion. Thus the vehicle and items of payload carried by it can be designed for very low stress loads as compared with a chemically propelled vehicle, and that will result in very large savings in the mass of the vehicles and the payload structures.

Another advantage of electrically propelled vehicles is that they avoid the high G's and associated safety issues of aerobraking maneuvers of chemically propelled vehicles when they come back to low-Earth orbit. Such maneuvers are necessary for chemically propelled vehicles if propellant mass is to be conserved. Designing the vehicle to absorb the mechanical stresses and to dissipate the heat involved in aerobraking becomes very acute if sizeable payloads are to be returned to low-Earth orbit.

An example of the advantages of such a "soft" entry back into low-Earth orbit from space, as opposed to a "hard" one, would be the removal of no longer operational and obsolete communication satellites in geostationary orbit where they will have become debris problems. The electric thruster propelled interorbital vehicle could be maneuvered into position near the satellite to be removed from orbit. A grappling hook could engage the satellite so that it could be brought gently back into low-Earth orbit for either refurbishing or to be burned up in the Earth's atmosphere.

In the past, a significant factor that has prevented the general acceptance of any Earth-based beamed power source for electric propulsion has been the necessity of locating all parts of the system, the transmitters as well as the satellites, in the equatorial plane. This necessity results from the need to maximize the time of contact between the microwave beam and the satellite. It is readily determined that only in the equatorial plane does the satellite in low-Earth orbit come directly over the source of microwave power each time it orbits the Earth. This frequency of contact is from 15 to 17 times as often as with any other geographical arrangement.

However, as time has passed and the problems of the current space transportation infrastructure have been identified, it has become generally recognized that electric propulsion with a low mass power source is a requisite for the further development of space. Accompanying this recognition

is general recognition that the development of space will assume a more international flavor with an accompanying movement away from current modes of space transportation and provincial containment of those modes within regional boundaries (8).

### 1.2 Brief Description of the Overall System.

The proposed transportronic system will be broken down into its component parts and they will be discussed in great detail in this report. However, it is important in this overview section to understand the basic principle of operation and the principal components of the system. In particular, this section will discuss the geopolitical implications of the use of the equatorial plane for any beamed power operations between the Earth and low-Earth orbit.

The all-electronic, or transportronic, LEO to GEO transportation system is shown in schematic outline in Figure 1.1 (3,4). Electronically , the system consists of the ground based transmitters, their microwave beams, and space-based rectennas and the ion thrusters. In the mature system depicted, four Earth based electronically steerable microwave beams track the orbital transfer vehicles throughout the large shaded area of figure 1.1. Each microwave beam tracks the OTV (orbital transfer vehicle) through a total angle of about 90 degrees. The total time of contact between the four beams and the satellites varies from about 6% at an orbital altitude of 300 kilometers to nearly 44% at an altitude of 5000 kilometers, to 61% at an orbital altitude of 10,000 kilometers.

The orbital transfer vehicles (OTV's) follow a spiral trajectory from low-Earth orbit to geostationary orbit. A mathematical relationship for transit time from LEO to GEO has been derived in section 3.4 that takes into consideration the reduced contact time between the microwave beam and the OTV at low altitudes in LEO. Because of the high acceleration made possible because of the low mass of ion thrusters and the microwave power supply, acceleration is very high for an electrically propelled vehicle. This compensates for reduced contact time. A four beam system can place a satellite with a 50% payload into geostationary orbit in from 30 to 40 days.

One potential layout of the Earth based transmitters for the transportation system is shown in association with transmitters to supply power to an orbiting industrial park system in Figure 1.2. The four high powered transmitters for the LEO to GEO transportation system are spaced about equally around the equator with transmitters in South America, Africa, the East Indies, and on Jarvis Island in the Pacific (8). The other transmitters are lower powered transmitters that are intended to supply power to orbiting industrial parks. The industrial park application of beamed microwave power will not be discussed in this report, other than to indicate the use of the lower powered transmitters to increase the contact time between the LEO to GEO transfer vehicles and the microwave beams when the satellites are in low-Earth orbit.

It will be observed from figures 1.1 and 1.2 that the complete system is

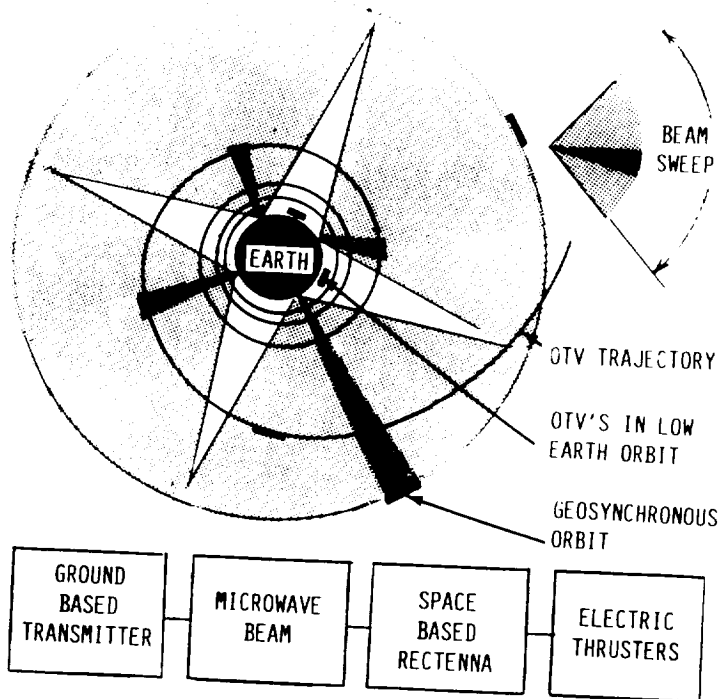


Figure 1-1. Transportronics Transportation System between LEO and GEO. Orbital Transfer Vehicles (OTVs) are Electrically Propelled and Execute a Circular Spiral as They Travel from LEO to GEO. The Microwave Beam Generated on the Earth Supplies Power for Electric Propulsion. The Microwave Beam Tracks the OTV's through an angular Sweep of 90 degrees.

350747

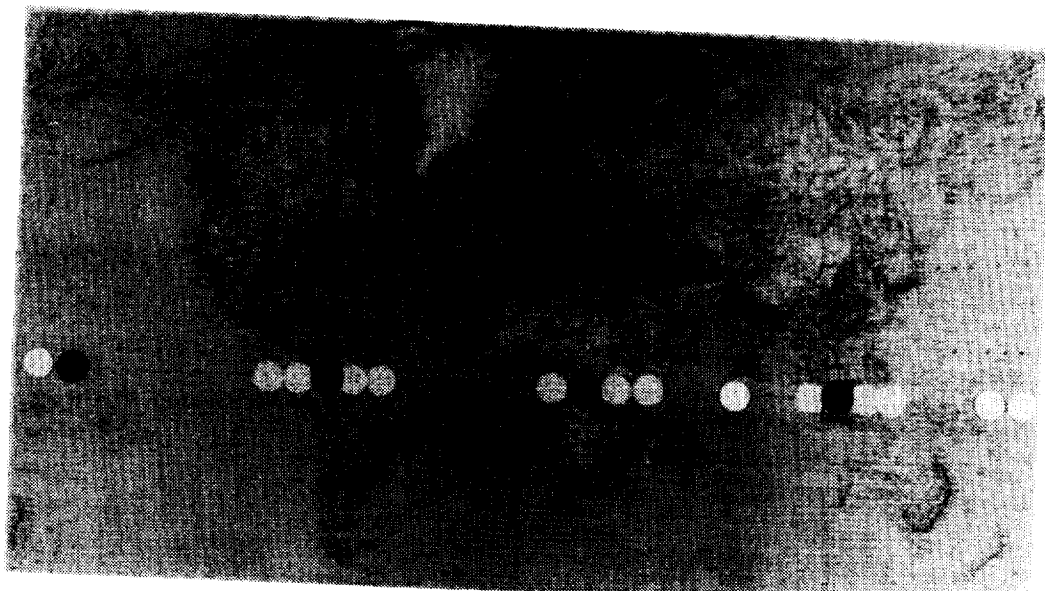
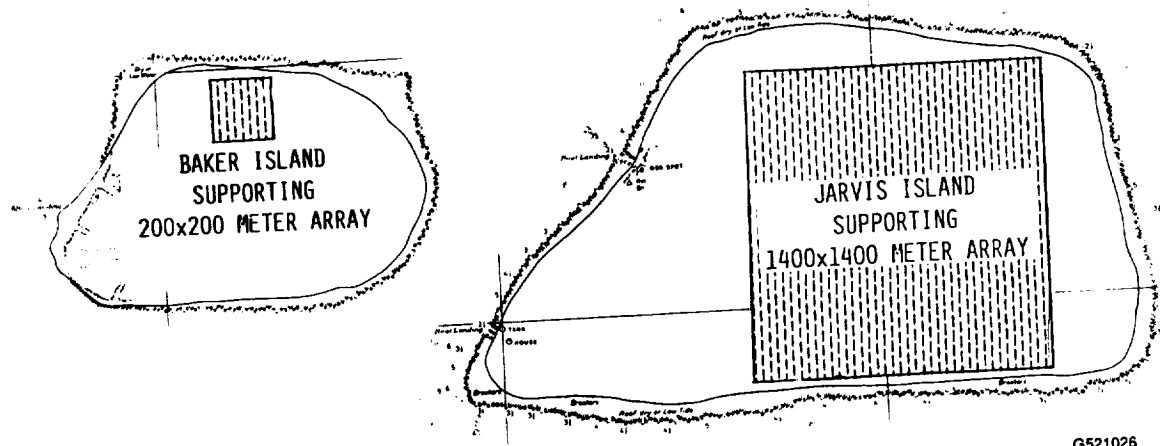


Figure 1-2. A Mature Equatorial Plane Power Transmission System may have 24 or More Ground Stations on the Equator. The Black Disks Represent Large Aperture Transmitters to Beam Power to Electric Propelled Vehicles Bound for Geosynchronous Orbit. The White Disks are Smaller Transmitters that could Assist LEO to GEO Vehicles but are Primarily Used to Supply Power to Orbiting Industrial Satellites.

86-3790CR2



G521026

Figure 1.3. Jarvis and Baker Islands in the Middle of the Pacific Ocean are Critically Important to a Mature System that Needs Four Earth Based Microwave Beams. Although Small in Area, Jarvis Island is Sufficiently Large for a Full Scale Transmitter that would be Two Square Kilometers in Area. Baker Island could be an Ideal Setting for the First Experimental Installation of a 40,000 Square Meter Array to Beam Power to an Orbiting Rectenna that could First Become an Orbiting Industrial Satellite and then, After Fitting with Ion Thrusters, Become a Transportation System.

TABLE I  
LOCATION OF POSSIBLE SITES ON THE EQUATOR FOR LAND-BASED TRANSMITTERS  
Survey starts with the 0° Meridian of Greenwich and proceeds Easterly

REGION	LOCATION	ISLAND OR MAINLAND	LATITUDE	LONGITUDE	APPROX. AREA IF AN ISLAND (SQ KM)
Africa	Sao Tome	Island	5°-30°N	6°-30°E	964
	Gabon	Mainland	Equator	9°-14°E	
	Congo	Mainland	Equator	14°-17°E	
	Zaire	Mainland	Equator	17°-30°E	
	Uganda	Mainland	Equator	30°-32°E	
	Kenya	Mainland	Equator	34°-41°E	
	Somalia	Mainland	Equator	41°-43°E	
Indian (Maldives)	Suvadiva *a Atoll		2°-N	73°E	<15 Ocean
Indonesia	Sumatri	Island	Equator	100°-113°	Large
	Borneo	Island	Equator	109°-117°	
	Celebes	Island	Equator	120°E	
	Hahnahera	Island	Equator	128°E	
	Waigeo	Island	2°-1.5°S	131°E	
Pacific Ocean	Nauru	Island	30°-S	166°E	230
	Abernama	Island	Equator	174°E	
	Baker	Island	11°S	176°W	
	Jarvis	Island	23°S	160°W	
	Isla Isabela *b	Island	Equator	90°W	
South America	Ecuador	Mainland	Equator	76°-78°W	0.6
	Columbia	Mainland	Equator	69°-76°W	
	Brazil	Mainland	Equator	49°-69°W	
Atlantic Ocean	St. Paul @ Rocks		55°N	29°W	
	St. Peter Rocks				

\*a not researched for area

\*b one of the Galapagos Islands

located in the equatorial plane. The principal reason for this is that only if the transmitters and the orbiting vehicles are located in the equatorial plane will each satellite pass over each transmitter and contact its microwave beam each time that it orbits the Earth, or approximately sixteen times in a 24 hour day. In any non-equatorial plane arrangement contact between each satellite and each transmitter will be reduced to once every 24 hours. Such a low frequency of contact makes the principle of beaming power from the Earth impractical for a space transportation system (8).

The necessity to use the equator for the installation of any beamed microwave or laser power system between Earth and low-Earth orbit raises many geopolitical issues and makes the LEO to GEO all-electronic transportation system an international program. However, it is noted that the United States possesses the only two strategically located Islands in the mid Pacific on which to locate one of the four high powered transmitters for a mature LEO to GEO transportation system.

Figure 1.2 indicates that there is ample opportunity to put three of the proposed transmitters into equatorial sites in South America, Africa, and the East Indies. However, between the East Indies and South America there are only two potential locations for transmitters located on or very close to the equator. It is indeed fortunate that one of these islands, Jarvis, is sufficiently large for the construction of the fourth high powered transmitter that would be necessary for the mature system. The other island, Baker, is sufficiently large to install a much lower powered transmitter and smaller area antenna that could provide some increased duty cycle when the LEO to GEO vehicle is orbiting at relatively low altitudes.

These two islands, together with a layout of the areas required for the respective antennas are shown in figure 1.3. Geographical data for these remote islands owned by the United States of America were obtained from chart 83116, "Islands in the Pacific Ocean", procured from the US Dept. of Commerce, National Oceanic and Atmospheric Administration, National Ocean Service.

Jarvis Island is located at 160° 1' West Longitude and 0° 23' South Latitude. Baker Island is located at 176° 29' West Longitude and 0° 12' North Latitude. Baker and Jarvis are 22 kilometers and 43 kilometers from the equator, respectively. While their ideal location would be directly on the equator, these locations are sufficiently close so that a permanent mechanical tilt to the transmitting array, and a larger electronic steering capability in the North-South direction could supply the interorbital vehicle with power at all orbital altitudes from LEO outward.

The islands are large enough for transmitting arrays but most of the service facilities for them would probably be located on adjacent Islands. Howland Island is close to Jarvis while Christmas Island is close to Baker.

Attention is drawn to the fact that these two islands are geographically so isolated from inhabited areas, with the exception of Christmas Island, that they would represent a desirable site for early development and the deployment of the first ground based transmitter. Although the microwave power density levels other than those directly in the path of the beam are so low as not to

represent a hazard, it would be only prudent to conduct the first tests in a relatively isolated area.

Table 1 lists the mainland and island land masses that may be available for placing the microwave transmitters. As previously indicated the transmitters need to be placed on or very close to the equator and the interorbital vehicles need to be in or very close to the equatorial plane.

### 1.3 Timeliness of the Transportronic Concept

The transportronic concept is introduced at a time when it is widely recognized that there are two major issues that are retarding the development of space. One is the survival of people in a hostile space environment. The other is the high cost of space transportation. Theoretically, at least, there could be a substantial development of space with a minimum of people being involved. However, if the barrier of the high cost of transportation is not broken, we can anticipate that anything beyond a few adventurous sorties into space will not occur. Certainly the commercialization of space will not occur.

It also occurs at a time when it is recognized that the future development of space will require much larger space vehicles capable of carrying payloads greater by a factor of at least ten than can presently be transported beyond low-Earth orbit. The demands of such vehicles for propellant mass, if they continue to use the current paradigm of chemical propulsion, are huge, and it must be brought up at high cost from the Earth. On the other hand, if the vehicles are electrically propelled vehicles to radically reduce these demands for propellant, their demands for electric power and energy are also very great. The need for large electrically propelled space vehicles fits into the ability of the ground based microwave beam power system to deliver huge amounts of electrical power to space at relatively low cost.

The problem of space transportation and the limitations of the chemical propulsion paradigm was effectively recognized in the recent report of the "Synthesis Committee" chaired by General Stafford in which the development of nuclear thermal propulsion and nuclear electric propulsion were recommended for missions to the moon and Mars (9). Such development tasks at the multimegawatt levels, and the reliability and safety levels required, would be an enormous undertaking. The specific impulse of nuclear thermal propulsion will not be greater than 1000 as compared with 4000 to 10,000 for ion thrusters. To power electric thrusters operating at high specific impulse in the 5000 second region will require multimegawatt nuclear power sources which for efficiency purposes will have to be dynamic systems with conventional heat cycles, rotating machinery, and enormously large radiators for the disposal of waste heat directly to space.

In any event, these developments that were largely inspired by the desire to send manned missions to Mars, have little or no application to transportation systems geared to climbing out of the high gravitational gradients close to the Earth, because they must be parked in high orbits for safety reasons.

Hence, there is an urgent need to look at other approaches to the transportation problem from LEO outward, particularly as it relates to geostationary orbit or the moon.

#### 1.4 Relationship of the Transportronic Transportation System to Other Applications of Beamed Microwave Power Transmission.

The transportronic LEO to GEO interorbital transfer system is closely related to two other space applications of beamed power transmission. The first of these is the Solar Power Satellite System that was studied extensively in the 1977 to 1980 time frame (10,11,12). The other is the concept of a number of orbiting industrial parks that are supplied with low cost electrical power and energy from transmitters placed on the equator (13).

The close relationship to the SPS (Solar Power Satellite) system is both technical and functional ; technically, because many of the details of the beamed power technology are very similar in the two systems, and functional in the sense that the SPS needs a low cost LEO to GEO transportation system before the SPS can be considered as an economically viable approach for electric power for use on Earth. In fact, it was the problem of transporting material for the deployment of SPS's in geostationary orbit that inspired the concept of what the author now terms "transportronics".(2)

The same close technological relationship exists with a proposed system of orbiting industrial parks where power and electrical energy is economically supplied to the parks from transmitters located on the Earth's equator. There is also a functional relationship in which the smaller scale transmitters for the industrial park system can also supply power to the LEO to GEO transportation system when the OTVs are close to the Earth.

All of these systems are either completely in the equatorial plane, or partially so as in the case of the SPS system where the transmitters are in equatorial or geostationary orbit while the rectenna sites may be at any latitude up to about 50 degrees on the Earth's surface.

Figure 1.4 shows a model which depicts the three closely related systems simultaneously.

There are also other proposed applications of beamed microwave power transmission. One of these, given some visibility by the Stafford report, is the concept originated by David Criswell (14) and others of harvesting the sun's energy on the moon and beaming it back to Earth by microwaves. A giant step toward this proposed approach to obtaining a pollution-free source of electrical power would be the construction and operation of the ground based transmitter for the all electronic LEO to GEO transportation system.

#### 1.5 Status of the Development of Transportronic Technology

The broad categories of Transportronic technology that apply to this study are electric thruster technologies and beamed power transmission technologies.

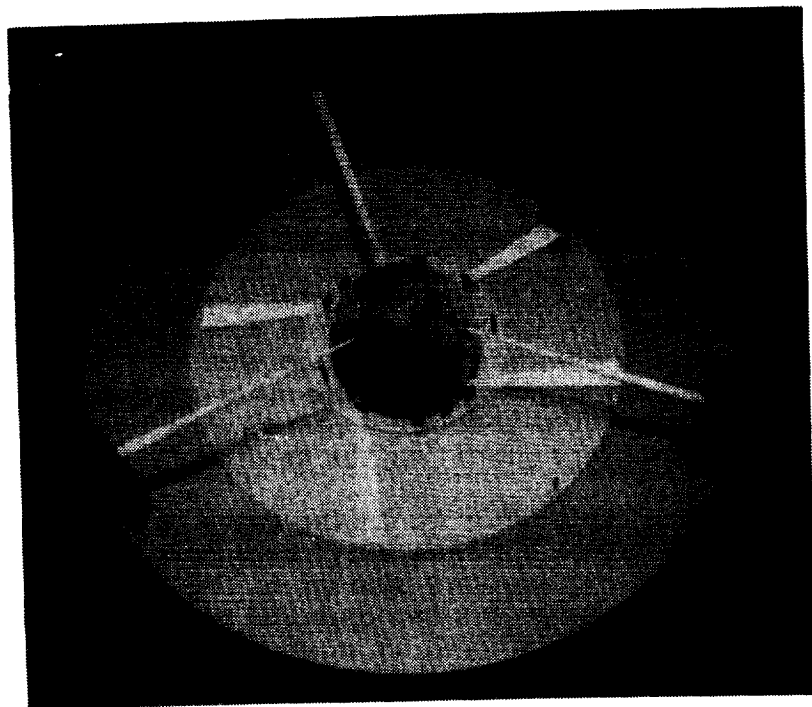


Figure 1-4. Plan View of the Three Space Systems Shown with the Aid of a Mechanical model with Three Rings Rotating at Three Different Speeds: (1) Outer Ring Rotating at Synchronous Speed with Earth Contains Solar Power Satellites, (2) Middle Ring Shows Orbital Transfer Vehicle Tracked by Beam in Midflight and (3) Inner Ring Contains Fast-Orbiting "Industrial Parks".

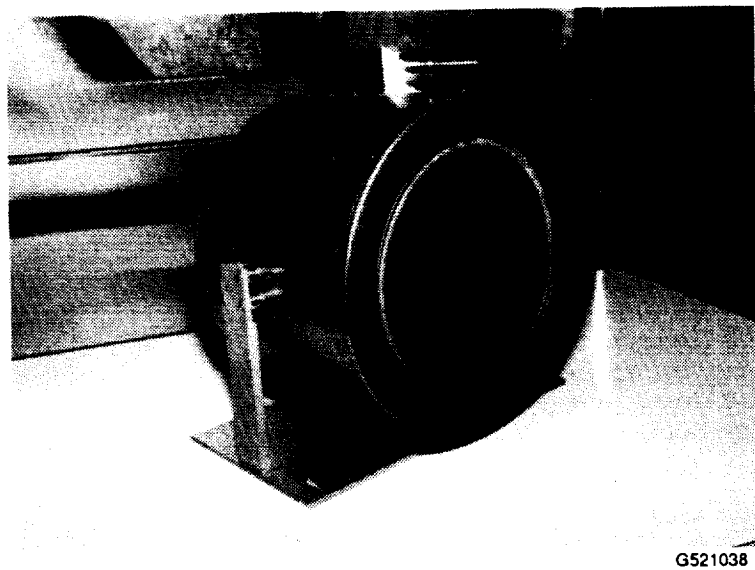


Figure 1-5. Photograph of a 30 cm Ion Thruster. Thruster Consumes 10 kW of Power and has a Mass of About 10 kg. Thrust Produced at a Propellant Velocity of 40,000 m/s is 0.37 Newtons.

However, specific branches of these technologies have been selected for this study. The branch selected for the electric thruster is the ion thruster, and the branch selected for the beamed power technology is technology at 2.45 GHz. The reasons for these selections are twofold. First it is believed that the specific technologies chosen are by far the furthest along in development in their respective fields. Secondly, it is noted that the two technologies complement each other in that the rectenna can be connected directly to the high-voltage input of the ion thruster with no power conditioning than a simple disconnect if the ion thruster fails.

The avoidance of extensive power conditioning with its added mass and heat dissipation complications is of the utmost importance. It is also noted that high voltage, low current operation is needed to avoid excessive  $I^2R$  losses in the power bussing from the rectenna to the ion thrusters. This subject is discussed in detail in section 4.0, including a mathematical analysis of the tradeoff between the mass of the busses and the electrical loss in them.

Ion thrusters have had a long and successful development experience, starting with the pioneering book on the subject "Ion Thrusters for Space Flight" by Ernst Stuhlinger (5), and now have reached a level of advanced development that would assure their successful use and permit them to be manufactured economically in the large numbers required for the all-electronic LEO to GEO transportation system. A representative ion thruster is the 30 cm ion thruster developed by the NASA Lewis Research Center is shown in Figure 1.4.

Although the ion thruster is of major importance in the transportronic engineering discipline, it will receive only a modest amount of attention in the body of this report because of the focus of this report upon the overall performance of the system and particularly the microwave portion of it. The ion thruster has reached an advanced state of development and is generally accepted by the research and engineering communities.

However, adequate attention will be given to the interface of the ion thruster with the rectenna portion of the beamed microwave power system because it appears to be possible to couple the rectenna directly to the bank of ion thrusters and thus avoid the costly and massive power conditioning that must be used with other power supply approaches. This interface is discussed in considerable detail in section 4.4.1.

The development of beamed microwave power transmission at 2.45 GHz likewise has had a long and successful development and now has reached an advanced stage of development (15) but it has not yet been accepted for the application of supplying ion thrusters in space vehicles with a reliable, safe, and low cost source of prime power. This report essentially addresses this issue.

The present state of development of beamed power transmission is best addressed with several pictorial references to demonstrations of power transmission and related applications. These are given in Figures 1.6 to 1.10 in chronological order. The first breakthrough in transportronic technology was the demonstration of the flight of a tethered microwave powered helicopter (figure 1.6) that received all of the power to operate its rotor from a microwave beam (16,17). This demonstration introduced the receiving device,

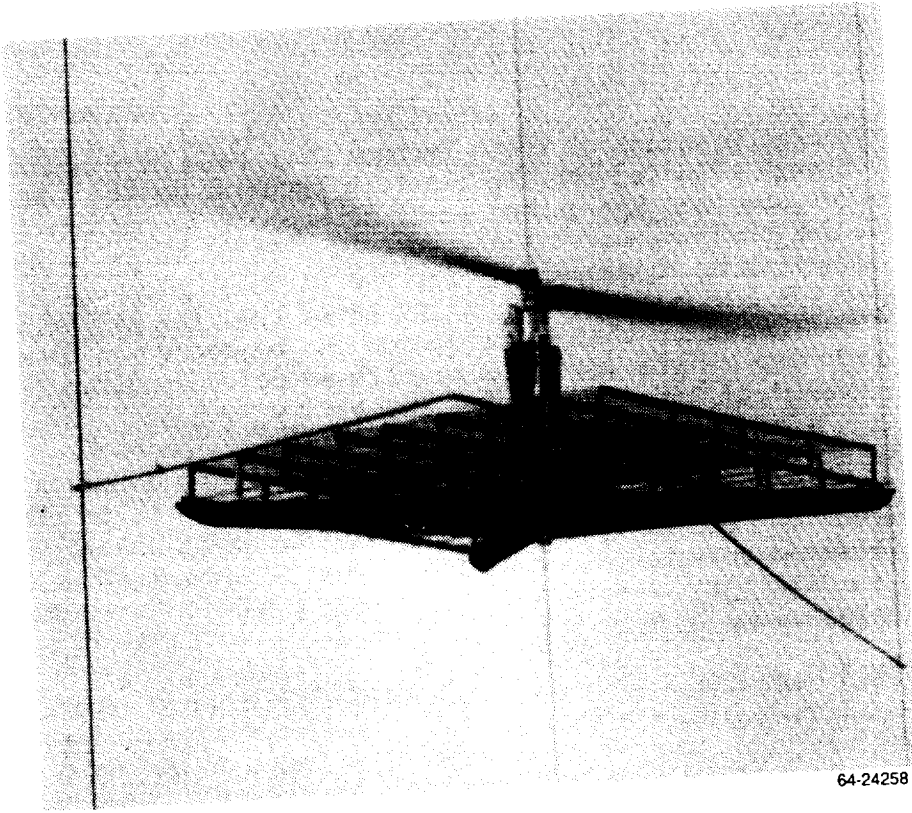


Figure 1-6. First Flight of a Microwave Powered Aircraft Occurred in 1964 at the Raytheon Company. 200 Watts of Power was Supplied to the Electric Motor from the Rectenna that Collected and Rectified Power from a Microwave Beam.

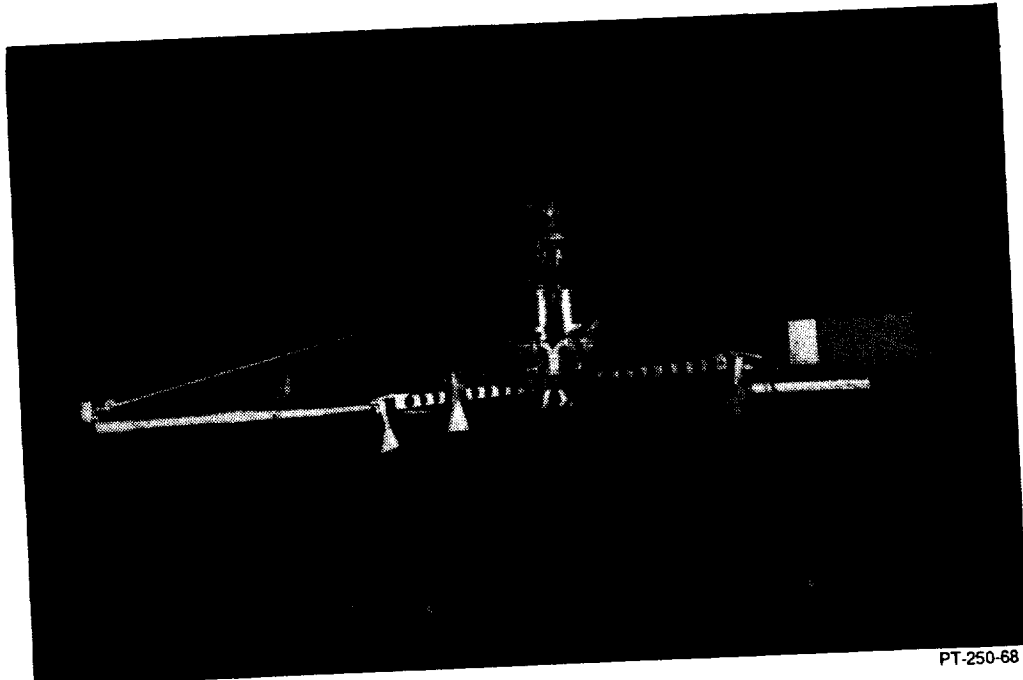
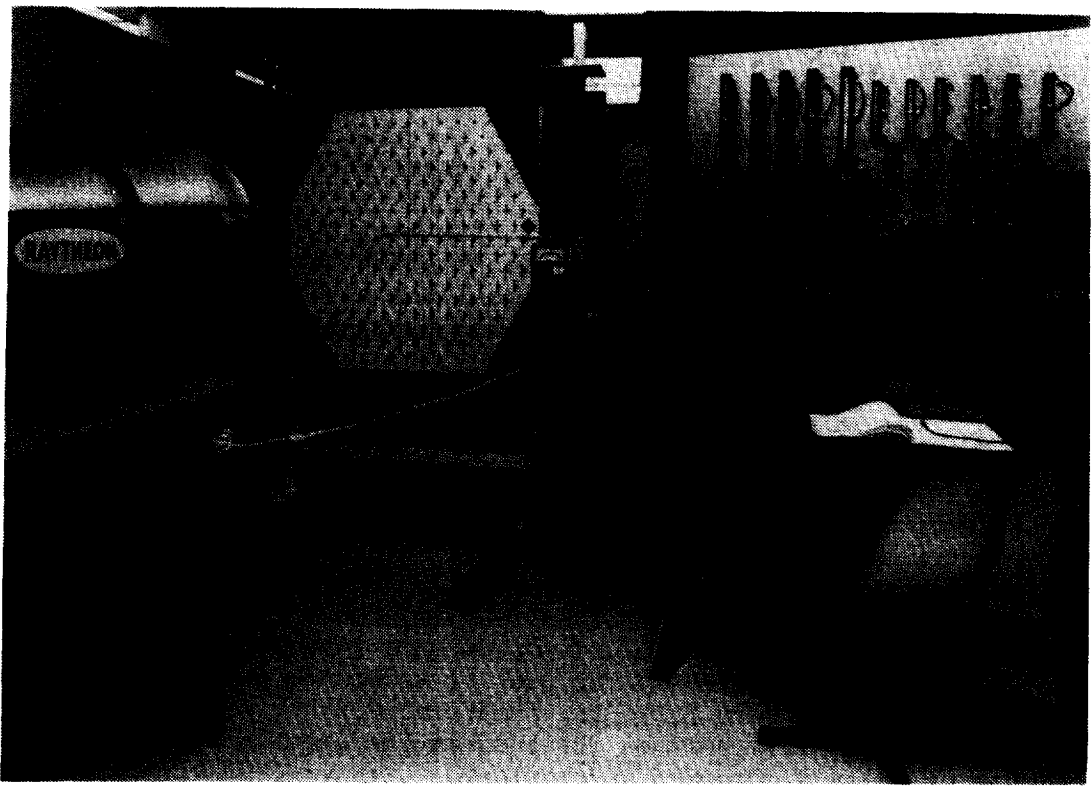
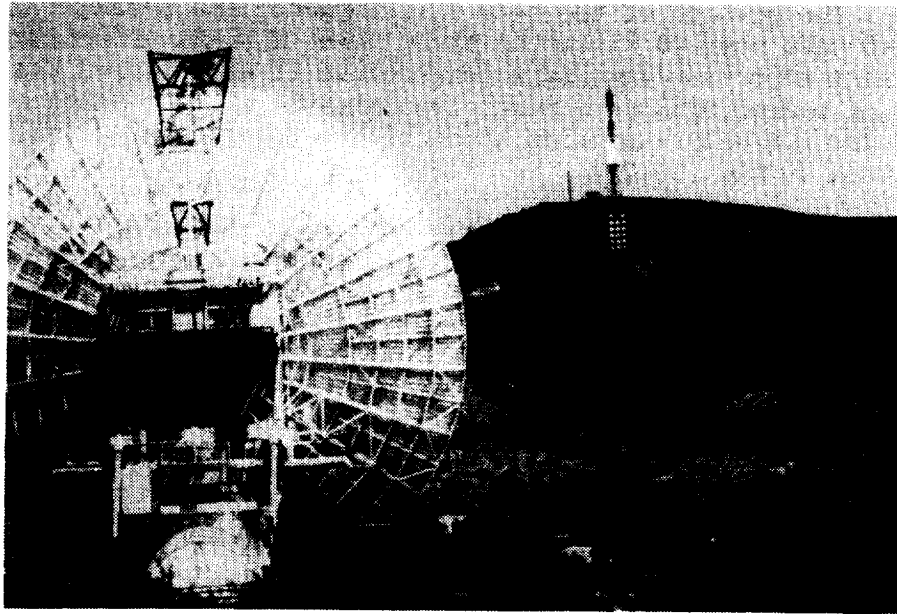


Figure 1-7. This Beam Riding Helicopter Self Guided Itself Over the Beam by Using the Microwave Beam as a Position Reference for Roll, Pitch, Yaw, and x and y Translation.



89-1837B

Figure 1-8. Microwave Power Transmission System that Provided a Certified Demonstration of 54% Overall DC to DC Efficiency. Rectenna DC Power Output was 600 Watts. Frequency was 2.45 GHz



444872

Figure 1.9. Demonstration of Beamed Power Over One Mile Distance at the JPL Goldstone Facility in the Mojave Desert. Of the Microwave Power Intercepted by the Rectenna Array, 82% was Converted into a DC Power Level of Over 30 Kilowatts. Frequency was 2388 MHz. Power was Used in Matrix of Illuminating Lamps in Front of Rectenna.

the "rectenna" that simultaneously captured the microwave beam and converted it into DC power for the electric motor that drove the rotor.

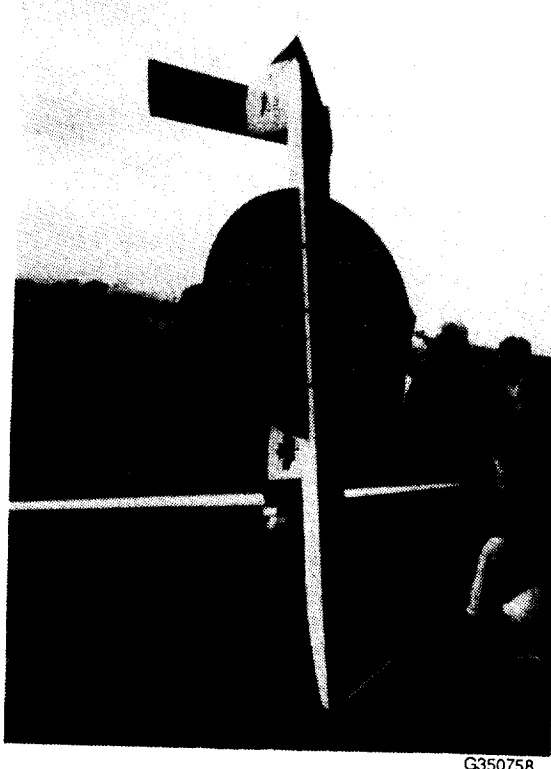
A related follow on demonstration was that of a beam riding helicopter (figure 1.7) that used the microwave beam itself as attitude references for roll, pitch and yaw, and as x and y translation position references. This technology is useful for keeping beam contact between the Earth-based microwave beam and the OTV and for keeping the OTV always parallel to the surface of the Earth and on the equator. This technology is discussed in section 5.2.4.

The second milestone in beamed microwave power transmission technology was the demonstration in the laboratory of an overall DC to DC efficiency of 54% (18). This overall efficiency was the product of three other efficiencies: (1) the efficiency of conversion of DC power into microwave power and the forming of a concentrated beam with it, (2) the transfer efficiency between the transmitting aperture and the receiving aperture, and (3) the efficiency with which the microwave beam was absorbed and converted back into DC power. The overall efficiency of 54% was certified by the Quality Assurance section of the Jet Propulsion Laboratory (figure 1.8). It is estimated that, today, an overall efficiency of close to 70% could be obtained if the experiment were repeated with the best of today's component technology. .

The third milestone was to increase the distance of transmission and the power level many fold over the Laboratory demonstration. At the Goldstone Facility of the Jet Propulsion Laboratory, an existing transmitter was used to beam power at a rectenna located on a tower one mile, or 1.6 kilometers away. (figure 1.9). The portion of the beam that impacted the rectenna was absorbed and converted into over 30 kilowatts of DC power with an efficiency of 82%. This was a very important demonstration because it established the basic credibility of beamed microwave power transmission without which it is doubtful if the DOE/NASA supported study of the Solar Power Satellite concept would have been funded (19,20).

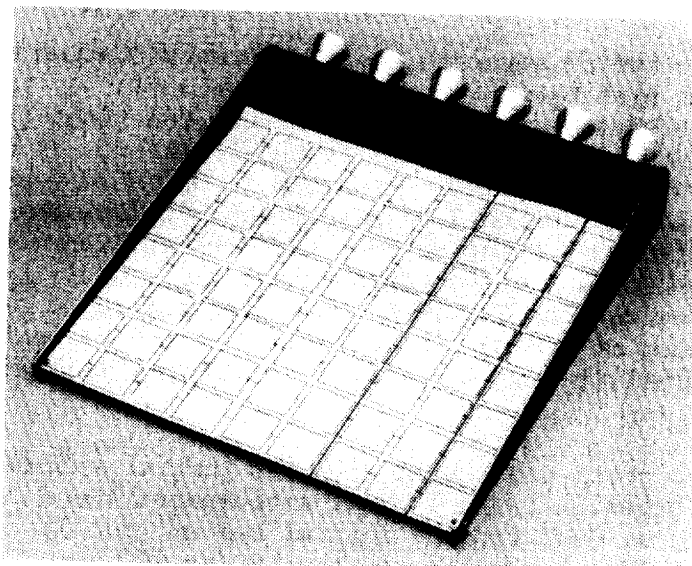
Although there is no pictorial illustration given, the study of the Solar Power Satellite concept not only established the feasibility of the SPS concept, but it also led to a different concept with respect to the transmitter that would be necessary not only for the SPS but also for the transportronic approach to space transportation. This new development was the electronically steerable phased array concept, composed of multitudes of radiating modules, each with its own microwave source. The orchestration of all of these modules to steer the beam and focus it was accomplished through a microprocessor that received its information from sensors on the receiving rectenna.

Another milestone of importance was the demonstration of the free flight of a microwave powered airplane by the Canadian Communications Research Center of Canada (figure 1.10). In this demonstration that took place in Ottawa in 1987, the microwave beam was slaved to the free flying airplane and followed it in flight to supply power to it. The demonstration was the first phase of the SHARP (Stationary High Altitude Relay Platform), whose fully functional altitude of operation would have been about 20 kilometers above the Earth. (21,22)



G350758

Figure 1-10. Underneath Surface of the Successfully Flown Canadian Microwave Powered Airplane Showing the Use of the Thin-Film Etched-Circuit Rectenna. Total Rectenna Weighed Less than One Pound and was Wired Directly to the Electric Motor without Power Conditioning.



86-3804C

Figure 1-11. Schematic of Orbital Transfer Vehicle (OTV). Rectenna Collects Microwave Power, Converts it into DC Power, and Transfers it to Side Busses which Carry Power to the Ion Thrusters. The Large Symbolic Thrusters would be Replaced with Hundreds of Smaller Ion Thrusters.

### 1.6 The Economics of the Transportronic Transportation System

As previously indicated the economic attractiveness of "transportronics" as applied to a space transportation system between LEO and GEO is based upon the use of prime energy sources on the Earth which are low in cost. This energy source can be efficiently converted into microwave beams that carry energy to the orbital transfer vehicles. Upon arrival the microwave beam is absorbed and efficiently converted back into DC power for the electric thrusters by a novel but well tested device, the "rectenna". Together, the low cost of the prime energy and the low mass of the receiving terminal aboard the OTV have the potential to reduce transportation costs in the region of space between LEO and GEO by a large factor.

The beamed microwave power transmission technology has reached such an advanced state that the cost of its implementation in various system scenarios can be estimated with a good degree of accuracy. What is found is that the cost savings become greater as larger and larger payloads are transported.

The system analysis in Section 3.0 of this report examines two kinds of costs associated with the proposed transportronic system. The first cost is the amount of prime 60 cycle power that is required to transfer payload from LEO to GEO or to closer orbits. The second cost is the capital cost of the terminals of the system, specifically the cost of the Earth based transmitter and the space based rectenna. The two figures of merit used in the analysis are the 60 cycle energy costs and the prorated capital costs to place a kilogram of payload into GEO. These costs are a function of the maturity of the system, being much less in a mature system than in an initial system.

To obtain a perspective on expected costs, a transportation scenario that would be consistent with the first stage of development of the system was selected and its parameters defined. This system consisted of a single Earth based transmitter and a single orbital transfer vehicle and had the capability of transporting 130,000 kilograms of payload to GEO each year. The analysis of this system scenario in section 3.6 is followed by examining the capability of a fully mature system consisting of four Earth-based transmitters and four orbital transfer vehicles that would then have the capability of transferring 16 times as much payload to GEO. Then, the power rating of the OTVs was increased by a factor of ten by similarly increasing the rectenna area to find that nearly 60,000 metric tons of material could be transported to GEO each year.

A comparison of the costs associated with the initial system scenario and the mature system are given in table 1.2. As anticipated there is a marked economy of scale. These costs, even for the initial system, are far below those of any competing transportation technology in the LEO to GEO space arena. And the transportronics approach reduces by a factor of at least ten the burden that is placed upon the Earth to LEO transport system.

These costs do not include that portion of the system identified with the ion thruster. However, as explained in the text, the design of the ion thruster lends itself to large scale manufacture. It is concluded that the additional

cost of the ion thrusters would not increase the overall capital costs of the all-electronic propulsion system by more than 10%. They would add nothing to the energy costs, of course.

The capital cost of the vehicle itself has not been included. It would be highly desirable to extend the cost studies to include the vehicle and the complete system. Two approaches to the vehicle design are considered in this report. The vehicle itself would be a framework on which to mount the rectenna and the ion thrusters but the bus bars for the power from the rectenna would be the main structural members of the vehicle. In the analysis of the initial system these bus bars were found to constitute about 5% of the mass of the rectenna. A mass of 14,000 kilograms was assigned to the vehicle structure. ,

TABLE 1.2

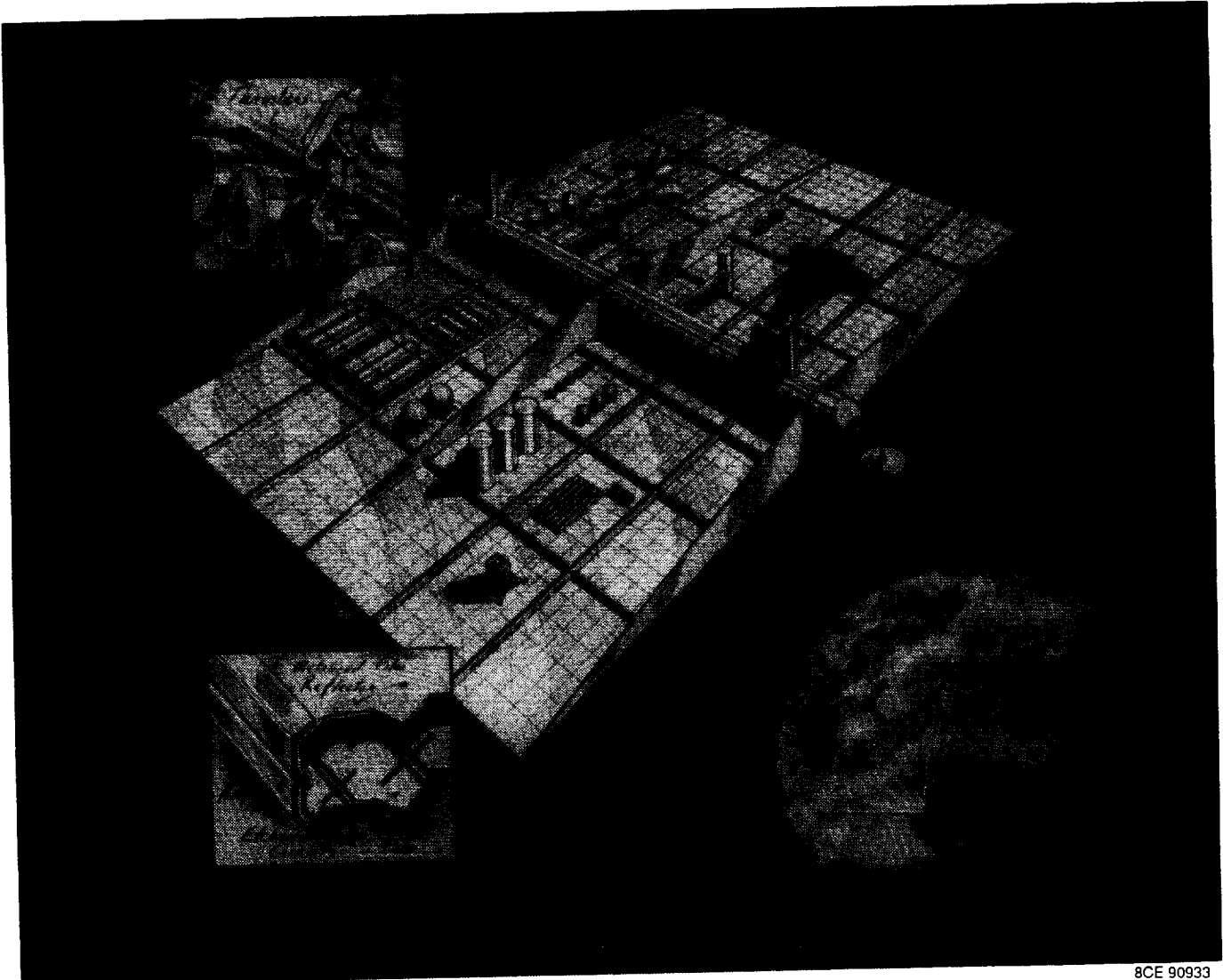
<u>System size</u>	<u>To place a kilogram of payload into GEO</u>	
	60 cycle energy costs at 10 cents/kwhr	10 year prorated capital costs
Initial system scenario 130,000 kg/year to GEO	\$392	\$276
Mature system 60,000 m tons/year to GEO	\$18	\$8

#### 1.7 Impact of Transportronic Transportation Concept Upon Space Ship Design

One of the surprising results of the application of transportronics to space transportation is that the resulting vehicle takes on a physical configuration that is radically different than conventional space vehicles. This is because the rectenna is characteristically very thin but of a very large area. Thus the vehicle is a very large flat structure. In fact, the larger the area of the rectenna, the more efficiently it intercepts the microwave beam (4).

The resulting configuration is shown schematically in Figures 1.11 and 1.12. Figure 1.11 is of a schematic nature, showing the large rectenna and how the power output of the rectenna is fed to the large busses on the two sides of the vehicle which also serve as the major physical structure of the vehicle. The size of the electric thrusters in the illustration are a hundred times larger than the ones that are proposed for the reference design and are therefore purely schematic.

Figure 1.12 was created by a professional illustrator with some engineering guidance, and the thrusters illustrated were one meter in diameter, more nearly the size that would probably be used in future designs. The reference, or base line design, makes use of either 30 or 50 cm thrusters, both of which



SCE 90933

Figure 1-12. The All Electronic LEO to GEO Transportation Vehicle Concept is a Logical Combination of the Electric Ion Thruster and Beamed Microwave Power to Supply the Thruster's Electric Power and Energy Needs. The Rectenna on the Bottom Side of this 50,000 Square Meter Vehicle Absorbs Microwave Power and Converts it with 85% Efficiency to 20,000 Kilowatts of Electric Power for Several Hundred Ion Thrusters. The total thrust is 750 Newtons to Provide the Empty Vehicle with an Acceleration of  $0.017 \text{ m/sec}^2$ . The Corresponding Specific Impulse is 4000 Seconds with Xenon as a Propellant. The Orbital Transfer Vehicle can Transport as much as 150,000 Kilograms of Payload to GEO.

are in an advanced stage of development.

In section 4.6, it will be pointed out that the direction of current flow in a spaceship of the configuration shown in Fig. 1.11 will produce an excessively large rotational torque when the spaceship is operating in the magnetic field characteristic of low Earth orbit. However this difficulty can be overcome with a shift to the design shown in Figure 1.12 where the torques generated in that configuration counteract each other.

It is generally accepted that the development of the moon and Mars, as distinguished from adventuresome Apollo like missions to them, will require large spaceships, not only to carry large amounts of materials and equipment, but also to support the necessary quarters for personnel. The use of beamed power transmission becomes more efficient as the size of the vehicle is increased and so fits well into large spaceship design.

Large space ship designs with electric propulsion have also been made using photovoltaic arrays and nuclear dynamic electric generators as power sources. The nuclear dynamic systems need very large cooling arrays which are also large flat structures (23). So all large spaceships that are electrically propelled share an essentially flat structure.

#### 1.8. Transporttronics for a LEO to Moon Transportation System and for a Prime Power Source for the moon.

It was not the original purpose of this study to include a study of a transportronic transportation system to the moon. On the other hand, as a result of events that have occurred since the onset of this study, there is now some interest in examining its application to get to the moon. One of these events was the Space Exploration Initiative that stressed using the moon's resources as well as using it as a way station on the way to Mars. Another is the recent willingness to consider a power beaming system from the moon to the Earth (14,9). Technologically, an Earth to the moon system is much simpler than vice versa, and any serious consideration of moon to Earth may well depend first upon the development of the Earth to the moon system.

In any event, it may be worth while to at least examine the geometry of such a system. It has already been established that it is necessary to use the equatorial plane for a transportronic LEO to GEO transportation system. It would therefore be logical to extend the transportronic system outward in the equatorial plane from geostationary orbit to the moon's orbit and to examine the rendezvous relationship between a spaceship and the moon.

Such a rendezvous can occur where the moon's orbit intersects the equatorial plane and this occurs twice each time the moon orbits the Earth. The moon orbits the Earth approximately every 27 days so there is a window for rendezvous every 13.5 days.

The moon's orbit is inclined to the equatorial plane by 18.5 degrees. The relationships between the geometrical elements of the arrangement can be visualized with a model, or the photograph of a model, as is shown in Figure

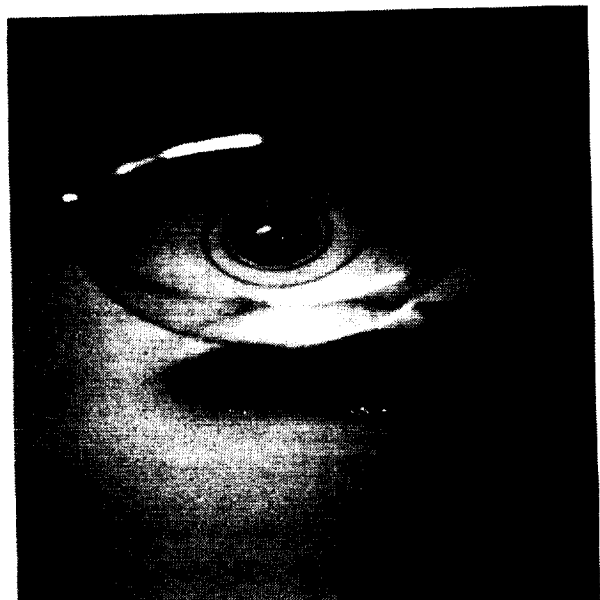
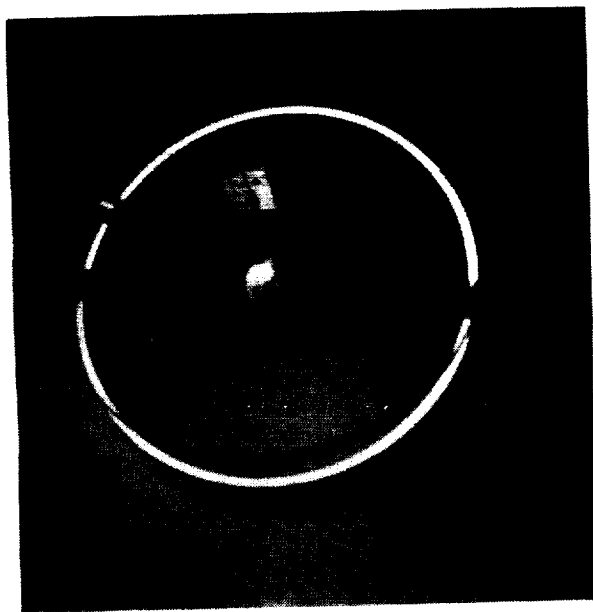
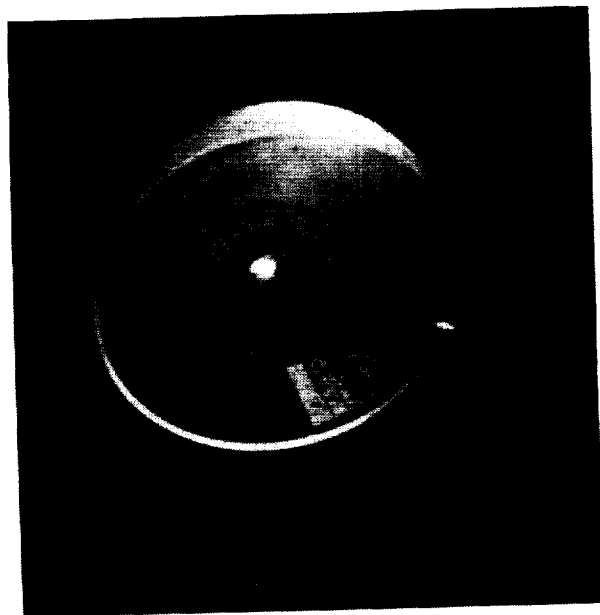


Figure 1-13. Conceptual All-Electronic Transportation System from LEO to the Orbit of the Moon. The Orbit of the Moon is Inclined 18.5 Degrees from the Earth's Equatorial Plane. The Moon Intersects the Equatorial Plane Twice During One Orbit of the Moon About the Earth.

### 1.13.

Some further discussion of the moon-spaceship rendezvous may be worthwhile. Although the orbital speeds of the moon and the spaceship will be the same, the 18.5° difference in inclination would require a delta V correction to place the spaceship into the same orbit as the moon.

The delta V required to get to the moon from an orbit 300 kilometers above the Earth via the low-thrust outward spiraling maneuver used for the LEO to GEO transportation system, is 6703m/s. This compares with 4652m/s required to get to geostationary orbit. Because the moon is about ten times further from the Earth than is geostationary orbit it would be necessary to scale up the area of the Earth array of 2 million square meters now being used in the reference LEO to GEO OTV system by a factor of 100 to obtain the same power density at the moon as the reference system has at GEO. This would seem to be out of the question, but scaling up the ground array by a factor of ten could be done at a reasonable cost of about 10 billion dollars. This would allow following the vehicle out to an orbital radius three times that of GEO where the orbital velocity of 1767m/s is only 745m/s away from that of the moon. At that point where 89% of the needed velocity change had been achieved, some auxiliary source of power could take over to allow the vehicle to achieve the orbital radius of the moon and to go into orbit about the moon.

It may be of interest that scaling up the present two million square kilometer Earth-based array by a factor of 10 would increase the power density available in GEO by a factor of 10 for the same total microwave power radiated from the transmitter. In fact, the OTV operating near GEO would be illuminated at a power density of 430w/m<sup>2</sup>, or nearly ten times that from the reference system. This would greatly reduce the cost of 60 cycle energy at the surface of the Earth.

The general conclusion that can be drawn from the discussion in this section, is that scaling up the area of the ground based transmitter by a factor of ten from the reference size has a two fold leverage. First, the microwave beam can supply an electrically propelled vehicle with 90% of the power that it needs to get to the moon. Secondly, the cost of 60 cycle Earth based energy for placing a kilogram of payload into geostationary orbit is greatly reduced from the reference design, although these costs were quite acceptable.

Any microwave beam or laser beam that could operate a space vehicle in the region of the moon inevitably leads to the possibility of that same beam supplying power directly to the moon's surface. This is of interest because of the difficulty of generating and storing electrical energy on the moon so that it remains continuously available to a settlement there. Because of the fact that the moon faces the sun directly only once every 27 days, and that any photovoltaic array on the moon's equator may be effectively exposed to the sun for a maximum of about ten days, there is the need to store energy for an extended period of time that leads to very large, massive, and expensive storage facilities, as well as an oversized solar array which is not collecting energy for an effective 2/3 of the time. The energy storage problem is the major argument for a nuclear power source on the moon's surface.

A single source of beamed energy, microwave or laser, from the Earth's surface would allow the transmission of energy to the moon once every 24 hours for a period of about 8 hours every day if the beam can be electronically steered over an angle of plus and minus 45 degrees from zenith. This would reduce the storage period from seventeen days to 18 hours, or a factor of 23.

However, there is a distinction between a microwave beam that will power vehicles enroute to the moon in the equatorial plane, and a beam that will also beam power to the moon on a daily basis. This is because of the 18.5 degree difference in the orbital plane of the moon from the equatorial plane of the Earth. So if the source of power on the Earth were located on the Earth's equator, the logical spot for it, the microwave or laser beam would have to be capable of being steered a maximum of 18.5 degrees in the north and in the south direction as well as 45 degrees in the East and West direction.

If the beam were a microwave beam, the transmitting array could be considerably more expensive than one with very little steering capability in the North-South direction. However, it may still be an option that should be examined.

### 1.9 Environmental and EMI considerations

It is outside of the scope of this study to discuss the environmental and EMI aspects of beamed microwave power transmission from a general point of view. At least one extensive study was made of these aspects of beamed power transmission during the study of the DOE/NASA study of the Solar Power Satellite in the 1977 to 1981 time period (12). The findings of this study are directly applicable to the LEO to GEO transportation system. However, it may be helpful to briefly discuss environmental and EMI considerations directly related to the all-electronic LEO to GEO transportation system (24).

First, in discussing the interference or EMI problem, it is assumed that all the Earth based microwave beams will be at one frequency that will not be shifted or intentionally modulated in any way. This simplifies the situation immensely and allows the use of narrow band-stop filters in the communications receiver, as well as the use of phase-locked loops to feed back out-of-phase energy to cancel power picked up at the beamed power frequency.

There are other less technically involved strategies. In the event that the illumination intensity, which will be at the maximum about  $500\text{W/m}^2$ , proves to be too much for some services, the microwave power beam can be either momentarily shut off or electronically steered away from an impending encounter with a satellite receiver. The microwave beam will be so narrow that the transit time across the beam for most satellite encounters will be for only a few milliseconds, allowing the interorbital vehicle to proceed unaffected if there is a minimal amount of energy storage carried aboard.

Another major area of interference concern are the harmonics and spurious signals generated in the transmitter and in the rectenna receiver. Those involved with the transmitter are discussed in some detail in section 5.0 of

this report (25). Those involved with the rectenna are discussed in considerable detail in section 6.0 of this report, and to some extent in section 4.0. In both cases it appears that the spurious and harmonic levels can be held to a level that will not interfere with other uses of the electromagnetic spectrum.



## 2.0 QUANTITATIVE COMPARISON OF "TRANSPORTRONICS" TECHNOLOGY WITH CONVENTIONAL CHEMICAL PROPULSION AND SOLAR AND NUCLEAR ASSISTED ELECTRIC PROPULSION.

"Transportronics" has been defined as the combination of electric propulsion with beamed power transmission to supply the needed electric power for the propulsion. "Transportronics" has transportation applications in both the Earth's atmosphere and in space. In the Earth's atmosphere, transportronics has been demonstrated for both helicopters and airplanes. Using the "weightless fuel" supplied with a microwave beam these vehicles could stay on station for months at a time. The subject of this report is the application of the technology of transportronics to a LEO to GEO all-electronic transportation system. The electric propulsion, specifically in the form of ion thrusters, is supplied with the power it needs by a microwave beam originating at the Earth's surface.

In this section, the potential of electric propulsion to radically reduce the amount of propellant that would have to be brought up from Earth for chemical propulsion beyond LEO will be examined first. Then after it is shown that large reductions can be made, the sources of power for electric propulsion will be examined with emphasis upon a comparison between a nuclear power source and a microwave beam source.

The principles of operation of the ion thruster are discussed in Section 4.0, "The Technology of the Orbital Transfer Vehicle".

This section will have the following subsections:

- 2.1 Comparison of propellant mass needed for electric propulsion and chemical propulsion beyond LEO
- 2.2 The electric power requirements for electric propulsion
- 2.3 Comparison of nuclear and photovoltaic power sources with the rectenna power source for ion thrusters.

### 2.1 Comparison of Propellant Mass needed for electric propulsion and chemical propulsion beyond LEO.

The expression for thrust in terms of the velocity of the propellant and the time rate of propellant flow is given by

$$N = v(dm/dt) \quad (2.1)$$

where  $N$  = thrust in Newtons (1 Newton = 0.2248 lbs. force)

$m$  = propellant mass, kg

$dm/dt$  = time rate of propellant flow, kg/sec

$v$  = velocity of the propellant, meters/sec

Expression 2.1 will be recognized as a variation of the familiar  $f = ma = m(dv/dt)$ , where the mass flow is the time variant and not the velocity.

From expression 2.1 it can be seen that for the same thrust, the propellant flow is inversely proportional to the velocity. With chemical propulsion a

velocity of 4000 m/s is approaching the limit, while for electric propulsion a figure of 40,000 m/s is readily obtained.

A simple application of expression 2.1 shows that for a sustained thrust of 1 Newton, and a propellant velocity of 40,000, 1 kilogram of propellant will last for 40,000 seconds or 11.1 hours; while for a propellant velocity of 4000 only 1.11 hours will have been achieved.

Assuming a flight path trajectory that is a circular spiral with continuous thrust, what difference, in terms of propellant required for a trip from LEO to GEO and then back to Earth, would a major difference in propellant velocity make? Assume also that no payload, or very little payload, is carried so that the vehicle mission is to go to GEO and return.

The answer to this may be found in using the basic equation for the ratio of mass at the termination of the trip to the mass at the start in terms of the velocity change to make the trip and the velocity of the propellant. It is assumed that the difference between the terminal mass and the initial mass is the mass of the propellant used during the trip. The expression is:

$$M_t / M_i = \exp - (\Delta u / v) \quad (2.2)$$

$M_t$  = Terminal mass

$M_i$  = Initial mass

$v$  = Ejection velocity of the propellant

$\Delta u$  = Change in vehicle velocity to reach objective

$M_i - M_t$  = Propellant Mass.

This expression may be applied to the spiral trajectory of a vehicle from LEO to GEO, where delta u is approximately 4600 meters/sec for one way transfer from a 300 kilometer orbit, and 9200 meters/sec for a transfer to GEO and return to LEO.

In applying this expression to a chemical rocket using oxygen and hydrogen it is assumed that the terminal velocity of the propellant is 3500 m/s, a value substantially higher than when a propellant other than hydrogen is used. By contrast, the exhaust velocity assumed for the ion thruster is 41,500 m/s, a value comfortably in the range of the propellant xenon which is also assumed. As indicated earlier, it is further assumed that both the chemical rocket vehicle and the electrically propelled vehicle would execute a spiral trajectory to GEO and that the terminal masses of the electrically propelled vehicle and the chemically propelled vehicle are the same.

The results of the application of expression 2.2 to these assumptions is given in table 2.1.

As noted in the table, there is a factor of 50 difference in the mass of the propellant for the round trip from LEO to GEO. Thus there is great leverage in the use of electric propulsion to greatly increase the velocity of the propellant and therewith reduce the amount of propellant.

The comparison in Table 2.1, however, is not fair to chemical propulsion. because it assumes that the chemical propellants would be used in a spiral trajectory mode whereas they would be used in a Hohman transfer mode in which

the delta  $\mu$  needed was acquired near low-Earth orbit so that the propellant required to attain it would not have to be boosted through the gravitational potential between LEO and GEO. And it neglects the fact that the chemicals during combustion generate the power needed to accelerate the combusted products to 3500 m/s. By contrast the ion thrusters need a very large amount of power supplied by an outside source to power them. Until recently this mass has been so great relative to the mass of the ion thrusters themselves as to make electric propulsion impractical for most applications. In addition the vehicle using chemical propulsion would use very little propellant in returning to LEO, but would rely upon aerobraking in the Earth's atmosphere.

TABLE 2.1

COMPARISON OF PROPELLANT NEEDED FOR CHEMICAL AND ELECTRIC PROPULSION

	Chemical Rocket	Ion Thruster Xenon
Ejection velocity	3500 m/s	41,500 m/s
<u>Starting Mass</u> Terminal Mass	3.72 one way	1.117 one way
<u>Propellant Mass</u> Terminal Mass	2.72 one way	0.117 one way
<u>Propellant Mass</u> Terminal Mass	12.8 round trip	0.25 round trip

Nevertheless, it is generally acknowledged that an orbital transfer vehicle using chemical propulsion would require much more propellant than an electrically propelled one. One study that has been made of a chemically propelled OTV that would carry payload to GEO only, has a propellant to payload ratio of 2.5 and a ratio of gross takeoff mass to dry weight of the vehicle of 13.5. The vehicle depends upon aerobraking to return it to a circular orbit in LEO, with an aerobrake sized to the dry weight of the vehicle. With a small payload on the returning OTV equal to the dry weight of the vehicle, the area of the aerobrake would have to increase by a factor of 2, and its mass by a much larger fraction. And any aerobrake structure would have to be replaced for the next journey.

By contrast the ratio of propellant to payload for the typical electric propelled OTV scenario of section 3.4, in which the OTV returns without aerobraking to LEO, is 0.3 or nearly ten times less. In addition, the OTV enters LEO with very low deceleration (small fraction of 1 G), so that it can bring back massive payloads without changing the structure of the vehicle itself, in contrast to the aerobraking of large return payloads with chemically propelled OTVs.

## 2.2 The Electric Power Requirements for Electric Propulsion

The work required to accelerate a mass  $m$  to a velocity  $u$  is  $1/2 mu^2$   
The corresponding power for a sustained acceleration process is:

$$P = 1/2 dm/dt v^2 \quad (2.2)$$

Where  $P$  = Watts of power

$dm/dt$  = time rate of propellant flow, kg/sec

$v$  = velocity of the propellant, meters/sec

How much power is associated with obtaining a thrust of 1 Newton at a propellant velocity of 40,000 m/sec. From equation 2.1, the flow rate of mass was found to be  $1/40,000$ , so the power requirement obtained from expression 2.2 is 20,000 watts or 20 kilowatts.

If equation 2.2 is divided by equation 2.1, the ratio of power to thrust is:

$$P/N = 1/2 v \quad (2.3)$$

and it is seen that the power requirements grow rapidly with an increase in the velocity of the propellant. Historically, since there have been until recently no suitable low-mass electric power sources, this has compromised the application of electric propulsion in space toward lower propellant ejection velocities or, equivalently, to lower values of specific impulse. This in turn has encouraged the development of electric propulsion devices that have inherently lower propellant terminal velocities.

## 2.3 Comparison of nuclear, solar photovoltaic, and rectenna power sources for ion thrusters.

Historically, power supplies that have been considered for electric propulsion in space have been either solar photovoltaic or nuclear. Generically, both of these sources suffer from a high ratio of mass to the delivered DC power output. The high mass of the supplies have to be transported to space at high cost, and then the high mass greatly reduces the amount of acceleration that can be achieved, resulting in the use of a large amount of propellant to achieve the final necessary velocity change.

In addition there are a number of other disadvantages of nuclear which seem to disqualify it for an orbital transfer vehicle which could interface with transportation from Earth to LEO. Safe orbits for nuclear supplies are in a 1000 kilometer orbit, necessitating auxiliary orbit raising from LEO to 1000 kilometer.

Table 2.2 has been prepared to compare the characteristics of the three power sources for OTV's in space.

An examination of table 2.2 reveals that the rectenna has many advantages over the two other power sources as a pure power source but suffers the disadvantage of low duty cycle in low-Earth orbit. However, the high acceleration of the vehicle because of the low mass power source compensates for this as Table 2.3 indicates. In table 2.3 the low duty cycle in low Earth

orbit has been taken into account with the use of expression (3.7) developed in section 3.4. It is assumed that the specific mass of the nuclear power supply is 30 kg/kW supply with power conditioning included to use with an ion thruster. The specific mass of the ion thruster is assumed to be 1 kg/kW which is close to the actual figure of the 30 cm ion thruster. The specific mass of the rectenna and associated power conditioning is assumed to be 1 kg/kW, and the structure designed for low acceleration loads is assumed to have equal mass to the rectenna and the ion thrusters. It is further assumed that the mission is an express one, that is, that the payload constitutes a negligible fraction of the gross mass and that the vehicle travels from a 300 kilometer orbit in LEO to GEO and back to LEO.

TABLE 2.2

COMPARISON OF CHARACTERISTICS OF ELECTRIC POWER SOURCES IN SPACE

Characteristic	Solar Photovoltaic	Nuclear	Rectenna
Specific mass	10-30 kg/kW	30 kg/kW	1-2 kg/kW
Use in LEO	yes	no	yes
Power Conditioning Mass	large	large	small
Power Conditioning Complexity	large	large	small
Vulnerability to Space Radiation	large	no	small
Production of harmful radiation	no	large	no
Electromagnetic interference potential	none	none	some
Ease of Manufacture	difficult	difficult	easy
Level of Technology Readiness	moderate	poor	advanced
Use of critical materials	high	high	low
Relative cost	high	high	low
Compatibility with ion thruster	marginal	marginal	high
Orbital limitations	none	none	equatorial plane
Duty cycle of full system at 300 km orbit in LEO	60%	not allowed	6%
Duty cycle of full system at 10,000 km orbit	80%	100%	60%

An inspection of Figure 2.3 reveals that 10 times as much propellant must be brought up from Earth if a nuclear power supply is used instead of a rectenna

as a source of power. And even though the OTV supplied with nuclear power has continuous thrust, its acceleration is so low that the transit time is slightly poorer than for the intermittently accelerated OTV with a rectenna and four times as poor as for a beamed power system with four Earth based transmitters.

**Table 2.3**  
**EXPRESS MISSION (SMALL PAYLOAD) TO GEO AND RETURN**

	DRY VEHICLE SPECIFIC MASS KG/KW	PROPELLANT MASS KG	TOTAL MASS KG	INITIAL ACCEL. M/S <sup>2</sup>	ROUND TRIP TIME DAYS
ION THRUSTER BY ITSELF	1	0.25	1.25	0.029	3.67
ION THRUSTER NUCLEAR POWER	31	7.5	38.5	0.001	106
ION THRUSTER RECTENNA 1 BEAM	3	0.75	3.75	0.01	100
ION THRUSTER RECTENNA 4 BEAMS	3	0.75	3.75	0.01	25

### 3.0 SYSTEM ANALYSIS OF THE ALL-ELECTRONIC LEO TO GEO TRANSPORTATION SYSTEM.

In its entirety a "transportronics" system is a complex system. It not only involves a broad range of electronic technology to generate the microwave beam at the transmitting end and then to absorb the microwave power and convert it back to DC power at the receiving end of the system but also much technology pertaining to the transportation aspect including electric propulsion, associated vehicle design, and the flight paths of the space vehicles. The system analysis is, of course, dependent upon determining a set of basic assumptions which narrow down the scope of the analysis. Then there will be the development of the analytic tools, followed by their use in a scenario from which the performance and costs of the system may be obtained.

In this section we will first state the objectives of the system analysis, followed by the statement of the general approach to the analysis, followed by a set of basic assumptions which restrict and direct the analysis. These will be followed by a section devoted to developing an equation for the transit time from one orbit to another, and a section on the expressions that will give the efficiency of energy transfer between transmitting and receiving apertures. The output of these sections will then be used in a transportation scenario from LEO to GEO that was selected as a compromise between initial cost of the system and the performance of the system, the latter in terms of cost to place a kilogram of payload into geostationary orbit. This scenario will then provide a reference system with estimated costs and other characteristics against which the impact of expansion and alterations can be compared. The subsections of the section are:

- 3.1 Objectives of the System Analysis
- 3.2 General Approach to the System Analysis
- 3.3 Basic Assumptions Used in the Analysis and Rationale for Them
- 3.4 Quantification of Transit Time From One Orbital Altitude to Another, Including LEO to GEO.
- 3.5 Aperture to Aperture Power Transfer Efficiency
- 3.6 System Analysis by Scenario
  - 3.61 Introduction and selection of set of parameters for scenario
  - 3.62 Estimation of 60 cycle energy cost and transit time for the system scenario.
  - 3.63 Initial cost of the microwave power transmission system for the system scenario.
- 3.7 The Payload and Cost Performance Associated With Various Degrees of Maturity of the System and With Various Payload Ratios.

#### 3.1 Objectives of the System Analysis

The objectives of the system analysis of the all-electronic LEO to GEO transportation system as shown in Figure 1.1 is to:

1. Determine likely system scenarios that are consistent with scenarios for the future development of space and that take into account the constraint that the system handle large payloads to reach its fullest potential to reduce the cost of space transportation.

2. Determine elapsed time of transport between LEO and GEO and intermediate orbital altitudes for likely system scenarios.
3. Determine the number of kilowatt hours of Earth based energy to transport a kilogram of payload between LEO and GEO and to intermediate orbital altitudes, for likely system scenarios.
4. Determine the cost of construction of the microwave power transmission portion of the system.

### 3.2 General Approach to System Analysis.

It will become evident that system analysis involves many different parameters that must be taken into account. Among them are:

1. The mass fractions represented by the propellant, payload, and dry vehicle at launch point in LEO.
2. Transmission efficiencies between apertures as function of separation distance.
3. Thrust and other characteristics of the electric thrusters.
4. Variation in contact time between beam and vehicle as a function of orbital altitude.
5. Efficiencies of the energy conversion devices at transmitting and receiving ends of the system.
6. Costs of 60 cycle electric energy and system construction costs.
7. Frequency of the microwave radiation.

There are other parameters that will be found as the system analysis progresses. To a large extent the number of the parameters and especially the range of their values can be reduced through a set of basic assumptions. Some of these assumptions, such as basing the analysis at a frequency of 2.45 GHz, and the selection of the ion thruster as the electric thruster, are quite restrictive, so that the system analysis is limited to a system that has been largely defined by a set of initial assumptions. Then even with those restrictions, the analysis is based upon a specific scenario that has been selected by the author on the basis of his experience with a multitude of scenarios.

Within this specific scenario the analysis will depend upon analytic expressions derived during the study that for simplification purposes are approximations. And some well established analytic expressions may be applied in an approximate manner. In both cases, the point to be made is that the errors introduced with the use of these approximations will introduce errors that will be no larger in magnitude than those introduced elsewhere into the analysis. In other words this is a "first-cut" analysis.

### 3.3 Basic Assumptions Used in the Analysis and Rationale for Them.

1. From a technology point of view the system starts with the input of DC power at the Earth based terminal and ends with the propulsive force of the ion thruster.
  - o The technology logically divides up into that for the Earth based transmitter, that for the orbital transfer vehicle, and the microwave beam that interconnects the two.
  - o The technology of the transmitter and that for the orbital transfer vehicle are discussed in separate sections, 4.0 and 5.0 of this report.
  - o The technology surrounding the microwave beam itself will be discussed in this section.
2. The components of the transportation system are located in the equatorial plane.
  - o The principal and overriding reason for this is that it is only in the equatorial plane that the satellite makes contact with the microwave beam each time that it rotates around the Earth. Any other arrangement reduces the contact time between satellite and microwave beam in low Earth orbit by a factor of at least fifteen.
  - o An important secondary reason is that the transmitter cost is greatly reduced if it has to electronically track the satellite around one axis only.
  - o A less important reason is that the equator is the logical place to launch any satellite because of the maximum velocity of the Earth at the equator. And, if the objective is to place the payload in geosynchronous orbit, no cross range correction of the satellite trajectory is needed.
3. The mathematics of electromagnetic wave diffraction determine the properties of the microwave beam (26,27,28)..
  - o The microwave beam is characterized by the diameter of the beam and the distribution of energy across the beam at any distance from the launching point. The parameters that determine this characterization are the launching aperture diameter, the distribution of power density and phase across that aperture, the frequency of microwave radiation, and the distance from the aperture.
3. The frequency to be used in the analysis is 2.45 GHz, corresponding to a wave length of 0.1226 meters.
  - o At this frequency there is little attenuation of the beam in the Earth's atmosphere under all weather conditions. See Figure 3.1.

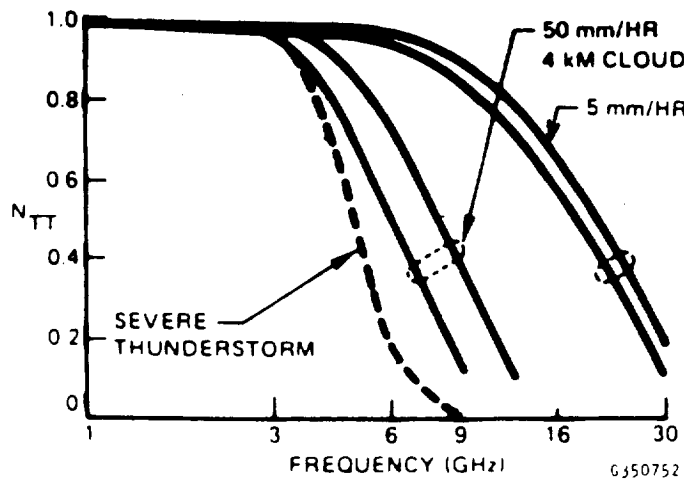


Figure 3-1. Transmission Efficiency through the Earth's Atmosphere as Related to Frequency and Condition of the Atmosphere.

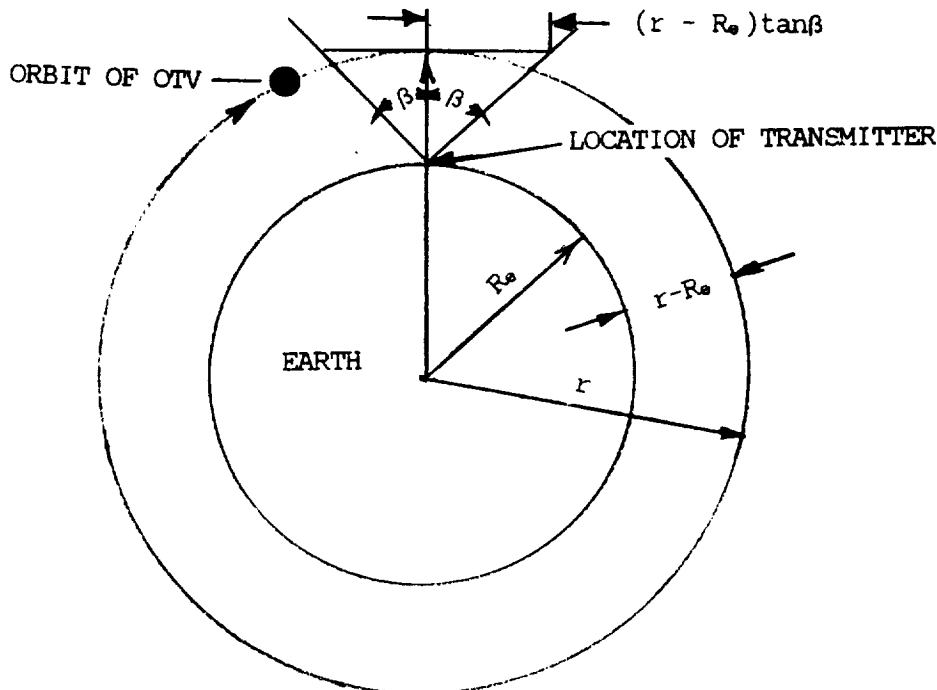


Figure 3-2. Geometry that Relates the Approximate Fraction of Time that the Microwave Beam Makes Contact with the Orbiting Transfer Vehicle to the Orbital Altitude  $r$  that is Measured from the Earth's Center. At Low Altitudes,  $r - R_E$ , and for Values of the Beam Sweep Angle  $\beta$  Less than 45 Degrees, the Term  $(r - R_E)\tan\beta/2\pi r$  Closely Approximates the True Contact Time. At High Orbital Altitude Some Error is Introduced but the Magnitude of Such Errors are Consistent with the Error Magnitudes of Other Approximations that have been Made.

- o It is at the center of the established ISM (Industrial, Scientific, Medical) band where experimental work may be carried out. It is logical that this would also be the allocation frequency most acceptable for beamed power transmission that exists below the next ISM band at 5.80 MHz. At 5.8 MHz there will be serious attenuation of the beam through the Earth's atmosphere under bad weather conditions.
  - o This is the frequency at which the technology has been developed and where the components are available at low cost compared to the cost at higher frequencies.
  - o The efficiencies of microwave power generation and rectification are greater at this frequency than at higher frequencies.
4. The characteristics of ion thrusters as developed or as projected at NASA's Lewis Research Center are used as a data base to determine the electrical rating, mechanical mass, propulsive thrust, and other parameters. Specifically the projected performance, mass, and other characteristics of the 50 cm. thruster now being developed at LeRC were assumed. These are discussed in section 4.2. The following is the rationale for the use of the ion thruster as a class of electric thruster.
- o Of the various electric thrusters, the ion thruster is the one most compatible with the rectenna.
  - o The ion thruster has a low specific mass. (Kilowatts/kilogram)
  - o The ion thruster is self cooled.
  - o The ion thruster is efficient.
  - o The fact that 80% of the power requirement of the ion thruster is at high voltage (2000 volts) is very favorable in reducing the power losses and the mechanical mass associated with the power busses from the rectenna. For large power needs from the rectenna, this is a very important factor.
  - o The ion thruster can be operated at high specific impulse, an outstanding advantage if a low mass source of electric power such as the rectenna is available.
  - o The ion thruster is so designed that it can be very economically fabricated in mass production.
  - o Although more development and evaluation of the ion thruster will be needed, it is believed that its state of evaluation from the viewpoint of life and other reliability characteristics is considerable better than for other electric thrusters.
5. The orbital trajectory of the satellite is a closely spaced spiral whose geometry is derived from the simplified assumption of continuous tangential acceleration in near circular orbit about a

central gravity field as derived from formulae given in section "Constant-thrust spiral" in section 4-3 of Stuhlinger, "Ion Propulsion for Space Flight", McGraw Hill, 1964.

- o Because there will be bursts of propulsion during the time of contact between the beam and the satellite vehicle it might be inferred that this propulsive pulse would result in a non circular orbit with the perigee established at the point of impulse and the apogee 180 degrees away. However, because the Earth is rotating at an angular velocity that is approximately sixteen times slower than the OTV (if it is in low-Earth orbit) the contact between the Earth based transmitter and the satellite will occur at different orbital angles and the perigees and apogees will frequently interchange with the passage of time. There should be an even lower probability of decircularizing the orbit in a fully mature system with four Earth based transmitters equally distributed about the Earth.
  - o Although this assumption probably applies in orbits close to the Earth, the situation may be sufficiently different as the satellite reaches near geosynchronous orbit to make corrective maneuvers necessary.
6. Time of transit of the orbital vehicle between any starting orbit at LEO and any terminal orbit, including geosynchronous orbit, is given by a unique formula, derived specifically for this study, to take into account the varying time of contact between beam and vehicle as a function of orbital altitude.
  5. The rectenna will be used to capture and rectify the incoming microwave beam at the interorbital vehicle. Its specific mass will be assumed to be 0.67 kilograms per kilowatt of power output when operated at the  $400\text{w/m}^2$  DC power output level. Its efficiency at this power level density is assumed to be 80%. It is also assumed that any harmonic radiation from the rectenna can be attenuated to acceptable levels, with improvements in rectenna technology as discussed in Section 6 of this report.

#### 3.4 Quantification of Transit Time From one Orbital Altitude to Another, Including LEO to GEO.

The time of transit of the electrically propelled OTV from one orbit to another is dependent upon (1) the physical laws that describe the motion of a self accelerated vehicle in a central gravitational field as described in section 4.3 of Stuhlinger, "Ion Propulsion for Space Flight" (McGraw Hill 1964), (2) the actual contact time between the microwave beam and the OTV and (3) the acceleration of the vehicle during the time of contact between the beam and the OTV.

For continuous time contact between the beam and the vehicle the time derivative of the increase in orbital altitude is given by the expression (4-211) in Stuhlinger (2)

$$\frac{dr}{dt} = \frac{2 a u r^2}{g_0 R_e^2} \quad (3.1)$$

where all parameters are given in MKS units, and  
 where  $a$  = the acceleration of the vehicle when in the beam  
 $r$  = the orbital altitude of the OTV as measured from the center of the Earth  
 $u$  = the velocity of the vehicle in circular orbit  
 $R_e$  = the radius of the Earth- 6,375,000 meters  
 $g_0$  = acceleration given to a mass at the Earth's surface by the Earth's gravitational field, 9.8 meters/s<sup>2</sup>

Expression (3.1) must be multiplied by the approximate fraction of time that the OTV is exposed to the microwave beam. This term is given by

$$2 \tan\beta / 2\pi r \quad (3.2)$$

where  $\beta$  is 1/2 the total sweep angle of the microwave beam from west to east.

The expression (3.2) is derived from Figure 3.2. The expression is quite accurate at low orbital altitudes but becomes less so at the higher orbital altitudes, where the term  $\tan \beta$  tends to become  $\beta$  instead. The use of this term also assumes that the output of the rectenna is independent of the angle  $\beta$ . This is another approximation which is justified on the basis of being able to vary the output of the transmitter to compensate for a larger separation distance at the angle  $\beta$  and the reduced projected cross section of the rectenna at the angle  $\beta$ .

$u$ , the velocity of the vehicle may be expressed in terms of  $r$  as

$$u = R_e \sqrt{g_0 / r} \quad (3.3)$$

When expression (3.1) is multiplied by expression (3.2) and the value for  $u$  in terms of  $r$  is inserted, and the resulting expression inverted we have

$$\frac{dt}{dr} = \frac{\pi R_e \sqrt{g_0}}{2 a \tan\beta} \frac{1}{\sqrt{r(r - R_e)}} \quad (3.4)$$

In the first term of expression (3.4) the acceleration "a" is a variable and is dependent upon the ratio of the thrust to the mass of the body. It may also be a function of orbital altitude if the microwave power reaching the OTV is not kept constant with altitude. In the practical scenario that will be examined the microwave power incident upon the OTV will decrease above 10,000 kilometers orbital radius. To take this and other changes in parameters into account, including possible changes in the angle  $\beta$ , the flight of the OTV may be broken up into several stages, and the time for each stage calculated. The total time to GEO will then be the sum of the times for the individual

stages.

The acceleration of the vehicle will be given by the following expression:

$$a = T / (M_{p1} + M_{pr} + M_v) \quad (3.5)$$

where  $T$  = Total thrust in Newtons

$M_{p1}$  = Payload mass

$M_{pr}$  = Propellant mass

$M_v$  = dry mass of vehicle

In a typical scenario the Payload mass represents 50% of the total mass, the propellant mass represents 16%, and combined mass of the rectenna, ion thrusters, and vehicle represent the other 34%.

The total thrust in Newtons is equal to the total dc power from the rectenna multiplied by the conversion factor of that power into Newtons of force. As seen in section 2.0 the force is dependent upon the velocity of the expelled propellant which is oftentimes expressed in terms of the specific impulse. In the scenario that we will examine, we will use some experimentally established ratios of thrust to power obtained from the performance of a 30 cm thruster, specifically 0.035 Newtons for each kilowatt of power input at a specific impulse of 4240, corresponding to a velocity of the propellant of 41,500 m/s.

The first term in expression (3.4) then becomes

$$\frac{\pi R_e \sqrt{g_0} (M_{p1} + M_{pr} + M_v)}{2 \tan\beta T_s P_{dc} A_r} \quad (3.6)$$

where  $T_s$  = specific thrust of ion thruster, N/kW

$P_{dc}$  = Average dc power density from rectenna, kW/m<sup>2</sup>

$A_r$  = Total area of rectenna on OTV

The expression for the transit time from one orbit to another then becomes

$$t_{r1-r2} = \frac{\pi R_e \sqrt{g_0} (M_{p1} + M_{pr} + M_v)}{2 \tan\beta T_s P_{dc} A_r} \int_{r1}^{r2} \frac{dr}{\sqrt{r(r - R_e)}} \quad (3.7)$$

where  $t_{r1-r2}$  is the time the OTV takes to go from  $r_1$  to  $r_2$  and the other parameters have been previously defined.

The second major term can be numerically integrated to produce Figure 3.3. In Figure 3.3 it can be seen that this term is a near logarithmic function of the orbital altitude as measured from the Earth's surface. This term is strictly a function of the orbital radius because the Earth's radius is a fixed quantity. If the first major term remains fixed during the vehicle flight then the ordinate of Figure 3 is linearly proportional to the flight time to reach any orbital altitude.

Expression (3.7) will be applied to the transportation scenario in section

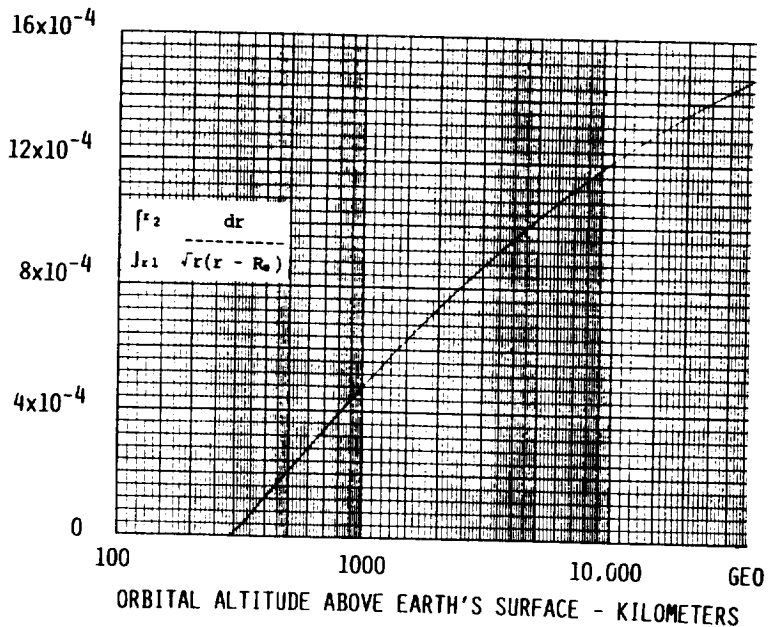


**Figure 3-3.** The Graph Above Gives the Integrated Value of the Second Major Term in Equation (3.7) as a Function of the Orbital Altitude. This Term Depends Only Upon  $r$  because the Diameter of the Earth,  $R_e$ , is Constant. This Term Takes into Account not Only the Increasing Time of Contact between the Beam and the OTV with an Increase in  $r$ , but also the Decrease in the Earth's Gravitational Field with an Increase in  $r$ .

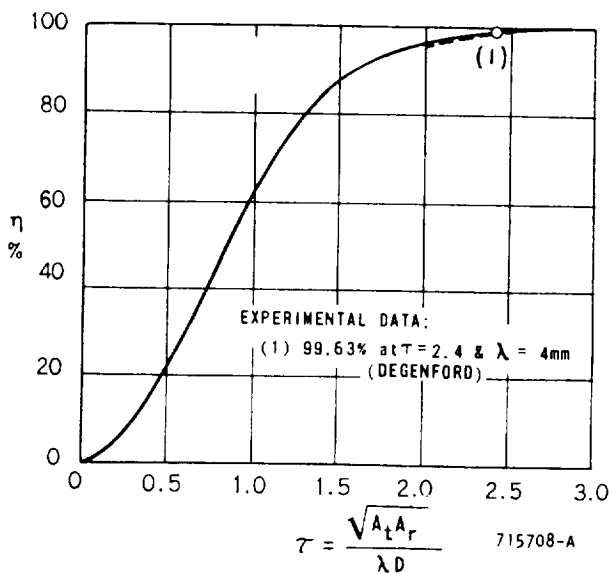


**Figure 3-4.** The Goubau Relationship between Maximized Aperture to Aperture Transfer Efficiency as a Function of the Aperture Areas  $A_t$  and  $A_r$ , the Wavelength of the Radiation, and the Distance  $D$  between the Apertures. Distribution of Power Over the Aperture is Given in Figure 3-5.

### 3.6.

The time that an Earth generated microwave beam sweeping through a 90 degree angle from West to East has to dwell on a satellite in low-Earth orbit is short. The result is that the vehicle is accelerated for only a short period of time and the change in velocity obtained is small so that the vehicle initially gains orbital altitude slowly. The dwell time of the OTV in low-Earth orbit is exacerbated by the large gravitational gradients close to the Earth through which it must climb. Nevertheless, because of the inherently low mass of the propulsion system made possible by the low mass of the rectenna and the ion thrusters, the vehicle has very high acceleration and climbs into regions of increased dwell time where it ascends rapidly.

The development of the expression 3.7 contains a number of simplifying assumptions that degrades its accuracy but it is believed to give transit times between LEO and 15,000 kilometers orbital altitude that are within 10% of the true value. At that altitude most of the energy required to place the vehicle in GEO has already been expended. Transit times to GEO predicted by this formula are believed accurate to within 15%.

### 3.5 Aperture to Aperture Power Transfer Efficiency.

Essential to any analysis is the determination of the overall DC to DC efficiency of the system. This efficiency is the product of three efficiencies (1) the efficiency with which 60 cycle power at the Earth is converted into radiated microwave power, which has been assumed to be 60% for all conditions, (2) the efficiency with which microwave power is transferred from the transmitting to the receiving aperture which can vary widely as a function of the separation distance between the Earth based transmitter and the altitude of the orbital transfer vehicle, and (3) the efficiency with which the microwave power is absorbed at the receiving aperture and converted into DC power, which will be assumed to be 80% as a conservative value derived from experiment. This subsection will discuss how the aperture to aperture efficiency is handled in the analysis.

The following expression developed by Goubau (28) gives the transmission efficiency between two apertures in terms of a parameter  $\tau$  which is defined as follows:

$$\tau = \frac{\sqrt{A_t A_r}}{y D} \quad (3.8)$$

where  $A_t$  = Aperture area of transmitting antenna  
 $A_r$  = Aperture area of receiving antenna (rectenna)  
 $y$  = Wavelength of microwave radiation  
 $D$  = Separation between transmitting and receiving apertures

The relationship between this parameter and aperture to aperture transfer efficiency is given in Figure 3.4. With each value of  $\tau$  is associated an illumination pattern of the two apertures which is given in Figure 3.5 as a function of  $\tau$ .

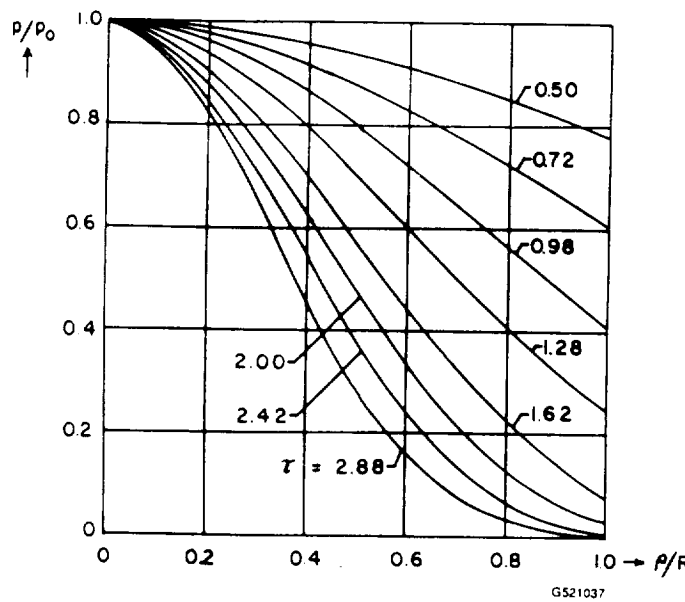


Figure 3-5. For Maximized Transfer Efficiency for Each Value of  $\Gamma$  the Power Distribution Over the Apertures Must Conform to the Above Figure.

### Vehicle mass breakdown when ion propulsion is used

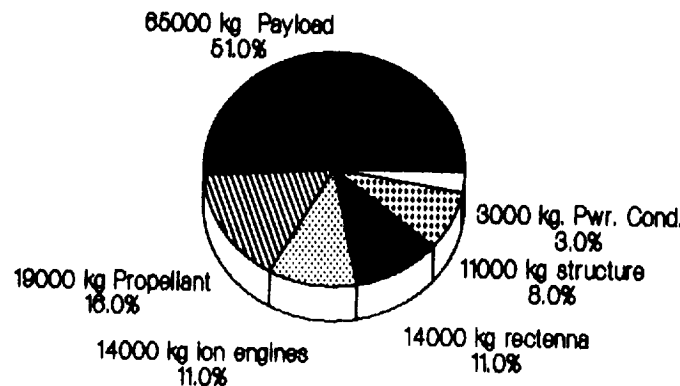


Figure 3-6. To Obtain Representative Performance of a "Transportronics" LEO to GEO Transportation System, in Terms of Transit Times to GEO and Operating and Capital Costs, a scenario that is described in Table 3-2 has been assumed. The Composition of the OTV as it Leaves LEO is Depicted Above. When the OTV Reaches GEO it Discharges its Payload and Returns to LEO in about 1/3 of the Transit Time for the up Link.

Referring to figure 3.4, it is noted that the aperture to aperture transfer efficiency can be very high, approaching 100% which has been confirmed experimentally. It is also noted that as the associated value of  $\tau$  decreases in value, the distribution of energy across the apertures becomes uniform. Under this condition the power density at the center of the rectenna and nearly that elsewhere is given by:

$$P_d = \frac{P_t A_t}{y^2 D^2} \quad (3.9)$$

where  $P_d$  = Incident microwave power density on the rectenna

$P_t$  = Total power radiated by transmitting antenna

$A_t$  = Total area of transmitting antenna

$y$  = wavelength of the microwave radiation

$D$  = Separation distance between apertures.

It follows that the power received will be  $P_d A_r$ , and the efficiency will be:

$$\eta = \frac{P_d A_r}{P_t} = \frac{A_t A_r}{y^2 D^2} \quad (3.10)$$

An examination of these equations indicate that high transfer efficiency between the transmitter and the OTV when it is near geostationary requires very large apertures. For example, using equation 3.9 and assuming both apertures of equal size, 60 % aperture to aperture efficiency would require apertures of 4.7 square kilometers. Although such large apertures for the rectenna on the OTV are conceivable for the distant future it would not be feasible to consider them at this time.

However, from the point of view of creating a lower cost LEO to GEO transportation system it would not be necessary to have high efficiency at high orbital altitudes if good efficiency can be achieved while pulling out of the intense gravitational field that exists in close proximity to the Earth and where the bulk of the effort is required to raise the orbital altitude.

In our analysis we will use expression (3.8) for separation distances between the apertures up to 2500 kilometers, and expression (3.9) beyond that. The purposes in doing so is largely motivated by the overall economics of the system as will be made more understandable in section 3.7 on "System Analysis by scenario".

### 3.6 System Analysis by Scenario

#### 3.6.1 Introduction and selection of set of parameters for scenario

As indicated in the objectives of this study, it was desired to evaluate system transit times from LEO to GEO, system installation cost, and system operating cost. Costs were to be expressed in terms of cost to place a

kilogram of payload into geostationary orbit.

Experience has indicated that there are just too many parameters to arrive at a minimum cost by analytical means. On the other hand, a large amount of experience in dealing with transmitter and rectenna costs as well as with preliminary tradeoffs between operating costs and initial installation costs suggests that a scenario approach may be a good approach to arrive at a set of installation costs, operating costs, and transit times to GEO. Such a system can be used as a reference system for making improvements, enlarging the system, etc.

The parameters of the scenario that we have selected are presented in Figure 3.6 and table 3.1. It is known a priori that the system must have a large payload capability to attain its potential to greatly reduce transportation costs. Such large payloads would be associated with the deployment of the Solar Power Satellite system and large scale development of the Earth's moon. It appears to be an economical choice over any other approach to putting one-trip payloads of 50,000 kilograms and over into GEO with the associated capability of bringing the OTV back to LEO, with or without a payload from GEO.

The technical aspects of the scenario may be divided into the microwave beam parameters and the OTV parameters. The microwave beam parameters involved are the transmitting aperture area and the radiated power. The OTV parameters are the rectenna mass, the rectenna area, the rectenna specific mass, power consumption and thrust rating of the ion thrusters, the payload mass, and the remaining mass of the vehicle and peripheral equipment.

The scenario assumes an empty vehicle mass of 42,000 kilograms, a payload mass and payload fraction of 65,000 kilograms and 51% respectively, and a propellant mass and propellant fraction of 29,000 kilogram and 16% respectively. With the use of one ground based transmitter it is capable of putting about 130,000 kilograms of payload into GEO each year. Although such a performance represents putting single payload masses into GEO that are an order of magnitude greater than present approaches, it is relatively small compared to those which could be accomplished with vehicles with a greater rectenna area or with convoys of smaller vehicles that are placed close to each other,

On the other hand, the ground based transmitter that involves an area of two square kilometers and a maximum radiated microwave power of 400,000 kilowatts is close to the size of a transmitter in a full scale system.

The parameters for the complete scenario is given in table 3.1. The basis for the selection of the parameters associated with the orbital transfer vehicle is found in section 4.0 that describes the associated technology. The basis for those associated with the Earth-based transmitter is found in Section 5.0.

Table 3.1

Parameter selection for the LEO to GEO transportation system.

1. Mission: Starting from a 300 km orbit in LEO to deliver a 65,000 kg payload to GEO and return to LEO

2. Orbital Transfer Vehicle

Total mass in LEO	126,000 kg
Dry vehicle mass	42,000 kg
Ion thrusters	14,000 kg
Rectenna	14,000 kg
Structure,etc	14,000 kg
Payload to GEO mass	65,000 kg
Propellant mass	19,000 kg
Rectenna	
Area	50,000 m <sup>2</sup>
Average DC power density	400 w/m <sup>2</sup>
DC power output	20,000 kW
Specific mass	0.7 kg/kW
Efficiency (dc output/microwave input)	80 %
Propulsion	
Ion thruster	
Propellant	xenon
Specific impulse	4200 sec
Physical size	50 cm. diameter
Power consumption, each	40 kW
Number of thrusters	500
Mass of each thruster	28 kg
Thrust of each thruster	0.37 Newton
Total propulsive force	740 Newton
Vehicle acceleration (empty)	0.0178 m/s <sup>2</sup>
Vehicle acceleration at LEO	0.0059 m/s <sup>2</sup>
3. Earth-based transmitter	
Aperture area	2 x 10 <sup>6</sup> m <sup>2</sup>
Maximum radiated microwave power	400 mgW
Frequency	2.45 GHz
Efficiency, 60 cycle pwr to microwave rad. pwr.	60%
West to east total scan angle	90°
North to south total scan angle	<1°
Location	equator

### 3.6.2 Estimation of 60 Cycle Energy Cost and Transit Time for the System Scenario

The subject of the amount of 60 cycle energy taken from an earth supply to put a kilogram of payload into orbit with the system scenario just discussed will be addressed first with the help of Figures 3.7 and 3.8. Figure 3.7 gives the aperture to aperture transfer efficiency and the power density available from the rectenna as a function of orbital altitude. These were derived, with the aid of expressions 3.8 and 3.10, from the aperture area of the transmitter and its radiated power as given in Table 3.1.

The efficiency curve shown in Figure 3.7 is the aperture to aperture transfer efficiency when the OTV is directly above the transmitter ( $\beta = 0$ ). It is, of course, not valid to assume that the same transfer efficiency will occur with  $\beta = 45^\circ$  at all orbital altitudes. The major argument for this simplification is that most of the electric power consumption is associated with high orbital altitudes where the efficiency is low but remains substantially the same over the entire sweep angle of  $90^\circ$ . At low orbital altitudes the efficiency can be maintained out to  $\beta = 45^\circ$  because of the large area of the transmitter, and the ability of the phased array to change the point upon which its beam is focussed.

Taking into account the conditions imposed by figure 3.7, figure 3.8 gives, as a function of orbital altitude, (1) the accumulative 60 cycle energy, (2) the accumulative delta V, and (3) total elapsed time in days, that includes the time during which there is no contact between beam and OTV.

The calculation of the first item, accumulative 60 cycle energy, will now be done, by breaking the mission down into three separate regions. The first region is at low orbital altitude where a 60% aperture to aperture efficiency can be maintained. The next region is where the output of the transmitter is gradually increased with increasing orbit altitude to provide 500 watt/m<sup>2</sup> until the full power output of 400 kW is reached. That limit is reached at an orbital altitude of 8,700 kilometers. The final region is where the power density is falling off rapidly with increasing orbit diameter.

In the first region, near LEO, the efficiency of transfer of power from Earth to the OTV is high. A typical efficiency breakdown at low altitude is :

Overall rectenna efficiency	85%
Ground aperture to OTV aperture transfer efficiency	60%
60 cycle power to microwave power radiated	60%
Overall 60 cycle power to DC rectenna power	30%

From Fig. 3.7, the overall efficiency of 30% holds until an altitude of 2500 kilometers is reached and beyond which the aperture to aperture transfer efficiency becomes less than 60%. To supply 20,000 kilowatts to the ion engines will therefore require a 60 cycle power of  $20,000/0.3$  or 67,000 kilowatts. With an acceleration of 0.0059 m/s, which is 1/3 that of the empty vehicle, the "on" time of the ion engines during which power is being consumed is 48.3 hours. The 60 cycle energy consumed is therefore  $67,000 \times 48.9$  or

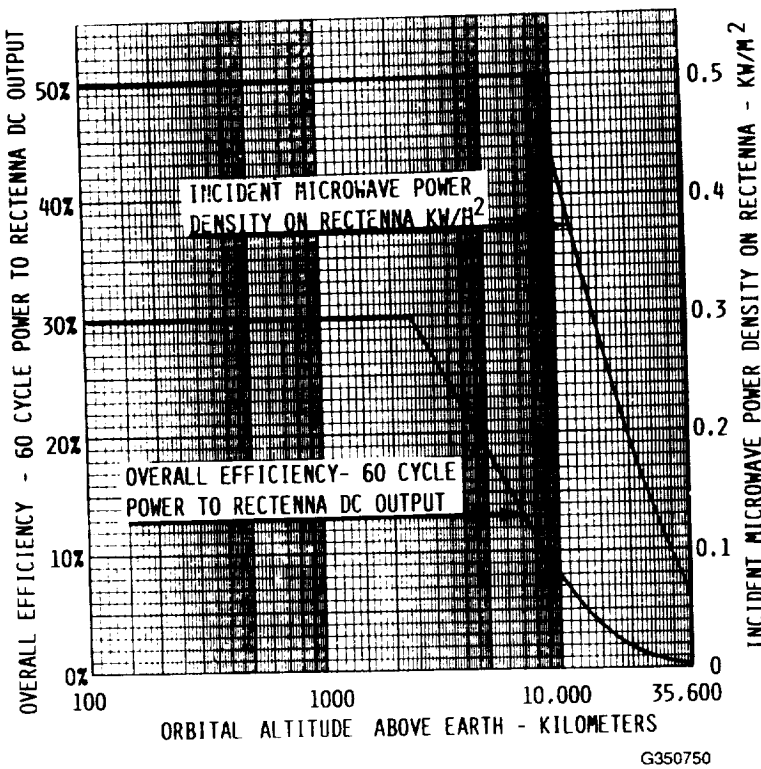


Figure 3-7. The Dependency of (1) Overall Efficiency of Microwave Power Transmission System, and (2) Rectenna Incident Microwave Power Density, Upon Orbital Altitude that Results from the Parameters Chosen for the System Scenario.

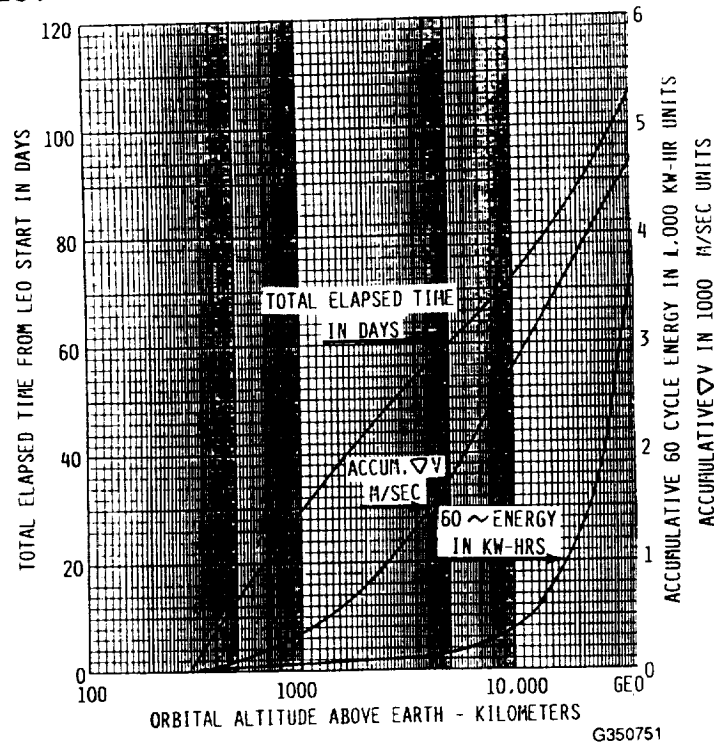


Figure 3-8. The Graphs Show (1) Accumulative 60 Cycle Energy, (2) Accumulative Delta V, and (3) Total Elapsed Time as a Function of Orbital Altitude with the Imposed Constraints Given in Figure 3-7.

$3.18 \times 10^6$  kwhrs, or 48.9 kwhr for each kilogram of the 65,000 kilogram payload boosted from a 300 kilometer orbit to a 2500 kilometer orbit. At 5 cents per kwhr this represents \$2.44 worth of 60 cycle electric power; at 10 cents per kwhr the cost is \$4.88. This is an extremely low energy cost for orbit raising.

It is interesting to compare the cost of energy with the amount of propellant used and the cost of bringing it from Earth to LEO. The propellant consumption during the 48.3 hours of acceleration is computed from the use of equation 2.1, where the propulsive force is 740 Newtons and the propellant velocity is 41,000. The propellant consumed is 3,138 kilograms, or 0.048 kilograms for each kilogram of the 65,000 kilogram payload placed into a 2500 kilometer orbit from a 300 kilometer orbit in LEO. At the current cost of \$5000 for each kilogram transported from Earth to space, the transportation cost for the 0.048 kilogram of propellant is \$240, or about 100 times the cost of the electric energy. It is interesting to note that such a disparity in costs would suggest that even higher specific impulses be used for orbit raising to reduce propellant transportation costs from Earth to orbit. Argon, inexpensive and readily available, could be used at twice the specific impulse in the same ion thrusters, and reduce the propellant transportation cost to \$120 while raising the 60 cycle energy cost to about \$10.00.

With respect to the total elapsed time, If the microwave beam swings through an angle of 90°, the total elapsed time, as derived from equation 3.7 is 48 days.

The delta V that is acquired at 2500 km represents slightly over 20% of that needed to go all the way to GEO as seen in Figure 3.7.

At orbits higher than 2500 km, the aperture to aperture efficiency falls off rapidly and impacts the overall efficiency as observed in Figure 3.7. However, the power density remains at 0.5 kw/m<sup>2</sup> until an orbital radius of 8300 kilometers is reached because the power output of the transmitter is gradually increased to a maximum of 400,000 kilowatts, corresponding to 670,000 kw of 60 cycle power input.

The 60 cycle energy that is used in ascending from 2500 km to 8300 km represents an additional 197 kwhrs, or \$9.85 of 60 cycle energy at 5 cents per kwhr, \$19.70 at 10 cents per kwhr. At an orbital altitude of 8300 km a total delta V of 2500 has been acquired or over half of that required to go to GEO.

At orbital altitudes greater than 8300 km, the power density will also decrease rapidly with altitude producing less acceleration of the OTV and taking longer to acquire an incremental delta V, while still consuming the maximum 60 cycle power of 670,000 kw. This segment of the flight from LEO to GEO requires the most energy- 3685 kwhrs, or 93% of the total 3,931 kwhrs of energy required. The curve of energy consumed versus altitude achieved is shown in Figure 3.7. The total energy charge at 5 cents/kwhr is \$196.00, or \$392.00 at 10 cents per kwhr..

The intuitive reaction to the high 60 cycle energy charge for the last half of the LEO to GEO flight is to increase the efficiency of power transfer over the

longer distances. On the other hand this energy charge of \$196.00 should be compared with the cost of bringing up the propellant from Earth to LEO. For each kilogram of pay load put into GEO, 0.3 kilograms of propellant will be required for the two way propulsion of the vehicle. At a cost of \$5000/kg to place material into LEO from Earth, the transportation cost would be \$1500, a charge greater than that of the 60 cycle energy charge.

Moreover, the energy charge can be drastically reduced when it becomes appropriate to do so by using very large OTV's or a convoy of smaller OTVs packed closely together.

The transit time is shown to be 106 days from Figure 3.7, obtained as the sum of many incremental times for incremental increases in orbital radii. With the shedding of the payload of 65,000 kilograms, and with only enough propellant mass to return to Earth, the return time from GEO to LEO will be very close to 1/3 of the up time, so that the round trip transit time would be 141 days. Since each payload is 65,000 kilograms, about 130,000 kilograms of payload would be transported per year, after allowing a total of 82 days for loading and unloading cargo.

It would be of interest to observe what happens to the cost of 60 cycle electrical power for each kilogram of payload placed into GEO if the rectenna area of a single orbital transfer vehicle, or aggregate area of several smaller ones locked together in convoy formation, were increased by a factor of five, and if the maximum microwave radiated power were increased from 400 megawatts to 800 megawatts. The payload delivered to GEO per year would now increase from 130,000 kilogram to 650,000 kilogram. By going through the same procedure shown in Figures 3.6 and 3.7 it is found that the cost of 60 cycle electric power for each kilogram placed into GEO is reduced to \$49 from the \$196 figure. It is further estimated that the transit time will be cut down to 100 days from 106 days because the incident microwave power density is maintained at 500 watts/m<sup>2</sup> to a higher orbit.

### 3.6.3 Initial Cost of the Microwave Power Transmission System for the System Scenario.

Another cost of concern is the initial cost of the transportation system portrayed in this section. In addition to the cost of the microwave portion of the system, the complete system cost includes the cost of the ion thrusters, and more importantly the cost of the vehicle itself which must be transported into space from the Earth. However, these costs are outside the area of the author's expertise and will not be estimated in this report.

The costs of the microwave transmission portion of the system are associated with the cost of the components of the Earth-based transmitter and of the cost of the rectenna. In addition there will be "one time" engineering design charges, but these are a small fraction of the costs of the fabrication of a mature system consisting of four ground based transmitters and more and larger orbital transfer vehicles and rectennas. Our procedure, therefore, will be to estimate costs for all the physical hardware associated with the first system, which will also be the basis of estimating costs for a mature system. To these costs will be added a large amount for engineering design of the hardware components, for their testing, and for tooling charges for the fabrication of

the hardware components, which will be found to lend themselves to mass production techniques. Testing of the system will be included under engineering charges.

The key aspect to accurate estimating of costs is the modularity of both the Earth-based transmitter and the rectenna. There are two million modules in the Earth-based transmitter, and tens of thousands of modules in the rectenna. The total cost of these modules represents the major cost of the transmitter. Therefore the emphasis has been to reduce the costs of these modules through the use of low cost sub components, minimum mass of raw materials such as aluminum, and low cost fabrication methods. Much work and ingenuity has gone into this, and much of this is reviewed in sections 4 and 5. .

As a result of this work, it is possible to estimate the cost of the modules used in the transmitter to be no more than \$200 each when built in such large quantities. Thus their cost would represent \$400,000,000. The cost of the ten foot high, concrete floor structure to support the modules and protect them from the weather is estimated at another \$300,000,000. These and other costs are outlined in table 3.2. The total costs estimated are one billion dollars.

TABLE 3.2  
ESTIMATED COST OF 2 SQUARE KILOMETER EARTH-BASED TRANSMITTER

Module Cost (2,000,000 units)	\$400,000,000
Slab and support structure (building)	\$300,000,000
Power conditioning and Distribution	\$50,000,000
Phase reference and beam guiding	\$100,000,000
Management and Engineering	\$150,000,000
Total Cost	\$1,000,000,000

If we assume that this cost can be amortized over a period of ten years at an annual cost of \$100,000,000, and that the yearly payload that can be delivered with the transportation system is 130,000 kilograms as previously estimated after allowance for turn around time, then the cost per kilogram of payload is \$769.00, or \$350.00 for each pound of payload.

Although building such a large transmitting antenna is necessary for an all-electronic LEO to GEO transportation system, it is not recommended that it be built without first building a much smaller system which would verify the technology that would be used in the full scale Earth-based transmitter. The scale of the interim transmitter would be large enough to merit the same tooling and other needs of the larger system. The scale would also be consistent with efficiently beaming power into space for use by a satellite in LEO. The recommended transmitter would be 200 meters on the side to produce a 40,000 m<sup>2</sup> aperture. Each of the 40,000 modules that comprise the transmitter would radiate a nominal 500 watts of power for a total radiated power of 20 megawatts.

The cost of this smaller transmitter is estimated at \$100,000,000, broken down as follows:

Radiating modules including tooling	\$12,000,000
Structure	\$10,000,000
Power conditioning and distribution	\$3,000,000
Phase reference distribution and beam steering control	\$8,000,000
Engineering, program management, misc.	\$67,000,000
Total cost	\$100,000,000

Although the major purpose of the smaller array is verification of the technology it could be very useful as a second transmitter for the OTV vehicle while it is still in LEO, approximately doubling its rate of ascent in the 300 to 600 kilometer orbit region.

Returning to the discussion of cost of the total system which includes the rectenna, a similar estimate has been made for the cost of the 50,000 square meter rectenna. Although it is estimated that the eventual cost of the rectenna at the end of the learning curve will be about \$350 per square meter, we have estimated the cost to include tooling and engineering at a total cost of \$50,000,000 or an average cost of \$1000 per square meter. This cost is small compared to that of the Earth based transmitter and so if its cost were spread over ten years, it would add only \$38.00 to the cost of placing a kilogram of payload into space.

In summary of this section 3.6, a set of parameters were selected that described the microwave power transmission system, the propulsion system, and that gave the mass of the payload, the mass of the propellant, and the mass of the vehicle broken down into rectenna, propulsion, and structure. From this we examined the performance in terms of the time taken to go from an orbit of 300 kilometers to geostationary orbit, and the costs associated with the 60 cycle energy required and the construction of the Earth-based array and the space rectenna. The cost results were given in terms of the cost per kilogram of payload delivered to geosynchronous orbit. Much of the data base for the costs associated with the construction of the system is derived either directly from the material in sections 4.0 and 5.0 or in reports on other studies. The system described by the set of parameters chosen is referred to as the reference system.

### 3.7 The Payload and Cost Performance Associated With Various Degrees of Maturity of the System and Various Payload Ratios.

A fully mature system is defined as one with four full scale Earth-based transmitters, and four orbital transfer vehicles. With this arrangement there is four times the use of each of the Earth based transmitters, while each of the OTVs is exposed to a microwave beam four times more often, so that the flight time between LEO and GEO is decreased by a factor of four. Each of the OTVs now delivers four times as much payload as the reference system, and because there are now four rather than one OTV, the amount of payload delivered is 16 times as great as for the reference system.

In addition, in a fully mature system as defined, it is possible to increase the payload fraction, the size and power handling capability of the rectenna, and the aperture area and radiated power of the Earth-based transmitter.

Increasing the payload fraction has an impressive impact upon the amount of payload that can be delivered to GEO in the same time period.

Table 3.3 shows the performance capability in terms of payload delivered as a function of various stages of maturity of the system. The procedure for obtaining the data for table 3.3 is given in Appendix A. Of particular interest is the set of parameters given below Table 3.3 for the annual delivery of 60,000 metric tons of material from a 300 kilometer orbit in LEO to GEO. Such a delivery would be capable of putting up two Solar Power Satellites each year from material originating at the Earth's surface or ten per year if 80% of the materials came from the surface of the moon. This is a long range objective that would be occasioned only by a deployment of the SPS system in GEO or some as yet non-predicted activity of equal size.

It may be of interest to estimate the number of 60 cycle kilowatt hours required to place a kilogram of payload into GEO with the system parameters tabulated below Figure 3.3 where there is a payload of 3620 metric tons that is placed into GEO in a single journey in about 90 days. We will simplify the procedure of estimating 60 cycle kwhrs by assuming that the transmitter will be operating at full power output during the contact time with the OTV. The actual contact time with the OTV will depend upon the acceleration and the velocity change that must occur between LEO and GEO. The change in velocity is 4600 m/s and with the acceleration of 0.00169 the corresponding time interval is 756 hours. During operation the power input into the transmitter is 800,000 kilowatts. Therefore the corresponding number of kwhrs for the 756 hour flight duration is  $605 \times 10^6$  kwhrs. When this is divided by the 3,620,000 kg payload, the number of kwhr per kilogram of payload delivered is 171 kwhr/kg. This would represent an energy charge of \$17.60 per kilogram of payload delivered.

We may also want to estimate the capital costs involved in various stages of maturity of the system, and see how they apply to placing a kilogram of payload into GEO. Table 3.4 has been prepared for this purpose. In determining the annual payload that each stage of maturity could deliver, we have assumed a payload factor of 0.8. As compared with corresponding payloads in table 3.3, the 10,000 kw OTV has been upgraded to a 20,000 kw OTV.

From table 3.4, it is seen that with the initial cost distributed over a ten year period, the capital cost to put a kilogram of payload into GEO can be less than \$10.00 in a fully mature system. This, of course, applies only to the microwave power transmission system in the transportation system.

However, it is pointed out in section 4.2 that the ion thruster is designed to be produced at relatively low cost. In lots of 5000, a generous cost would be \$10,000 each so that their cost in a mature system would be \$50,000,000 for each 200,000 kw rated OTV. For 4 OTV's with that power rating the total cost would be \$200,000,000. This would increase the total cost of the mature system as given in table 3.4 to \$4,600,000,000 or only 5% greater. Even if the estimate of the cost of the ion thrusters was low by a factor of three or four, the difference between the complete propulsion system and that of the microwave transmission portion of it alone would not be very great, percentage wise.

Table 3-3

NUMBER OF METRIC TONS OF PAYLOAD DELIVERED TO GEOSYNCHRONOUS ORBIT PER YEAR  
AS FUNCTION OF OTV POWER RATING, SYSTEM MATURITY, AND PAYLOAD FRACTION

NO. OF BEAMS AND OTV'S	1 BEAM - 1 OTV		2 BEAMS - 2 OTV'S		4 BEAMS - 4 OTV'S	
	10,000 KW	100,000 KW	10,000 KW	100,000 KW	10,000 KW	200,000 KW
PAYOUT FRACTION	TONS	TONS	TONS	TONS	TONS	TONS
0.2	29.2	292	117	1170	467	9340
0.3	47.5	475	190	1900	759	15180
0.4	65.7	263	263	2630	1051	21020
0.5	87.6	876	350	3500	1400	28000
0.6	117	1170	467	4670	1868	37360
0.7	150	1500	600	6000	2400	48000
0.8	190	1900	759	7590	3036	60000

G447213

ABBREVIATED SET OF SYSTEM PARAMETERS  
FOR YEARLY TRANSPORT OF 60,000 METRIC TONS TO GEO

Space Vehicle	200,000 kw DC from rectenna	Earth based transmitting antenna
Power Rating	0.4 kw/m <sup>2</sup> DC power	Frequency 2.45 GHz (ISM Band Center frequency)
Average Power Density	500,000 m <sup>2</sup>	Area 2,000,000 square meters
Area of rectenna	80% minimum	Maximum microwave power radiated 500,000 kw
Rectenna efficiency		Microwave Generator - high-gain, phase-locked, micro wave oven magnetron combined with ferrite circulator
Vehicle mass		Average generator output 250 watts
Ion thruster mass at 0.68 kg/Kw	136,000 kg	Number of magnetrons 2,000,000
Rectenna mass at 0.68 kg/Kw	136,000 kg	Input 60 cycle AC power 800,000 kw
Vehicle, tank, and other structure	136,000 kg	Type of antenna structure 2,000,000 radiating modules
Dry mass of vehicle	408,000 kg	each a section of waveguide with 100 radiating slots
Payload mass at 80% of total	3,620,000 kg	fed in middle from one magnetron amplifier.
Propellant mass at 11% of total	459,000 kg	
Total initial vehicle mass	4,487,000 kg	
Electric Propulsion		Beam pointing control by phasing radiating modules
Type	ion thruster, 50 cm. (Ref. 10)	Beam tracking of space vehicle - interferometers on transmitter track beacon at center of rectenna in open loop mode, and by amplitude sensors on periphery of rectenna sense beam amplitude and close control loop.
Power input	40 Kw each	Beam focussing for near and far distances by phasing radiating modules
Quantity	5000	
Propellant	Xenon	
Specific Impulse	4200 sec. (41,000 m/s)	
Specific thrust	0.038 Newton/Kw	
Total thrust	7600 Newtons	
Acceleration of the vehicle		Angular sweep of beam - 120° total in direction along equator; less than 1° in north-south direction. Note that only 90° sweep is practical at low altitude. However, at altitudes of 5000 km or more the distance to satellite and the angle between beam and satellite tend to be independent of pointing angle so that a larger angular sweep could be used.
Acceleration of dry vehicle	0.0186 m/s <sup>2</sup>	
Acceleration of vehicle with payload and propellant	0.00169 m/s <sup>2</sup>	
Acceleration of geosynchronous distance	0.00015m/s <sup>2</sup>	
Approximate round trip times, assuming empty vehicle return to earth	90 days	

3.8 Comparison of estimates obtained from the system analysis for the scenario assumed in section 3.6 with that from data in table 3.3.

It is of interest to compare the 130,000 kilograms of payload delivered to GEO each year as derived in section 3.6 with the nearest corresponding point in table 3.3. . This point is in the left hand column where the payload fraction of 0.5 corresponds to the payload fraction of 0.51 in the scenario assumed in section 3.6. Table 3.3 shows 87.5 metric ton (87,500 kg) delivered annually to GEO by a 10,000 kW rated OTV. This would be upgraded to twice that or 175 metric ton with the 20,000 kW rated OTV used in the scenario, or a factor of 1.35 greater. However, table 3.3 assumes no allowance for turn around time while 77 days was allowed in the analysis in section 3.6. The delivery of 130,000 kg would have been increased to 165,000 kilograms if turn around time had been omitted. Thus the estimated two annual payloads are nearly the same, when adjusted for turn around time allowance.

TABLE 3.4

CAPITAL COSTS ASSOCIATED WITH VARIOUS DEGREES OF SYSTEM Maturity AND ASSOCIATED IMPACT UPON PRORATED CAPITAL COSTS TO PLACE A KILOGRAM OF PAYLOAD INTO GEO

Level of System Maturity			
	1 Transmitter 1 20,000 kW Rectenna	4 Transmitters 4 20,000 kW Rectennas	4Transmitters 4 200,000 kW Rectennas
1. Transmitter Acquisition cost	\$1,000,000,000	3,400,000,0000	3,400,000,000
2. Rectenna Acquisition Cost	50,000,000	170,000,000	1,000,000,000
3. Total Acquisition Cost (1+2)	\$1,050,000,000	3,570,000,000	4,400,000,000
4. Annual Cost Distributed Over 10 years (3/10)	\$105,000,000	357,000,000	440,000,000
5. Annual Payload Delivery 0.8 Payload fraction	380,000 kg	6,000,000 kg	60,000,000 kg
6. Time Distributed Acquisition Costs Divided by Annual Payload Delivery (3/4)	\$276/kg	\$59.5/kg	\$7.33/kg



#### 4.0 TECHNOLOGY OF THE ORBITAL TRANSFER VEHICLE

The technology of the proposed orbital transfer vehicle is a unique combination of electric propulsion technology and the technology of power transmission via a microwave beam. This section will first discuss the physical format of the vehicle. Then, in sequence, it will discuss the ion thruster as the preferred form of electric propulsion, and the rectenna as the portion of the beamed microwave power transmission carried on board the orbital transfer vehicle. It will also discuss the interface between the rectenna and the ion thrusters, a subject of prime importance. In addition the bussing of the power from the rectenna to the ion thrusters will be analyzed in terms of the mass required for the bussing and the power that is dissipated in the bussing. Finally, there will be a preliminary discussion of the interaction of the current in the busses with the Earth's magnetic field. These subjects together with their numerical identification are given below.

- 4.1 Overall description of the vehicle.
- 4.2 Description and simplified analysis of the ion thruster
- 4.3 Description of the rectenna
- 4.4 The interface between the ion thruster and the rectenna
- 4.5 Interrelationship of rectenna size with bussing mass and electrical loss
- 4.6 Interaction of the electrical busses with the Earth's magnetic field

Attention is called to the fact that items 4.4, 4.5, and 4.6 have been quantitatively evaluated during this study and the results have been incorporated for the first time in a report. They have not been included in any published paper. Each of them is very important in the design of a practical orbital transfer vehicle.

##### 4.1 Overall Description of the Vehicle

The overall format of the vehicle is depicted in Figures 1.11 and 1.12 in section 1.0 of this report. Figure 1.11 is a photograph of a model representing the vehicle in its simplest form. A large rectenna collects the energy and the power is bussed through the side members of the vehicle. These side members are also the major structural members of the vehicle and their shape and mass represent a tradeoff study between increased mass to reduce the  $I^2R$  losses and area to radiate the heat loss. This aspect of the design is discussed in section 4.5.

The ion thrusters are located at one end of the vehicle. They are purely schematic in the illustration. In their place would be several hundred ion thrusters of the current 30 cm. or 50 cm. design.

The area of the rectenna is large, primarily for the purpose of increasing the efficiency of the microwave beam coupling between the earth and OTV apertures. The result is a rectenna that would be rated at 20 megawatts, with a rating of

several times that and even up to 200 megawatts a distinct possibility for second generation vehicles. Power levels of 20 megawatts and more are consistent with the need for the large thrusts required to deliver the large mass of material needed for the construction of Solar Power Satellites in geostationary orbit. Such a large vehicle could also be considered as the staging for vehicles that would go on to the moon or Mars, and to receive cargos of material coming from the moon or Mars and destined for low-Earth orbit or Earth.

Figure 1.12 of section 1.0 shows an artists rendering of a second generation OTV conceived by the author (4). This design is an attempt to diminish and possibly cancel the torquing of the ship by the interaction of the current in the busses with the Earth's magnetic field. It also cuts down the bussing losses and the mass of the busses by feeding power into the ion thrusters from the front and the back of the vehicle.

In this design, the ion thrusters are mounted at an angle in the hope and expectation that their plume of ions will not erode the structure. Because the thrust of the ion thrusters must be parallel to the Earth's surface, the angle of the mounting does mean that the rectenna will be inclined at a slight angle to the Earth's surface. The most serious aspect of this is that the drag of the vehicle in the atmosphere in low Earth orbit will be substantially increased. A more recent thought is that perhaps the ion thrusters should still be mounted on the axis of the vehicle but outboard of its sides so that the direction of the thrust of the ion thrusters may be independent of the orientation of the rectenna with respect to the Earth.

In this study no serious consideration has been given to the detailed structural design of the vehicle. However, the work of A.P. Coppa has been used for estimating the mass of the vehicle. (33)

#### 4.2 The Technology of the Ion Thruster

The principles of operation of the ion thruster are first principles of charged particle ballistics as given, for example, in "Fundamentals of Engineering Electronics" by W. G. Dow, John Wiley, and in reference 5. Advanced technology from which performance parameters were taken for the study are given in references 29, 30 and 31.

The ion thruster was selected from a number of different kinds of electric thrusters. It is not the purpose of this section to also describe the other thrusters and their good and bad characteristics. However, the ion thruster was selected for the following reasons.

- o Works well over a wide range of specific impulse values.
- o Efficiently converts electric power into thrust power -80%
- o Gets rid of any inefficiency by direct radiation of heat to space.
- o Operates at a high voltage- essential to hold down current bussing losses from the rectenna.
- o Has a low ratio of mass to power consumption, 1 kg/kw in 30 cm design. less than that for projected 50 cm. design.
- o Easy replacement of parts.
- o Is designed to be largely constructed from sheet metal parts.

- o Operation is well understood theoretically.
- o More good life test experience than other approaches.

#### 4.2.1 Principle of operation of the ion thruster

A photograph of a representative ion thruster is shown in Figure 1.4 in section 1.0 of this report. Figure 4.1 is a schematic that describes the principle of operation of the ion thruster. First, a gas is ionized in a chamber. Positively ionized atoms of the gas are then extracted through holes in a wall of the gas chamber and accelerated to high velocity by the potential that exists between the wall of the chamber and an accelerating grid.

In this subsection we will analyze the performance of the ion thruster using the physical laws that relate to the acceleration of ions between two plates, as shown in Figure 4.1. From these laws we can predict the approximate behavior of the ion thrusters. However, the measured performance of ion thrusters deviates somewhat from these predictions for reasons best understood by experts in the area of ion thrusters. The performance of the 50 cm. thruster as projected by experts is given in Table 4.1. and the ratio of its mass to power consumption may be obtained from Table 4.2 (31).

Table 4.2 is also included to indicate the very large power conditioning mass that is necessary when operating with a non-rectenna power source, in this case a nuclear power source that has a relative low DC voltage output which must be stepped up for application to the ion thruster.

The analysis is started by determining the terminal velocity given to an ionized particle moving between two charged plates. This is

$$v = \frac{(5.97 \times 10^5) V^{1/2}}{\sqrt{m_i/m_e}} \text{ m/s} \quad (4.1)$$

where  $v$  = velocity of accelerated ion, meters per second

$V$  = the applied potential , volts

$m_i/m_e$  = ratio of the mass of the propellant ion  
to the mass of the electron

Substitution of the mass of the ions for argon and xenon into the above equation, together with an assumed applied potential of 1500 volts, give velocities of 77,000 and 42,000 , respectively. These velocities are greater by ratios of 19.2 and 10.5 than that achieved with chemical propulsion. For a given thrust, the propellant mass expelled is inversely proportional to the velocity, so the propellant consumption is down from that of chemical propulsion by the factors of 19.2 and 10.5.

The number of positive ions and therefore the total mass that is extracted from the ionized gas chamber may be approximated by the solution of Poisson's equation applied to a diode consisting of two plates separated by a distance  $s$ , with a potential  $V$  between the two plates, one of which is a cathode that can emit unlimited amounts of charged particles so that the limitation of current flow between the plates is limited by the build up of space charge between the plates (34). This equation is given below:

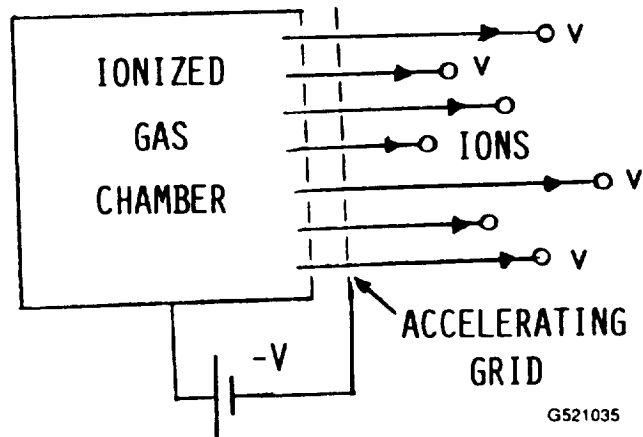


Figure 4-1. Principle of the Ion Thruster. Positively Charged Gas Ions are Accelerated between Grids with Voltage  $V$  to be Ejected with Velocity  $v$ .

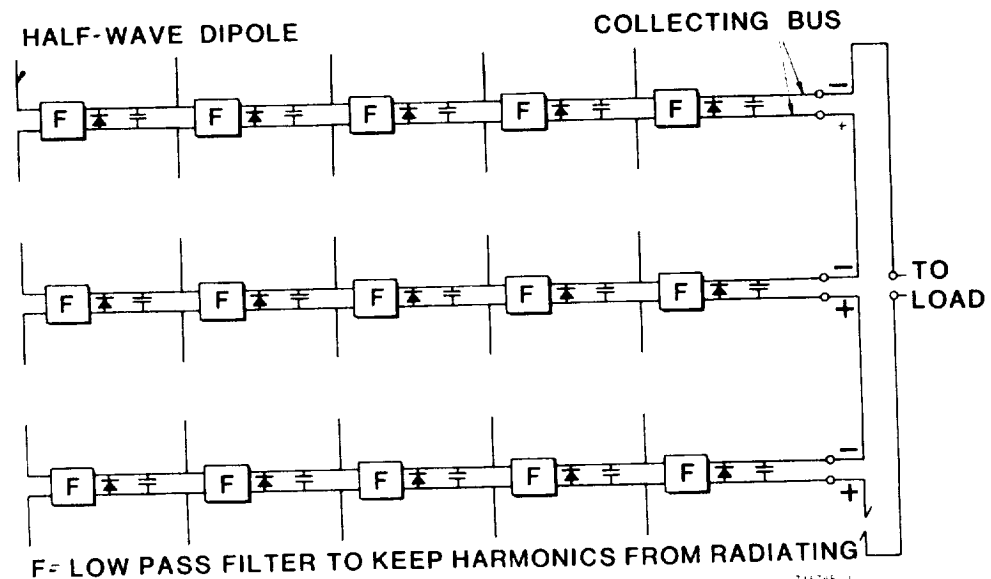


Figure 4-2. Schematic Diagram Showing the Functions Performed on the Foreplane of the Two Plane Rectenna Format. These Functions are Absorbing the Microwave Beam, Rectifying it into DC Power, Harmonic Filtering, and Bussing of the DC Power to Terminals for Series or Parallel Combining with Other Busses.

$$J = \frac{(2.331 \times 10^{-6}) V^{3/2}}{\sqrt{m_i/m_e} s^2} \text{ amperes/m}^2 \quad (4.2)$$

where:  $J$  = current flow, amperes/ $\text{m}^2$   
 $V$  = potential applied across the plates in volts  
 $m_i$  = mass of the ion  
 $m_e$  = mass of the electron  
 $s$  = separation between the grid plates.

If  $s$  is taken as 1.3 mm or 0.0013 m, a representative spacing between the grid plates, the voltage is taken as 1500 volts, and xenon is used as the ionized gas, whose ratio of ion mass to that of electron mass is 237,000, then the current flow is determined as 164 amperes per square meter.

It is found that the flow of current between the two plates in an ion thruster which are not simple flat plates but have holes in them through which the ions can flow is not proportional to the  $3/2$  power of the potential but to an exponent which is somewhat less than that.

Note that the number of atoms flowing per second and therefore the total mass flow rate can be determined from this expression. Current flow is expressed in coulombs of charge per second, so that the total number of particles is given by the coulombs of space charge flow divided by the value of charge on a single particle. The number of particles then can be multiplied by their mass to give the mass flow rate  $dm/dt$  from the ion thruster.

$$dm/dt = (J \times m_i) / e \quad (4.3)$$

$dm/dt$  = mass flow rate in kg/s  
 $J$  = current flow density in amperes/ $\text{m}^2$   
 $M_i$  = mass of ion = proton mass  $\times$  atomic weight  
 $= (1.672 \times 10^{-27}) \times$  atomic weight  
 $e$  = unit charge =  $1.602 \times 10^{-19}$  coulombs

The atomic weight of argon is 40 while for xenon it is 130. For these two gasses the flow rate as given by 4.3 is  $1.35 \times 10^{-6}$  kg/s for xenon and  $0.42 \times 10^{-6}$  kg/sec for argon, for each ampere of current.

Expression 4.3 gives the mass flow per unit area or one square meter. The current flow in the actual thruster will be proportional to the area of the grids of the thruster. Ion thrusters are usually referred to in terms of the diameter of their grid structure through which the positively charged ions flow. Thus the well developed 30 cm thruster has an aperture area of  $0.07 \text{ cm}^2$ . and the 50 cm. thruster now being developed has an aperture area of  $0.20 \text{ cm}^2$ . The projected current for the 50 cm. thruster then is  $(.2)(164)$  is 32.8 amperes, so that the anticipated propellant flow rate would be  $(32.8)(1.35 \times 10^{-6}) = 4.6 \times 10^{-5}$  kg/second.

It should be noted that the current flow actually experienced between the grids in the ion thruster, may not be as great as that theoretically predicted by equation 4.2, because the number of atoms of the gas being used may be limited by valves which control the flow of gas into the ionizing chamber.

The total thrust is given by:

$$N = v \frac{dm}{dt}, \quad (4.4)$$

where  $N$  = thrust in Newtons

$v$  = velocity of expelled ion, m/s

$\frac{dm}{dt}$  = mass flow rate in kg/s

Using the expected flow rate of  $4.6 \times 10^{-5}$  kg/second as derived from equation 4.2 and 4.3 and as applied to a projected 50 cm ion thruster, the projected thrust would be 1.93 Newtons.

The predicted performance of a 50 cm thruster as projected by D.L.Galecki and M.J.Patterson of NASA's Lewis Research Center is shown in Table 4.1 (31). The predicted current flow of 25.8 amperes for a specific impulse of 4138 (corresponding to a velocity of 40,500) and propellant flow rate of  $3.51 \times 10^{-5}$  kg/sec are both lower than the 1.93 Newtons and the  $4.6 \times 10^{-5}$  kg/sec computed by the procedure given above. Some difference would certainly be expected. The procedure given above, would certainly need some fine tuning to allow for secondary factors. One of these is that the ion thruster may not be operated at the space charge saturation limit because of the throttling possible in allowing gas into the chamber.

A listing of the sources from which three critical parameters were obtained for use in section 3.6 which evaluates the performance of the system as a whole is important. These parameters are the ratio of thrust to electric power, the ratio of the mass of the ion thruster to the power consumed, and the ratio of propellant consumed to the thrust. They are:

Ratio of thrust to electric power -----	0.035N/kw
Ratio of the ion thrust mass to power consumed -----	0.67kg/kw
Ratio of rate of propellant consumption to thrust -	$2.245 \times 10^{-5}$ kg/N

The ratio of thrust to electric power, 0.035 Newtons/kW was obtained from the following table 3.2 on ion thruster experimental data that was published in paper AIAA-85-1999, "NASA Electric Propulsion Technology" at Electric Propulsion Conference Sept. 3-Oct. 1, 1985, by authors F.D. Berkopac, J.R. Stone and G. Aston (29).

### 3.2 DEMONSTRATED 30 CM ION THRUSTER PERFORMANCE

Xenon propellant

Thrust	0.37	0.71
Specific Impulse, sec.	4240	4740
Power , kW	10.6	21.6
Thruster Efficiency	0.72	0.76

With 20,000 kilowatts of power, the resultant thrust is the 740 Newtons

TABLE 4.1  
PROJECTED 50-cm ION THRUSTER PERFORMANCE

Beam current, A	Thrust, N	Thruster input power, kW	Specific impulse, sec <sup>b</sup>	Thruster efficiency	Beam voltage, V <sup>a</sup>	Net-to-total voltage ratio	Propellant flowrate, kg/sec <sup>b</sup>
<b>Propellant = Xenon</b>							
25.8	1.50	39.39	4138	0.77	1375	0.55	3.51 E-5
24.2	1.59	46.02	4669	0.79	1750	0.70	3.29 E-5
25.6	1.79	55.08	4991	0.80	2000	0.80	3.48 E-5
23.0	1.71	55.24	5294	0.80	2250	0.90	3.13 E-5
<b>Propellant = Argon</b>							
45.2	1.45	68.97	7498	0.77	1375	0.55	1.86 E-5
48.4	1.75	92.00	8459	0.79	1750	0.70	2.00 E-5
42.7	1.65	91.85	9043	0.80	2000	0.80	1.76 E-5
38.3	1.57	91.96	9591	0.80	2250	0.90	1.58 E-5

<sup>a</sup>The screen grid voltage was used as an approximate value for the beam voltage.

<sup>b</sup>These were used in the trajectory analysis as the values of exhaust velocity and spacecraft mass loss rate which produced useful thrust; precise thruster Isp, and total flow rates used in the calculation of total propellant mass, vary by less than 5 percent.

**0.038 N/kW**

**0.64 KG/kW**

TABLE 4.2  
ION PROPULSION SYSTEM COMPONENT MASSES

(a) Nuclear start orbit spiral, Xenon, 300 kW

Mission scenario	NSO spiral	NSO spiral	NSO spiral	NSO spiral
Propellant Isp, sec	Xenon 4138	Xenon 4669	Xenon 4991	Xenon 5294
Total power, kW	300	300	300	300
Number of thrusters	7	6	5	5
Thruster/Gimbal, kg	191	164	137	137
Thermal control, kg	648	648	648	648
Power processor, kg	560	519	476	475
Thruster structure, kg	59	51	42	42
Total interface module (dry), kg	206	203	199	199
Total dry mass, kg	1664	1585	1502	1501
Propellant, kg	6685	5956	5569	5321
Tankage, kg	669	596	557	532
Tankage structure, kg	294	262	245	234
Total propulsion system mass, kg	9312	8399	7873	7588

that was listed in table 3.1.

The ratio of propellant consumption to thrust was derived from equation 3.4. At a propellant velocity of 41,600 (corresponding to the 4200 value of specific impulse) the propellant consumption is  $2.45 \times 10^{-5}$  kg/sec for each Newton of propulsive force. The results of this procedure for calculating propellant consumption may be checked against the projected consumption rate in Table 4.1 (obtained from reference 31) for the comparable specific impulse of 4138 in that table. The rate of consumption so obtained is  $2.34 \times 10^{-5}$  kg/sec. With 740 Newtons of thrust the propellant consumption will be 0.0179 kg/sec.

#### 4.3 Description of the Rectenna

The technology of the rectenna is key to the revolutionary performance of the proposed electrically propelled orbital transfer vehicle. It has many desirable characteristics, but it can be briefly described as a source of power that when illuminated by a microwave beam will produce 1 kilowatt of continuous power in space with a mass of from 0.7 to 2.0 kilograms. This mass to power ratio, frequently called specific mass, contrasts sharply to that of the 100 kw nuclear power source now under development which has a projected mass of 30 kilograms to produce 1 kilowatt of power. It also contrasts with the specific mass for solar photovoltaic arrays, which currently is very high, but which is projected to be as low as 10 kilograms for a kilowatt of power output. The low specific mass of the rectenna matches that of the ion thruster, so that with a similarly low specific mass of the orbital transfer vehicle structure, unprecedented accelerations are possible for an electrically propelled vehicle.

##### 4.3.1 Desirable characteristics of the thin-film rectenna format for space.

In addition to the low specific mass of the rectenna it has many other desirable characteristics. These and other identifying properties are:

- o Frequency- 2.45 GHz. Other frequencies are possible but the following set of characteristics are based upon performance at 2.45 GHz.
- o Frequency sensitivity - relatively insensitive because it is a non-resonant type of device. Therefore, it can be built without exacting tolerances.
- o Low specific mass - as low as 0.7 kg/Kw
- o High power density -  $400\text{w/m}^2$  in current system scenario as compared with  $200\text{w/m}^2$  for solar photovoltaic arrays. New designs can operate at levels of as high as  $5\text{ Kw/m}^2$ .
- o High efficiency - Space rectenna has operated at 85% efficiency. Has been measured as high as 90% in non-space application.
- o Disposal of waste heat- all space rectennas have been designed to be

self cooled, radiating directly into the vacuum of space.

- o Use of critical material GaAs - 1.0 gram per kilowatt of power output, or about 10 kilograms for a 10 megawatt array. This contrasts sharply with a GaAs solar photovoltaic array.
- o Life and reliability - Extensive Life tests of rectifying diode under sea level atmospheric conditions indicate life of tens of years. Tests in vacuum have been limited but indicate long life in space.
- o Protection from space radiation - The package for the GaAs diode represents considerable shielding from radiating from space. More shielding could be added with little penalty in the mass of the diode.
- o Output voltage - Output voltage of one rectenna element will be from 15 to 30 volts as contrasted to 0.6 volts for a solar photovoltaic cell. Like solar cells they may be connected in series and parallel to produce almost any desired voltage and almost any level of power.
- o Sensitivity to direction of incoming radiation- DC output of original rectenna with diode per rectenna element followed  $\cos^2$  law with respect to angle of incoming microwave radiation. Newer rectenna designs are equally insensitive about one axis but not the other.
- o Sensitivity to load- Highly insensitive to small variations in load. Efficiency losses follow relationship of  $(R-R_0)/R_0)^2$ . A 10% load variation thus leads to a 1% power and efficiency loss. A 2-to-1 load variation will lead to a 25% power loss.
- o Failure modes related to load- rectenna must be protected against an open load or one that appears transiently as an open load, such as a highly inductive load.
- o Ease of manufacture - The rectenna can be made in large quantities with existing equipment. .
- o Modular nature of rectenna- rectenna area can be easily increased by just adding new rectenna modules.

#### 4.3.2 Description and performance of the thin-film format of the rectenna .

The rectenna is a two plane device, in which the foreplane carries out the function of absorbing the microwave power, rectifying it, filtering it, and the bussing of the DC power. The back plane which can be a low- mass, plastic film with a metalized surface, positioned about one quarter wavelength from the foreplane , is necessary to capture 100% of the microwave beam that is incident upon the foreplane (6,7).

A schematic of the foreplane is shown in Figure 4.2. It may be seen from this schematic that a microwave transmission line serves not only as part of the

microwave circuitry but also as the DC power collecting bus. The general format is that a number of rectenna elements are paralleled across a DC bus line whose terminals may then be connected in series or parallel to other DC collecting busses. Thus any combination of total output voltage and current may be obtained. The typical voltage output of an individual rectenna element is 25 volts. To achieve the typical 1500 volts needed by an ion thruster 60 parallel banks of rectenna elements would be coupled in series. This compares with having to connect 2500 banks of solar photovoltaic cells together to provide 1500 volts.

The question may arise as to what happens when a diode develops an open circuit or a short. The open circuit is not a problem because it removes the diode from the line and the microwave power involved is either reflected from the dipole or is picked up by adjacent elements, or both. A hard short, however, would cause some problems. Fortunately, the diode package is designed so that a one mil wire couples the rectified power in the diode to the outside. If the diode shorts the other rectenna elements in parallel with it also see the short and the total rectified current from them flows through the one mil wire and burns it out.

Many of the principles of the series and parallel connecting of rectenna elements and the fuse principle was put into practice in the rectenna built for the Goldstone demonstration as seen in Figure 1.8. Here 6 banks of 50 parallel connected rectenna elements were connected in series to produce 200 volts of DC power output. At no time were there any failures caused by shorted elements (19,20).

It was necessary, however, to protect the output of the rectenna from an open circuit load or one that appeared to be an open circuit on a transient basis because the diodes can burn out very rapidly if the peak inverse voltage is exceeded. To protect the Goldstone array from the open circuit failure mode fast acting shorting bars were designed into the array to protect the array if its output voltage exceeded an agreed upon value.

One of the rectenna elements is shown in greater schematic detail in Figure 4.3. The incident microwave power is captured by the dipole. It then flows through the two section low pass filter which acts as both a harmonic filter and as an energy storage element, and then into a low-Q rectification circuit tuned to the incoming frequency. A 30 picofarad bypass capacitor on the output has a number of functions. It appears as a near microwave short across the two wire line and so its physical distance from the rectifying diode determines the value of inductance that resonates the rectification circuit. It also greatly reduces the harmonic power that would otherwise get into the DC output.

The electrical design of the low pass filters was originally made for individual bar-line, plug-in type rectenna elements. These elements were mechanically assembled from formed sidebars and disks of teflon acting as capacitors. This design was based upon theory and its performance as a harmonic filter follows the theoretically predicted results. Section 6.0 of this report covers that subject. This same electrical design was used in the thin-film format for the rectenna.

Some of the details of the construction of the rectenna are shown in Figure

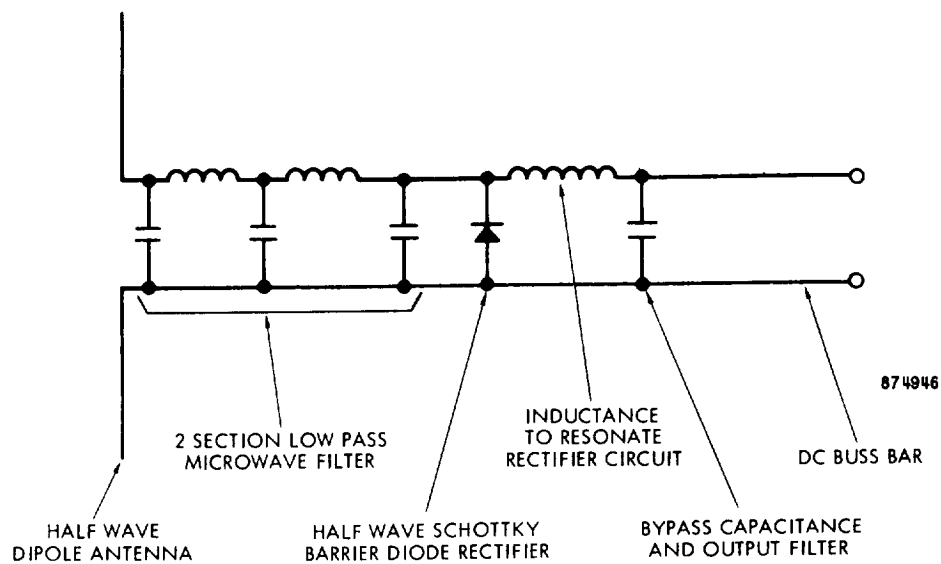


Figure 4-3. Simplified Electrical Schematic for the Rectenna Element.

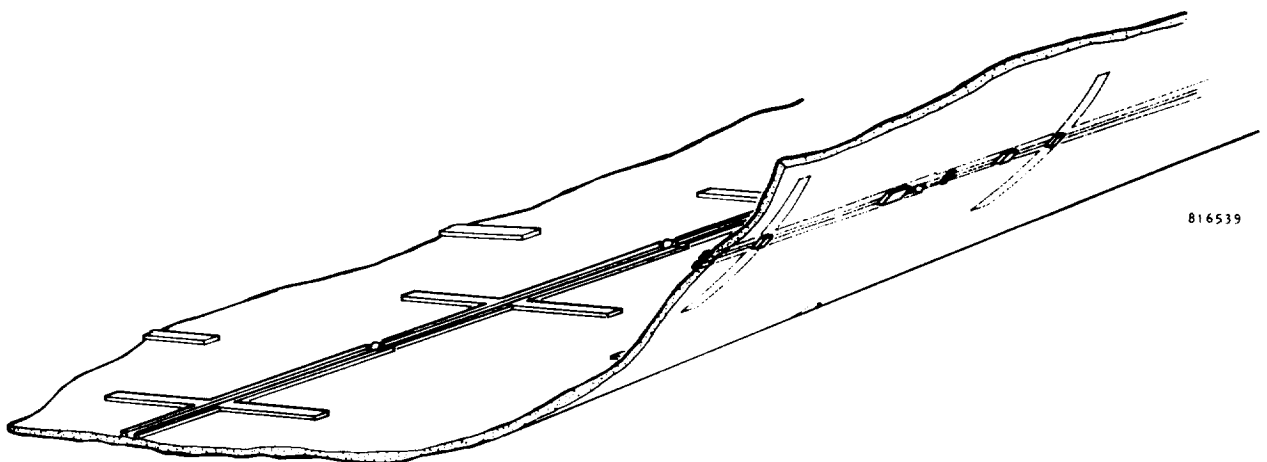


Figure 4-4. Principle of the Thin-Film, Etched-Circuit Rectenna. Circuit Elements are Etched on Both Sides of Dielectric Film. There are No Interconnects between Etched Elements. The Needed Capacitors Shown in Figure 4.3 are Formed with the Aid of a Metal Patch on the Back Side of the Dielectric Film.

4.4 (6). The rectenna is etched from a 5 layer sandwich of material consisting of one ounce copper (1.2 mil thick) on the two outer faces, a central core of one mil kapton with two 0.5 mil sheets of teflon between the copper and the Kapton which serve as a bonding agent between the copper and the Kapton. The bonding of the copper to the film is done under high pressure at an elevated temperature, considerably greater than that used for bonding copper directly to Kapton with an epoxy. It was found that the epoxies generally used are very lossy. The combined loss in the Kapton and teflon is quite low.

Etching is carried out on both faces. The shunt capacitance shown across the line in figure 4.4 is physically two capacitors in series.

Some of the properties of the thin film format for the rectenna foreplane are shown in Figure 4.5. The flexibility of the film is exhibited by rolling it up on a drum and then unwinding it. In figure 4.6 the film is shown applied to an airplane wing which was thoroughly checked out for its electrical properties. The output of the rectenna was connected directly without power conditioning to a DC motor that was driving a propellor.

#### 4.3.3 Experimentally measured performance.

Figure 4.7 shows the efficiency performance of the thin-film rectenna element as a function of DC load resistance and the DC power output of the element. The performance is limited by the reverse voltage break down of the diode.

The experimentally measured diode efficiency as a function of a variation in load is shown in Figure 4.8 (4). As previously indicated a 10% variation in load away from a matched load results in a 1% decrease in efficiency. A 2-to-1 variation results in a 25% decrease in efficiency.

Of paramount importance is the ability of the diode in the rectenna to operate without failure in the vacuum of space. A substantial amount of analysis was performed and reported upon in reference 33 in which a glass packaged diode was used. The finding was that there should be good confidence for long life if the diode were operated with a dc output of 1 watt per diode. Later, with the diode packaged in a ceramic package this projection was raised to 2 watts per diode or 400 watts of DC power for each square meter of rectenna area.

In more recent work as outlined in Section 6.0, the new rectenna format allows the diode to be mounted in a very low mass circular radiator as shown in figure 6.28. With this arrangement the diode was operated with three watts of dissipation in a vacuum for an extended period of time and with the diode package not exceeding 110 degrees Celsius. This temperature is considered to be low enough to give the diode long life. Because the diode itself will give an efficiency of 90%, the 3 watts of diode dissipation represents operation of the diode as a rectifier with 27 watts of DC power output. In the new rectenna format described in section 6.0 it is planned to operate the diode at 8 watts of power output. Figures 6.28 thru 6.31 provide additional information.

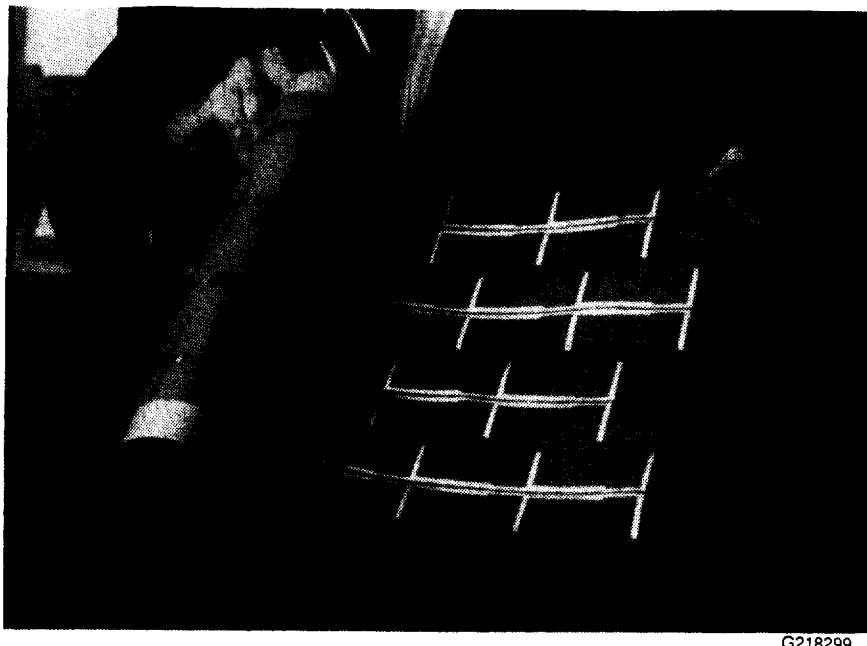


Figure 4-5. Photograph Showing the Flexibility of the Foreplane of the Thin-Film Etched-Circuit Rectenna.

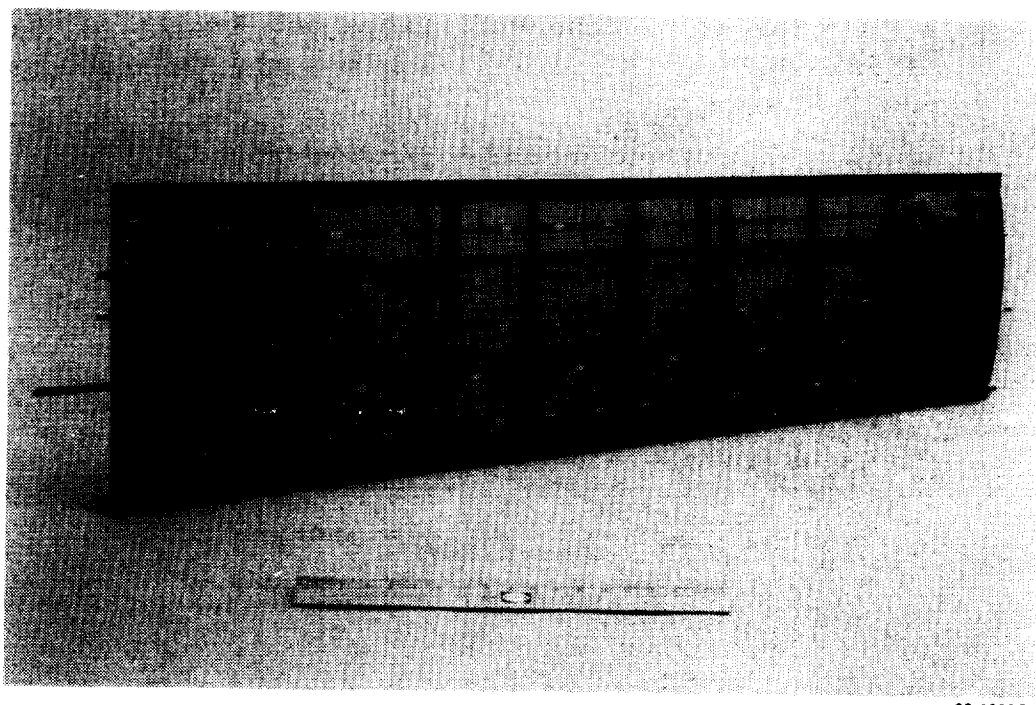


Figure 4-6. An Area of the Thin-Film Rectenna was Applied to an Airplane Wing and Tested. Output of the Rectenna was Fed Directly to an Electric Motor that was Driving a Propellor.

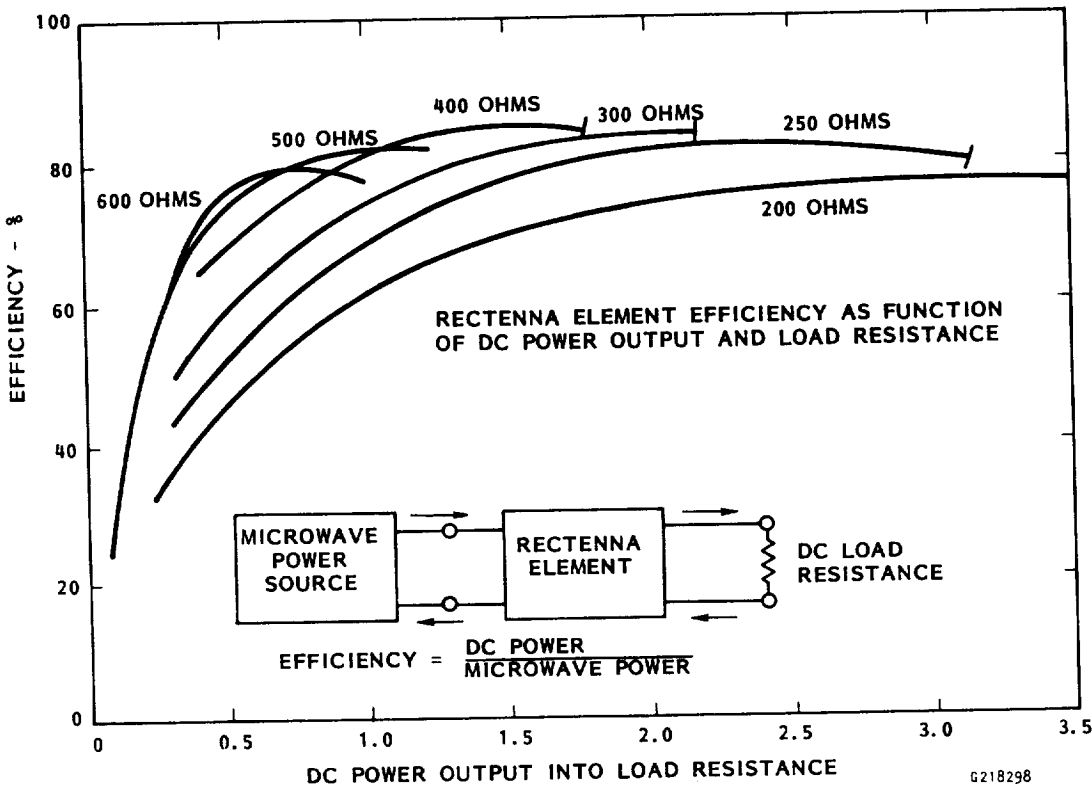


Figure 4-7. The Efficiency of a Single Thin-Film Rectenna Element as a Function of DC Load Resistance and Rectified DC Power Output Level.

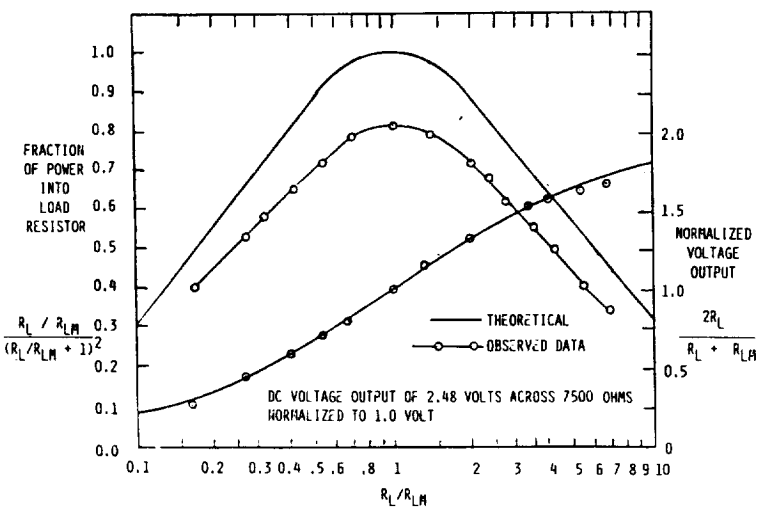


Figure 4-8. Theoretically Derived and Experimentally Observed Curves for Normalized DC Voltage Output  $V_L$  and Normalized DC Power Output (Denoted as "Fraction of Power into Load Resistor") as Functions of the Ratio  $R_L/R_{LM}$  Where  $R_L$  is the Value of the DC Load Resistance and  $R_{LM}$  is that Value that results in Zero Reflected Power.

#### 4.4 The Interface Between the Ion Thruster and the Rectenna; Minimization of Power Conditioning.

One of the problems with the acceptance of the ion thruster principle is that the power conditioning associated with it has been a major complication. The ion thruster requires a number of different power supplies. In addition to the large amounts of high voltage power needed for accelerating the ions, there is the power supply for the cathode, the power supply for the ionization chamber, and the power supply for the space charge neutralizing electrode. However, with a beamed power transmission system as a source of power, it appears that there is a major opportunity to minimize the amount of power conditioning necessary for the thrusters.

These different power requirements are marked by a wide variation in the level of power and voltage. As discussed in the previous section the rectenna modules can be connected in parallel or series to provide the desired voltage. Although the general need is to provide voltages higher than 30 volts, the nominal voltage output of the basic rectenna element, the rectenna elements themselves may be designed with microwave impedance transformers to produce voltages as low as 6 volts, for possible power sources for filamentary cathodes, etc. Thus we can dedicate portions of the rectenna to the various needs of the ion thrusters. Those requirements of the thruster that need high current but low voltage can be placed adjacent to the thrusters to minimize the mass of the bussing.

Of all the diverse power requirements for the ion thruster, that required to accelerate the ions between the grids of the thruster represents more than 80% of the total power requirements. Further it must be at high voltage, and to avoid complicated and massive power conditioning of the power the ion thrusters should be connected directly to the high voltage bus, with only a fuse to disconnect the thruster from the bus in case of a hard short between the grids of a thruster and an inductance of the proper impedance to momentarily reduce the voltage between the grids to clear a transient arc. The high voltage power supply and its connections to the ion thrusters is discussed in the next section, 4.4.1. This work is new work performed under this contract.

##### 4.4.1 The rectenna power source for the ion thruster accelerating grids and its interface with the ion thrusters.

As shown in Figure 4.9 a large number of rectenna modules are connected in series to provide a source of high voltage for the grids of the ion thruster. This principle was experimentally confirmed with the test of the 30 kilowatt rectenna at the Goldstone Facility of the Jet Propulsion Laboratory. Six rectenna modules, in which all internal elements were connected in parallel, were connected in series to produce 2 kilowatts of power at a potential of 200 volts (19,20).

As shown in Figure 4.9, there is a build up of voltage across the array to the side members which bus the power to the ion thrusters. The total voltage generated across the array and the voltage gradients between the side busses is probably of importance in minimizing leakage through any plasma that may exist. The existence of this plasma may result from operating the OTV in low-

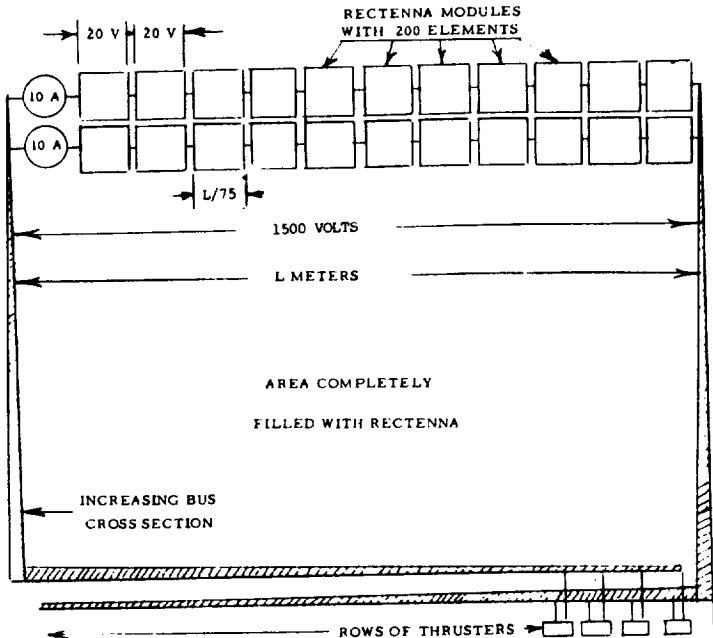


Figure 4-9. Composition of the Rectenna for the Orbital Transfer Vehicle. The Requirement of the Ion Thrusters for Potentials of the Order of 1500 Volts is Met by Placing 75 Small Rectenna Arrays in Series. Each Array Produces 20 Volts. The Power Collected Flows Laterally to Two Larger Tapered Busses that Carry power Directly to the Ion Thrusters.

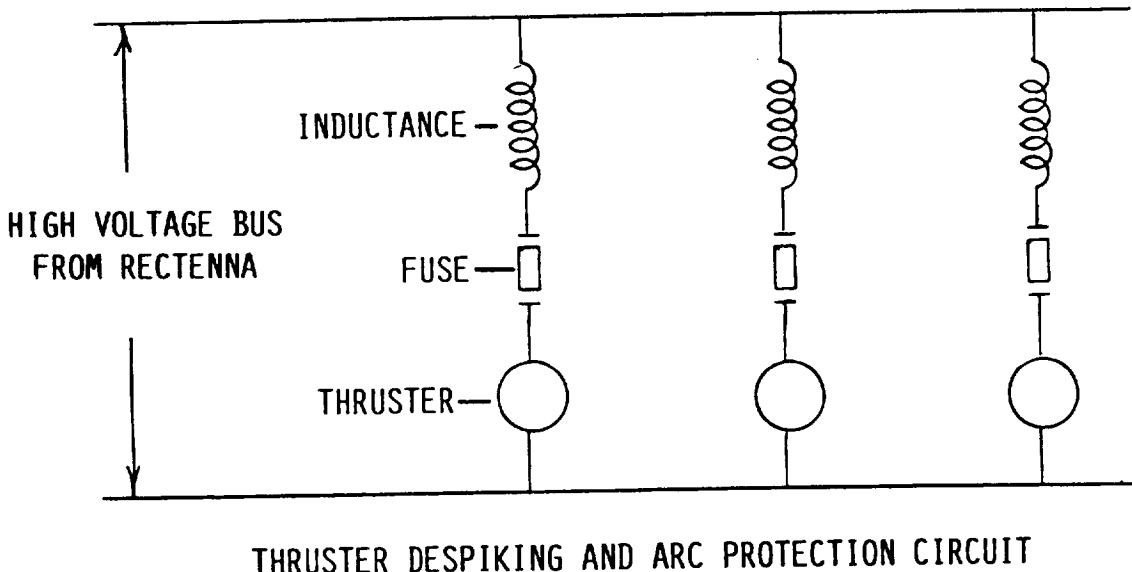


Figure 4-10. The Rectenna is Connected Directly to the Bank of Ion Thrusters without Power Conditioning Other than that Shown Above. Transient Arcing in the Thruster is Accommodated by a "Small Mass" Series Inductance which Lowers the Voltage Momentarily on the Ion Thruster and Clears the Arc. In the Event of Sustained Arcing a Fuse Blows and Removes the Thruster from the "Hard Bus".

Earth orbit where some natural plasma exists, or it may come from the plume of the exhaust of the ion thrusters where low velocity ionized gas may be generated.

In the scenario of the OTV that we have assumed, the rectenna is a square array of 50,000 square meters so that the side members of the array are 234 meters apart. The voltage gradient between these side members for a 1500 volts between the busses is then 6.4 volts per meter. Such a low voltage will minimize leakage through the plasma.

As shown in Figure 4.9 the high voltage appears at the terminals of a 234 meter long bus which extends the length of the ion thruster bay. If necessary the ion thruster bay could be either evacuated or pressurized to avoid leakage between the busses.

The proposed arrangement for connecting the grids of the ion thrusters directly across the hard bus from the rectenna is shown in Figure 4.10. If there is a hard short between the grids, the fuse in series with the thruster will blow. To handle a momentary arc that would clear itself if the voltage across the thruster grids were suddenly reduced, an inductance has been inserted in series with the thruster.

#### 4.4.2 The impedance match between the rectenna and the terminals of the ion accelerating grids of the ion thrusters.

The voltage current characteristics of the rectenna and of the ion thruster are such that a direct connection may be made between the two. The characteristic of the rectenna is that when exposed to a microwave beam of constant power level, the rectified DC power will be nearly constant, even though the load resistance may be varied over a substantial range. This leads to the voltage-current or V-I characteristic shown in Figure 4.11.

The V-I characteristic of the ion thruster depends upon whether it is always operating space charge limited between the grids, or whether the flow of gas into the thruster is choked down so that only a limited number of atoms can enter the ionization chamber. In the first case the current flow tends to be proportional to the  $3/2$  power of the applied potential as given by equation (4.2). Experimentally it has been found that the exponent is a little less than  $3/2$ . In any event there is a stable intersection between the respective V-I characteristics of the rectenna and the ion thrusters as shown in Figure 4.11.

The values of current at the operating points (where the lines intersect) may be found by equating the voltage characteristics of the microwave power system (as expressed in terms of the current and system constants) and the ion thrusters (likewise expressed). Similarly, the operating voltage can be found by equating the current characteristics for the microwave system and the ion thrusters.

Referring to figure 4.11, it is seen that in the case of space charge limited emission in the ion thrusters, the intersection of the V-I characteristics of the rectenna and ion thrusters is determined by the total power output of the rectenna,  $P_w$ , and the multiplying factor  $K_M$  in the expression for current into the ion thrusters.  $K_M$  may be interpreted as being proportional to the total

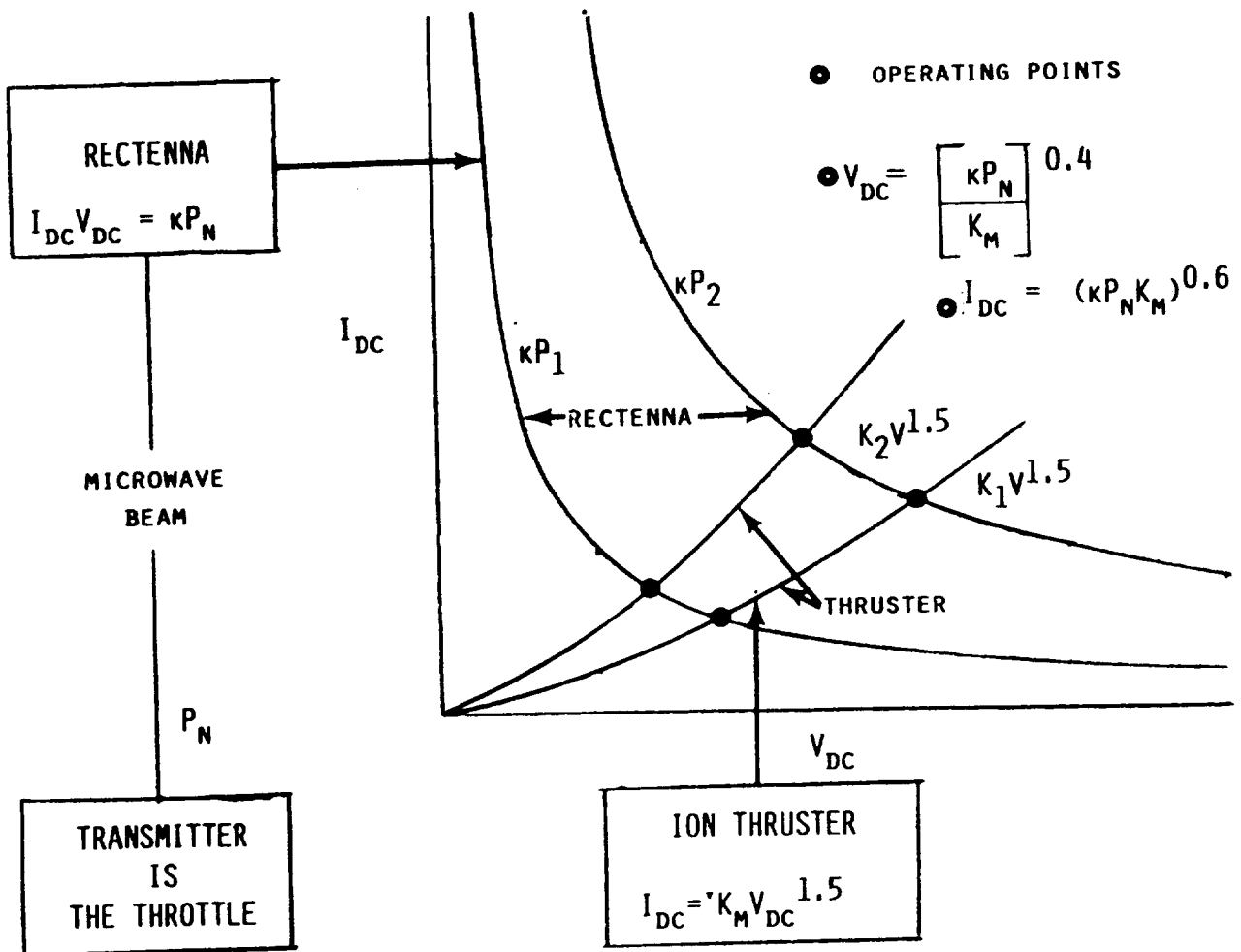


Figure 4-11. The Interaction of the Power Delivered by the Rectenna with the Power Consumed by the Ion Thrusters is Shown Above. With Constant Microwave Power Input to the Rectenna, the Output DC Power Tends to be Constant Over a Wide Variation in Load Resistance, Leading to a Voltage-Current Characteristic that Shows a Drop in Voltage with an Increase in Current. By Contrast the Voltage-Current Characteristic of the Ion thrusters Shows an Increase in Current with an Increase in Voltage. As a Result, the Overall System Automatically Adjusts Itself as Shown by the Intersections of the V-I Curves. The Throttle in the System is the Intensity of the Microwave Beam which can be Controlled in the Earth-based Transmitter.

ion thruster grid area, so that it reflects the number of ion thrusters connected to the high voltage bus. If some ion thrusters are taken off the line, and the microwave power input is not changed, the voltage applied to the thrusters will increase somewhat.

For the second distinct mode of operation, the mass flow of gas into the ionization chamber may be limited and in that case the V-I characteristic will be a horizontal line at a fixed value of current. However, the intersection of that line with the V-I characteristic of the rectenna will still represent a stable operating point.

It will be noted in figure 4.11 that the throttle controlling the thruster propulsive output can be traced to the amount of power radiated from the Earth-based rectenna. The throttle can be adjusted to most efficiently propel the vehicle. Thus at low altitudes, where there is efficient flow of power from the Earth to the rectenna, the power into the rectenna can be increased to operate the ion thrusters at their maximum power or maximum voltage rating, similar to the operation of aircraft engines on takeoff. Both the total thrust as well as the specific impulse can be increased. As the OTV ascends to higher orbits and the coupling efficiency decreases, ion thrusters may be taken off the line or operated with limited mass flow of propellant to preserve a high specific impulse. On the other hand, when the OTV approaches geostationary orbit and the flow of microwave power to the OTV is greatly reduced, it may be desirable to operate the thrusters at a relatively low specific impulse to increase the level of thrust. The control of the throttle will probably also be associated with the ratio of payload mass to the rest of the mass, etc.

The flexibility of controlling the specific impulse of the thrusters makes it possible through analysis and experience to optimize the performance of the LEO to GEO all-electronic transportation system for different payloads and missions, in much the same sense that it is possible to optimize airplane flights, say from the East coast to the West coast of the United States.

#### 4.4.3 Discussion of other dedicated power sources.

Only a limited amount of effort to address this subject has been expended. However it is possible to make some general remarks.

The present and probably the eventual source of electrons in the ion thruster that are used to ionize the gas is a low voltage filament requiring high current and low voltage. This can be provided by a dedicated section of the rectenna that is close to the ion thrusters to minimize the mass of the bussing to carry the high currents involved. However, as the microwave power reaching the rectennas of the OTV is substantially reduced, as is the case for the scenario discussed in section 3.6, there will not be enough power to keep the sources for ionizing the gas in all the ion thrusters active so that it will be necessary to remove ion thrusters from the line. However, such a tactic is consistent with also keeping the ion thruster bank as a whole operating at high efficiency and high specific impulse.

The same procedure can be followed with respect to the power supply for the ionization chamber, and for the electron emitter to neutralize the positive charge on the gas atoms as they leave the thruster.

#### 4.5 Interrelationship of Rectenna Size, Mass of Bus, Electrical Loss in Bus, and Structural Considerations

The portraits of the OTV in figures 1.9 and Fig. 1.10 show that the electrical conductors used to transfer the rectenna output power to the electric thrusters are the major structural members of the OTV as well. Figure 4.9 indicates how the power and current flow from the rectenna sections into the side conductors.

It is intuitively recognized that as the area of the rectenna increases the difficulty of conducting the power to the ion thrusters increases disproportionately. It is further evident that there will have to be some tradeoff between the mass of the conductors and the electrical or  $I^2R$  losses in the conductors. It is also recognized that operation of the conductors (and the ion thrusters) at a high voltage will reduce the value of current and therefore the  $I^2R$  losses in the conductors. Finally it is recognized that the electrical conductors must radiate any heat that is generated within them directly to space. This requirement suggests a high ratio of surface area to cross sectional area be pursued.

The object of this section of the report is to quantitatively study the interrelationships of the size of the rectenna area, the DC power output density of the rectenna, the mass of the conductors, and the electrical loss in the busses. The details of this analysis is given in Appendix B.

The conclusions of the analysis indicate that the electrical losses and mass of the busses is highly sensitive to the bus voltage and to the area of the array. The electrical loss is inversely proportional to the square of the bus voltage and proportional to the square of the power collected. Both depend upon a parameter "k" which defines the cross sectional area of the bus and therefore both the mass and electrical losses of the bus. There is therefore a tradeoff between bus mass and bus loss.

In general, it is found that the area of the rectenna and the power collected from it can be quite large before serious penalties in the form of bus mass and loss are encountered. For example with the system scenario of section 3.6, the bus loss is 5% of the rectenna power output if the bus mass is 5 % of the rectenna mass. A further insight into the relationship between size and losses and mass is given in Figure 12, where a higher bus voltage has been chosen and a rectenna mass 2.5 times that of the rectenna scenario in section 3.6.

For the analysis, the following assumptions and reasons for the assumptions are made:

- o The current flow into the side conductors per unit length of the conductor is uniform.
- o The side conductors have a cross section that is vanishingly small at the outer edge of the rectenna but becomes linearly greater as the terminals to the ion thrusters are approached.

Although it is not a priori evident that a linear increase

in cross sectional area is the most effective arrangement, it is evident that it is better than maintaining the same cross sectional area from both an electrical loss and structural point of view. It is simple to handle mathematically.

- o The rectenna area is square in shape.

It is assumed that the ground based transmitter will be square in shape and that the cross section of the beam at the OTV will therefore be similar, although this is true only in LEO. The analysis is greatly simplified by this assumption .

- o The microwave illumination of the rectenna is uniform.

This will be the approximate case only when the OTV is far removed from the Earth. Nevertheless, it is used because of the simplification of the analysis and also because it tends to be a "worst case" situation as far as the dissipation and sizing of the conductors are concerned.

- o Aluminum is used for the conductors.

Although the analysis will be general with regard to the material used for the side conductors it is assumed that aluminum represents the best choice because of its good electrical conductivity, low density, and good mechanical properties.

Figure 1 in Appendix B and the analysis there defines parameters that are listed below:

y = width of the rectenna, meters  
x = distance along the length of conductor  
L = total length of the conductor  
I = current flow in the bus  
 $I_L$  = current flow at end of the conductor  
 $P_d$  = DC power output density of the rectenna w/m<sup>2</sup>  
V = potential of the side conductors in volts.  
k = a parameter defining the conductor cross section  $kx$  at distance x  
 $\delta$  = density of the material of the side conductors.  
 $\epsilon$  = conductivity of the material of the side conductors.  
 $\beta$  = ratio of  $I^2R$  loss in both conductors to power output of rectenna  
 $m_d$  = mass of rectenna per unit area kg/m<sup>2</sup>  
 $r_m$  = ratio of mass of two conductors to rectenna mass  
 $P_b$  = Power dissipated in one side conductor  
 $M_c$  = mass of one conductor

The mathematical analysis has yielded several relationships.

$$P_b = \frac{P_d 2 y^2 L^2}{2 k \epsilon V^2}$$

in which k can be found in terms of  $\beta$

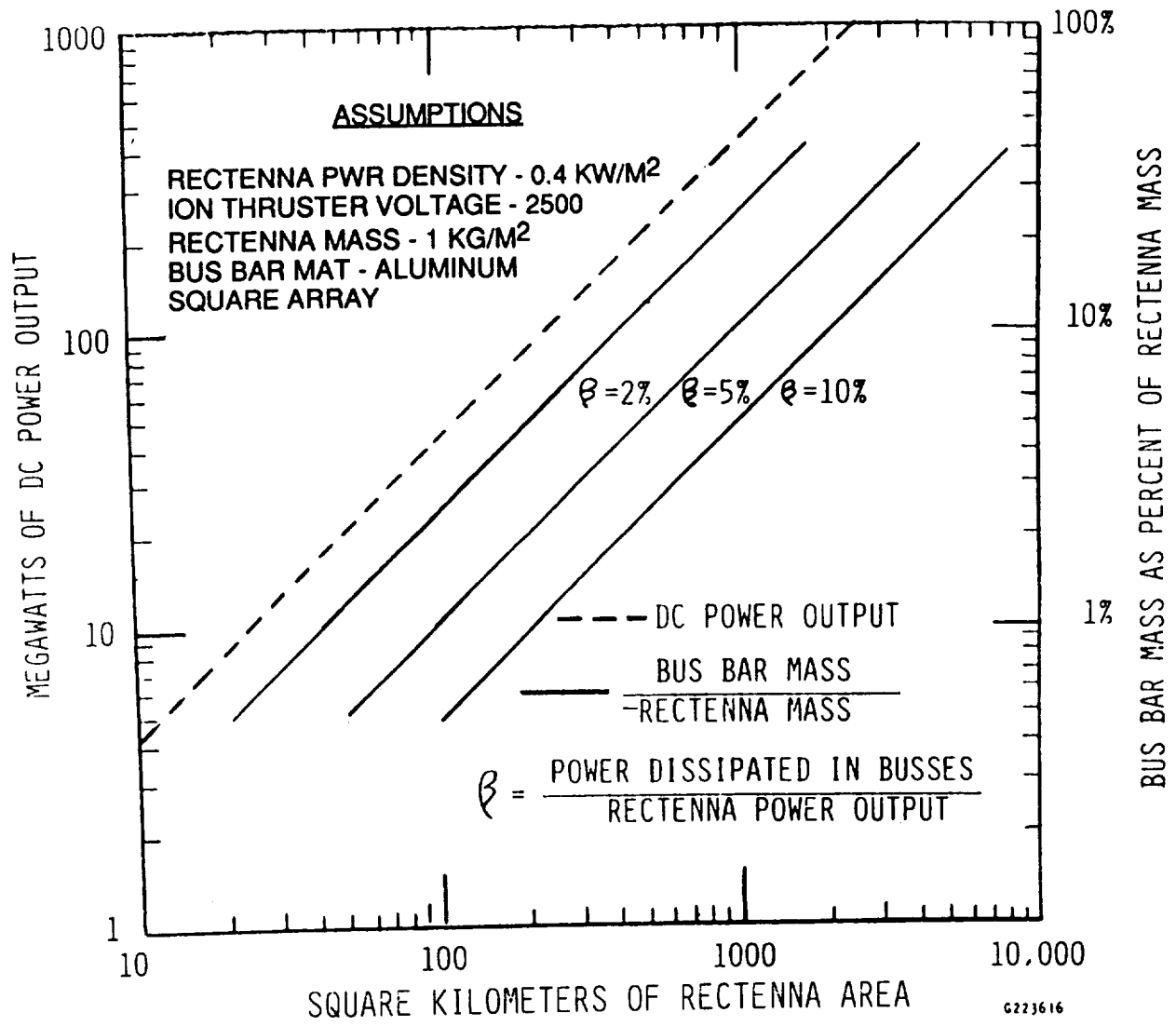


Figure 4-12. The Above Chart Provides Information with Respect to a Tradeoff between Bus Bar Electrical Loss and Bus Bar Mass, as a Function of Rectenna Area which is Proportional to Power Output. As an Example of Use of the Chart Assume a 50,000 Square Meter Rectenna. Project a Vertical Line from the Ordinate Value of 50,000 Square Meters. It Intersects the Power Output Line of 20 Megawatts. It also intersects the  $\beta$  Curves. If the Bus Bar Loss is Limited to a  $\beta$  of 2% then the Horizontal Projection of the Intersection Shows that the Bus Bar Mass is About 1.3% of the Rectenna Mass. For a 200,000 Square Meter Rectenna the Bus Bar Mass would Go Up to 6% of the Rectenna Mass, etc.

$$k = \frac{P_d \gamma L}{\epsilon \beta V^2}$$

$$M_c = \frac{k \delta L^2}{2}$$

$$r_m = \frac{P_d \delta L^2}{\epsilon \beta m_d V^2}$$

Figure 4.12 is a result of the analysis and indicates a tradeoff between the mass of the conductors and the power dissipated for the conditions of (1) the use of aluminum as the conductor material, (2) a DC power output density of 400 w/m<sup>2</sup>, (3) a rectenna specific mass of 2.5 kg/kW (a value 2.5 times that assumed in the analysis), (4) an operating voltage of 2500 volts (a value greater than the 1500 volts assumed for system analysis) on the ion thruster, and (5) a conductor cross section which varies linearly with distance from the outboard edge of the rectenna.

To use the figure to study tradeoffs between the mass of the conductors and the electrical losses in them, select a value of rectenna area on the abscissa and project this vertically to one of the lines denoted as  $\beta$ .  $\beta$  is the ratio of power dissipated in the busses to the DC power output from the rectenna. As an example let  $\beta = 2\%$ . Then project the intercept to the right hand scale of the graph and read off the ratio of bus bar mass to the mass of the rectenna, which is approximately 1.5%.

#### 4.6 Interaction of the Current in the Conductors With the Earth's Magnetic Field

In low-Earth orbit the Earth's magnetic field is of the order of 0.5 gauss or 0.0005 Tesla. If the current in the bus bars from the rectenna is large and flowing at right angles to the Earth's magnetic field and the conductor is of considerable length, a significant force can be generated. The force that is generated in Newtons is

$$N = BLI$$

N = Force in Newtons

B = Magnetic field in Tesla

L = Length of the conductor, meters

I = Average current flowing in the conductor, Amperes .

In the vehicle scenario that has been chosen the conductors that collect the current from the rectenna are at right angles to the magnetic field of the Earth and are 224 meters long. The average current flowing in them is 4000 Amperes. If the magnetic field is 0.5 gauss, the resultant force generated in each conductor is 44.8 Newtons. Because the current flow is reversed in the two conductors, the force will be away from the Earth for one conductor and will be toward the Earth for the other. Thus a strong mechanical couple

results which would rotate the vehicle around an axis whose direction coincides with that of the motion of the OTV.

This force is very strong relative to the 740 Newtons generated by the full component of ion thrusters operating at 20 megawatts of input power and a specific impulse of 4000 seconds. It is therefore not practical to counter this strong mechanical couple with ion thrusters.

Fortunately, it is possible to eliminate the rotation forces caused by the flow of current in the side conductors by breaking up the collecting area into two areas in which the mechanical couples that are generated are in opposite directions so they cancel out. This is illustrated in the design of the OTV shown in Figure 1.10. In this design the current flow in the two outer conductors is in the same direction while the current flow in the center conductor is in the opposite direction. Hence two mechanical couples are generated with rotational forces in the opposite directions so they cancel out.

However, to get complete cancellation it will be necessary to have the same current flowing in the two systems. Thus the microwave beam must be exactly centered on the vehicle in the North-South direction. In fact, the difference in the flow of current in the two conductors may be used to monitor the centering of the microwave beam.

It is of interest that as long as there is no rotation of the vehicle there is no back emf generated.

## 5.0 THE EARTH BASED TRANSMITTER

The Earth based transmitter is defined to include the radiating antenna, all phases of generating the microwave power with the exception of the DC power supplies for the microwave generator, and a guidance of the microwave beam to track the interorbital transfer vehicle. Any discussion of the guidance of the microwave beam will include sensors that are put aboard the OTV to be certain the beam is centered on the vehicle.

With this definition the following requirements are placed upon the transmitter:

1. It must emit a sufficiently narrow beam to transmit power with acceptable efficiency to the interorbital vehicle.
2. The beam must be electronically steerable in the West to East direction along the equator over an angle approximating 90°.
3. The beam must track the interorbital vehicle with high accuracy.
4. The transmitted beam should have relatively low side lobes.
5. The efficiency of the transmitter should be high.
6. The cost of the transmitter must be acceptable.
7. The random noise and harmonic content of the generated microwave power must be very low.

A transmitter has been designed to meet this set of requirements. Its design is discussed under the following sub topics.

- 5.1 The overall design of the transmitting antenna.
- 5.2 The design of the electronic steering and tracking system.
- 5.3 The design of the radiation module
- 5.4 Interaction of the transmitter with other uses of the electromagnetic spectrum.

There are a number of assumption that are made a priori to the design of the transmitter. These are:

1. The frequency used will be 2.45 GHz, free from any modulation.
2. The transmitter is placed on the equator.
3. A total of 90 degrees of electronic steering is required in the direction along the Equator, but only a small fraction of a degree is required in the North to South direction.
4. The maximum range required for the beam is to geostationary orbit.

5. The factor of cost is of major concern and this has been of central concern since the onset of the study. Approaches to minimize the cost will be discussed under each sub topic.

### 5.1 The Overall Design of the Antenna.

The striking feature about the transmitting antenna is its size. In the scenario that we have selected it is two million square kilometers. Although an optimization of the design of the overall system might indicate another value, it is believed that it will still be a large transmitter and that the same principles of design will apply.

This large size places great pressure upon arriving at a design that will hold costs to a minimum. Consequently, the design is based upon using a very large number- perhaps as many as two million- of identical sub arrays or radiation modules, each of which consists of a long section (approximately 5 meters) of slotted waveguide radiator (only one waveguide wide) and a phase locked source of microwave power for each module. Such repetitive manufacturing should reduce the cost of the subarrays to a very low figure, if the components of the module are also low in cost. This will be shown to be the case in section 5.3.

A layout of the transmitting antenna is shown in figure 5.1. The swept footprint of the beam formed by this antenna is shown in figure 5.2.

A feature of the construction of the antenna is the low cost method of constructing the slotted waveguide radiators. As suggested by the figure, the low cost approach features the use of relatively thin aluminum metal (0.08 cm) which is folded up to represent three sides of a waveguide with welded-on slotted plate to become the 4th side of the waveguide. This method has been well worked out and experimentally checked for use in a ground based array with steering capability over a limited angle of scan in all directions. Figure 5.3 illustrates the method of fabrication, Figure 5.4 shows a section that was fabricated, and Figure 5.5 shows its nearly theoretical antenna pattern (36).

The method of fabrication lends itself to making up several long sections of slotted waveguide array, each section representing the slotted array portion of a radiating module, as shown in Figure 5.1. One of the advantages of this method of fabrication is that the dimension of the waveguide can be held to high accuracy which is essential when constructing the proposed five meter length of the slotted wave guide module.

With the cost of the tooling, estimated to be no more than one million dollars, spread out over two million modules, and the labor cost largely eliminated by the automatic fabrication, it is evident that the major cost will be the material itself. The amount of aluminum for the two million square meter array has been estimated to be 9,000,000 kilograms or 4.5 kilograms for each of the 2,000,000 radiation modules. As of January 1992 this mass of aluminum represents an aluminum ingot cost of \$12,000,000, or \$6.0 for each of the radiation modules.

PHYSICAL FORMAT FOR ELECTRONICALLY STEERABLE PHASED ARRAY ANTENNA

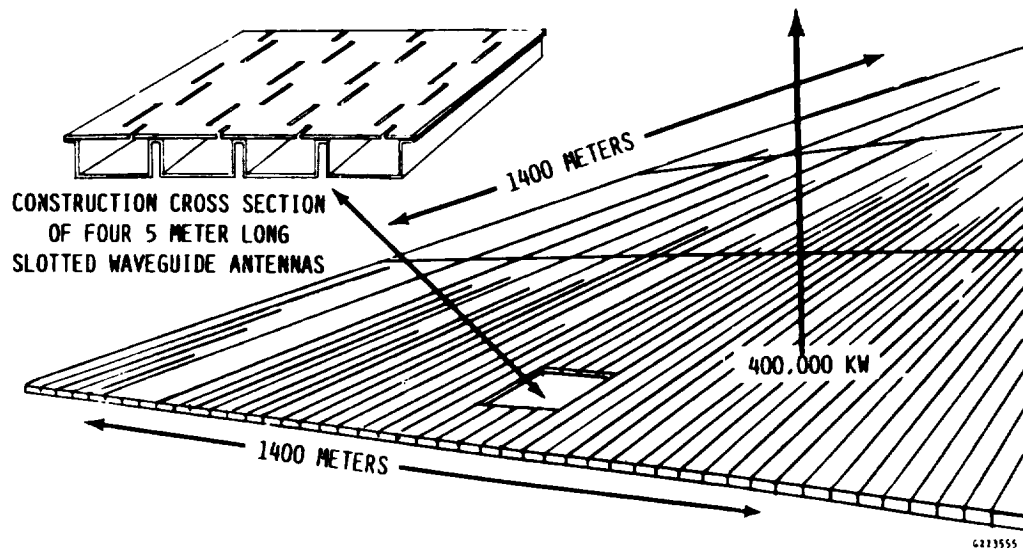


Figure 5-1. Layout of Earth-Based Transmitter Showing Folded Slotted Waveguide Formed from Thin Sheet Aluminum. Each Radiation Module is a Slotted Waveguide Several Meters Long.

ELECTRONICALLY SCANNED FOOTPRINT OF ACTIVE PHASED ARRAY  
CONSTRUCTED FROM LOW COST MICROWAVE TECHNOLOGY

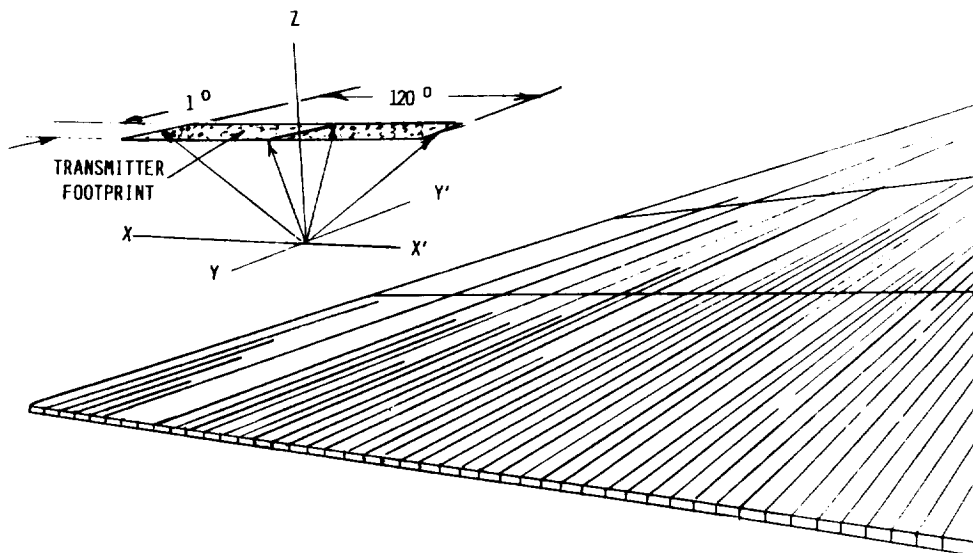
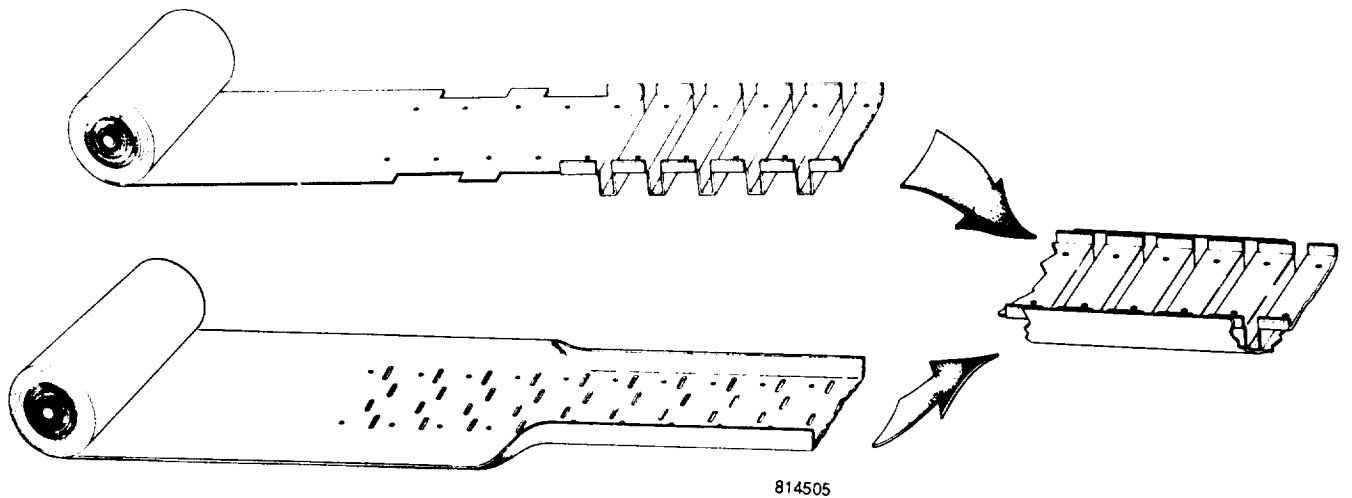
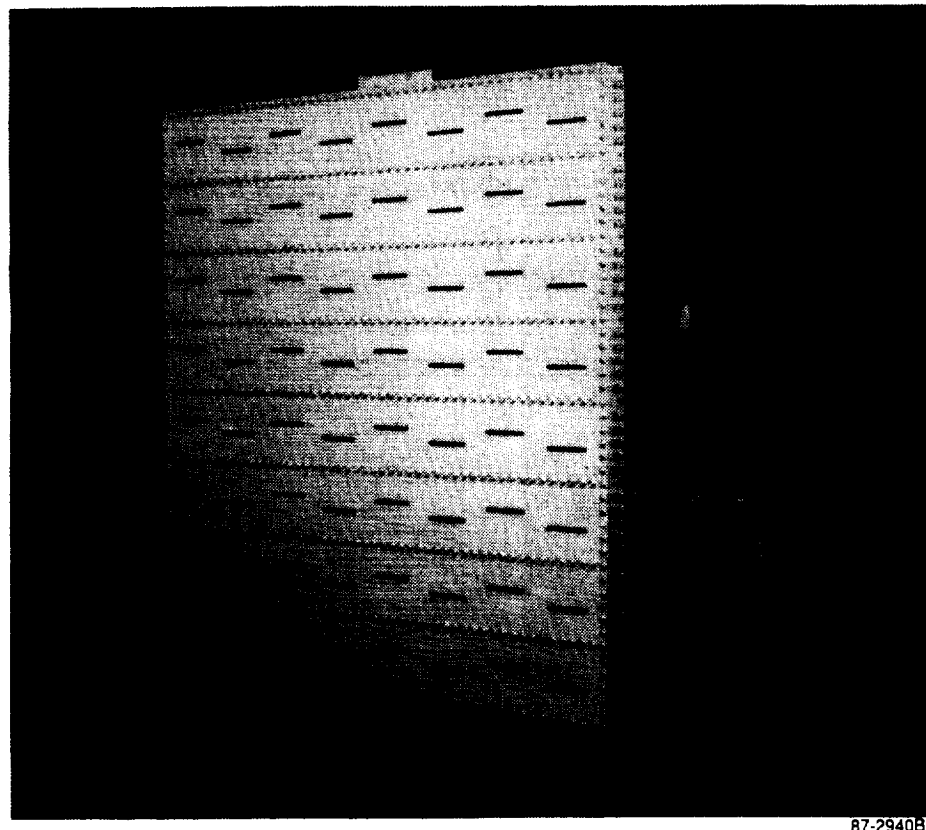


Figure 5-2. The Electronically Scanning Beam Generated by the Transmitter of Figure 5-2 can Sweep as Much as 120 Degrees in the West to East Direction. Scan is Severely Restricted in North-South Direction but the Application does not Require it.



814505

Figure 5-3. Proposed method for Precision Forming and Assembly of Low-Cost, Thin-Wall, Slotted Waveguide Arrays. Method, Modified to Use Temporary Forming Tools, was Used Successfully to Fabricate 64 Slot Arrays in Square Format that Performed Well on Test Range. Same Method Could be Used to Fabricate Long Slender Modules for LEO to GEO Transmitter as Shown in Figure 5-1.



87-29408

Figure 5-4. Radiation Module Composed of a Slotted Waveguide Antenna and a Phase-Locked, Magnetron Directional Amplifier. Radiated Power Output of About 600 Watts.

## 5.2 The design of the electronic steering and tracking system, including beam steering, beam focussing, bore sighting and use of the beam for controlling OTV attitude and positioning of the OTV in the equatorial plane.

There are several aspects of the system that is used to generate and steer the microwave beam. The same system can be used to refocus the microwave beam which may be desirable when there is a short distance between the Earth based transmitter and the OTV. The beam can also be used to supply attitude references ( roll, pitch, and yaw) and North-South positioning reference to the OTV. These will be discussed under separate headings.

### 5.2.1 Beam steering.

The microwave beam is steered to and kept focussed upon the rectenna on the LEO to GEO vehicle by means of two guidance principles as shown in Figure 5.6 and discussed in reference (36). First, in an open loop type of tracking, two microwave interferometers or monopulse receivers, revolving about an X and Y axis, respectively, keep themselves pointed as accurately as possible on the microwave beacon installed in the center of the rectenna. This is an open loop system and therefore incapable in itself to accurately center itself on the rectenna under all meteorological conditions.

The second guidance principle closes the guidance loop by putting sensors on the rectenna. There are two approaches. One approach is to put two pairs of amplitude sensors on the rectenna- one pair at the rectenna extremities in the West to East direction and one pair at the rectenna extremities in the North to South direction. If the individual sensors in each pair do not sense equal amplitudes, the difference is used as an error signal and relayed to the microprocessor in the transmitter on the ground where is used to repoint the beam.

The other method would be to divide the rectenna into quadrants and monitor the power in each quadrant. For monitoring the beam centering in the West-East direction the sum of the power from the West quadrants would be balanced against the sum of the power from the two East Quadrants, while for monitoring the beam in the North-South direction the sum of the power from the two North quadrants would be compared with the sum of the power from the two South quadrants. The latter arrangement would be the most sensitive.

At the ground station the information received from the tracking interferometers and the amplitude sensor on the rectenna are fed to a computer that generates two sets of digitized signals that are sent out along the X and Y axes and then distributed from there to each of the multitude of radiating modules as shown in Figure 5.7. It is known how far each module is physically and therefore number of wavelengths from the X and Y axes and therefore the digitized signal input can be multiplied appropriately to update the phase of the microwave power it is radiating. Almost all of this updating will involve steering in the West-East direction. It is planned to update the digitized signal for every 10 meters in the shift of the position of the satellite. Since the satellite will have an orbital velocity of as high as 7700 meters per second, the update would occur 770 times a

**BEAMED RF POWER TECHNOLOGY**  
**8-SLOT X 8-STICK SLOTTED WAVEGUIDE ANTENNA**

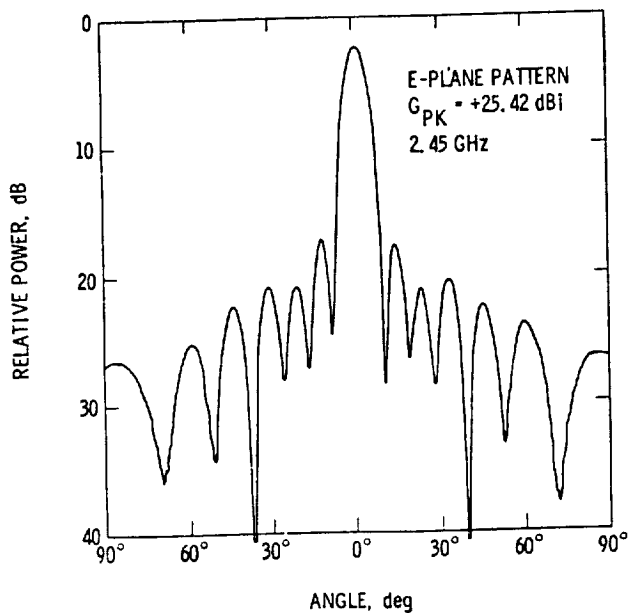


Figure 5-5. Radiation Module Shown in Figure 5-4 had Nearly the Theoretically Predicted Radiation Pattern.

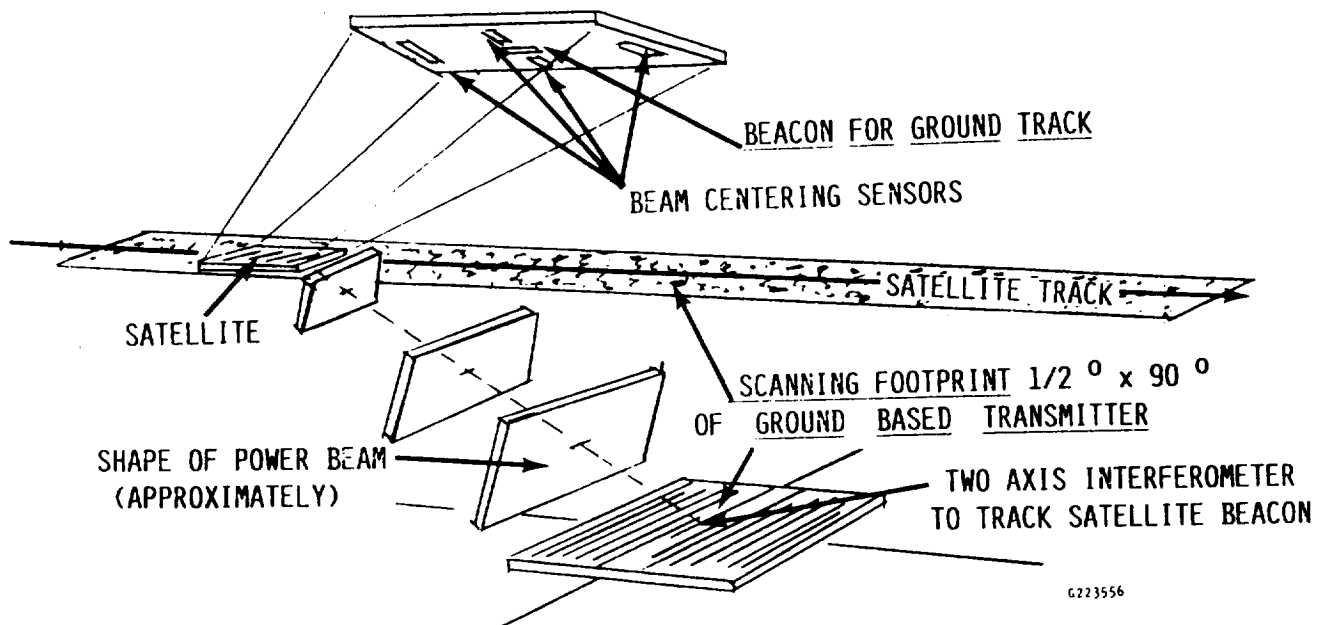


Figure 5-6. Beam Steering Technology that Keeps Beam Precisely on the Orbital Transfer Vehicle with Aid of (1) a Beacon in Space Vehicle which is Tracked by Interferometers on the Earth Coupled to the Beam Steering System, and (2) Sets of Amplitude Sensors which Send Error Signals to Earth if Beam is Not Precisely on Target.

#### HOW THE PHASED ARRAY IS STEERED

Inputs to the X and Y microprocessors from the ground-based interferometers and the air vehicle-based position sensors are used to generate incremental phase shifts which must occur between successive columns and rows of radiating elements to steer the beam. These incremental phase shifts in digital form are multiplied by an integral number corresponding to the position of the row or column of the processing elements located along the X and Y axes. The resulting phase shifts in digital form are sent along the respective rows and columns. Another processing element located in each radiating module adds the two incoming phase shifts. The resulting digital signal is converted to an analog phase by means of a low-power 4-bit phase shifter and added to the "clock" or "boresighted" reference phase to provide a new reference phase by which the phase of the power emitted from the radiating element is controlled.

Although the phase shift increment between centers of adjacent radiating modules is of prime concern, the physical symmetry of the antenna around X and Y axes requires that the phase shift signal of the first radiating module correspond to only half a radiating module width, so that the sequence of phase shifts is a, 3a, 5a, and b, 3b, 5b, etc.

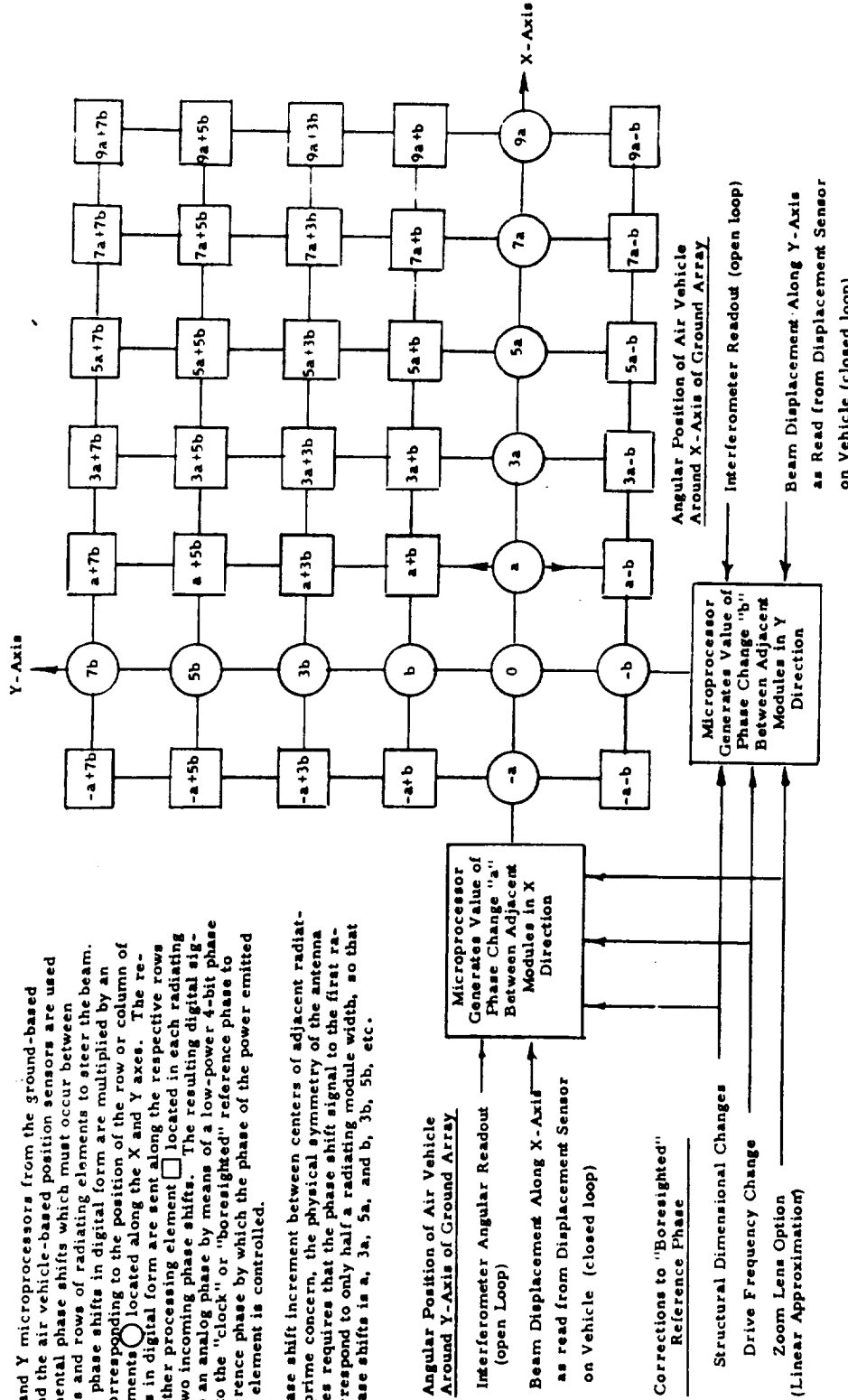


Figure 5-7. Row and Column Steering Matrix that is Activated with Input from Interferometers on Earth and Position Sensors in the Satellite.

second.

The digitized signal that is fed to the radiating modules will have to have a high resolution. The accumulated phase shift of the peripheral radiation modules as the beam is steered from zero to a 45 degree inclination is of the order of 2,000,000 electrical degrees and if the output phase is to be held within 20 electrical degrees from that value, the resolution of the signal fed to the peripheral modules must be one part in 100,000. This will require a 17 bit signal to be generated by the central processor.

### 5.2.2 The reference phase for each module, and the associated bore sighting of the array.

The digitized signal sent out to all of the radiation modules needs a reference phase at each radiation module to interact with. This reference phase is the same throughout all of the radiation modules, and is distributed to them through a waveguide or coaxial bus. The digitized signal sent out from the central processor through the row and column matrix interacts with this reference signal by means of a phase shifter which adds up to 180 degrees phase shift to the reference phase or, conversely, subtracts up to 180 degrees from the reference phase.

As indicated the phase reference is sent out through a waveguide or coaxial cable to each of the radiation modules. The reference signal is adjusted by a phase shifting device at each module to a multiple of 360 degrees by means of a laser beam that is sent out from a fixed location at the center of the array. The laser beam is modulated at the 2.45 GHz frequency (36). The laser beam is reflected from a mirror placed above the center of the radiation module and the returned phase compared with the outgoing phase. At the same time the phase of the reference signal is compared with the phase of the modulated laser beam at the radiation module. The phase shifter in cascade with the distributed reference signal is then adjusted for zero phase difference between it and the modulated laser beam, taking into consideration one half of the phase difference between the outgoing modulated laser beam and the returning one. The latter information is telemetered to the location of the radiation module from the center of the antenna array.

This procedure is equivalent to boresighting the array when it is pointed toward the zenith. It is also equivalent to radiating the beam with a flat phase front on it so that it is focussed at infinity. However, the boresighting procedure could proceed on a more sophisticated level and provide the reference for a slightly spherically shaped beam which is required for the maximum aperture to aperture beam efficiency. ,

A schematic for the use of the laser beam in the above context is shown in Figure 5.8.

It is obvious that some highly automated procedure must be used to bore sight the 2,000,000 radiation modules. It is premature to discuss this, but it would be possible to have a mirror permanently installed for each of the 2,000,000 modules. Each module would have a code number giving its row and column position, and the laser beam would be programmed to point to each of the module mirrors upon command of the software.

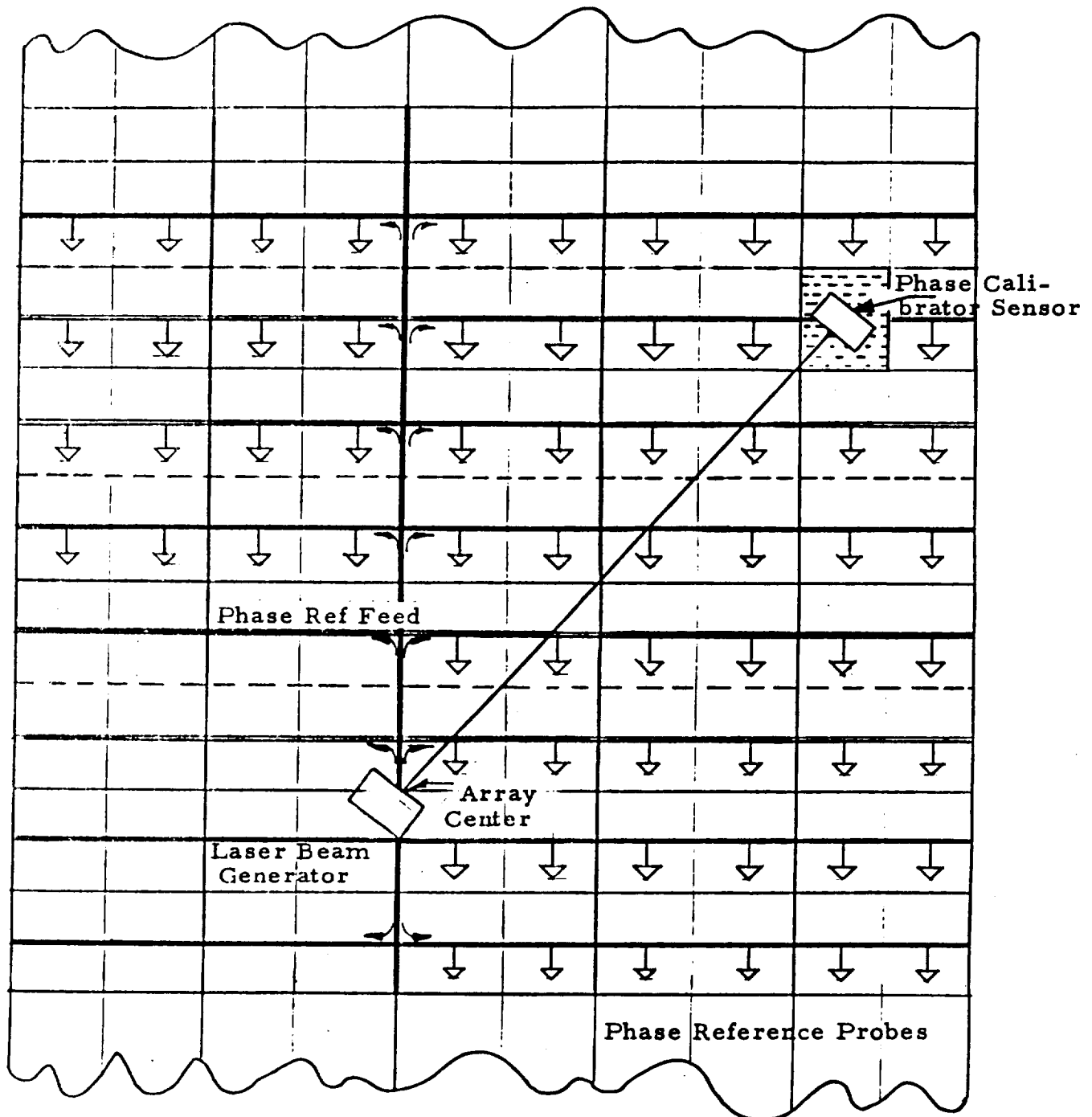


Figure 5-8. Arrangement for Boresighting the Transmitting Antenna to Zenith Position. Illustration Shows (1) Distribution of Microwave Frequency to Each Radiating Module, and (2) Arrangement for Use of Laser Beam, Modulated with Microwave Frequency, to be Used as a Reference Phase and to Set the Phase at Some Integral Multiple of  $2\pi$  at Each Radiating Module.

5.2.3 Control of the focussing of the beam and compensation for phase shift in the reference phase system caused by a change in the physical length of the system caused by temperature or other change.

As indicated in Figure 5.7, the digitized signal that is sent out to the radiation modules can also be used for a first order correction for expansion of the reference control system caused by a temperature change and to change the radius of the spherical phase front. The latter control could be adjusted in real time so that the total power reaching the OTV is maximized. The details of how this is done is given in reference 36.

5.2.4 Use of the microwave beam as an attitude (roll, pitch and yaw) control reference for the OTV and also to position the OTV in the equatorial plane.

A microwave beam can be used as a precise reference for five of the six degrees of freedom available to an object in space (37). This is shown in Figure 5.9. The phase front of the beam provides a reference for roll and pitch. The polarization of the beam provides a reference for yaw. And the change in the intensity of the beam with angle off boresight provides a reference for position in the plane.

The use of a microwave beam to provide these references was successfully demonstrated with the use of a helicopter that was kept over a microwave beam in precise position and whose attitude position was at right angles to the beam (37,17). The sensors on this helicopter are identified in Figure 5.10.

These same sensors could be applied directly to the OTV. The roll and pitch sensors could be activated only when the OTV is directly over the transmitting antenna. The yaw sensor could be used at any time. With respect to positioning the OTV, the microwave beam is slaved to the OTV in the West to East direction, but it would be logical to slave the OTV to the microwave beam in the North -South direction and thereby keep it precisely in the equatorial plane.

The forces necessary to change the attitude and position of the OTV can be obtained from electric thrusters. If there were no external forces at work to change position or attitude the work required from the thrusters would be minimal. However, the current collecting busses can react with the Earth's magnetic field to produce pitch or roll unless a design can be worked out to completely neutralize these forces. The possibility of doing this was discussed under section 4.6.

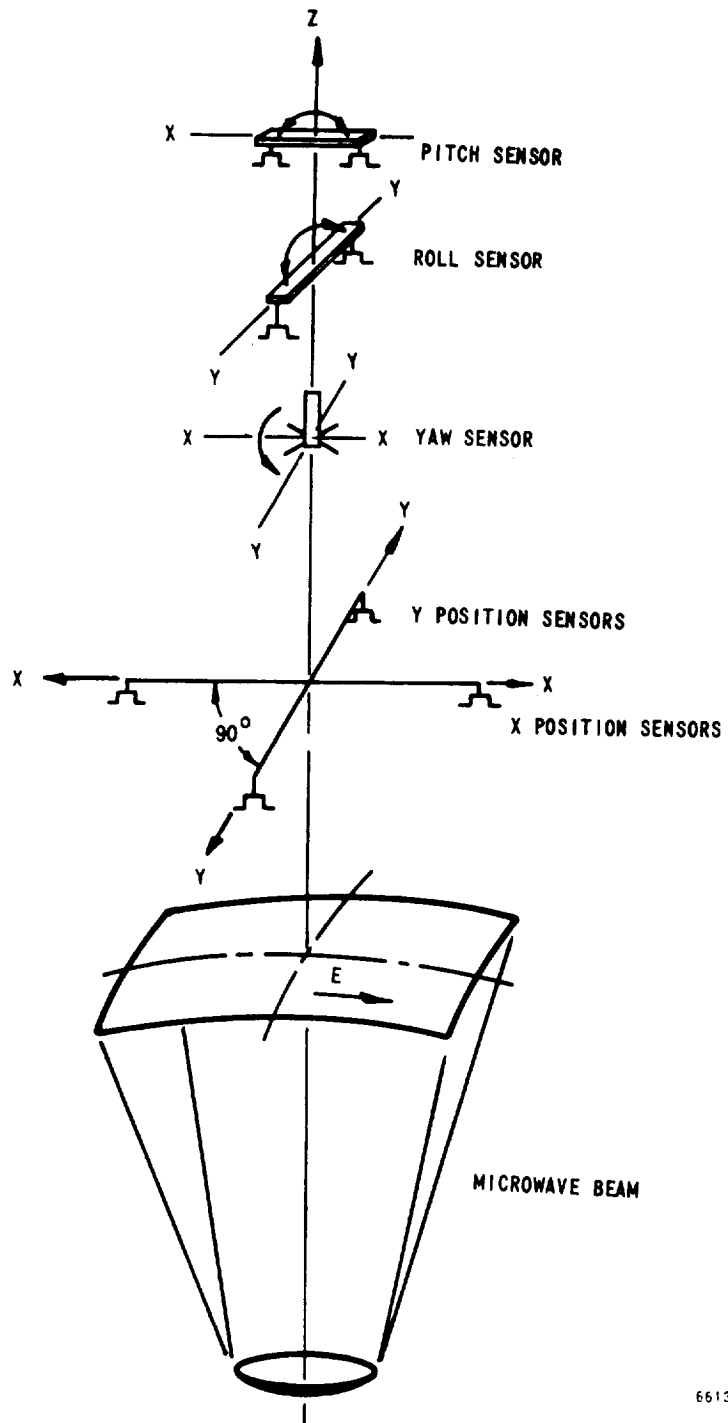


Figure 5-9. General Configuration of the Five Sensor Elements Used with a Microwave Beam as an Attitude and Position Reference for Roll, Pitch, yaw, and x and y translation.

### 5.3 The Design of the Radiation Module.

A schematic of the radiation module is shown in figure 5.11. It consists of three parts. One part is the antenna portion, or slotted waveguide array which has already been discussed. The second part is a proposed monolithic integrated circuit which contains (1) a phase shifter which responds to the digitized phase control signal from the central microprocessor, (2) a high gain low signal level amplifier to drive the power amplifier. This monolithic component is a straightforward application of the technology now being used and when made in the large quantities expected its cost should be very low. The third part is the phase locked high gain amplifier. This latter portion is the unique portion of the radiation module. It is not so well known or established but from the cost and performance point of view it is the critical element in the radiation module. It will therefore be discussed in considerable detail (35,38,39).

#### 5.3.1 The requirements placed on the power amplifier.

- o The output phase of the amplifier must be locked to the input phase obtained from the driver. By this is meant that if the input phase is say 10 degrees from the master phase reference, the output phase of the amplifier must be very close to 10 degrees from the master reference. In other words the output phase must be same integral multiple of 360 degrees from the input driver phase (39).
- o The power amplifier should have high power gain to couple to the necessarily low power output level of the monolith integrated circuit driver.
- o It should be possible to control the amplitude of the microwave output over a large range with a minimum of efficiency loss. . This is desirable for two reasons. First, the illumination intensity over the transmitter should be tapered from the middle to the edges to reduce the radiated side lobes. Second, the adjustment of the output power level should be independent of the status of the power bus which presumably would service many radiation modules.
- o The power amplifier should have very high efficiency.
- o The power amplifier should be very low in cost.
- o The radiated spurious noise and harmonics should be very low
- o The power amplifier should have a very long life.
- o The power amplifier must have a power level that matches the design power level to be radiated from the slotted waveguide section of the radiation module.

#### 5.3.2 The phase locked magnetron directional amplifier as a low cost approach to meeting the requirements of the power amplifier in the radiation module.

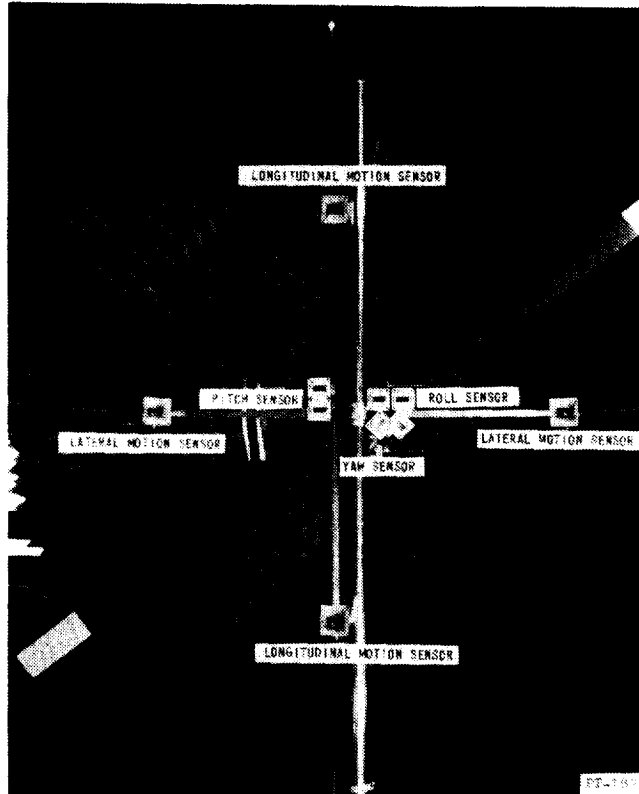


Figure 5-10. Array of Sensors Described in Figure 5-9 as Applied to the Attitude and Position Control of a Helicopter as Shown in Figure 1-7. Sensors are Arrayed on Bottom Side of Helicopter.

#### ANATOMY OF RADIATION MODULE WITH PHASE LOCKED LOOP

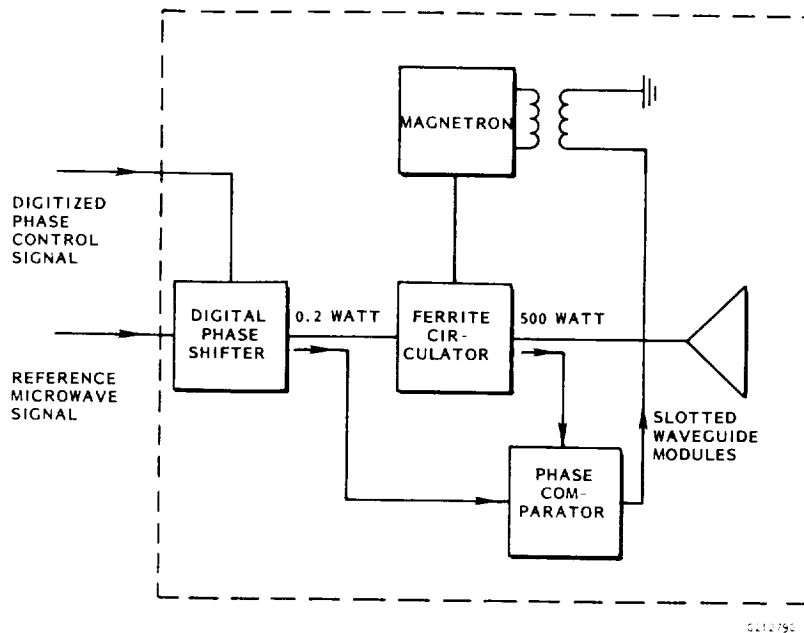


Figure 5-11. Schematic Circuit for a Radiation Module Consisting of the Slotted Waveguide Antenna and a Phase-Locked, High-Gain (30 dB) Magnetron Directional Amplifier.

It is a remarkable coincidence that the very low cost and highly available common microwave oven magnetron, when fitted with external circuitry, potentially meets all of these requirements. Following are the properties and characteristics of the microwave oven magnetron:

#### Electrical characteristics without external circuitry

Frequency	2.45 GHz centered in 2.4-2.5 ISM band
CW power output	100 to 1000 watts
Efficiency	65% to 70%
Operating voltage	3.5 kilovolts
Operating current	50 to 400 milliamperes
Filament power, start	30 to 40 watts
Filament power, run	0 (at 200 to 1000 watts output)
Random noise outside 2.4 to 2.5 GHz band	spectral noise (in 1 HZ bandwidth) 170 db below the carrier.
Harmonic level unfiltered	70 db. below carrier
Life	10 years projected at 300 watts output

#### Additional electrical characteristics with added external circuitry

Gain	30 db
Amplifier bandwidth with full efficiency	15 MHz
Phase locking between input and output	Within 10 degrees
Output Amplitude range with elec. control	200 to 1000 watts

#### Mechanical characteristics

Form factor	See figure 5.12
Mass	Less than 1 kilogram
Cooling	Air
Packaging	Fully packaged with integral magnets
Output connection	Antenna probe for waveguide

The magnetron with external circuitry is known to meet all of the requirements for the Earth based transmitter simultaneously with the exception of simultaneously meeting the three requirements of high gain, amplitude control of the output, and phase locking of the output to the input. The key phrase here is "simultaneously meeting three requirements" because simultaneous phase locking and amplitude control has been demonstrated (25), as has simultaneous operation at high gain with phase locking (39,40). However, it appears that all three of the requirements can be achieved simultaneously if phase locking is achieved by varying the reactive load on the output of the magnetron rather than by changing the input current to the magnetron as was the procedure to achieve high gain with phase locking. The latter procedure, of course, changes the power output of the magnetron, and is inconsistent with the need for independent amplitude control.

To properly understand the issues involved it is desirable to review just how

the magnetron is used as an amplifier and how high gain is related to the phase shift between the input and output of the amplifier.

In the first place the magnetron, which is a single port device and normally runs as an oscillator with the frequency being determined by its internal characteristics and the reactance of the load into which it operates, can be converted into an amplifier with the use of an external passive directional device. The simplest such external device is the ferrite circulator. The circuit relationship between the magnetron and the circulator is shown in figure 5.11. In various papers and references this arrangement is referred to as a magnetron directional amplifier and this phrase will be used throughout the subsequent discussion.

The phase shift between the input and the output of the magnetron directional amplifier is given by the following expression .

$$\phi = \sin^{-1} \frac{(f-f_0)Q_0}{f \sqrt{P_i/P_o}} \quad (1)$$

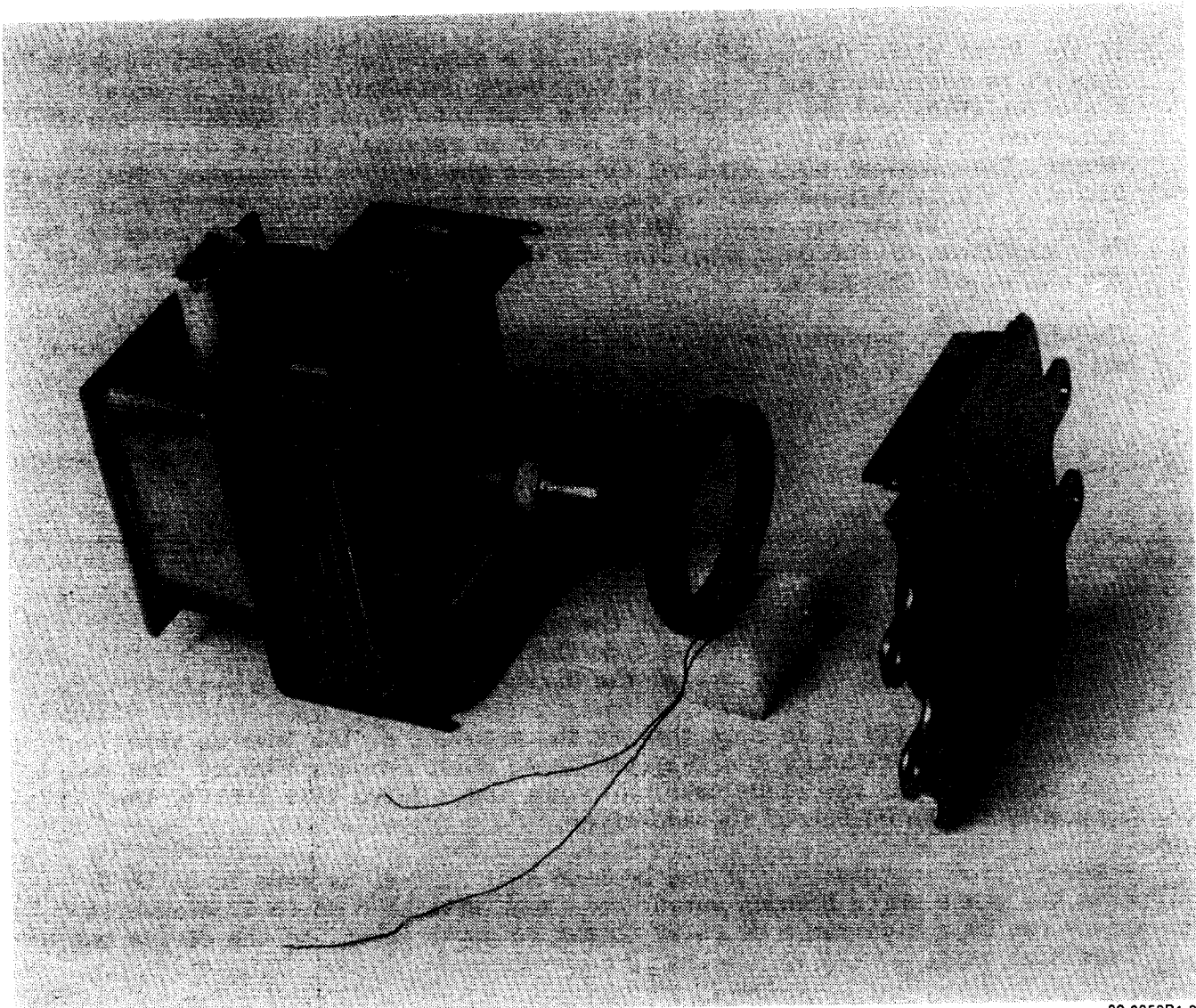
where  $\phi$  = phase shift between input and output of amplifier  
 $f$  = free running frequency of the magnetron  
 $f_0$  = frequency of the driver  
 $Q_0$  = external Q of the magnetron  
 $P_i$  = power input from the driver  
 $P_o$  = power out of the directional amplifier.

From expression (1) it is seen that if the argument of the inverse sine reaches either a ratio of 1 or -1, the phase shift reaches  $+90^\circ$  or  $-90^\circ$  and that is the end of the range over which the input drive will control the frequency of the output of the amplifier.

However, from expression 1 it can be seen that if  $f-f_0$  is made to go to 0 , then the phase shift between output and input will also go to 0. Meanwhile there can be a high ratio of power output to power input, so the device can have high gain.

To make  $f$  equal to  $f_0$  it will be necessary to change the free running frequency of the magnetron in some way. This can be done in two ways. One of these ways is to change the reactance of the external load. The other is to use the frequency change caused by changing the current into the tube. In either case the error signal that is used to produce the frequency change is obtained from a phase comparator that compares the phase of the output of the magnetron directional amplifier with the phase of the input drive. In one case, as shown in Figure\_5.11, this error signal is used to change the current in a buck boost coil that in turn changes the current that flows into the tube that in turn changes the free running frequency of the magnetron to match that of the driver. The installation of such a small buck boost coil on the tube is shown in Figure 5.12. This approach has been used experimentally and much pertinent data has been obtained.

In the other case, that of changing the reactance of the external load, it appears that there is no completely electrical way to do this ( such as the use of an electron tube or solid state device ) that is satisfactory and that



82-0959B1-3

Figure 5-12. Conventional Microwave Oven Magnetron Fitted with a Small Buck-Boost Magnetic Coil to Increase or Decrease the Value of the Magnetic Field. This Coil Addition can be Used Either to Precisely Control the Power Output of the Magnetron, Even if it is Connected to a Common Power Supply with Many Other Magnetrons, or in Combination with a Ferrite Circulator to Convert the Magnetron into a Phase-Locked, High-Gain Amplifier.

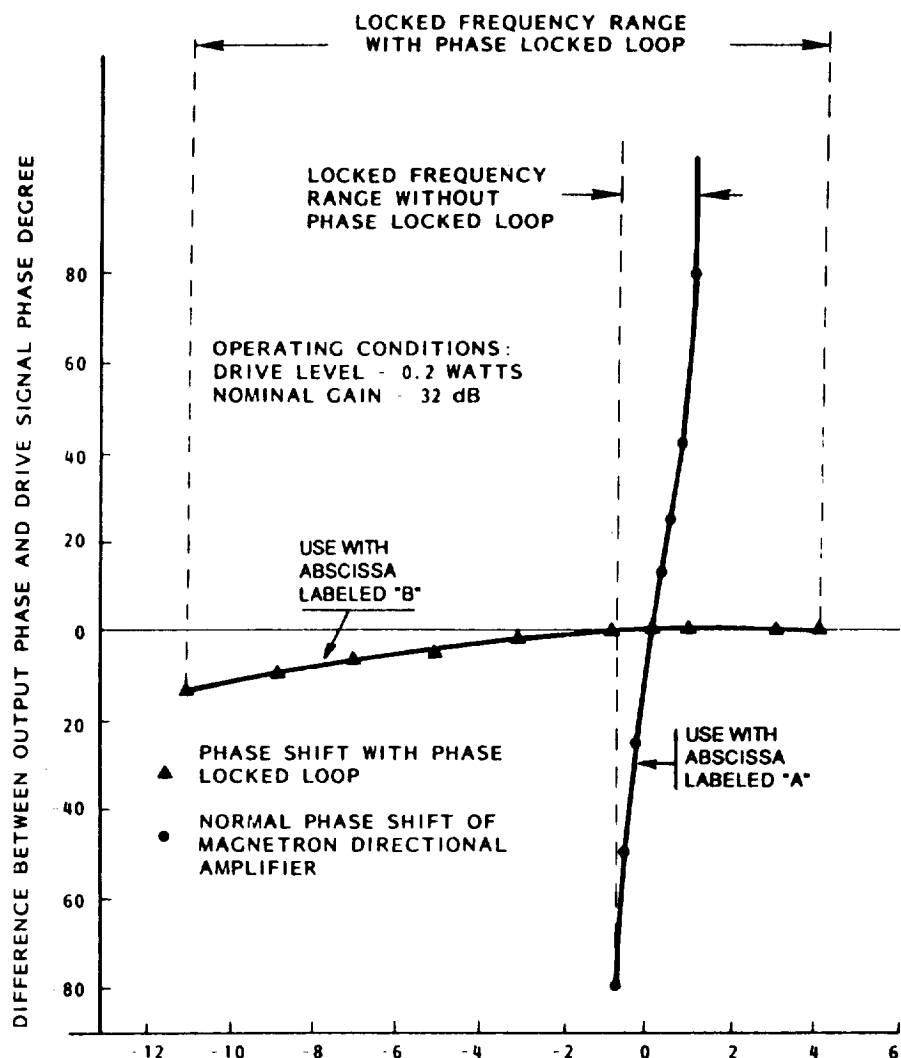


Fig. 8 A. DIFFERENCE BETWEEN FREQUENCY OF DRIVE A AND FREE RUNNING FREQUENCY OF MAGNETRON FOR THE CONVENTIONAL FREQUENCY LOCKED MAGNETRON DIRECTIONAL AMPLIFIER  
 B. CHANGE IN DRIVE FREQUENCY FOR PHASE LOCKED MAGNETRON DIRECTIONAL AMPLIFIER IN WHICH MAGNETRON FREE RUNNING FREQUENCY IS TUNED TO THE FREQUENCY OF THE DRIVER

Figure 5-13. A Comparison, or Contrast, of the Phase Versus Drive Frequency Behavior of a Magnetron Directional Amplifier in (1) the Conventional Locked Mode which is Characterized with Much Phase Shift Over a Small Change in Drive Frequency, and (2) the Much Preferred Phase-Locked, High-Gain Mode in which the Input Phase is Compared with the Output Phase and the Error Signal Used to Tune the Free-Running Frequency of the Magnetron to the Drive Frequency.

the use of some mechanical motion such as a screw tuner will be necessary. However, because movement of the tuner would be required only infrequently in most application, this would probably be a very satisfactory approach to reactance tuning.

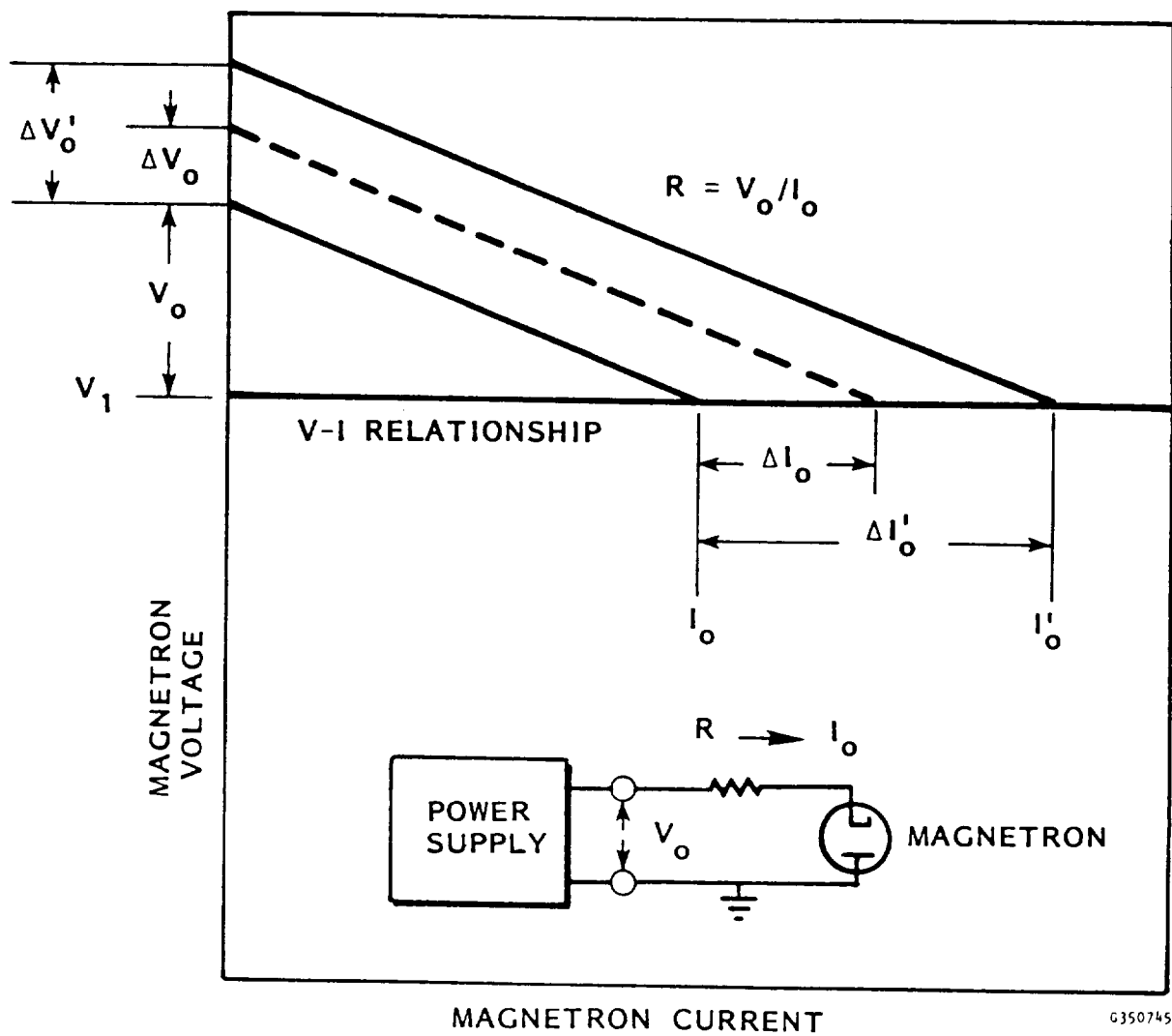
Although the electrical energy consumption for either of the approaches to change the free running frequency of the magnetron will be low, it is noted that the flow of energy is continuous in the case of the use of the buck-boost coil, while the reactance change in the external circuit would require electric motor drive and therefore power consumption only infrequently.

Either of these two approaches will give the same degree of control of matching the output phase to the input phase. Experimentally, however, only the buck boost coil approach has been used to obtain data. The preliminary data as shown in Figure 5.13 indicates that a high degree of phase control can be obtained over a relatively wide range of driving frequency. In the real application being considered, the drive frequency would remain fixed while other parameters changing the free running frequency of the tube would be the variable. Some of these changing parameters would be a change in the dimensions of the tube because of a change in operating temperature, changes occurring with life, a change in the impedance of the rf load, and changes occurring in the magnetic field produced by the permanent magnets. Relatively small changes in the current flow in the buckboost coil and in the flow of current into the magnetron would compensate for all of these changes except for a large change in the reactance loading on the tube. Once the relationship between the magnetron directional amplifier and the antenna has been established, however, there should be no change in the reactive load but if there were a 4 port circulator can be used to eliminate these variations in reactive loading to the magnetron.

### 5.3.3 The use of the buckboost coil for controlling the amplitude of the power output.

For a number of reasons it would be desirable to control the amplitude of the power output of each radiation module. This could be done by having a current regulated power supply for each radiation module, or it could be done with the use of a buck-boost coil, operating in conjunction with a stiff power bus. The assumption is made, a priori, that the use of the buck boost coil is a more efficient and more cost effective way to achieve a variation in power output.

The relationship between the stiff power buss (negligible voltage shift with a change of current into an isolated radiation module), the magnetic field across the magnetron, and the current drawn through the magnetron from the power supply is shown in Figure 5.14. For all practical purposes the current voltage relationship in the microwave oven magnetron for any value of magnetic field is a horizontal line. If the magnetic field is changed then the position of the horizontal line is shifted up or down, giving control of the anode current in the presence of a fixed applied voltage to the magnetron. Therefore the current drawn through the magnetron is highly sensitive to both the applied bus voltage and the magnetic field. Because of the flatness of the current voltage characteristic, it became necessary to introduce a small dropping resistance between the stiff power bus and the magnetron. Typically this is 200 ohms so that with 0.2 amps of current into the magnetron, a total



G350745

Figure 5-14. The Interaction of a Change in the Power Supply Voltage with the Flat Voltage Current Characteristic of the Magnetron is Shown. A Change in Magnetic Field Occasioned by the Buck Boost Coil will Shift the Flat Voltage Current Characteristic of the Magnetron Up and Down, and thus will Compensate for Changes in the Power Supply Voltage to Keep the Power Output Constant. The Buck Boost Coil can be Part of a Feedback Loop in which the Power Output of the Magnetron is Compared to the Desired Value and the Error Signal Used to Change the Current through the Buck Boost Coil to Provide the Type of Data Given in Figure 5-15.

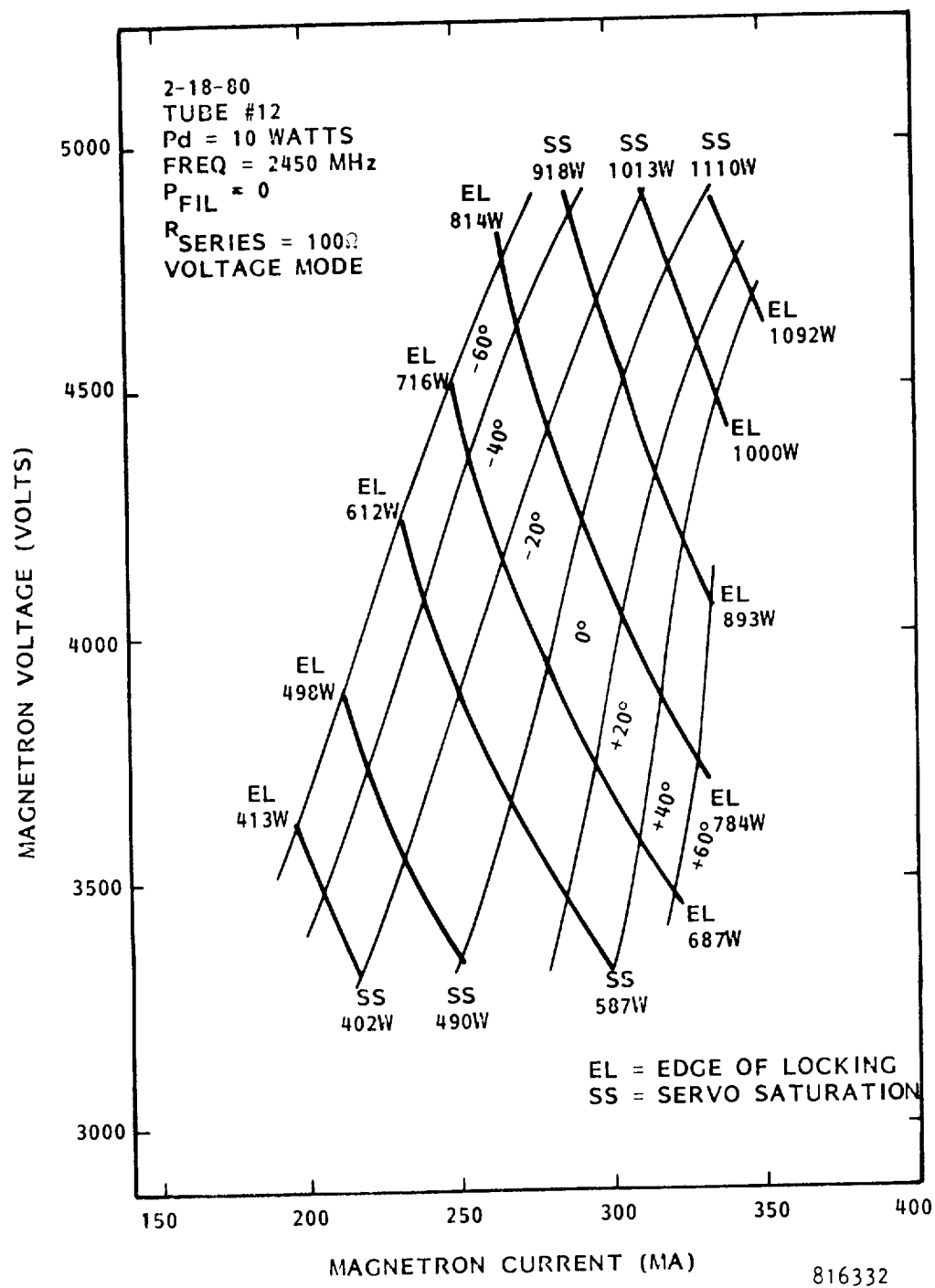


Figure 5-15. The Results of Applying an Error Signal to the Buck Boost Coil to Keep the Power Output Constant Over a Wide Range of Voltage Applied to the Magnetron is Shown. For Example, if the Reference Power Output is Set at 700 Watts then the Experimental Data Obtained from the Control Circuit Indicates that the Power is Maintained between 687 and 716 Watts While the Power Supply Voltage is Varied Between 3400 and 4500 Volts.

of 8 watts would be dissipated. In addition, on the average, about 5 watts would be taken from the 12 volt power supply for the control system that supplies current to the buck boost coil. As a result, the power conditioning is done at the cost of about 13 watts of power. This represents about 2% of the DC power input into the magnetron itself, so that the power conditioning system is 98% efficient.

The cost of such a power condition system is very low. A magnetron supplier has estimated that the additional cost of making and inserting the buck boost coil on a magnetron in production would be about 50 cents. It is estimated that the control circuitry to control the input to the buck-boost coil would be no more than two dollars.

The control of the amplitude of the power output is accomplished by sampling the microwave power output through a probe, rectifying it to a DC voltage and comparing that with a reference voltage which is the controlling parameter. The error signal in this comparator is then sent to the DC amplifier that controls the current flow through the buck -boost coil. The amplitude control system has been analyzed in reference 25. The effectiveness of such a system is shown in Figure 5.15, where the data is explained in the caption.

#### 5.3.4 Estimated cost of radiation module in volume production.

Following is as an estimate by the author as to the total cost of a radiation module and the breakdown of that cost by the principal components within.

Slotted waveguide array -----	\$15.00
Magnetron with buck boost coil-----	\$14.00
High gain microwave monolithic integrated circuit with----	\$20.00
low power level phase shifter	
4 Port circulator (integrated into magnetron package) ----	15.00
Motorized reactance insertion (for tuning magnetron)-----	\$10.00
Phase detector, control circuit, and DC amplifier-----	\$10.00
Amplitude comparator, control circuit, and dc amplifier--	\$10.00
Cooling fan -----	\$4.00
DC power supply (+ and - 12 v) for DC amplifiers )-----	\$8.00
Assembly and testing-----	\$20.00
	-----
	\$126.00
Contingency-----	\$74.00
	-----
Total Cost-----	\$200.00

This cost is believed to be very conservative. Aside from the magnetron and the 4 port circulator, there are no microwave power components. The rest of the module consists of components which can largely be integrated together.

#### 5.4. Interaction of the microwave beam with other uses of the electromagnetic spectrum.

The major use of the radio frequency spectrum with which the LEO to GEO transportation system might interfere is with communication services,

particularly satellite communication services. Would it interfere with them? This question cannot be easily answered, but the interference between a comparable microwave beam and communication satellites was studied and reported upon extensively during the 1977-to-1981 DOE/NASA study of the Satellite Power System in which a similar but higher power microwave beam was used to transfer several gigawatts of electrical power from geostationary orbit to Earth. The following quote is taken from the abstract of that study: "Mitigation techniques for SPS effects are examined and recommendations are made which would allow satellites to operate satisfactorily in an SPS environment" (12,24).

. Although it would be premature to assume that interference could be avoided between communication satellites and the microwave beam system proposed for the LEO to GEO transportation system, it may be informative to discuss some of the problems and the mitigating approaches that might be used in the event of interference. It should be noted that some of the problems perceived with today's technology and practices may be diminished in the future. For example, it is expected that by the time the proposed all-electronic LEO to GEO transportation system would be fully activated the bulk of the traffic in communication satellites will have shifted to much higher frequencies where the interference problem will be enormously reduced. And in anticipation of the improved transportation system, many steps could be taken to reduce or eliminate the interference problem.

First, in discussing the interference problem, it is assumed that all the Earth based microwave beams will be at one frequency that will not be shifted or intentionally modulated in any way. This simplifies the situation immensely and allows the use of narrow band-stop filters in the satellite receiver, as well as the use of phased locked loops to feed back out-of-phase energy to cancel power picked up at the beamed power frequency (41).

There are other less technically involved strategies. In the event that the illumination intensity which will be at the maximum about 500 watts per square meter proves to be too much for some satellite service, the microwave power beam can be either momentarily shut off or electronically steered away from an impending encounter with a satellite. The microwave beam will be so narrow that the transit time across the beam for most satellite encounters will be for only a few milliseconds, allowing the interorbital vehicle to proceed unaffected if there is a minimal amount of energy storage carried aboard.

Another major area of interference concern are the harmonics and spurious signals generated in the transmitter and in the rectenna receiver. In the case of the transmitter composed of many radiation modules in which the microwave oven magnetron is the phase locked generator, it has been found and documented in reports that the microwave oven magnetron when operated on a well filtered power supply, and with the normal input power to the filament removed so that the tube operates with an internal feedback mechanism to provide just the right amount of electronic backbombardment power to keep the cathode at the proper emission temperature, the spurious noise is at a very low level. During the DOE/NASA study of the SPS, special sensitive noise measuring equipment was made to permit making noise measurements within the guard band of plus and minus 50 megahertz around the center frequency of 2.45 GHz (25).

The sensitivity of this equipment made it possible to measure the spectral

noise density (noise in a one hertz bandwidth) from a magnetron directional amplifier that incorporated the microwave oven magnetron that was 190 db below the carrier at a frequency removed from the carrier by 10 MHz. In the context of a solar power satellite that was generating an 8 gigawatt beam, such a low noise level is translated into a total radiated power of  $3 \times 10^{-6}$  watts in a 4 KHz bandwidth. After taking the gain of the  $0.3 \text{ m}^2$  radiating module and the distance to the Earth into account there was a 60 db safety factor in meeting the CCIR requirements of -154 DBW/M<sup>2</sup>/4 KHz at the Earth's surface.

These noise measurements were made on microwave oven magnetron manufactured during the late 1970's, and such low noise levels may not be characteristic of the microwave oven magnetrons available today and some investigation may be needed as to the design characteristics that will insure such low noise levels. However, it is of interest that on the specific magnetrons used for the noise measurements there was no attempt made to optimize the design for low noise, so that an optimizing procedure may result in magnetrons of even lower spurious noise level.

The harmonic level from magnetrons is characteristically much lower than for other power generators such as klystrons. When harmonic noise measurements were made directly at the output of the magnetron it was found that the levels were characteristically 70 to 90 db below the carrier for 2nd, 3d, and 4th harmonics. (29). Data taken by JPL on reduction in measured gain for the harmonics caused by the slotted waveguide array that would be used in the transmitting antenna introduces another 50 db. for these same harmonics. In addition, of course, harmonic filters could be placed in the output of the magnetron to reduce the level even further. It is therefore likely, that with reasonable mitigation techniques that the harmonic levels of the transmitter could be held to the necessary level to avoid interference problems.

Finally, the rectenna with its rectification function could be a rich source of harmonics that could be reradiated from the rectenna. However, a recently developed format for a rectenna designed for use on a satellite confined to the equatorial plane can reduce the reradiation of harmonics to a negligible level, with the insertion loss for the filtering being offset by the increased efficiency gained by operating the diodes at a higher power level in the proposed format. It is expected therefore that an overall efficiency of greater than 80% from the rectenna can be obtained.(7). This new design is discussed in section 6.0 of this report.



## 6.0 An Alternative Rectenna Design

### 6.1 Introduction

The proposed transportronics technology as used in the equatorial plane for both the all-electronic interorbital transfer vehicle as well as orbiting industrial parks provides an opportunity to design a new rectenna which eliminates the harmonic radiation problem of the conventional thin film rectenna design. This is its chief advantage but it also reduces the number of diodes used by a factor of eight or ten, and also allows the diodes to be used at higher efficiency because they are operated at a higher power level. Because the diodes represent the greatest cost element in the rectenna, and the unit cost of the high power diodes will be no greater than the low power diodes, there will be a great reduction in rectenna cost.

These additional advantages of the proposed design must be balanced against the fact that the rectenna will be highly directive around one axis although it will remain as "non-directive" as the conventional thin film rectenna around the other axis. While the high directivity around one axis disqualifies the use of the alternative rectenna design for airplane use because of the roll and pitch of the airplane, it is quite compatible with the rectenna in the interorbital or industrial park vehicle because they will not theoretically require any North and South steering of the beam. In the event that they should drift away from the equatorial plane the rectenna will still be efficient up to a deviation of a degree or so.

The proposed rectenna design has already had a considerable amount of development as the result of an important phase of the contract having to do with collecting microwave energy at a low power density from a broadside antenna array into a single 50 ohm port. The microwave power is then passed into a low loss, multi-stage, low pass filter, and then into an impedance changing transformer and finally into the microwave diode rectifying circuit.

For documentary purposes the important features of the development of the low power density rectenna will be reviewed. However, the reader who is primarily interested in the alternative rectenna may want to proceed to section 6.3.

### 6.2 Documentation of the low power density rectenna.

#### 6.2.1 Overall description and performance.

The objective of the low power density rectenna was to produce a rectenna that would operate at incident microwave power density levels several orders of magnitude lower than the conventional rectenna. This development involved abandoning the principle of using a single diode on each rectenna element dipole, and using a single diode to process microwave power captured by many dipoles. This development resulted in a 48 element dipole antenna array and two separate cartridges, one containing the low pass filter and the other containing the impedance matching transformer and the rectification circuit.

The hardware resulting from the development, except for the low pass filter which will be discussed separately, is shown in figure 6.1. The impedance changing and rectification cartridge is shown on the left hand side of Figure 6.1.

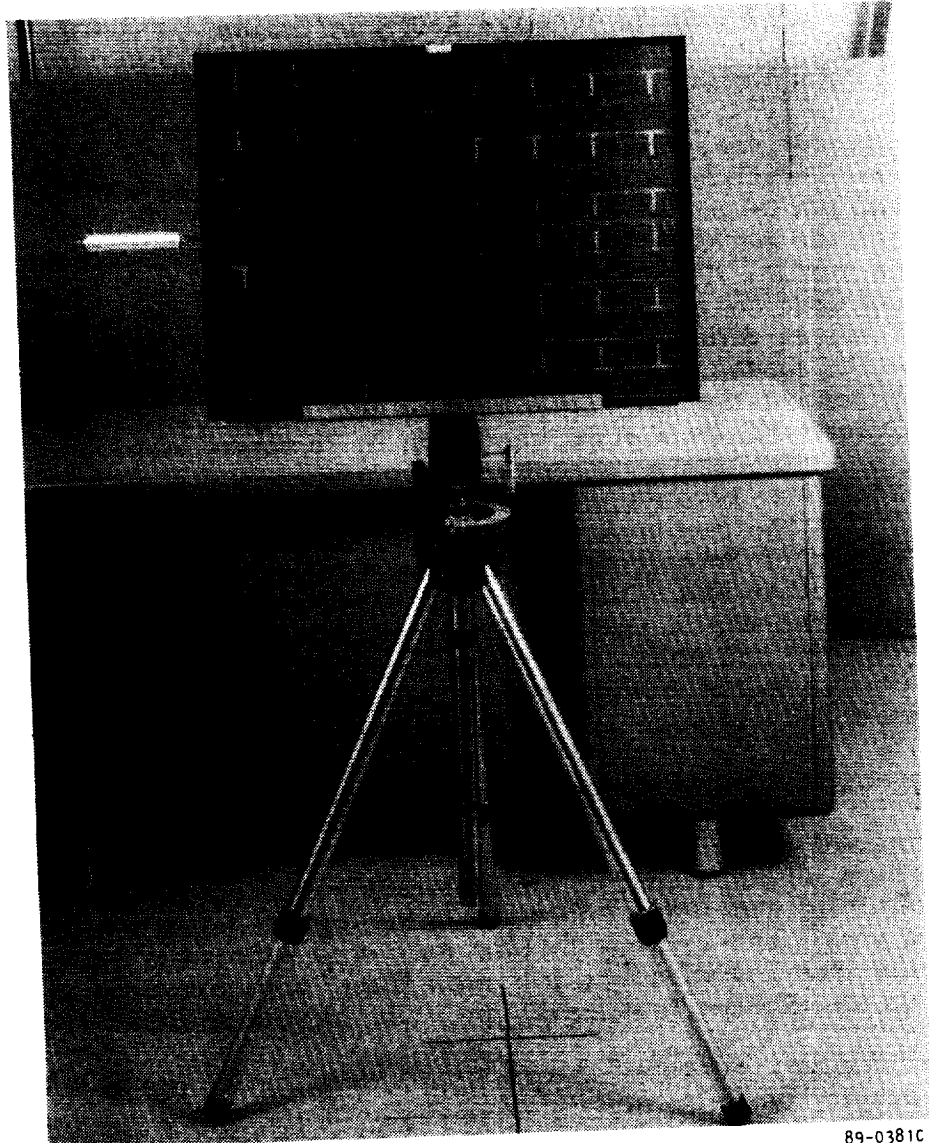


Figure 6-1. The low power density rectenna shown above consists of a 48 dipole broadside array that feeds into an impedance changing and rectification cartridge shown on the left side of the broadside array. In addition there may be a harmonic filter interposed between the antenna and the cartridge. This arrangement allows the achievement of five volts at an output level of 10 milliwatts that corresponds to an incident microwave power density level that is about ten thousand times lower than that for the typical rectenna which operates at an incident power density level of about 500 watts per square meter.

The general schematic of the 48 dipole broadside antenna, filter, impedance transforming and rectifier circuits is shown in Figure 6.2. The impedance level of each dipole receptor is of the order of 120 ohms but the dipole elements and interconnecting transmission lines are combined in series and parallel arrangements to present a 40 ohm output impedance, close enough to match well into a standard 50 ohm impedance circuit.

### 6.2.2 The impedance changing and rectification cartridge

Figure 6.3 shows a view of two impedance changing and rectification cartridges with their external shields removed. Both cartridges employ the same microwave circuits but the top one in the photograph has been refined mechanically and also makes provision for the changing of the diode rectifier without the need for a soldering operation. This circuit, in association with the antenna is represented in the simplified schematic of figure 6.4.

The impedance transformer in the cartridge steps up the impedance level from the input level of  $Z_a = 50$  ohms to an output impedance of 2500 ohms, or a factor of 50 in impedance. In addition the half wave rectifier circuit gives an additional effective step up of 2 so that the value of the DC load resistance is 5000 ohms. This was the value of the load specified as an objective of the development. The result of the impedance transformation is a step up in voltage by a factor of ten. The impedance transformation is made with the use of a simple balanced quarter-wavelength section of transmission line with a characteristic impedance of 350 ohms.

Figure 6.5 shows the performance of the impedance changing and rectifying cartridge in terms of overall efficiency as a function of DC load resistance,  $R$ , and the output power level in milliwatts. A typical power output of cartridge is 10 milliwatts which compares with typical output from a single standard rectenna element in traditional format of from 1 to 10 watts. Moreover, the cartridge receives the power from 48 dipoles so each dipole is operating at the  $2 \times 10^{-4}$  watt level, or lower by a factor of 10,000 than the standard rectenna element.

In the context of impedance changing with the quarter-wavelength section of transmission line it should be noted that the impedance may be stepped down as well as up and that this may be desirable for applications in which the diode rectifier may be handling ten or more watts of power.

### 6.2.3 Harmonic filter design and experimental evaluation.

Historically, a general problem of the rectenna has been the radiation of harmonic power. Harmonic power is radiated both by the dipole antennas and the rectifier circuit itself unless it is well shielded. This study provided the opportunity to design and evaluate a low-pass filter with very low loss at the operating frequency of 2.45 GHz but very high loss at the harmonic frequencies. More specifically, as a result of the development effort on an eight section low pass filter, we are able to report a loss of 1.13% or 0.049db per filter section at 2370 MHz and 13.1 db at the second harmonic frequency. The resultant ratio of second harmonic loss to loss at the fundamental frequency, 2370 MHz, is 1805.

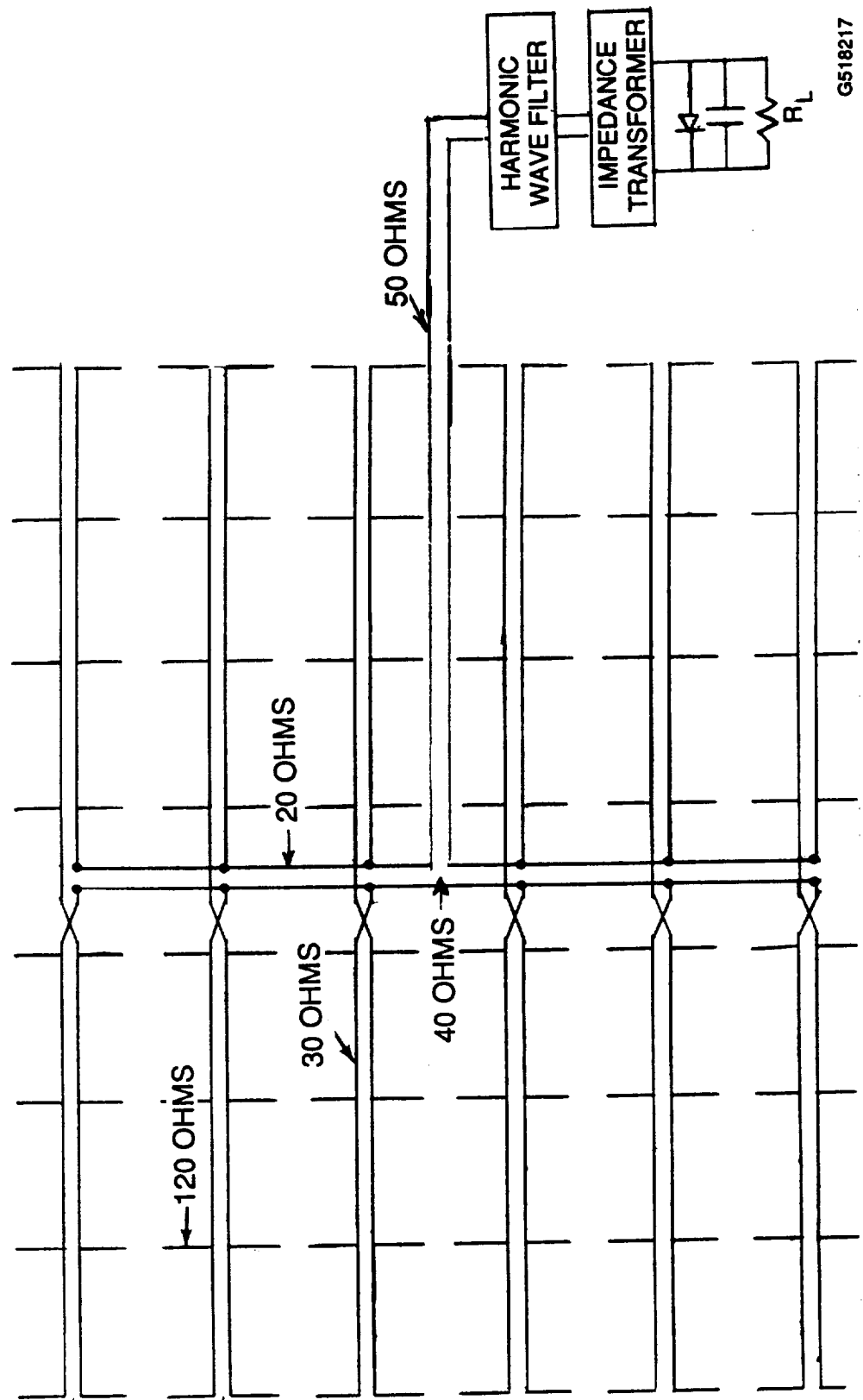
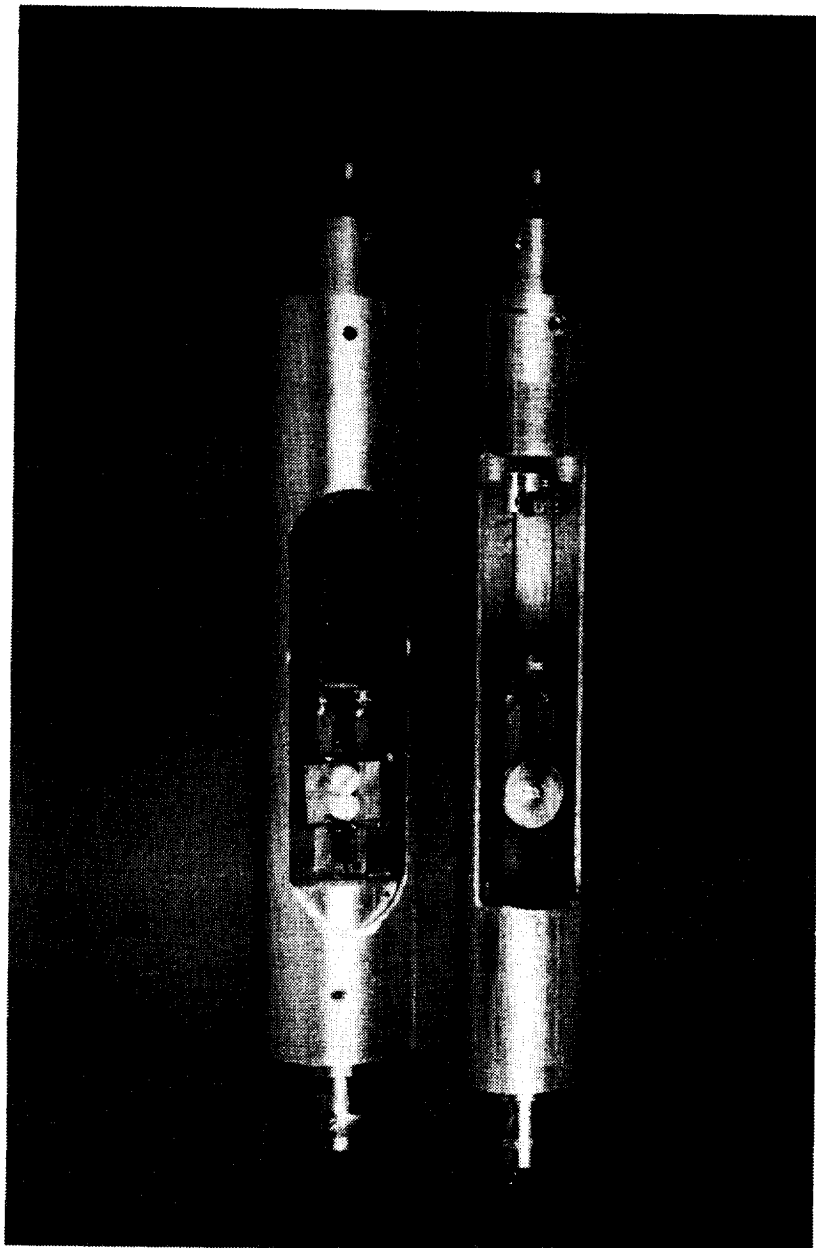


Figure 6-2. The electrical schematic for the 48 dipole antenna. Each dipole has an impedance of about 120 ohms. The dipoles are connected in parallel to 30 ohms transmission lines and the transmission lines are then connected in series and parallel to reach an output impedance level of 40 ohms which is very close to a standard 50 ohm impedance level for test equipment, etc.



89-0377C

**Figure 6-3.** The impedance transformation and rectification cartridge. The circuit schematic for these cartridges is shown in Figure 6-4 and the performance chart in terms of DC power output and efficiency as a function of DC resistive load is shown in Figure 6-5. The quarter-wavelength long balanced-wire transmission line that changes the impedance level from 50 ohms to 2500 ohms may be seen at the bottom of the cutaway section. The diode rectifier was a HP 2900 diode

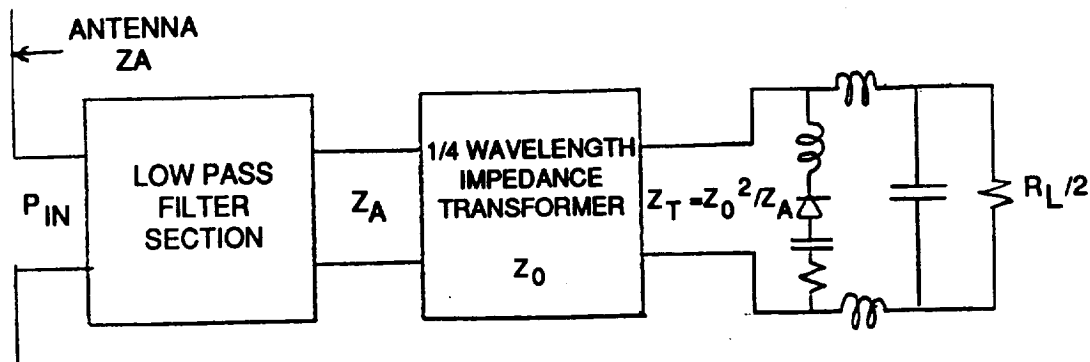


Figure 6-4. Circuit schematic for the impedance transformation and rectification circuits.

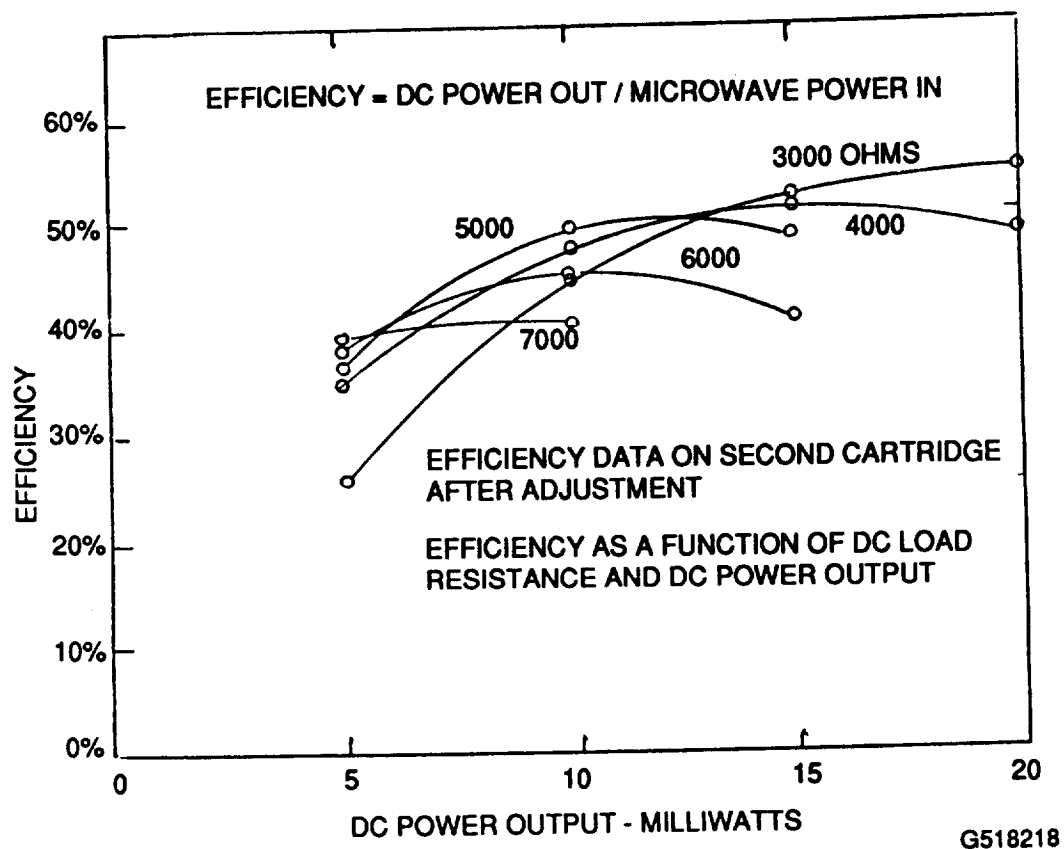


Figure 6-5. Performance chart of the impedance transformation and rectification cartridge. Output voltage can be obtained from the square root of the product of the DC load resistance and the DC power output. For example, at 10 milliwatts output into a load resistance of 5000 ohms, the output DC voltage will be 7 volts. Efficiency is defined as the ratio of DC power output to microwave power input.

An eight section low pass filter was used for these measurements for two reasons. First, the measurement sensitivity of the loss at the fundamental frequency was greater than for a filter with a relatively small number of sections. Secondly, it may be necessary to have filters with second harmonic attenuation in the 100 db range for very high power rectennas. Filters with such high attenuation may have idiosyncrasies unless the filter is so constructed that there are no other modes of propagation for the harmonic frequencies than a single TEM mode.

The experimental results from the specially constructed eight section filter are shown in Figure 6.6. The attenuation losses are shown per individual section. At the second harmonic frequency the attenuation is 13.1 db per section or a total of 104.8 db which was measured and from which the average attenuation losses per section were derived.

The eight section filter with its outer case removed is shown in Figure 6.7. It consists of bar type filter sections with which there has been considerable experience. In fact, the standard rectenna element whether of the bar type or thin-film type utilizes two sections of the same filter circuit in a balanced mode configuration. The balanced mode configuration, however, cannot be used in a high loss filter which must have an external shield to prevent the radiation of harmonics directly from the transmission line. A two wire line inside a shielded enclosure allows for another mode of transmission which cannot be tolerated. However, the balanced microwave circuit can be easily converted into an unbalanced circuit by running a ground plane physically through the center of the filter. This results in doubling the lumped capacitance and halving the effective inductance of the section of transmission line which has been used in place of the lumped inductance of the low pass filter. The characteristic impedance of the circuit will thereby be halved to 60 ohms from the 120 ohms of the balanced circuit but the other properties of the filter will remain unchanged.

The filter design is based upon that outlined in "Communication Networks, Vol. II" authored by E.A. Guillemin (John Wiley and Sons). More specifically we have used the "constant k" filter design which produces the theoretical attenuation characteristic shown in Figure 6.6. As can be observed, there is excellent agreement between the theoretically predicted and the experimentally measured attenuation characteristic.

The design shown in Figure 2.7 with its "SMA" connectors at either end could be easily connected between the broadside antenna output and the impedance changing and rectification cartridge. However, this could not be done because the two 48 element antenna arrays that had been constructed had been delivered to the customer prior to the work on the low pass filter. However, it was possible to connect a two section low pass filter in cascade with the second impedance changing and rectifying cartridge and compare the results with those in which no filter had been connected. The test circuit in which this comparison was made is shown in Figure 6.8. The backward directional coupler that was used was designed for the 4 to 10 gigahertz range.

The results of this comparison are shown in figures 6.9 and 6.10. A comparison shows that without a filter, the second harmonic reflected toward the input is down only about 8 db from the fundamental power input whereas with a two section filter it is down 35 db or about what one would anticipate

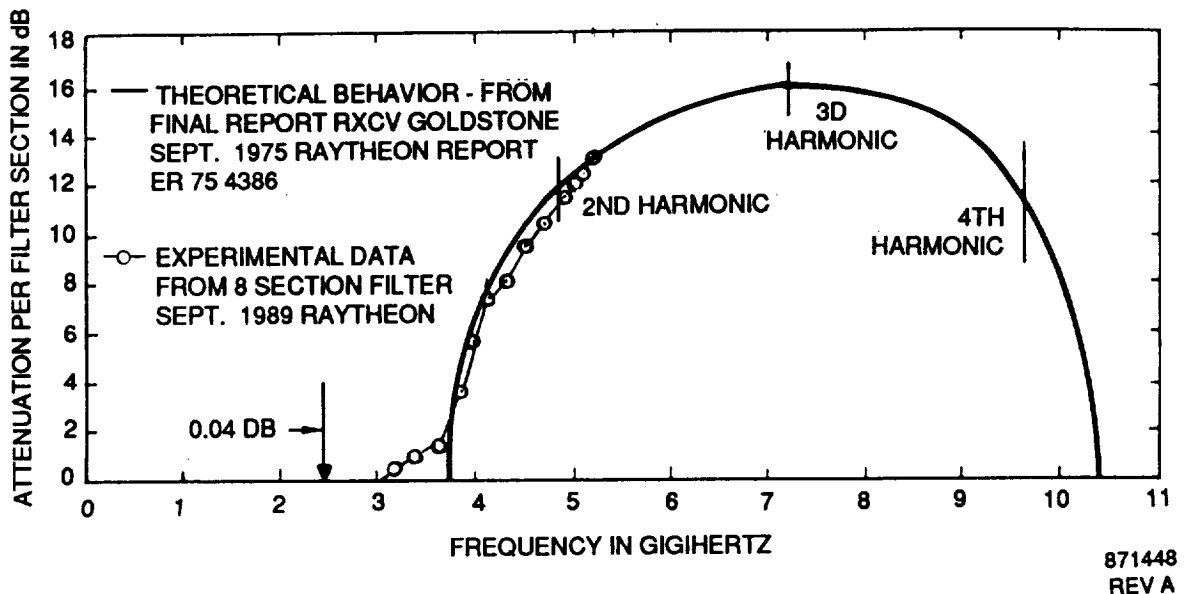
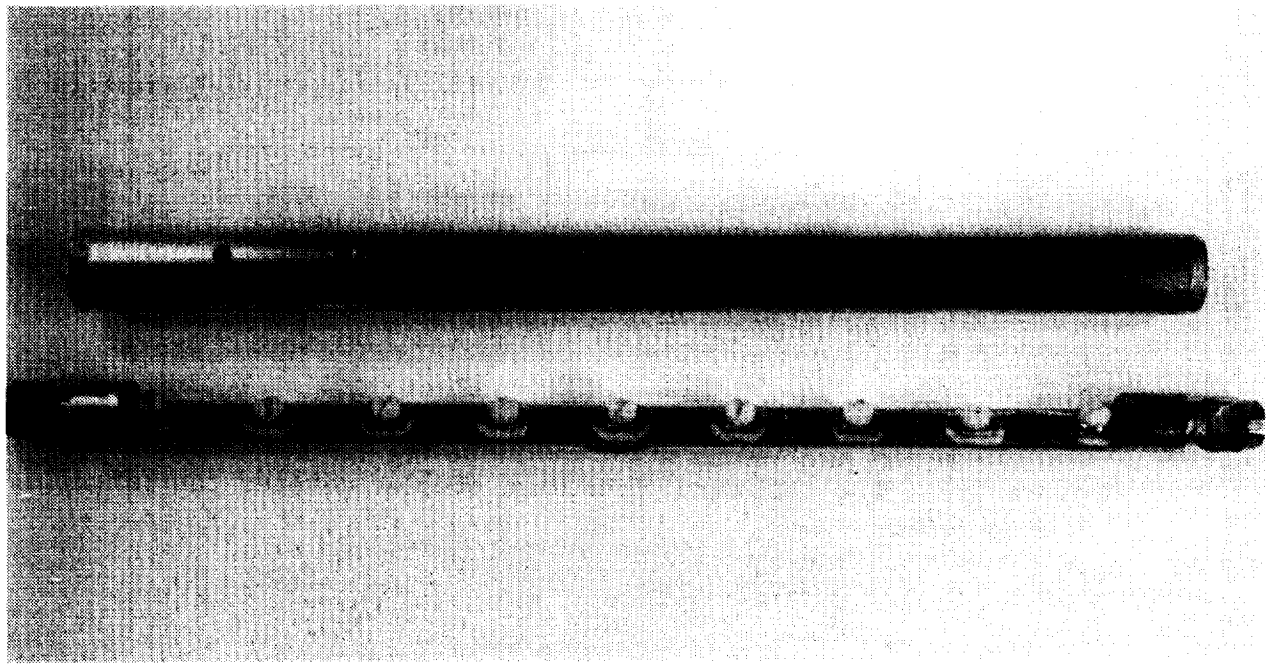
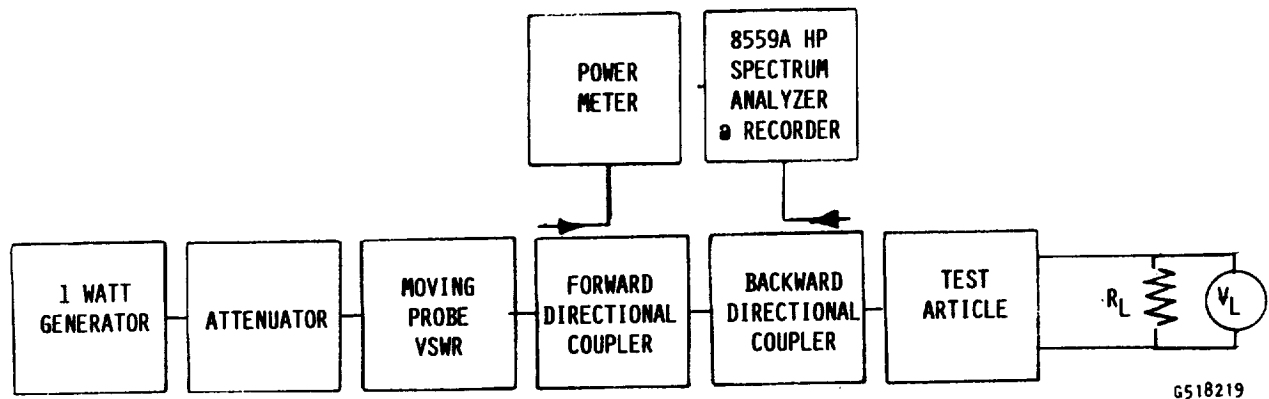


Figure 6-6. Performance of a single section of the 8-section filter shown in figure 6-6, as derived from the overall performance of the 8 section filter. The experimental observations follow closely the behavior predicted by filter theory.

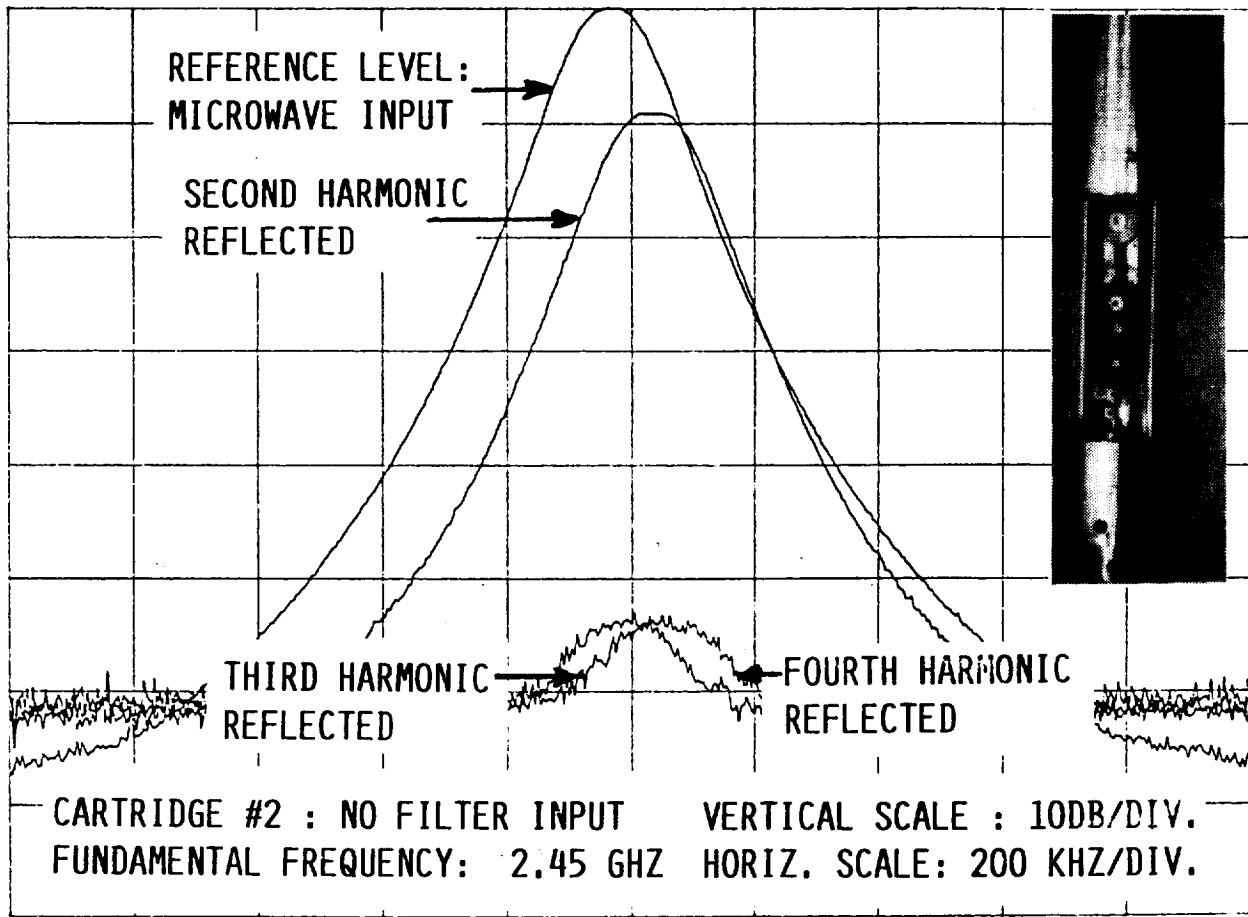


G518216P

Figure 6-7 An 8 section low-pass filter with a ratio of the attenuation of the second harmonic to the attenuation of the fundamental of  $1.12 \times 10^{26}$ . More specifically, the total loss was 0.39 db (9.4%) at the fundamental frequency and 104.8 db at the second harmonic frequency, with even more anticipated at the third harmonic frequency. Note that it was necessary to establish contact between the outer cylindrical shield and the interior ground plane at each filter section to avoid transmission of harmonic power from the output of the filter to its input. See figure 6-7 for details of filter performance and close agreement with filter theory.



**Figure 6-8.** Schematic of the arrangement that was used to check the impedance transformation and rectification cartridge for its harmonic generation. The backward directional coupler covered the range of 4 to 10 GHz.



G 518-220

Figure 6-9. Harmonic power generation of the impedance transformation and rectification cartridge without an input filter. Note that the second harmonic power is less than 10 db down from the reference level of microwave power input.

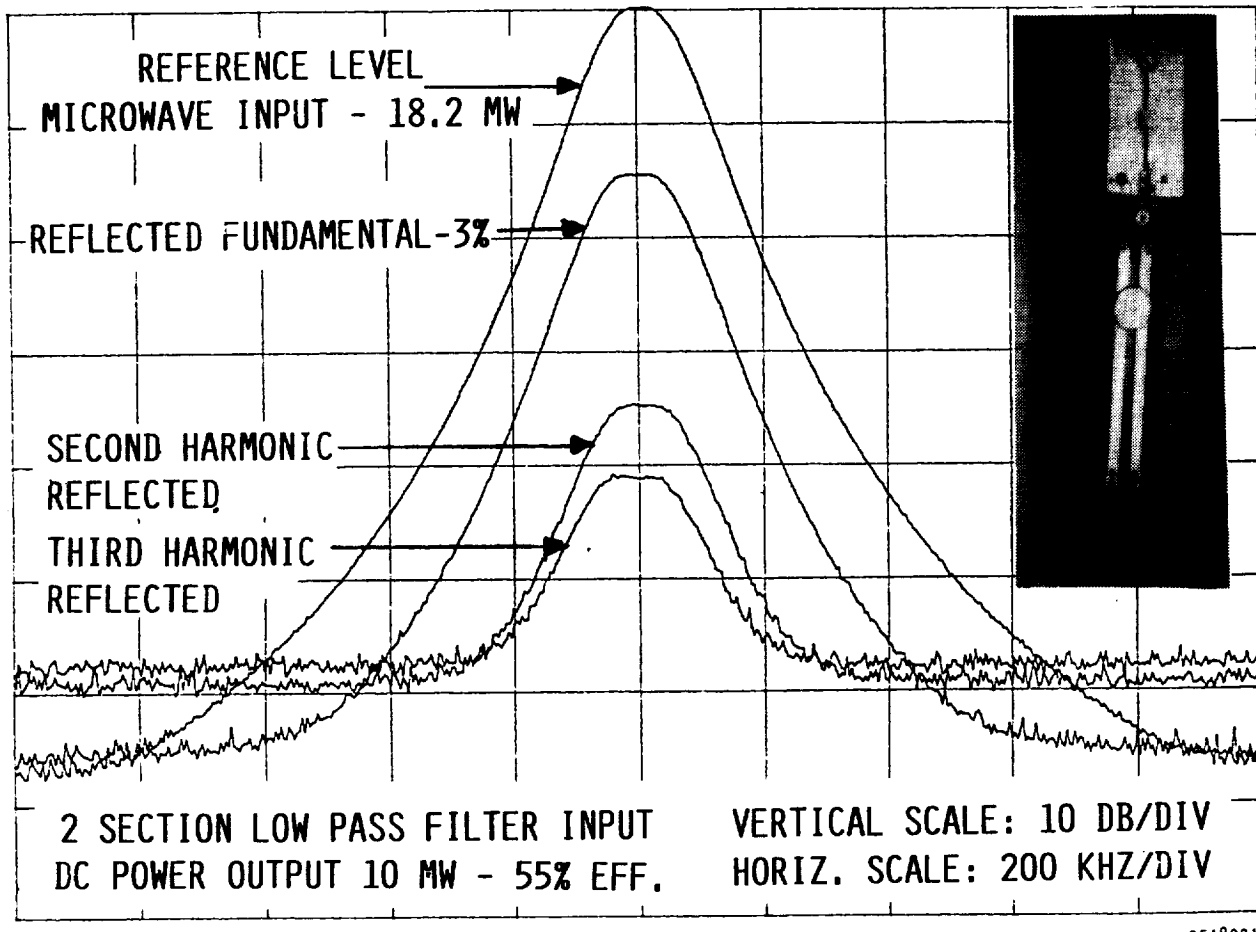


Figure 6-10. Impedance transformation and rectification circuit preceded with a 2-section low pass filter. The second harmonic is now down to a level that is 35 db below the microwave input reference level. Figure 2-7 indicates that a 2-section filter should provide 24 to 26 db. of attenuation at the second harmonic frequency. Figure 6-9 indicates the second harmonic to be down about 8 db. without a filter. If this 8 db is added to the theoretical attenuation of the wave filter, close to the observed experimental value of 35 db. is obtained.

from a two section filter. Interestingly, the level of the third harmonic is higher with the filter than without it. There is no explanation for this observation.

#### 6.2.4 Design and Construction of the thin, 48 element dipole, broadside antenna array.

The 48 dipole broadside array is shown mounted on a tripod in figure 6.1. the array measures 19 x 26 inches in area and is currently 1 1/4 inch thick as contained in a commercial picture frame. The array is constructed as shown in Figure 6.11. It is composed of twelve etched sections, each consisting of 4 dipoles and the interconnecting transmission line. The twelve etched sections are mounted on a front plate made from 3/16 inch thick "polygal" which is a ribbed extruded plastic sheet of very low density and low effective dielectric constant close to that of air. The plastic sheet also adds rigidity to the assembly and protects the etched surfaces. Then 5/8 inch thick styrofoam plates are placed on the backside of the front assembly. A 0.020 inch thick sheet of aluminum is then placed over the styrofoam to form the back reflecting plane. For convenience of assembly and disassembly the resulting sandwich of material has been inserted into a rugged aluminum picture frame molding.

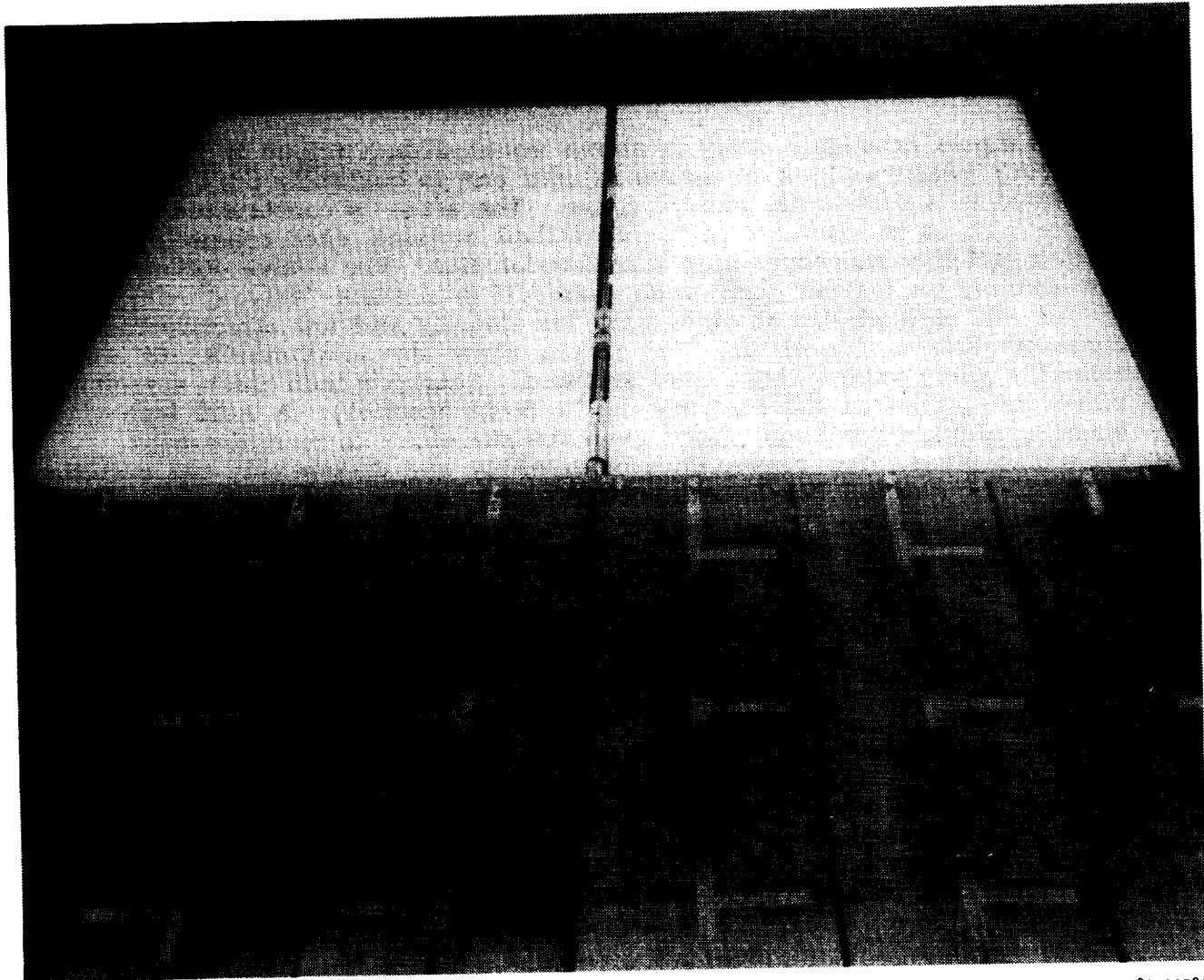
The electrical schematic of the antenna is shown in Figure 6.2. The circuit elements are interconnected in a series-parallel format to match the 120 ohm impedance of each of the 48 dipole antennas to one 50 ohm output. The interconnections are made in such a manner that only the back side of the 48 dipole array is involved with connections.

The key to the construction of the antenna array is the 4 dipole etched section, shown in Figure 6.12, whose dimensions and construction are shown in figure 6.13. The dimensions were determined by making a series of dimensional changes and subsequent testing for input impedance and coherent phasing of dipoles. Note that a section of transmission line was left on the outboard side of the line to allow for a movable short for trimming purposes .

Two 48 dipole arrays as shown in figure 6.1 were made. The first array used sections fabricated from Norplex-Oak GY 601 material with a 20 mil thick teflon-glass fiber dielectric with a 2.55 dielectric constant bonded on both faces to 1 ounce (1.4 mil thick) copper. Norplex-Oak, the supplier, is located on King Street in LaCrosse , Wisconsin.

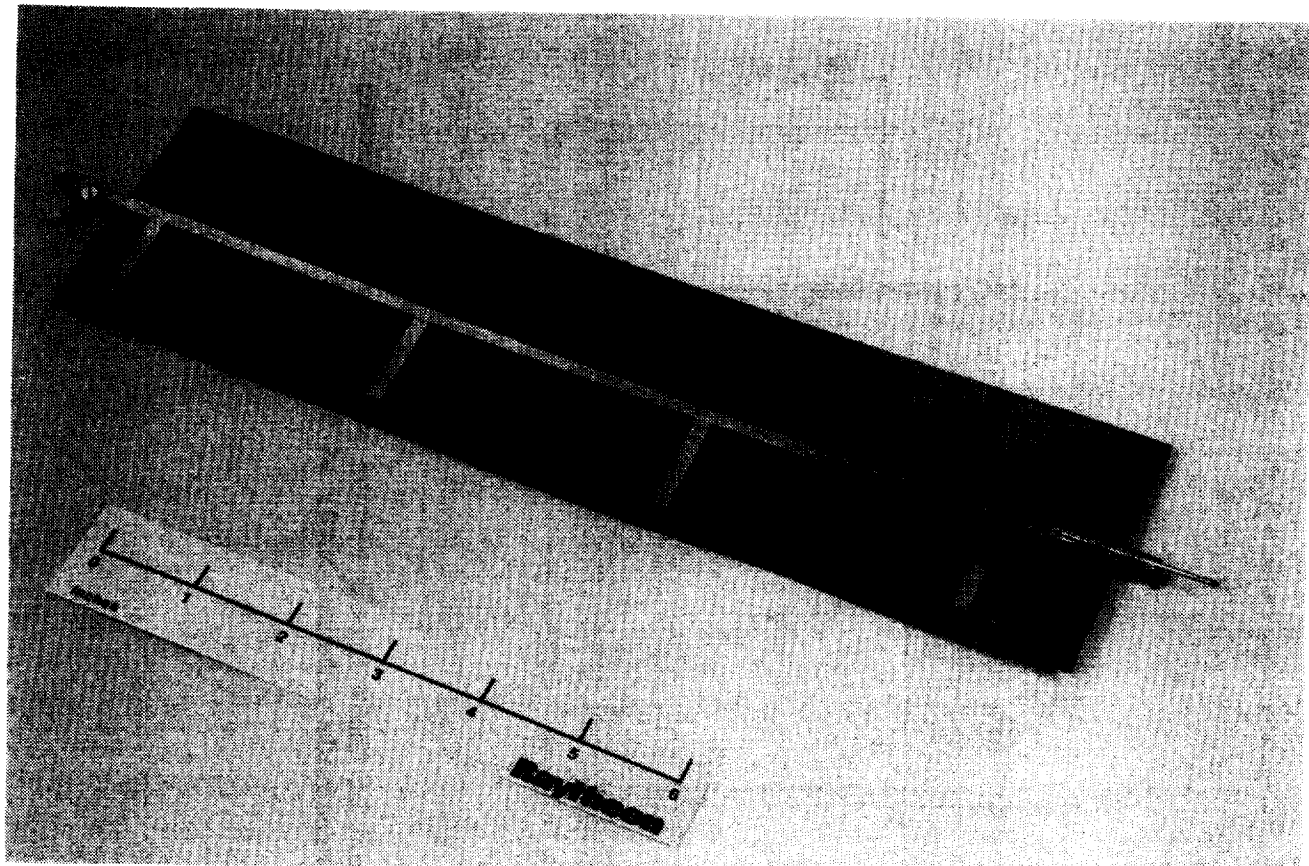
The material for the second 48 dipole array was procured from Keene Corporation Laminates, located in Bear, Delaware. It was a similar material but with a dielectric constant of 2.43 and a dielectric thickness of 19.3 mils. It was purchased in place of a repeat order to Norplex-Oak because of much faster delivery time. The original development effort of the 4 dipole section used the Norplex Oak material.

There were two known differences between the two 48 dipole arrays that were constructed. The first was the use of slightly different composite material. The second was that the first 48 dipole array had a balun inserted between the output 50 ohm transmission line and the parallel plane transmission line that interconnects the rows of dipoles. Whether it was these differences or other factors is not known, but there was a substantial difference in the input



89-0378C

Figure 6-11. View of 48 dipole array with back cover (reflecting plane) removed. Top half of picture shows the 5/8 inch thick styrofoam that spaces the front plane of the antenna from the back plane. Bottom half of picture exposes the back side of the front plane showing one arm of the dipoles and the back side of the 30 ohm transmission lines that connect the dipoles in parallel. The 20 ohm parallel plane transmission lines that connect the rows of dipoles in parallel is exposed in the center of the photograph. The 50 ohm output transmission line and the balun is shown connected to the center of the 20 ohm transmission lines in a series format.



88 3107C

Figure 6-12 The 4-dipole section is the electrical and mechanical building block of the 48 dipole array. Two of these 4 dipole sections are connected in series to form a 8-dipole row with a nominal series input impedance of 60 ohms. Test data on the 8 dipole array are given in figures 6-24 and 6-25. The physical dimensions of the array and directions for its fabrication are given in Figure 6-13.

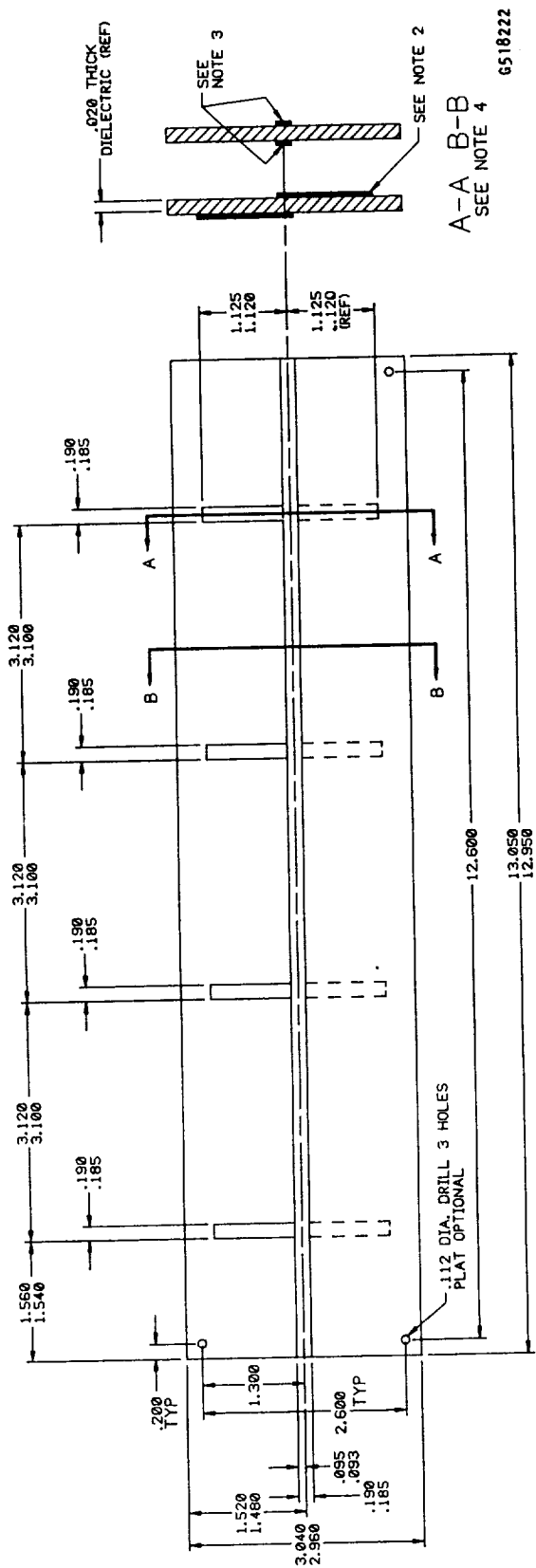


Figure 6-13. Mechanical layout of the 4 dipole section which was the building block for the broadside antenna array of 48 dipoles.

matches to the arrays. The second array had a reflection factor of about 0.14 or power reflection of 2%, while the first array had a reflection factor of 0.3 or a power reflection of about 10%.

The integration of the already developed 4 dipole sections into the 48 element array followed an orderly progression of steps, as follows:

STEP 1. Two 4 dipole sections were connected together to form a 8 dipole row. The connection of the parallel-plane transmission line bus into the 8 dipole row was a series connection which causes the pattern reversal of the dipoles as viewed from the front face as is evident in Figure 6.1. If it is assumed that the individual dipole is 120 ohms, as shown in Figure 6.2, then the input impedance to a 4 dipole section is 30 ohms because the dipoles are all in parallel with each other. Now, if the inputs to the 4 dipole sections are connected in series, the input impedance to the row of 8 dipoles as seen by the vertical interconnecting bus is 60 ohms.

STEP 2. Three of the 8 dipole sections are connected in parallel to a 20 ohm parallel plane transmission line bus. The remaining three 8 dipole connections are also connected in parallel to another 20 ohm transmission line.

STEP 3. The inputs to the two 20 ohm transmission lines are then connected in series to a 40 ohm transmission line, which then becomes the single input or output port to the antenna, depending upon its operation as a transmitting or receiving antenna. This connection results in another pattern reversal from top to bottom, as viewed in figure 6.1 again.

The complete 48 dipole array, except for the connecting busses, can be made in one printed circuit operation. The connecting busses can then be attached by a soldering operation. The layout of such a single printed circuit is shown in Figure 6.14.

#### 6.25 Testing of the 48 element dipole array.

The completely assembled 48 element dipole broadside array consisted of both far field patterns around both axis, and very local measurements of the phase and output amplitude of each dipole element. The local measurements will be discussed first.

The local measurements were made with a short dipole probe which was positioned directly over a rectenna element with a fixed separation from the dipole. This procedure is shown in Figure 6.15 for two rows of elements but the same procedure was used for the complete 48 element array. The source of power was the output port of a network analyzer. The output of the dipole probe was fed into the input port of the network analyzer and the output phase picked up by the probe was compared with the phase of the power going into the input port of the 48 element antenna.

The resulting data is shown in figure 6.16. Phase data is shown of the left side of the figure. The root mean square value of the phase variation is 15.7 degrees. This variation results in an antenna efficiency degradation of about nine percent and by itself is probably an acceptable figure. However, there is also a substantial variation in the amplitude which may further degrade the performance.

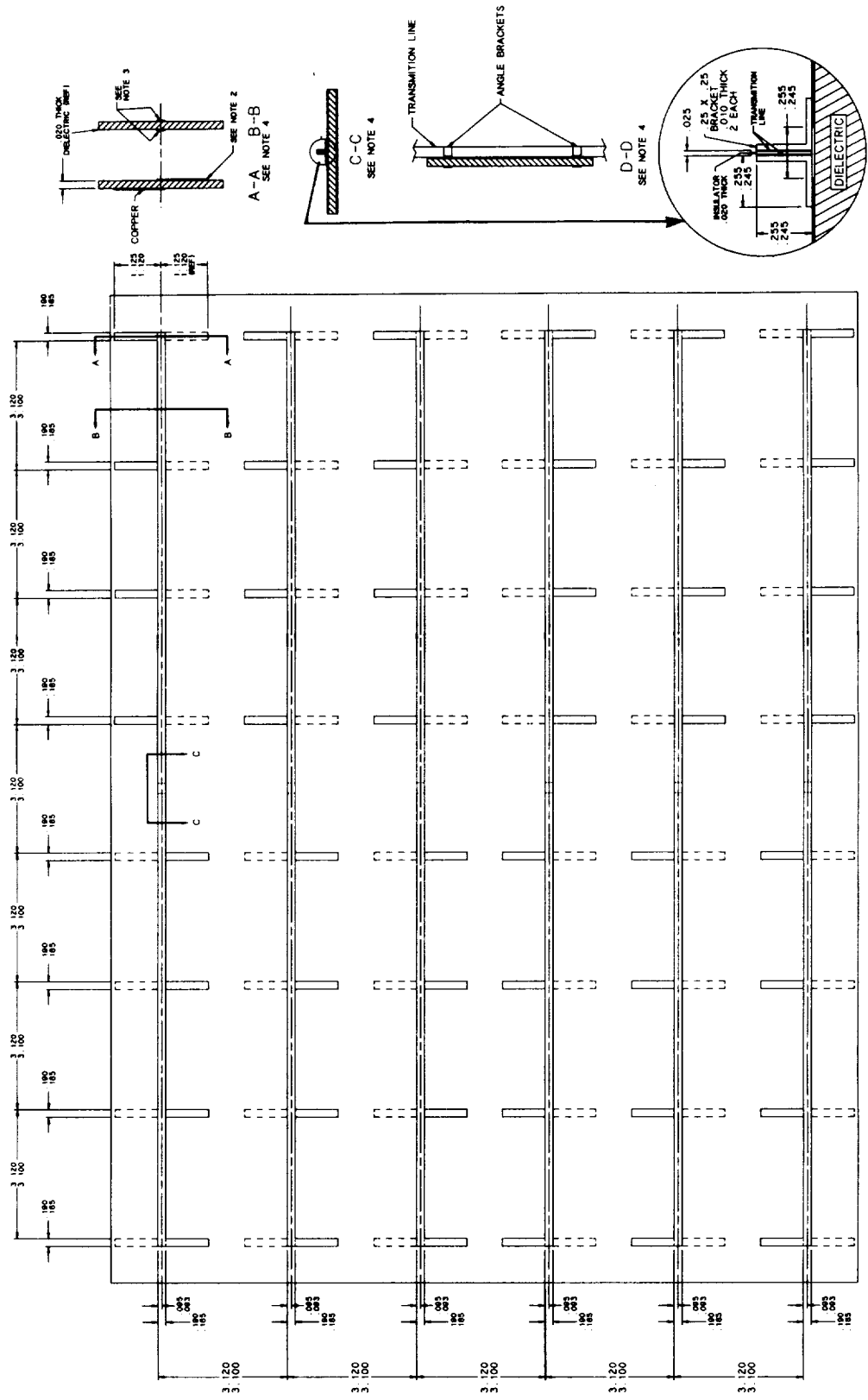
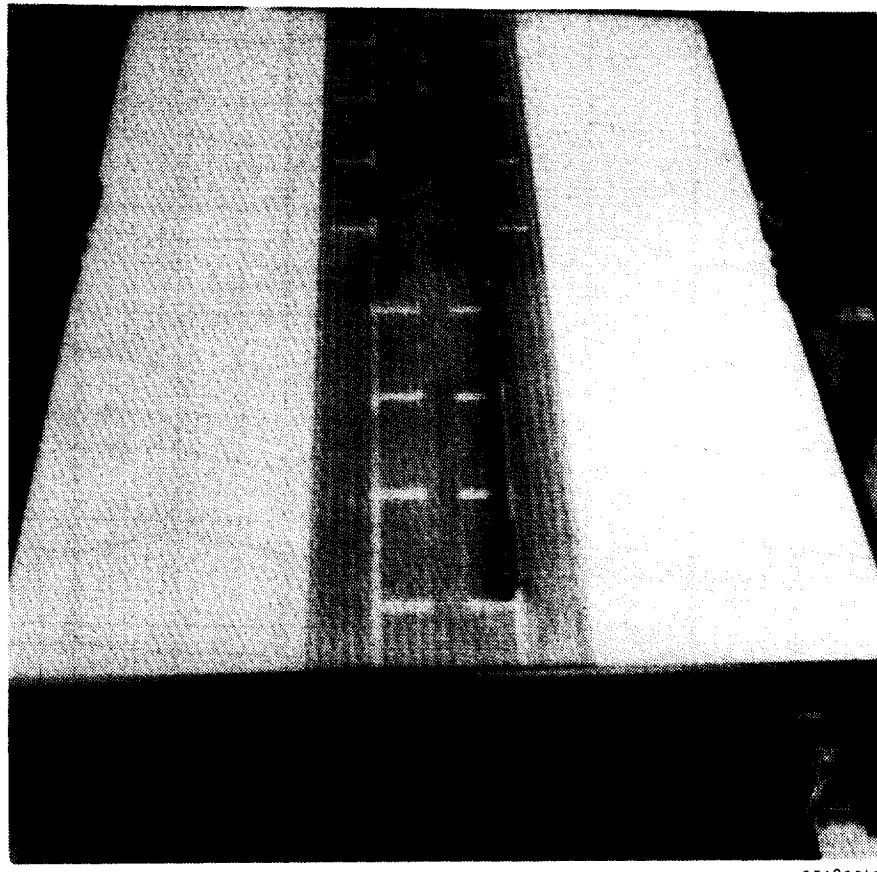


Figure 6-14. The complete 48 dipole array, except for the connecting busses, can be made in one printed circuit operation. Such an assembly is shown above. The connecting busses can be attached by a soldering operation.

G518223



G518224P

Figure 6-15. Phase and amplitude data were taken with a dipole probe with very short arms to minimize its impact upon antenna performance. Input of the array was fed from a network analyzer output while the output of the probe was fed back into the input port of the network analyzer. Same probe that was used successfully on a 64-slot, slotted waveguide array was used. In the test above the probe is being applied to two rows of dipoles as described under STEP 2 of the antenna development in the text.

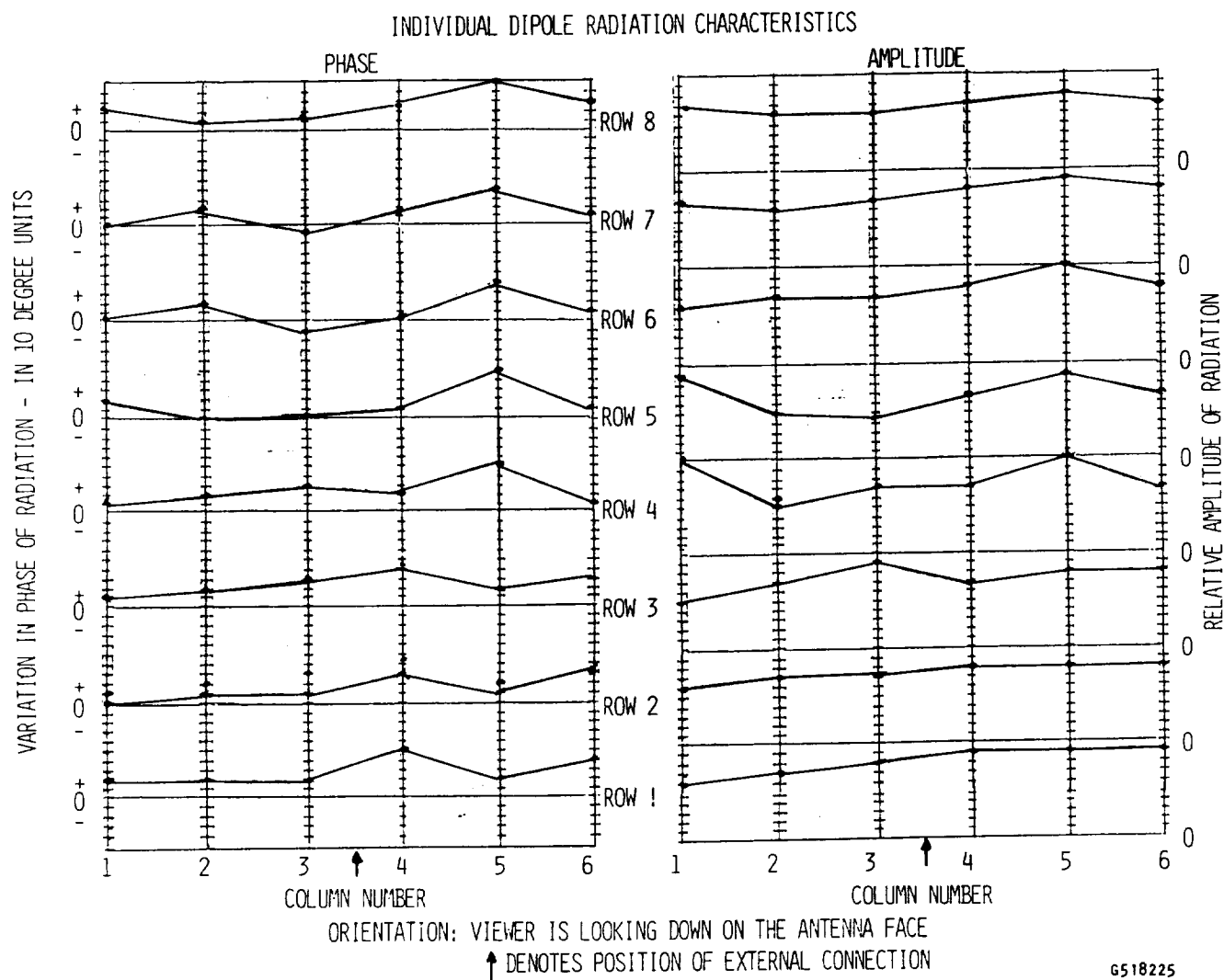


Figure 6-16. The above figures give the phase and output amplitude of the radiation from each of the 48 dipoles as obtained with the technique shown in figure 6-15. As derived from the data above, the rms random phase variation was found to be 17 degrees which is considerably more than that computed from the phase data given in figure 6-25 for the 8 dipole row. A 17 degree random variation in phase results in 10% scattering and degradation in antenna efficiency. Combined with the very substantial variation in amplitude the losses may be greater.

The antenna field patterns were taken by rotating the antenna around its vertical and horizontal axes. Figure 6.1 shows the adaptation of the tripod mounting for this purpose. It was possible to take these patterns without the use of an anechoic chamber or outside test range because of the use of a dual mode horn shown in Figure 6.17. This horn puts out a nearly theoretical gaussian beam and has very low side lobes so that reflections from the floor or ceiling are very low.

The dual mode horn as it was used in the test area is shown in Figure 6.17. It was used to illuminate the 48 dipole antenna array shown in Figure 6.1 at a distance of 145 inches from the phase center of the dual mode horn or approximately 140 inches from the mouth of the horn. The gaussian nature of the illumination at this distance is shown in figure 6.18 as obtained in earlier work. Because of the spherical phase front, the illumination of the 19 x 16 inch antenna array was not uniform in phase. With respect to the center, the phase at the corners, the sides, and the top and bottom lagged that of the center by 70, 46, and 25 degrees respectively. The amplitude is also not uniform. The power density of the beam varies as

$$p_d = p_0 \exp(-(r/r_k)^2)$$

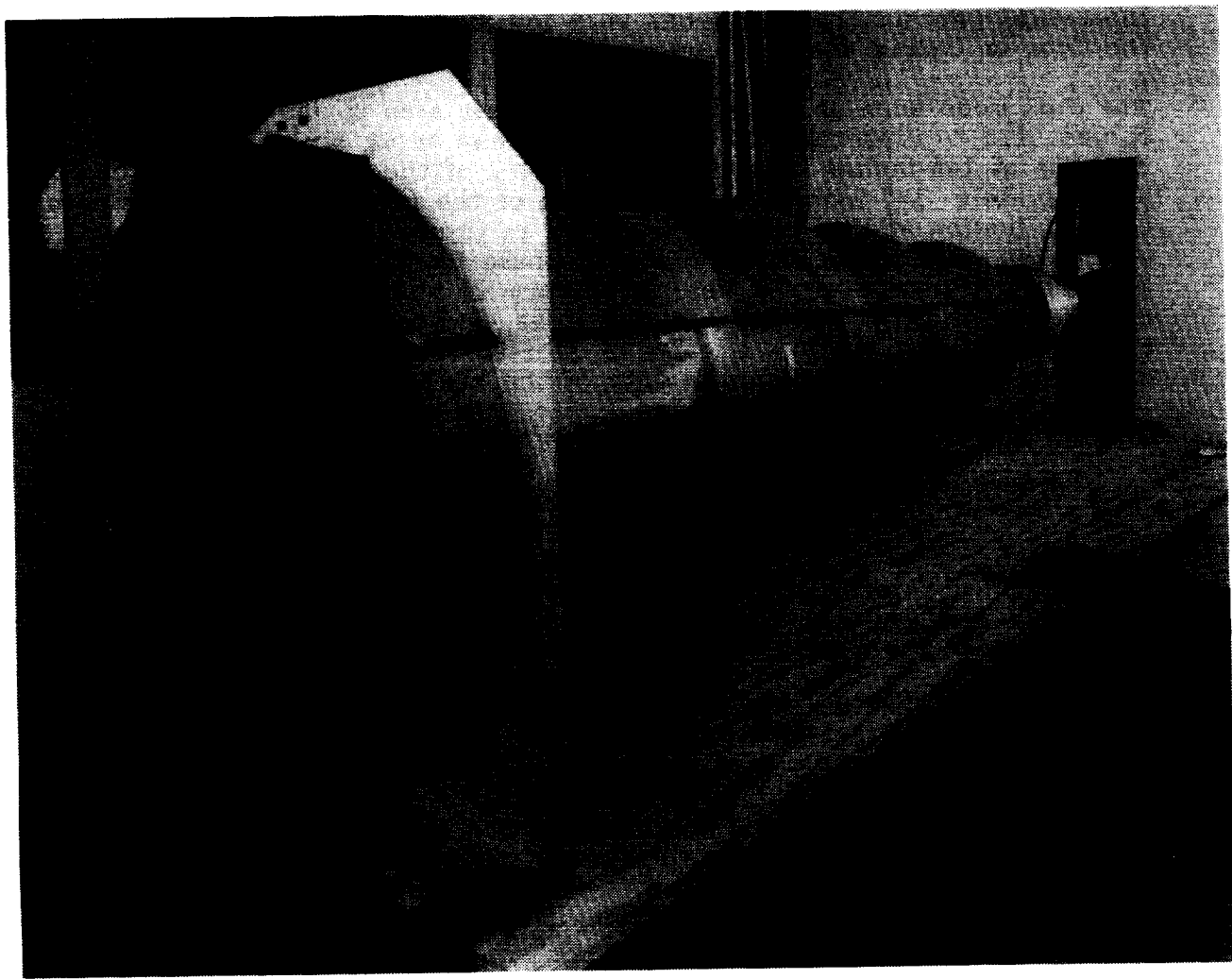
where  $p_d$  = power density at distance  $r$  from the center  
 $p_0$  = power density at the center  
 $r_k$  = distance at which power density is  $p_0/e$   
where  $e = 2.718$

At the distance of 145 inches,  $r_k = 22.0$  inches.

Therefore with the use of the above equation the power density at the corners, sides, and top and bottom will be down by the multiplying factors of 0.607, 0.705, and 0.83, respectively.

From the above discussion it may be seen that the illumination was less than ideal, and possibly responsible for some of the relatively low capture efficiency of the 48 dipole array as determined by the procedure that was used for measuring the power density at the receiving array location.

There were three approaches to determining the power density at the antenna receiving location. A crude method was to use an exposure meter manufactured by Narda. However, this instrument provides only a rough order of magnitude and is subject to both validity and repeatability errors. A second method is to compute the density at the center of the gaussian beam based upon theory. This computation gives the ratio of the power density at 145 inches from the phase center to the power injected into the throat of the horn, under the assumptions of perfect performance of the horn including no losses within the horn structure itself. This turned out to be  $1.02 \times 10^{-4}$  mw/cm<sup>2</sup> for each milliwatt injected into the horn throat. However, because of the power density falling off from the center, the average power density over the face of the 48 dipole receiving array would be down by the multiplication factor of 0.85, or down to 0.86 mw/cm<sup>2</sup> for each milliwatt of power into the throat. This computation is based upon a knowledge of how the power density falls off from the center of a gaussian beam and how it can be integrated to find the power within a given distance from the beam center.



89 0380C

Figure 6-17. The dual-mode horn which has negligible sidelobes has made it possible to obtain much good data, including antenna field patterns of the 48 dipole array, in an inclosure bounded by side, floor, and ceiling that were untreated with absorbing material. It is also possible to easily compute the curvature of the beam phase front and the amplitude variation at the test position of the 48 dipole array which was about 12 feet away. See figure 6-18 for a comparison of the experimental antenna pattern that was obtained and a gaussian beam configuration.

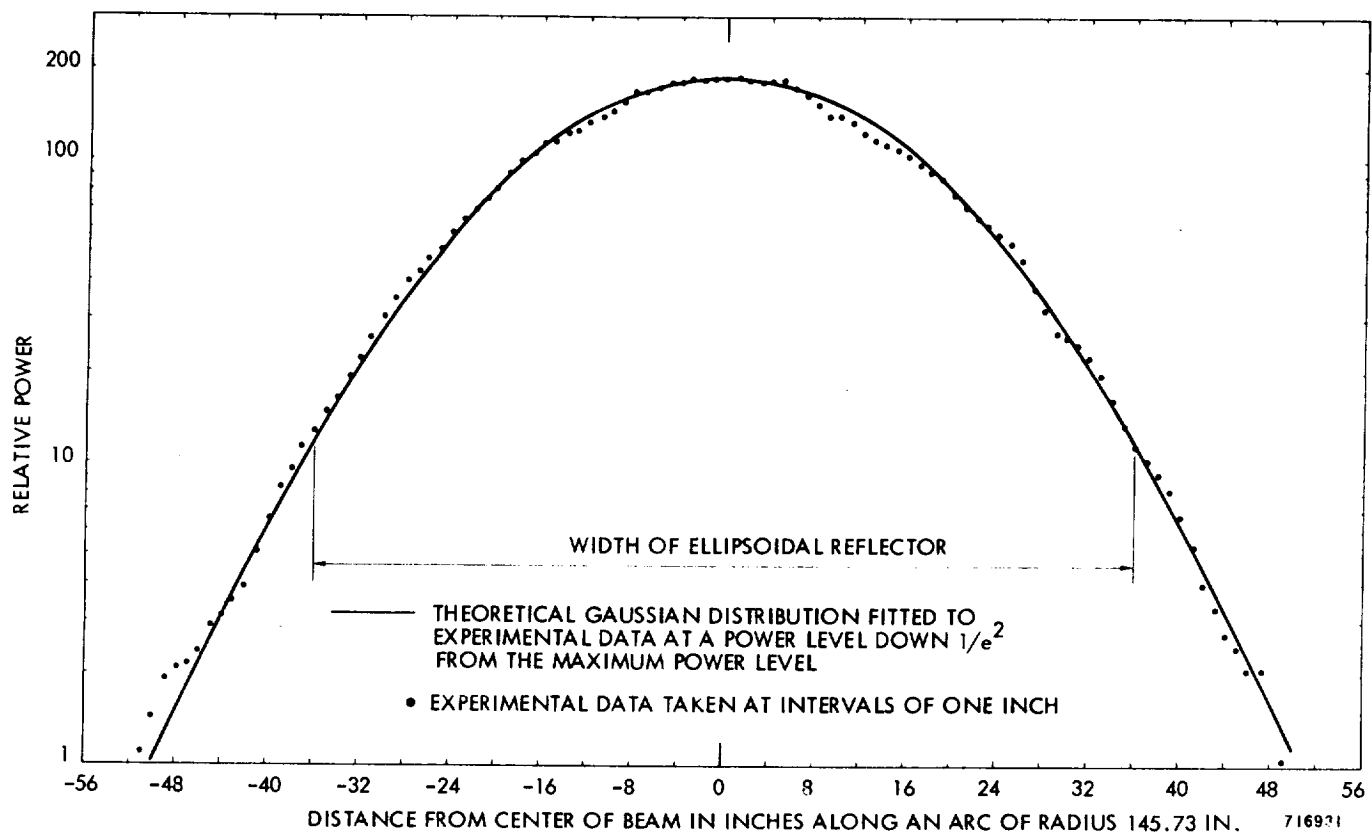


Figure 6-18. Dual mode horn beam pattern at a distance of 145 inches from the phase center at the mouth of the horn.

The value of power density that was used in the capture efficiency measurements, however, was based upon the use of the Polarad Calibrated Directional log periodic antenna, Model CA-LPR. A side view of this antenna and its effective area as a function of frequency is shown in Figure 6.18. This antenna has a physical interception area of about 254 sq. inches or 1640 sq. cm. as compared with 3186 for the 48 dipole array. Its effective capture area, however, as obtained from Figure 6.19 is only 410 sq. cm. With an injected power of 500 milliwatts into the horn throat, 16 milliwatts was picked up by the Polarad antenna, thus giving a ratio of power density to injected power input of  $0.78 \times 10^{-4}$ . This compares favorably with the value computed for the gaussian beam, particularly so if there are some  $I^2R$  losses in the dual mode horn and the formation of a less than ideal or theoretical beam.

If the value of  $0.78 \times 10^{-4}$  mw/cm<sup>2</sup> is used and multiplied by the total interception area of the rectenna which is 3186 sq. cm., the total power pickup would then be 0.248 mw for each milliwatt injected into the throat of the horn.

The actual power absorbed by the 48 dipole antenna arrays was considerably less than this. The first array absorbed only 0.083 mw for each mw of power injected into the throat of the horn while the second antenna that had a much better match to the 50 ohm output absorbed 0.110 mw for each mw injected into the horn. Thus the apparent absorption is only 45% of the incident power.

To explain this difference various multiplying factors corresponding to several different kinds of losses can be introduced:

- o losses from  $I^2R$  losses in the internal transmission lines of the 48 element arrays 0.85
- o losses caused by failure to introduce side lobes back into the illumination pattern of a uniformly illuminated aperture. 0.86
- o losses caused by lack of phase coherency across the radiating surface-also amplitude variation 0.8

The multiplication of these factors reduces the efficiency to 58%

In addition to the above factors there appears to be one associated with the size of the aperture. These are edge effects that affect the gain and the absorption efficiency. In the case of a 64 slot array, not too much larger than the 48 element array, the measured gain was decreased by one db or a factor of 0.79, and this agreed with the gain obtained when the radiation from each of the slots was computed and then summed. This would reduce the efficiency further from 58% to 46% and the factor could be larger for a smaller element array. However, as will be noted in the following discussion on antenna patterns, the position of the first side lobes indicate that the correction factor is only about 6% for effective aperture reduction.

#### 6.26. H-plane and E-plane antenna patterns

The interfering reflections from the walls, floor, and ceiling were so reduced

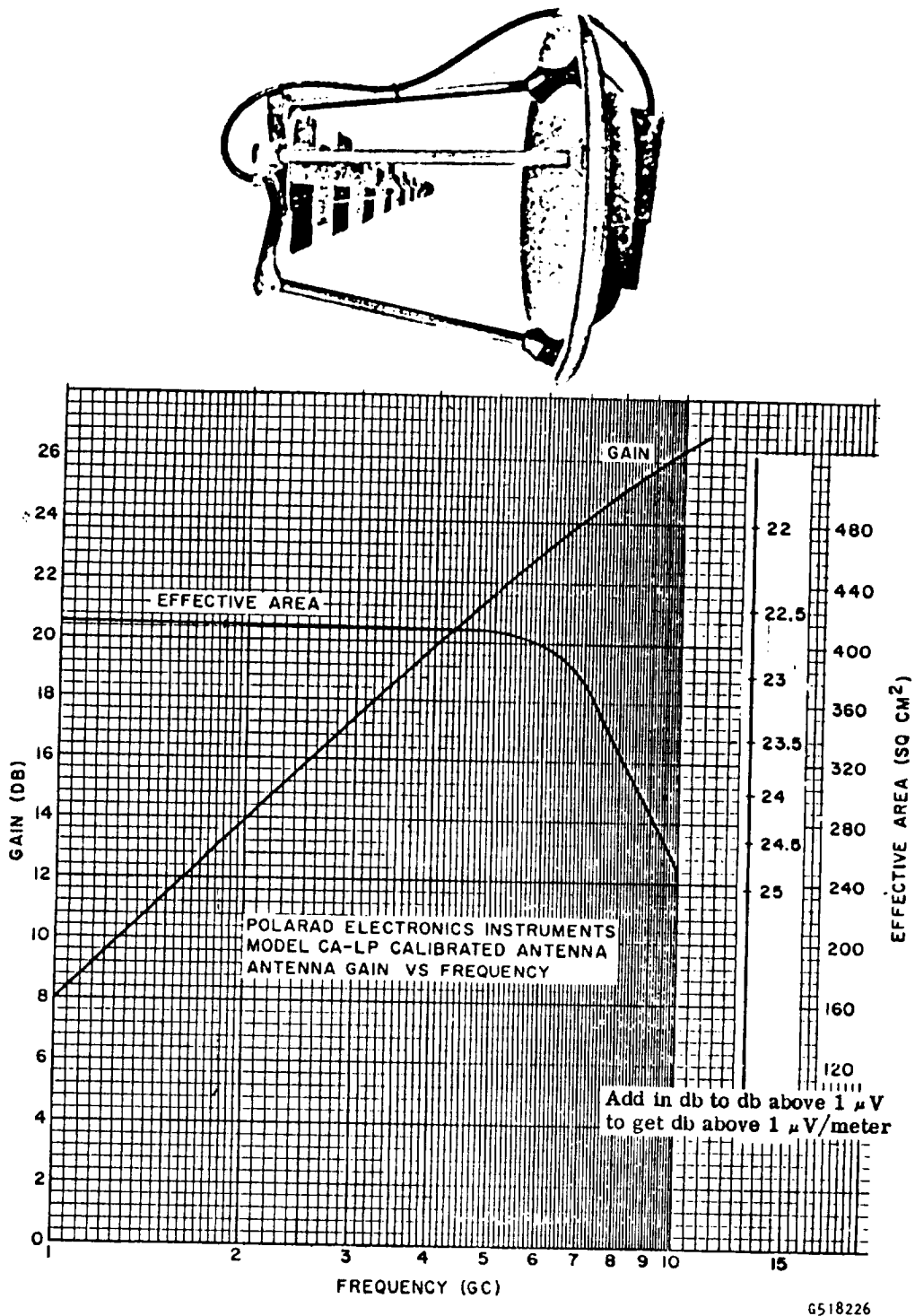


Figure 6-19. This field intensity measuring antenna was mounted on the tripod shown in figure 6-1, and measurements made of intercepted power from the dual mode horn . This measurement of power density, although subject to validity criticism was used to evaluate the efficiency of the 48 dipole array.

with the use of the dual mode horn that relatively good antenna patterns could be obtained by rotating the 48 dipole array around its vertical and horizontal axes while mounted on the tripod. (Figure 6.1) There did appear to be some interference from floor reflections in taking the E-plane pattern.

The H-plane and E-plane patterns are shown in Figures 6.20 and 6.21. respectively. The H-plane pattern shows first sidelobes at 17 degrees of rotation from normal incidence.

The angular position of the sidelobes can be used for an indication of the effective width or height of an array. This follows from the dependency of the position of the sidelobes upon the dimension of the antenna, as given for example by Silver (pages 180 and 181 of "Microwave Antenna Theory and Design") according to the following expression:

$$\theta = \sin^{-1} \frac{\lambda u}{\pi b}, \text{ where}$$

b = long dimension of the array  
 $\lambda$  = wavelength of the radiation (12.26 cm.)  
u = 4.4 for a uniformly illuminated array  
(Fig. 6.3 of Silver)

If the 26 inch width of the picture frame is used as b, the predicted sidelobe should be at 15 degrees.

Conversely, the above equation can be used to solve for b if the position of the sidelobe is found experimentally. The b that corresponds to 17 degrees is 23.1 inches. So that the effective aperture is reduced from the actual aperture of 26 inches by the factor 0.88.

On the other hand if we examine the E-plane pattern which applies to the height of the array, the effective aperture in that dimension is larger by the factor of 1.05.

So if these two corrections are multiplied together to obtain an effective aperture area for the array, the effective aperture is smaller than the physical aperture of 19 x 16 inch which has been used for efficiency collection computations by the factor of 0.933. This factor would further reduce the efficiency from 58%, as discussed in the previous section, to 54%.

It is apparent that the 48 dipole array is far from 100% efficient for the variety of reason just discussed. However, many of the factors have been quantified by estimate only, and before improvement of those factors is undertaken, the validity of the overall efficiency measurement should be improved by placing both the 48 dipole array and the Polarad calibrating antenna on a more nearly uniformly illuminating beam that has minimal phase front deviation from a plane wave front. This would require separating the illuminating horn and the 48 dipole array by a factor of at least two over the present separation. An outdoor range or a very large anechoic chamber would seem to be necessary for this undertaking.

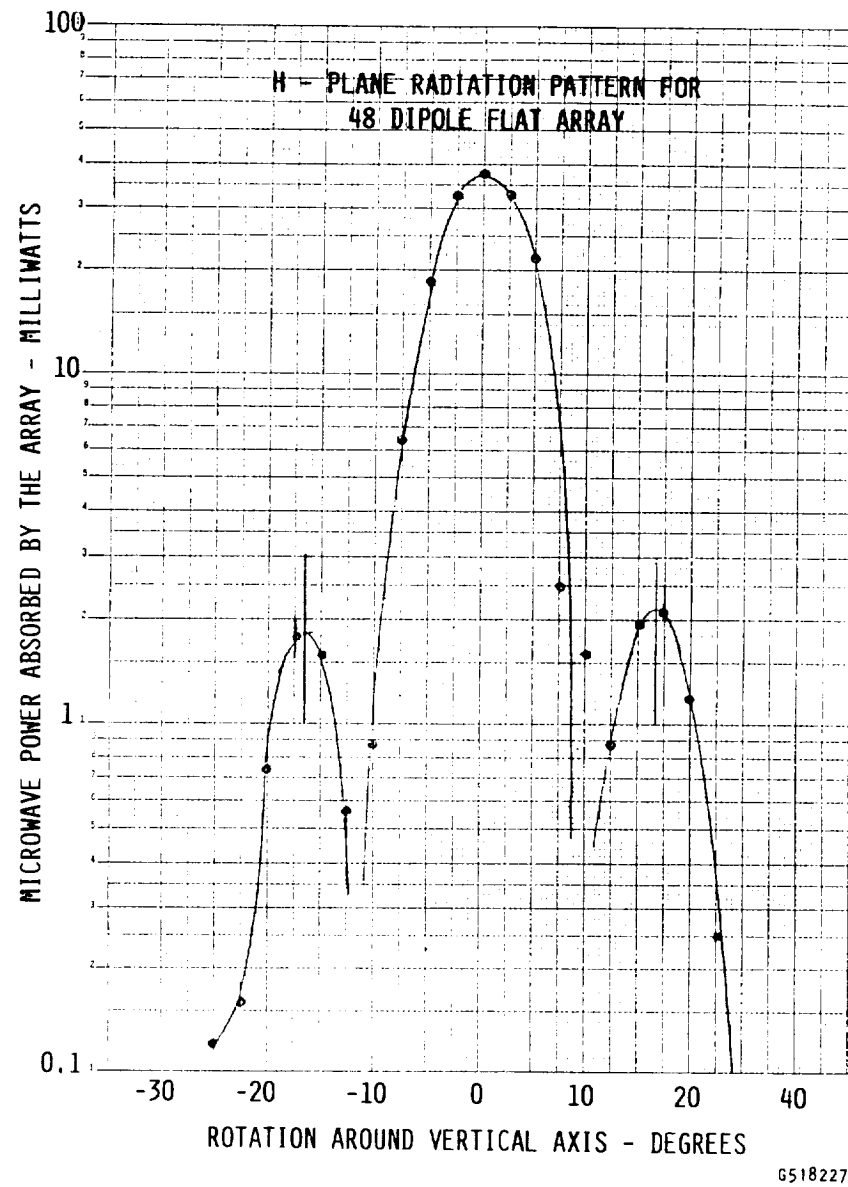


Figure 6-20. Angular position and amplitude of side lobes provide interesting information about the 48 element array. Theoretically, for a uniformly illuminated array, the first side lobes should be down by a factor of 20. They are down by a factor of 19. They are also slightly further removed in angular position than theory predicts.

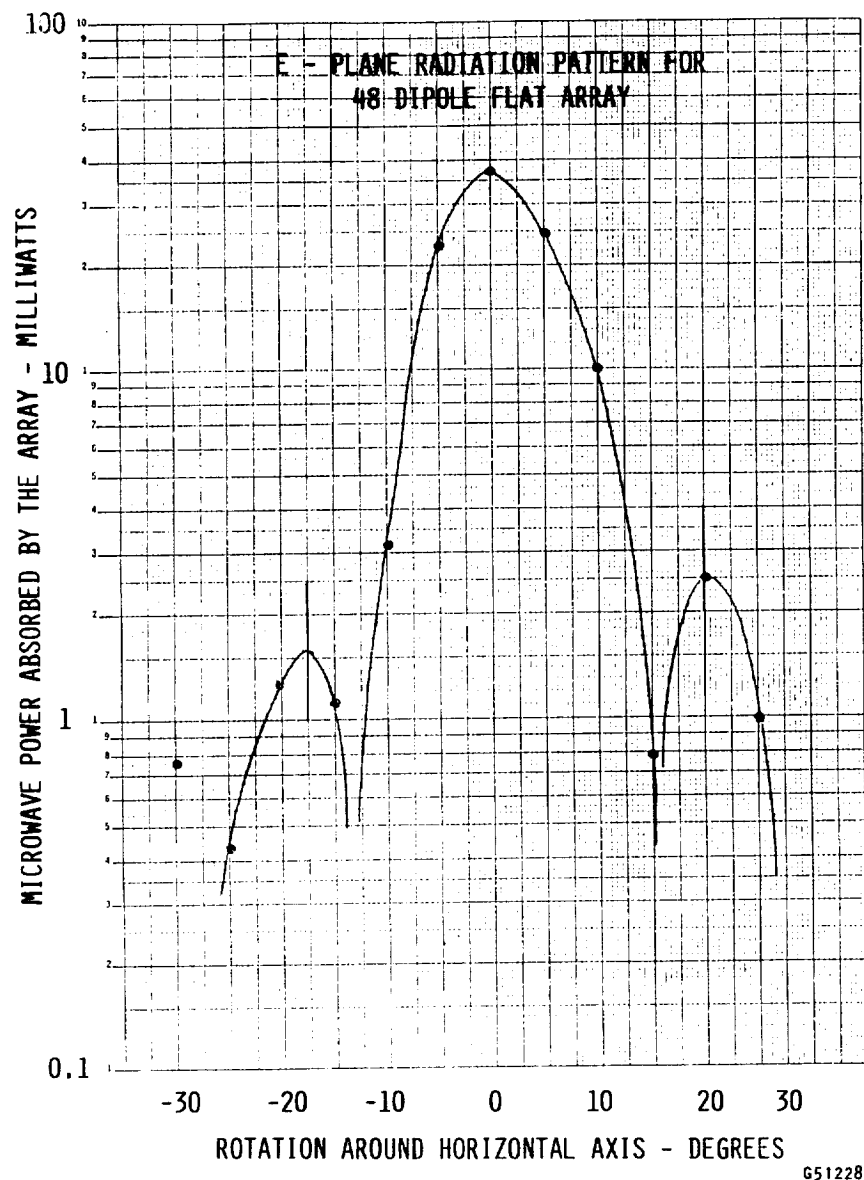


Figure 6-21. E-Plane antenna pattern data. This pattern is not symmetrical and not as good as the H-plane pattern, probably because there was some power reflected from the floor which distorted the left hand side of the above pattern which corresponded with the rotation of the antenna toward the floor.

## 6.3 An alternative rectenna design for use in the equatorial plane

### 6.3.1 Introduction

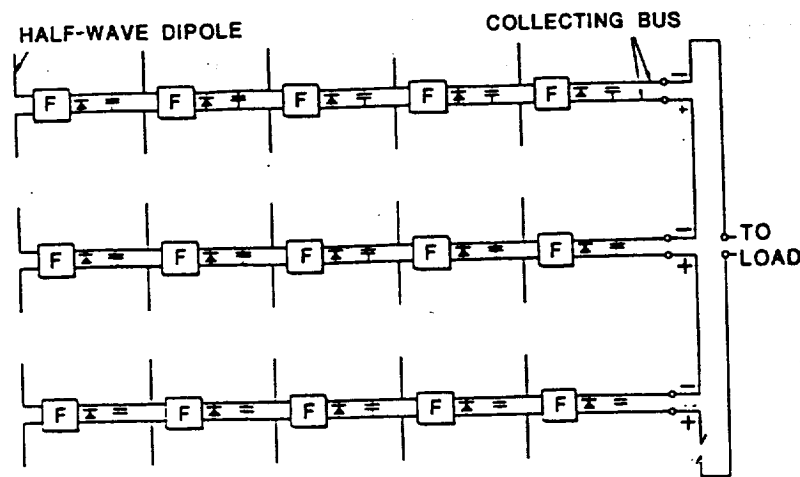
As it was explained in the introduction, for a rectenna that is used solely in the equatorial plane and that is illuminated from Earth transmitting stations placed on the equator, there is no necessity for "non-directivity" in the north-south direction. This relaxation in the performance requirements allows the collection of energy along a conventional linear array of dipoles by a transmission line which is connected to a termination consisting of first a low pass filter and then the rectification circuit to convert the microwave energy back into well filtered DC power. A rectenna consisting of many such linear arrays placed in parallel and closely together will be highly nondirective around the axes of the linear arrays. As indicated in the introduction such a rectenna has a number of advantages that includes (1) a means of attenuating to almost any degree the harmonics that result from the rectification process, (2) the operation of the diode rectifiers at a higher efficiency, and (3) a considerable reduction in the number and cost of the diodes. Typically, there will be a decrease in the number of diodes by a factor of 8 or 10 with an accompanying reduction in cost in the same proportion because the individual diodes will cost about the same. Eventually, as a result of learning experience, the individual diodes will be very low in cost, but initially the diodes will represent the predominant cost element in early rectenna production.

To help put the proposed linear rectenna into perspective, Figure 6.22 shows its relationship both physically and historically, to first the conventional rectenna in which there is one diode rectifier for each dipole antenna element, and then to the broadside array in which there is only one diode for the whole array. The proposed linear array with a single diode for a limited number of dipole antenna elements is shown at the bottom of the figure.

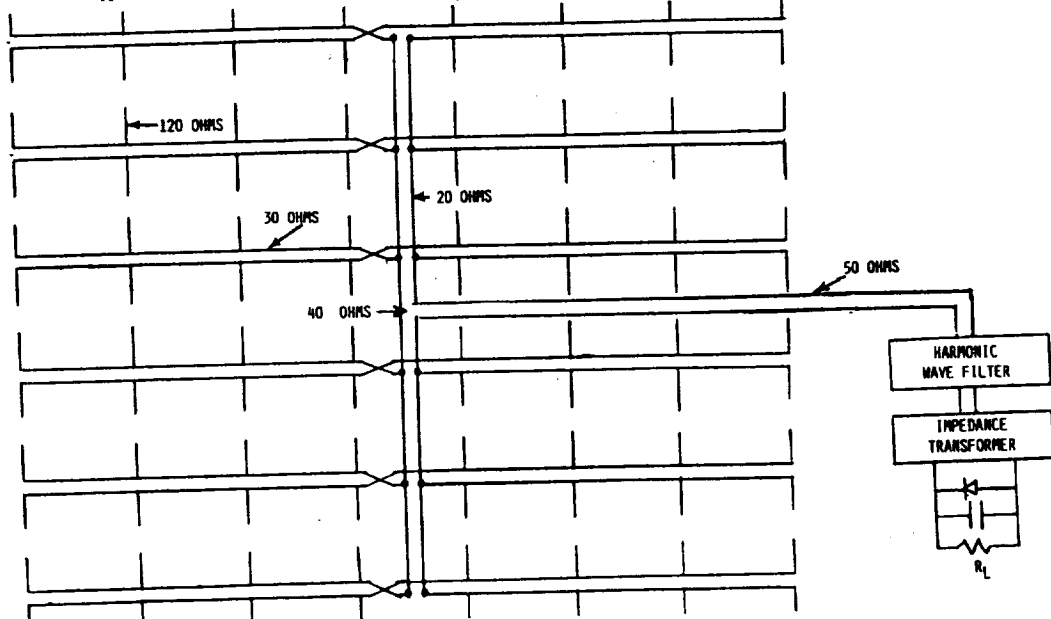
### 6.3.2 The linear dipole array

In section 6.2.4 , "Step 1" of the construction of the broadside array resulted in the construction of the prototype for the linear dipole array that is now being discussed. This prototype linear dipole array is shown in figure 6.23. Figure 6.24 shows how two sets of four 120 ohm dipoles which are connected in parallel to 30 ohm transmission lines are then connected in series to provide a nominal input impedance of 60 ohms.

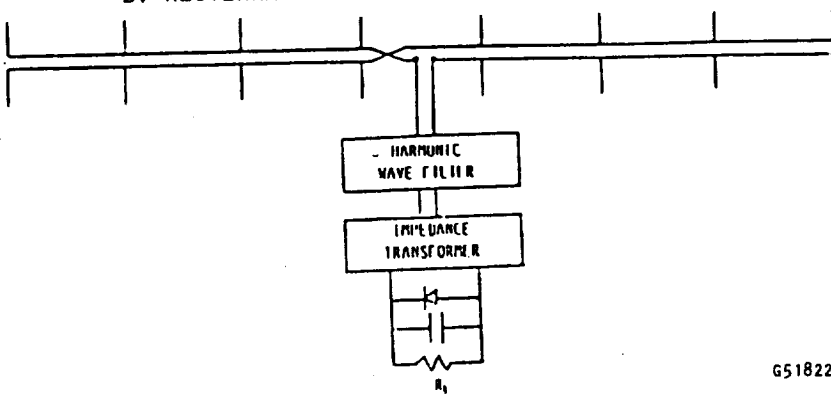
As was done for the entire array in figure 6.16, the phase and amplitude of the radiation from each of the eight dipoles in the linear array were made. Figure 6.25 presents this data. For comparison purposes, the rms phase variation was 9.9 degrees which would result in negligible scattering. The amplitude variation is also very small. The performance of the linear array with respect to phase and amplitude variation is considerably better than for the complete broadside array as presented in figure 6.16.



A - STANDARD RECTENNA-NON DIRECTIVE ABOUT BOTH AXES

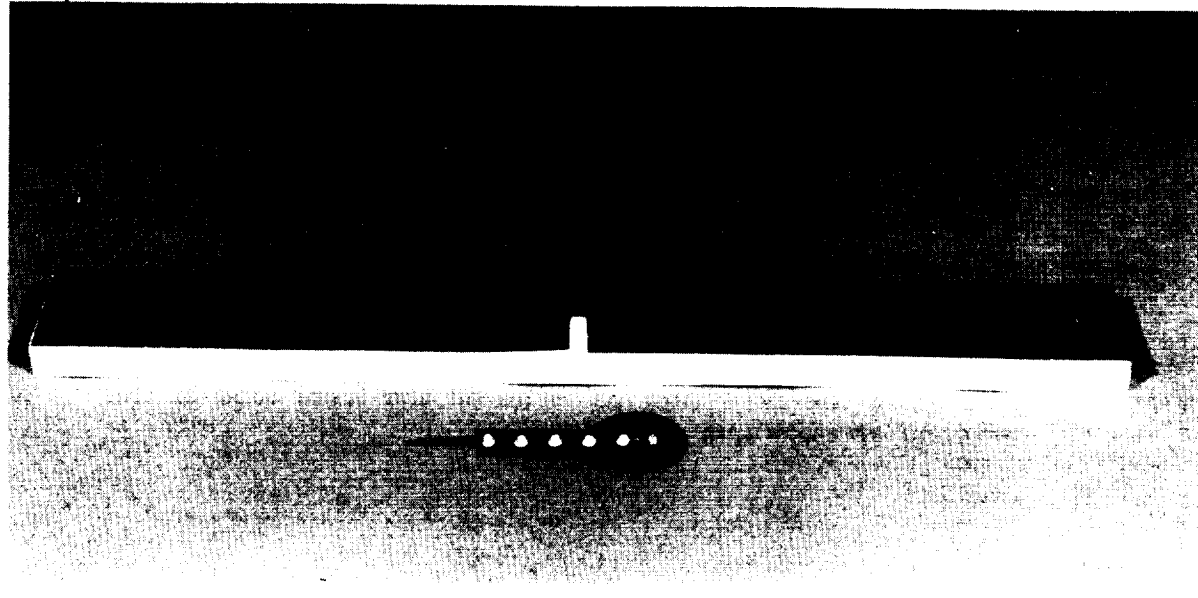


B. RECTENNA THAT IS DIRECTIVE ABOUT BOTH AXES

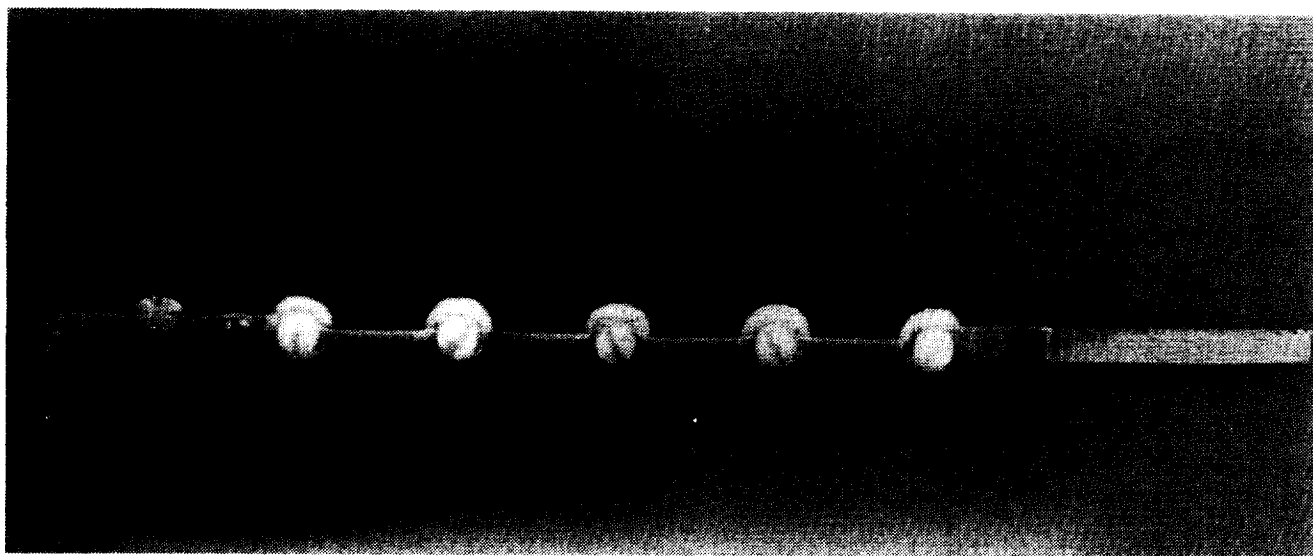


C. PROPOSED RECTENNA, NON-DIRECTIVE ABOUT ONE AXIS

Figure 6-22. A comparison of the proposed new rectenna design shown at the bottom of the above figure with the standard rectenna approach at the top and the broadside array approach shown in the middle.

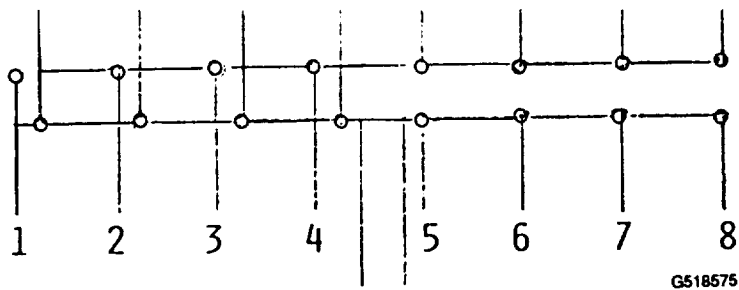


89-3768C



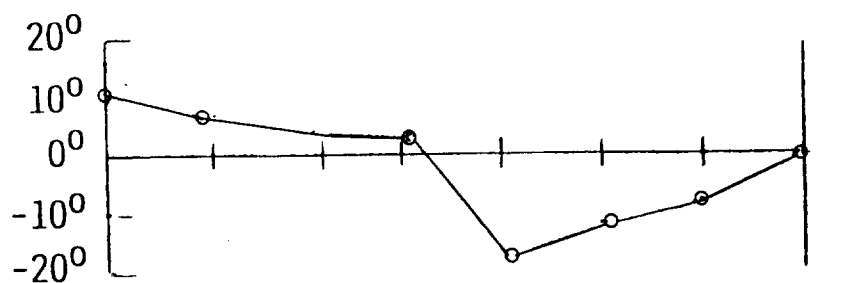
89-3769C

Figure 6-23. Proposed rectenna design that consists of an eight dipole linear array that is terminated with a four section low pass filter and the microwave rectification circuit. The banjo shape of the filter-rectification termination results from surrounding the diode with a circular radiator fin to radiate the heat resulting from any diode inefficiency directly into space.



SCHEMATIC OF DIPOLE INTERCONNECTION WITH TRANSMISSION LINE

Figure 6-24. Schematic of the connection of dipoles to two transmission lines which are then connected in series. This arrangement results in generating the reversing patterns on the front side of the rectenna as shown in figure 6-1.



PHASE VARIATION WITH DIPOLE POSITION

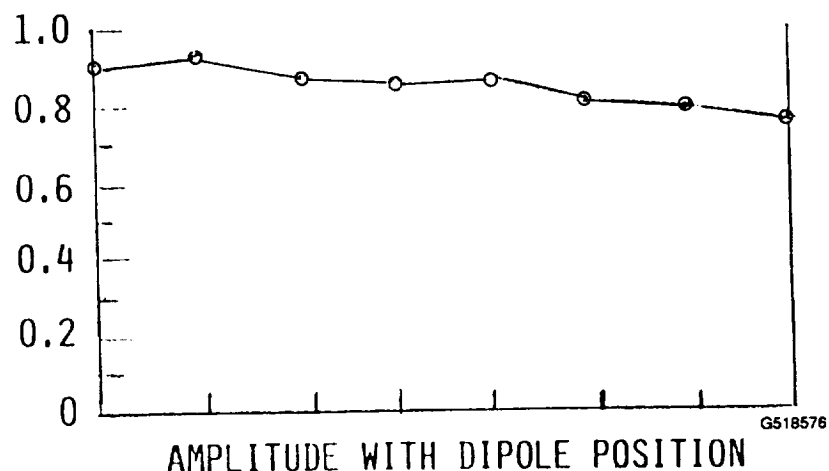


Figure 6-25. Phase and amplitude of the radiation from each dipole in the 8 dipole array. The rms phase variation is only 9 degrees which would result in minimum scattering and loss of efficiency of the beam.

### 6.3.3 The microwave filter and rectification cartridge.

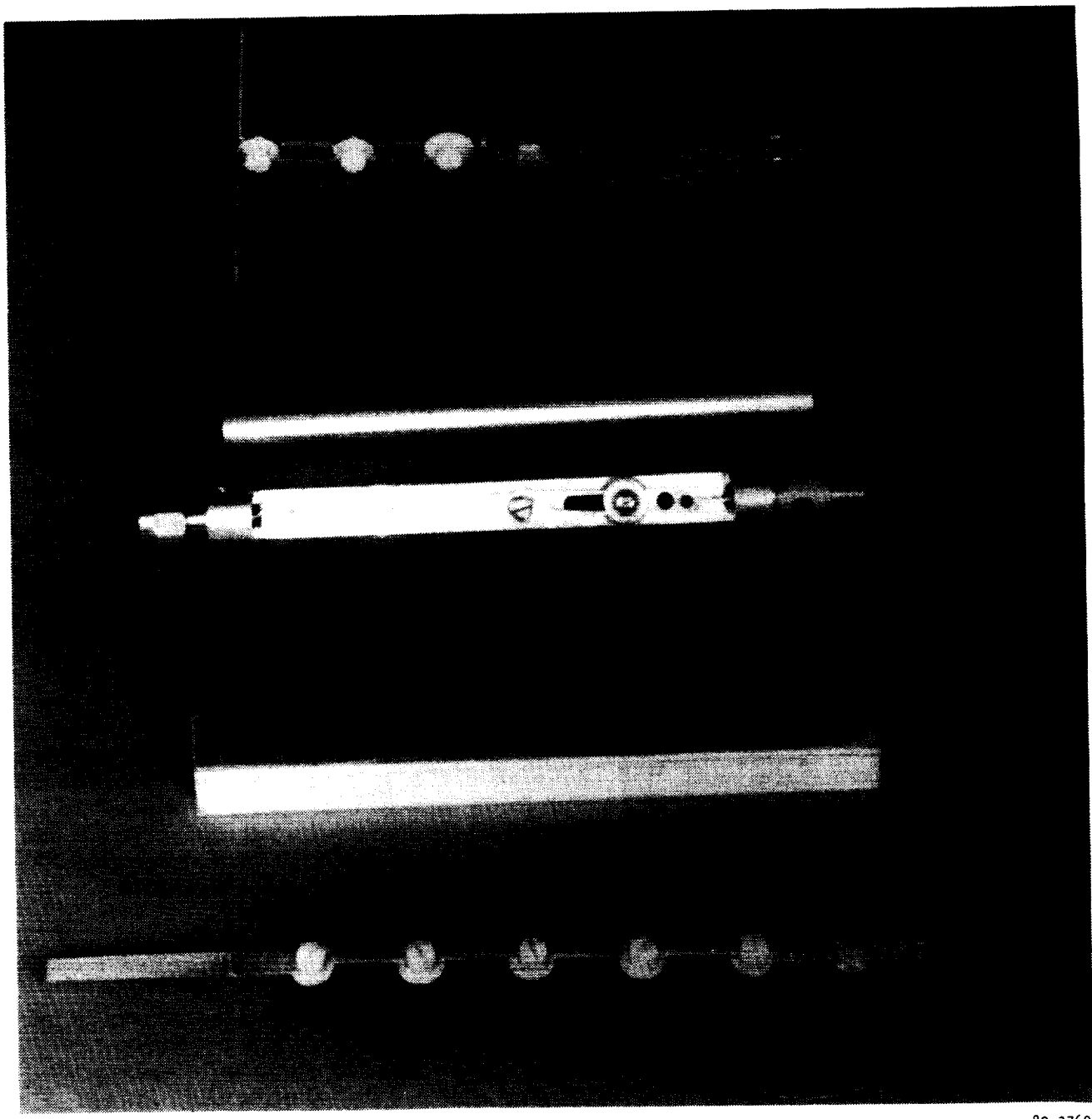
The microwave filter and rectification functions can be physically combined in one structure. This unification can be considered as a historical derivative of the standard rectenna element as shown at the top of figure 6.26 . This plug in element was used in the highly successful demonstrations of 54% overall DC to DC efficiency in the laboratory and in the demonstration at the Goldstone facility of the Jet Propulsion Laboratory when over 30 kilowatts of rectified DC power was obtained from a microwave beam source located one mile away.

This plug in unit has a balanced circuit with a characteristic impedance of 120 ohms which is matched to the 120 ohm dipole antenna. However, it can be converted into an unbalanced circuit by mechanically and electrically splitting the balanced circuit with a ground plane passing through its center. When this is done the propagation characteristics of the filter remain the same except for its characteristic impedance which is halved to 60 ohms. If the dipole antenna is removed, the remaining structure can be converted into coaxial structure shown in the middle of figure 6.26.

However, the coaxial structure has a number of disadvantages. It is comparatively massive and the diode does not have an opportunity to pass the heat generated by its inefficiencies along to a large sized radiator for radiation of heat into space. Also it is awkward to pass the cylindrical shield over the active part of the capsule and if there are many sections of low pass filter the shield will have to be electrically bonded to the center core in many locations to prevent transmission of harmonic power from the rectifier back to the input. For a discussion of this see section 6.2.3.

The construction of the cartridge at the bottom of figure 6.26 is more nearly of a prototype nature , although the mass of its components could be reduced considerably. In this construction the diode sits in the middle of a large radiating fin which can adequately dissipate at relatively low temperature the two or three watts of heat that result from the diode's inefficiency. Tests of the ability of the diode to so dispose of the heat resulting from its inefficiency have been made and are discussed in section 6.3.5

The construction shown at the bottom of figure 6.26 is very attractive from the parts fabrication and assembly point of view. The ground plane and heat radiating fin can be one contiguous piece of black anodized aluminum of five or ten mil thickness. The low pass filter sections should probably consist of sections of an open air transmission line, to minimize dielectric losses, and lumped capacitors constructed from material with the lowest dielectric loss possible. As discussed in section 6.2.3 filter losses should be minimized as much as possible. Finally, the shield can be formed from very thin sheet metal and bonded to the rest of the ground plane to prevent any radiation as well as to provide the whole assembly with an element of mechanical stiffness if it is wanted or needed. Ultimately, if mass of the assembly becomes an important issue , it will probably be found that the mass of the heat radiator will predominate . In this case, it should be pointed out that if the radiator is made from pyrolytic graphite, which has a density slightly less than aluminum but heat conductivity about six times that of aluminum, the mass of the radiator can be greatly reduced.



89-3769c

Figure 6-26. Historical evolution of the proposed filter-rectification package shown in experimental form at the bottom of the illustration. It has evolved from the balanced circuit format shown at the top of the illustration and which was used in rectennas for many years. The embodiment of an unbalanced version in a coaxial line format is shown in the middle. The coaxial approach, however, has a number of problems that are discussed in the text. These problems are resolved by the proposed construction shown at the bottom of the illustration.

### 6.3.4 High diode efficiency at high power levels.

In the introduction it was noted that the efficiency of GaAs diodes operating at high power levels was considerably better than when operating at lower power levels. And in the context of efficiency at high power levels , GaAs Schottky barrier diodes are very much superior to silicon Schottky barrier diodes.

In fact, few developments have had the impact upon the potential of beamed microwave power transmission that the heat-sunked GaAs Schottky-barrier diode has had. It is highly efficient, can handle large amounts of microwave power input, and can operate at a high temperature consistent with the need to radiate into space any heat that may result from any inefficiency in its operation. As shown in Figure 6.27, the diode is packaged in a format that is excellent for conducting heat away from the diode.

The diode has received a large amount of operational experience in such projects as the JPL-Raytheon Mojave Desert demonstration of the transmission of more than 30 kilowatts of continuous power by microwave beam over a distance of one mile. And it has withstood rigorous life testing as reported upon in section 4.2 of NASA CR-135194.

A comprehensive experimental investigation into diode efficiency as a function of operating power level was made under Contract NAS3-19722 and reported upon in the final report NASA CR-135194. Under this contract, a method was developed to directly and accurately measure the heat resulting from the microwave power being dissipated in the diode when the diode was part of an unbalanced circuit with a ground plane, exactly analogous to the arrangement that is being currently discussed. Table 2-1 from that report is reproduced as table 6.1 in this report. Table 6.1 indicates that the respective diode losses (see column F) for incident microwave power levels of 1,2, and 8 watts were 14.3%, 11.3% and 7.4% , respectively.

In the conventional rectenna design for space applications, a microwave power input of from 1 to 2.5 watts per dipole is being proposed. Hence, in the case of a single diode per each dipole element, the diode inefficiencies will be greater than 10% of the microwave input. On the other hand, if power is collected from eight dipoles, a situation corresponding to that of the linear dipole array shown in figure 6.23, then the incident power on the diode will range from ten to 25 watts, a region in which it appears that the diode inefficiencies should be well below 10%.

There is only a limited amount of experimental data on diodes being operated at power level in excess of ten watts, but the experimental data that does exist as well as the data resulting from theoretical considerations indicate that the high efficiencies should continue or even increase at power levels of as much as 25 watts per diode. The data that does exist is given in tables 6.2 and 6.3. In examining these tables it should be noted that overall rectenna element efficiency is being considered and that the diode accounts for only a portion of the corresponding inefficiency. It is also noted that the diodes that are designed for higher power will have larger junction areas and therefore greater heat dissipation capability at the junctions. it is also noted that these GaAs diodes are of the mesa type of construction and that

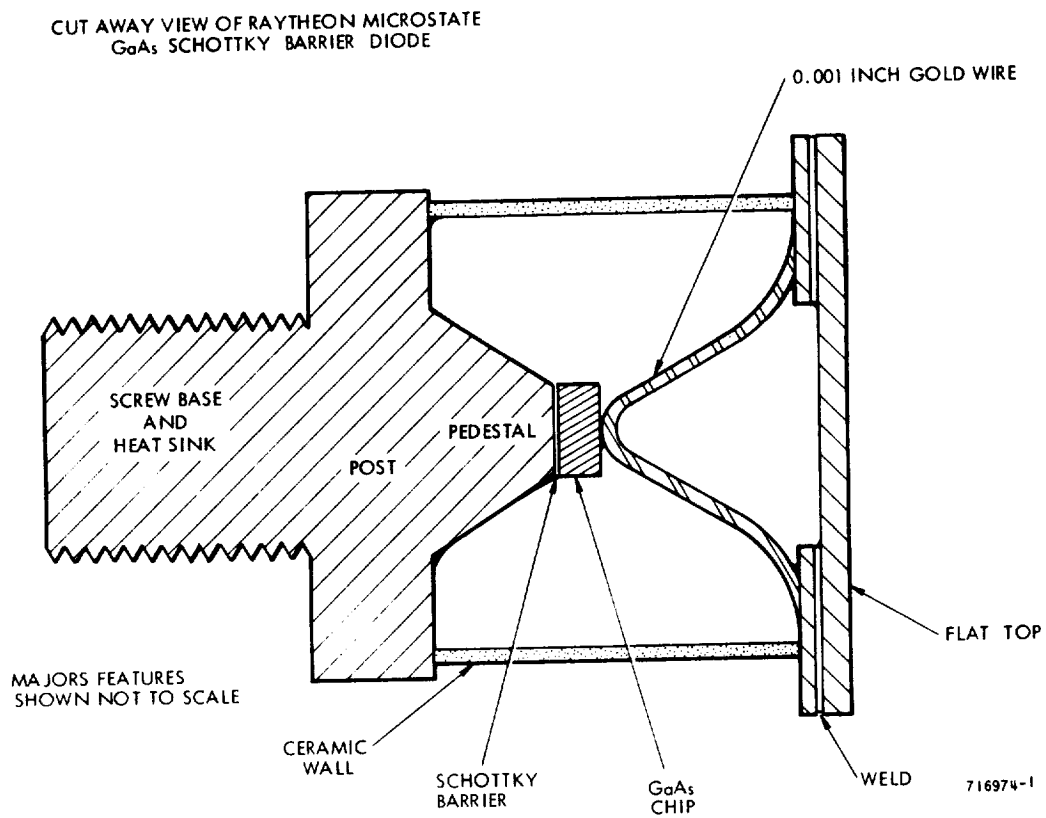


Figure 6-27. The efficient heat-sunk gallium arsenide diode shown above in its packaged form is a key component in the proposed new rectenna approach. When operated at the ten watt or more level the losses in the diode can be as low as 7% of the microwave input power. The diode can easily transmit 3 watts of heat to a radiator of the form shown in figure 6-26 which in turn can radiate the heat to space at a temperature much below the operating temperature limits of the diode. It follows that the diode can easily handle the twenty watts of microwave power at which it may be required to operate in the new rectenna approach.

**TABLE 6-1**

DC Power Output, Diode Losses and Circuit Losses  
as % of Absorbed Microwave Power \*

A Incident Microwave Power Level	B DC Load Resistance (ohms)	C Absorbed Power in Element (Watts)	D Reflected Power (Watts)	E DC Output as % of C	F Diode Losses as % of C	G ** Measured and Computed Circuit Losses % of C	H Total Measured Losses and DC Power Output E + F + G	I 100% - H
0.100	80	0.085	0.015	56.50	36.0	2.62	95.12	4.88
0.200	80	0.180	0.020	66.70	28.26	2.62	97.58	2.92
0.400	80	0.375	0.025	74.30	21.86	2.62	98.78	1.22
0.600	80	0.573	0.027	77.80	18.84	2.62	99.26	0.74
0.800	80	0.772	0.028	80.00	17.34	2.62	99.96	0.04
1.000	80	0.991	0.009	82.30	14.30	2.62	99.22	0.78
2.000	80	1.997	0.003	86.12	11.33	2.62	100.07	-0.07
3.000	80	3.000	0.000	87.60	10.17	2.62	100.39	-0.39
4.000	80	3.998	0.002	88.45	9.24	2.62	100.31	-0.31
5.00	80	4.992	0.008	89.06	8.77	2.62	100.45	-0.45
6.00	80	5.984	0.016	89.50	8.39	2.62	100.51	-0.51
7.00	80	6.972	0.028	89.95	8.11	2.62	100.68	-0.68
8.0	80	7.957	0.043	90.26	7.93	2.62	100.81	-0.81
8.0	90	7.958	0.062	90.59	7.51	2.62	100.72	-0.72
8.0	100	7.850	0.150	90.54	7.40	2.62	100.56	-0.56

\* Test made use of grounded-plane test fixture and diode No. 40593 - CPXIG No. 13, a GaAs-Pt standard reference diode.

\*\* This value is a composite of following measured and computed inputs.

Measured loss at fundamental frequency in microwave input filter is  $2.37\% \pm 0.3\%$

Computer simulation of loss including harmonics in input filter is  $1.83\%$ .

Computer simulation of other circuit losses is  $0.25\%$ .

Computer simulation of all circuit losses is typically  $2.08\%$ .

The decision was to add the measured input filter loss at  $2.37\%$  to the  $0.25\%$  "other circuit losses" computed by computer and add an uncertainty factor to give  $2.62 \pm 0.4\%$ .

TABLE 6-2

SPECIAL HIGH CAPACITANCE DIODES CHECKED OUT AT HIGH POWER OUTPUT  
 IN A RECTENNA ELEMENT WITH AN IMPEDANCE INPUT OF 60 OHMS.  
 (WORK REPORTED IN REPORT #11, MAY 1976 OF LERC CONTRACT NAS 3-19722)  
 DIODE  $C_{TO}$  = 7.5 PF,  $V_{BR}$  = 70 VOLTS.

DC Power Output (Watts)	Load Resistance (Ohms)	Efficiency (%)
9.45	80	86.7
10.7	80	86.9
15.1	80	87.3
16.46	70	87.5

TABLE 6-3

COMPARISON OF PERFORMANCE OF HIGH CAPACITANCE DIODE  
 WITH THAT OF THE FIRST 500 DIODES FOR THE GOLDSTONE RXCV

	First 500 RXCV Diodes	Special High Capacitance Diode
$C_{TO}$ Capacitance	3.7 (Avg.)	7.5
Input Microwave Power	6 watts	10 watts
Load Resistance	160 ohms	80 ohms
Reflected Power	0.040 (typical) Watts	0.125 watts
Efficiency	86.3% (Average)	87.1%

(NOTE) EFFICIENCIES GIVEN ARE FOR THE COMPLETE RECTENNA  
 ELEMENT - NOT JUST THE DIODE.

diodes with larger junction areas are easier to fabricate. These diodes should therefore be no more expensive than low power diodes.

#### 6.3.5. Experimental data on radiation cooling of diodes in vacuum.

In the previous section it was noted that GaAs diodes when operated at the ten watt level or above can easily have inefficiencies of 10% or less. If the inefficiency is 10% then it follows that if power dissipation is the limiting factor the diode can handle an amount of microwave power input that is ten times greater than the dissipated power. Thus, if the diode can dissipate 3 watts, a power input of 30 microwave watts and a rectified dc output of 27 watts follows.

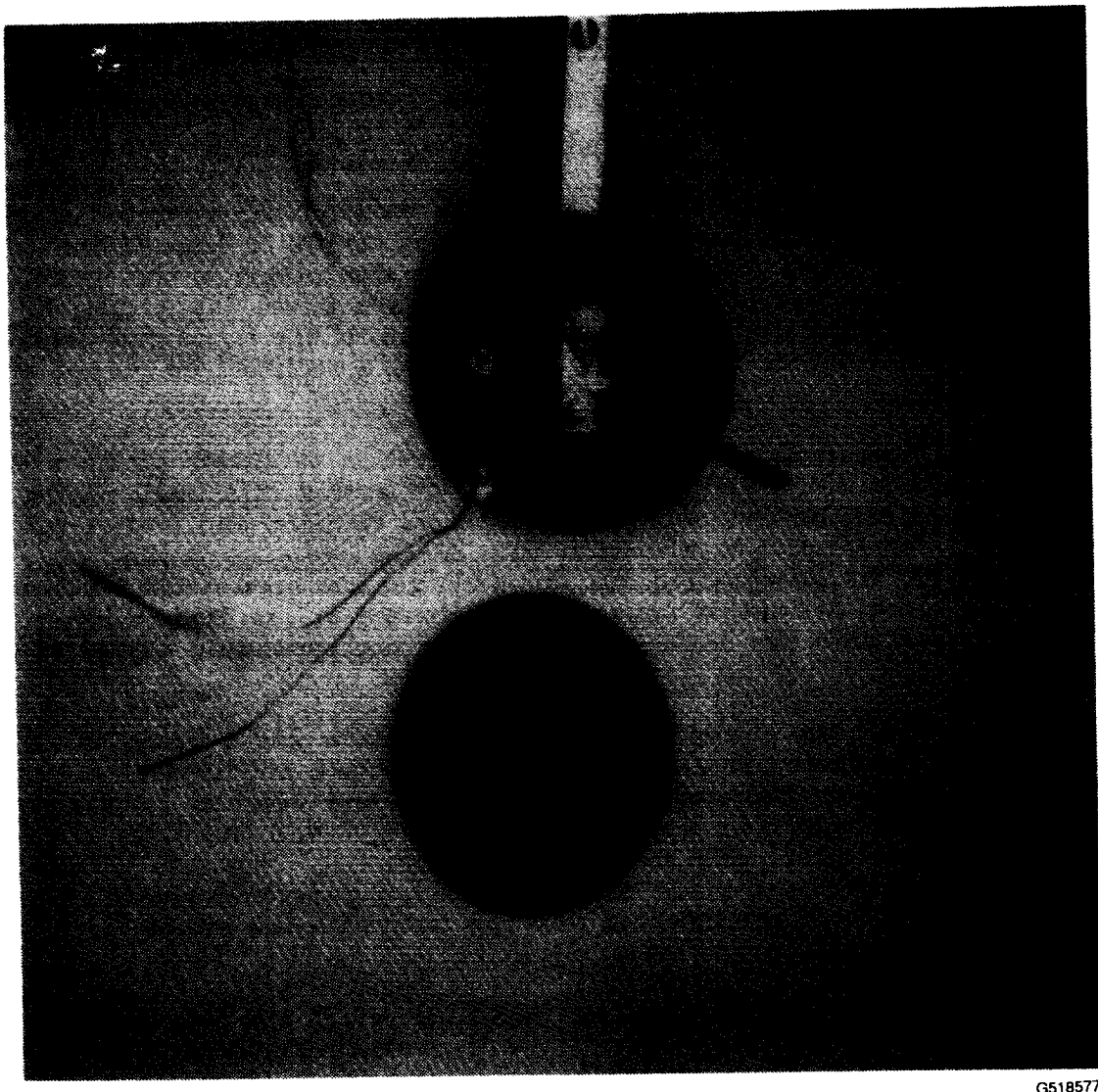
What has been needed is some experimental operation of diodes within a vacuum to determine if the dissipated power which is generated in a small region within the diode can be conducted to an external radiator and gotten rid of as radiated heat. Some initial experimental data on the radiation cooling of diodes in vacuum by an attached circular radiator has been obtained. In this experiment a known amount of power was dissipated in the diode simply by running dc power into the diode and noting the corresponding values of current and voltage.

In the specific test, the power inserted into the diode was 3 watts. All of this power was conducted to and radiated from a black anodized aluminum disk that was two inches in diameter and 20 mils thick and weighed 2.8 grams. A thermocouple was placed half way between the center and the outer edge of the disk so that the transient and steady state temperature response to a sudden insertion of power into the diode could be noted. Figure 6-28 shows both the radiator disk and the diode inserted into the disk with the attach thermocouple and power input leads.

Figure 6-29 shows the vacuum bell jar facility in which the test was made. The facility was also used for tests on a radiation cooled magnetron which is the item shown in the bell jar in Figure 6-29.

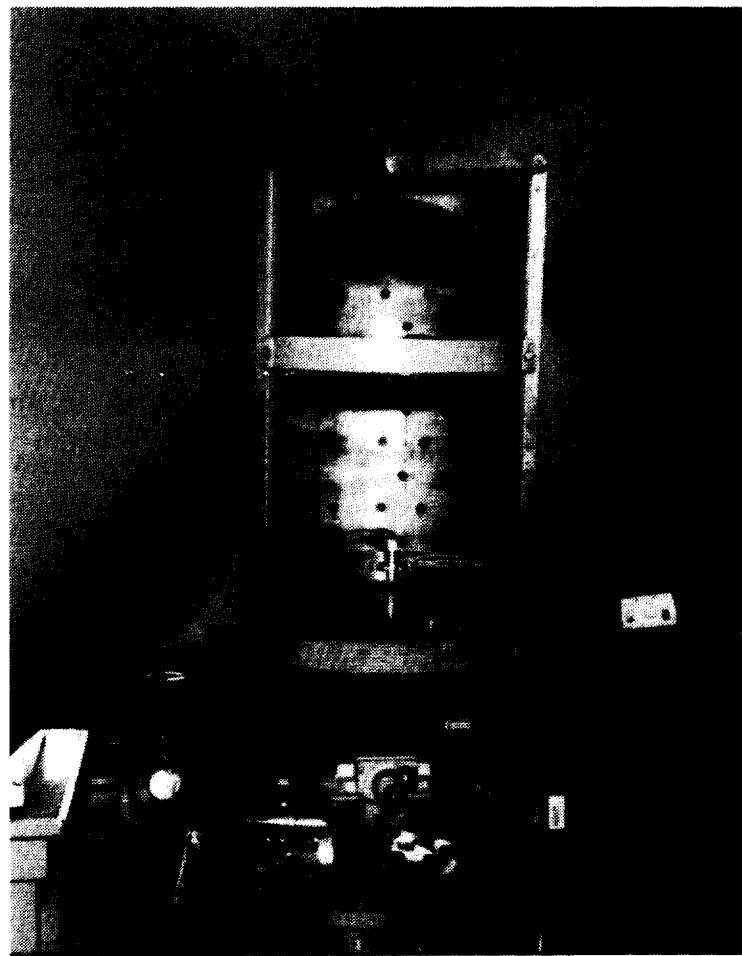
The response curve to a sudden insertion of three watts of power is shown in figure 6-30. It is noted that the steady state temperature reaches 115 degrees Celsius. This is certainly a low enough temperature to allow the diode to keep its Schottky barrier diode interface below 200 degrees Celsius, a temperature where the diode should have very long life.

It is of interest to know what the temperature of the disk is as a function of radial distance from the center. It was not possible to obtain this experimentally, but a worst case situation can easily be determined if it is assumed that all of the dissipated power is conducted from the center of the radiator to its outer edge without any radiation into the vacuum. Under these circumstances the temperature drop in the radiator as a function of radius follows the expression below:



G518577

**Figure 6-28.** Arrangement for disposing of heat generated by the inefficiency of the diode. The diode is inserted into a 2" diameter aluminum disk that has been black anodized. The disk with an emissivity coefficient of over 0.8 radiates the heat into the vacuum of space.



89-3765C1 #15

Figure 6-29. Vacuum bell jar in which the diode with its radiator is placed. Shown in the bell jar is a radiation cooled magnetron for generation of microwave power in space.

$$\Delta T = -\frac{0.038 H \ln r/r_0}{k d}$$

where:  $H$  is the heat in watts being transmitted through the disk  
 $r$  is the value of radius to compute  $T$   
 $r_0$  is the inner radius where the heat is inserted  
 $k$  is the heat transfer coefficient for the conducting material  
 $d$  is the thickness of the material in centimeters

A plot of  $\Delta T$  as a function of radius of the aluminum disk is shown in figure 6-31. Because  $r_0$  is so small, only 0.15 cm, most of the temperature change takes place close to the center of the disk so that the radiating area is so small as to have a negligible influence on the temperature change in that area. Hence the "worst case" expression gives data very close to the real situation when used close to the center of the disk.

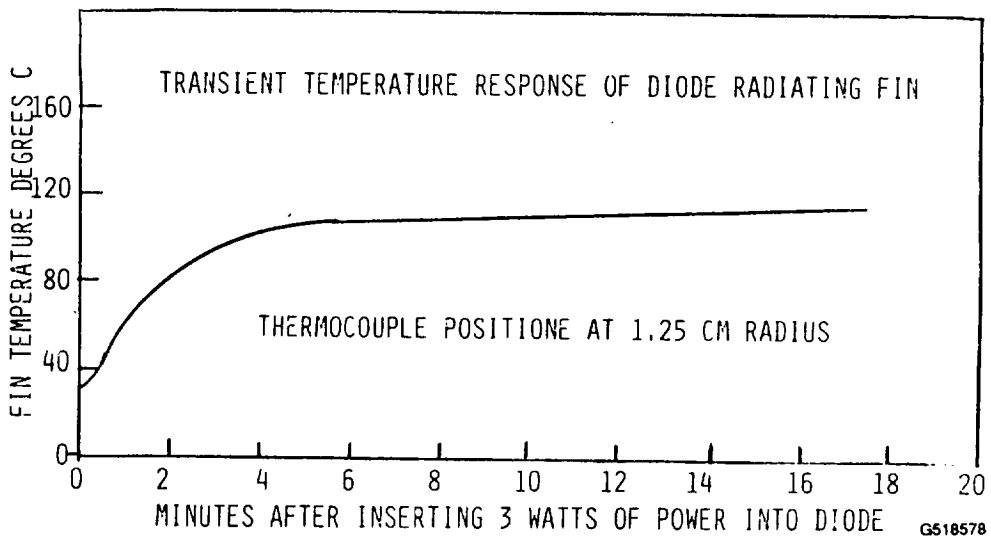


Figure 6-30. Temperature-time response of diode-radiator assembly to sudden insertion of 3 watts of power to be dissipated. Thermocouple was placed at a point half way between center and outer radius.

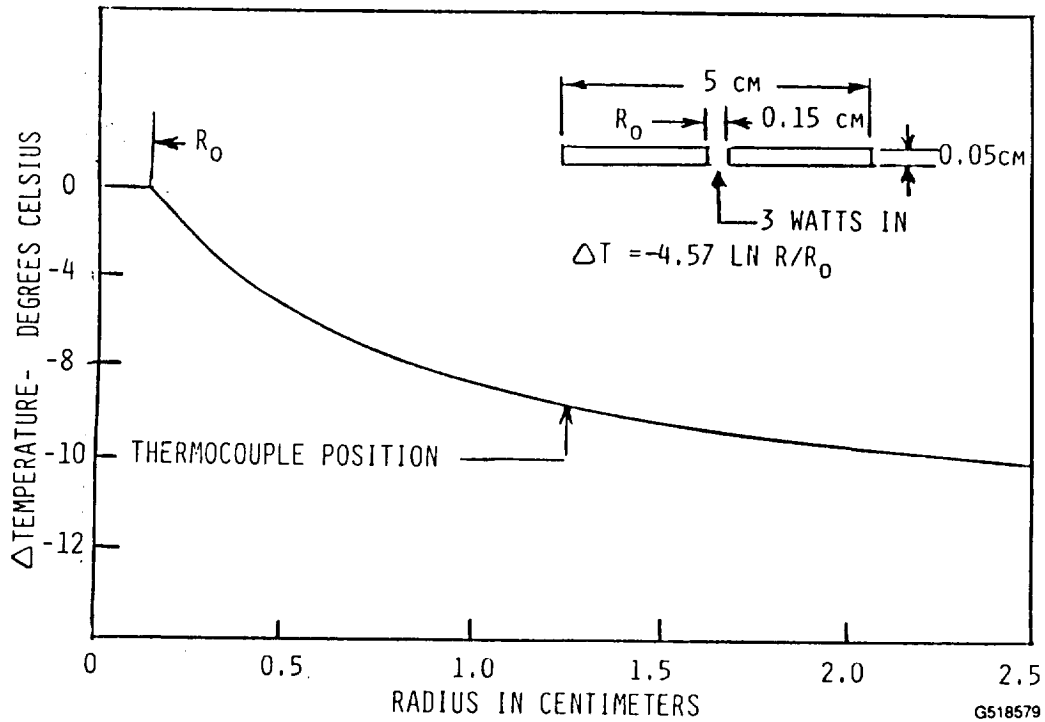


Figure 6.31. "Worst case" steady state distribution of temperature on radiating disk in which it is assumed there is flow of 3 watts of power from center to edge of disk without heat radiation.



### III. CONCLUDING REMARKS

The combination of two electronic technologies to provide all-electronic propulsion and transportation in an aerospace environment has inspired the term "Transportronics" to describe this new technology. This report has covered an important application of this technology in which electric propulsion in space is supplied with power beamed from the Earth by microwaves.

Although a number of papers have been written on this application, it is believed that this is the first report on any work supported by NASA or any other government agency. As such it provides more background material and more depth of discussion than any previous document and discusses for the first time the interface between the microwave technology and the electric thruster technology.

The report has first sought to establish a better perspective on where the new technology is positioned in the unfolding development of space, and then it performed a systems analysis to establish some baseline performance characteristics for a "transportronic" system for transportation between LEO and GEO. These characteristics were transit times from LEO to higher orbits including GEO, energy costs to place a kilogram of payload in GEO and lower orbits, and capital costs. The analysis was based upon a "scenario" selected by the author to represent a compromise between the full potential of a mature system to reduce transportation costs and the reduced capital cost of an initial system.

Those who have studied the proposed system recognize its merits and the fact that the basic technology at both the transmitting and receiving ends of the system are in an advanced state of development. However, in the usual learning curve on the application of new technology, a sizeable step has to be taken from the demonstrated beaming of tens of kilowatts of power over a distance of one mile on the Earth to transmitting tens of megawatts of power into space and applying it to electric thrusters. Just how this sizeable step can be successfully taken needs a substantial amount of study. In the absence of a compelling reason to take a giant step into space with the technology, some additional steps should be taken to ready the technology for that step. It is beyond the scope of this report to examine what all of those steps should be, but it is obvious that a complete system including the ion thrusters and most of the elements of the microwave subsystem should be demonstrated in some facility that exists on the Earth's surface.



## REFERENCES

1. W. C. Brown, "Transportronics-An Electronic Technology for Transportation of Both Energy and Material", 17th International Symposium on Space Technology and Science, Tokyo, Japan May 20-25, 1990.
  2. W. C. Brown and P. E. Glaser, "An Electrical Propulsion Transportation System from Low-Earth Orbit to Geostationary Orbit Utilizing Beamed Microwave Power Given at the Symposium on Energy from Space at the United Nation's Conference on the Exploration and Peaceful Uses of Outer Space, Vienna, Austria, August 1982. Paper published in Space Solar Power Review, Vol. 4, pp. 119-129, 198.
  3. W. C. Brown, "LEO to GEO Transportation System Combining Electric Propulsion with Beamed Microwave Power from Earth", AAS Goddard Memorial Symposium on Transportation Issues, Goddard Space Flight Center, March 1987. Published in Volume 69, AAS Science and Technology Series, pp. 185-219.
  4. W. C. Brown, "All Electronic Propulsion; Key to Future Spaceship Design", Paper AIAA 88-3170, AIAA/ASMA/SAE/ASEE 24th Joint Propulsion Conference, Boston, MA, July 1988.
  5. Ernst Stuhlinger, "Ion Propulsion for Space Flight, McGraw Hill Book Co., 1964.
  7. W. C. Brown, "Electronic and Mechanical Improvement of the Receiving Terminal of a Free-Space Microwave Power Transmission System", NASA Report CR-1135194, Raytheon PT-4964, August 1, 1977, Contract NAS 3-19722.
  8. W. C. Brown, "The Equatorial Plane - The International Gateway to Space". 10th Biennial SSI/Princeton Conf. on Space Manufacturing, May 1991.
  9. "America at the Threshold", Report of The Synthesis Group on America's Space Exploration Initiative. Submitted to the National Space Council on May 3, 1991 by Thomas P. Stafford, Chairman.
  10. P. E. Glaser, "Power from the Sun: Its Future" Science Vol. 162 pp. 857-861, November 22, 1968.
  11. W. C. Brown, "Satellite Power Stations -- A New Source of Energy?", IEEE Spectrum, Vol. 10, No. 3, pp. 38-47, March 1973.
  12. Final Proc. Solar Power Satellite Program Rev. DOE/NASA Satellite Power System Concept Develop. Evaluation Program, Conf. 800491, July 1980.

PREVIOUS PAGE BLANK NOT FILMED

72:152. - 1970-1971

## REFERENCES (Continued)

13. W. C. Brown, "A Microwave Powered Orbital Industrial Park System", Proceedings of the 8th Biennial SSI/Princeton Conference on Space Manufacturing, May 1987, pp. 242-251. Published by AIAA.
14. D. R. Criswell and R. D. Waldron, "Results of Analysis of a Lunar-Based System to Supply Earth with 20,000 Gigawatts of Electric Power", Paper A3.6 at SPS 91 Power from Space Conference in Paris/GIF-Sur-Yvette August 27 to 30.
15. W. C. Brown, "Status of Beamed Power Transmission Technology and Applications at 2.45 GHz. IAF Space Power Conference in Cleveland, June, 1989. Published in Volume 8 (1989) No. 3 of Space Power, pp. 339-355.
16. W. C. Brown, "Experimental Airborne Microwave Supported Platform", Technical Report No. RADC-TR-65-188, Dec., 1965. Contract AF30 (602) 3481.
17. W. C. Brown, "Experiments Involving a Microwave Beam to Power and Position a Helicopter", IEEE Trans. on Aerospace and Electronic Systems, Vol. AES-5.
18. R. M. Dickinson and W. C. Brown, "Radiated Microwave Power Transmission System Efficiency Measurements," Tech. Memo 33-727, Jet Propulsion Lab., Cal. Inst. Technol., Mar. 15, 1975.
19. R. M. Dickinson, "Evaluation of a Microwave High-Power Reception-Conversion Array for Wireless Power Tranamission," Tech. Memo 33-741, Jet Propulsion Lab., Cal. Inst. Technol., Sept. 1, 1975.
20. "Reception-Conversion Subsystem (RXCV) Transmission System," Raytheon Final Rep. Microwave Power, ER75-4386, JPL Contract 953968, NASA Contract NAS 7-100, Sept. 1975.
21. J. Schlesok, A. Alden, T. Ohno, "A Microwave Powered High Altitude Platform" Paper K-4, page 283-286, Vol. I, 1988 IEEE MTT-S International Microwave Symposium Digest.
22. Arthur Fisher, "Beam-Power Plane", Popular Science, January 1988, pp. 62-65.
23. J. M. Hickman, H. B. Curtis, et al., Solar Electric Propulsion for Mars Transport Vehicles, NASA Lewis Res. Ctr.
24. W. B. Grant, et al, "SPS Effects on LEO and GEO Satellites," Batelle Labs.
25. W. C. Brown, "Satellite Power System (SPS) Magnetron Tube Assessment Study," NASA Contractor Report 3383, Feb., 1981, Contract NAS8-33157.

REFERENCES (Continued)

26. G. Goubau and F. Schwering "On the Guided Propagation of Electromagnetic Wave Beams," IRE Trans. Antennas Propagat., Vol. AP-9, pp. 248 256, May 1961.
27. H. Kogelnik, T. Li "Laser Beams and Resources," Proc. of IEEE, Vol. 54, No. 10, October 1966.
28. G. Goubau, "Microwave Power Transmission from an Orbiting Solar Power Station," Journal of Microwave Power, Vol. 5, Dec. 1970.
29. F. D. Berkopac, J. R. Stone, G. Aston, "NASA electric Propulsion Technology," AIAA-85-1999 Electric Propulsion Technology Conference, Sept. 30 - Oct. 2, 1985.
30. M. Patterson, V. Rawlin, "Operation of a 50 CM Diameter Cusp-Field Ion Thruster" AIAA Paper 88-2915, 24th Joint Propulsion Conference, July 11, 1988.
31. D. L. Galecki, M. J. Patterson, "Nuclear Powered Mars Cargo Transport Mission Utilizing Advanced Ion Propulsion," NASA Tech. Memo 100109, Prepared for 23rd Joint Propulsion Conference, July 1, 1987.
32. W. C. Brown, "Design Definition of a Microwave Power Reception and Conversion System for Use on a High Altitude Powerer Platform", NASA Contractor Report CR-15866, Contract NAS6-3006, Wallops Flight Facility.
33. A. P. Coppa, "A General Truss System for Very Large Spacebase Foundations," Space Manufacturing Six Nonterrestrial Resources, Biosciences, and Space Engineering. 1987, pp. 286-274,. Pub. by AIAA ISBN0-930403-35-5.
34. W. G. Dow, "Fundamentals of Engineering Electronics, " Second Edition, John Wiley and Sons, Equation 5-13.
35. W. C. Brown, "Microwave Beamed Power Technology Improvement," Final Report, JPL Contract No. 955104, Raytheon Report PT-5613; May 15, 1980.
36. W. C. Brown, "Design Study for a Ground Microwave Power Transmission System for Use with a High-Altitude Powered Platform", NASA Contractor Report 168344, June, 1983, Raytheon Report PT-6052, May, 1982, Contract No. NAS6-3200.
37. W. C. Brown, "Experimental Sytem for Automtically Positioning a Microwave Supported Platform", Technical Report No. RADC-TR-68-273, Oct., 1968. Contract AF 30 (602) 4310.

REFERENCES (Continued)

38. W. C. Brown, "The SPS Transmitter Designed Around the Magnetron Directional Amplifier", *Space Power*, Vol. 7, No. 1, 1988, pp. 37-39.
39. W. C. Brown, "The Sophisticated Properties of the Microwave Oven Magnetron", 1989 IEEE MTT-S International Microwave Symposium Digest, Volume III, pp. 871-874. IEEE Cat. No. 89CH2725-0, ISNN 0149-645X.
40. Internal Work at Raytheon Company, not Published.
41. "Analysis of a Phase-Locked Loop to Suppress Interference from a Solar Power Satellite," NTIA-Report 81-64. SPS Study Report SPS PO/EC-10.

## APPENDIX A

### PAYOUT DELIVERY TO GEOSYNCHRONOUS ORBIT AS A FUNCTION OF ELECTRIC THRUSTER POWER RATING, PAYLOAD FRACTION, AND SYSTEM MATURITY

Note: This appendix constitutes a section of one of the many monthly reports that were prepared under the contract. The procedure for determining transit times and payload delivery and propellant required is similar to that assumed for the "system scenario" in section 3.6 of the text of the final report. It is, however, more directed toward maximizing payload delivery and minimizing costs that are associated with very large systems.

Some additional simplifying assumptions are made to those made in the analysis in section 3.6. Two that make the results more optimistic are that no allowance for turn around time is made and that the acceleration of the vehicle is assumed to be constant throughout its journey. This latter assumption gives trip times that are from 15% to 20% less than those in the section 3.6 scenario analysis. One that makes the operating costs for the fully mature systems less optimistic is that the transmitters are assumed to be operating at full power output during the time that they are in contact with the OTVs.

One of the outcomes of the forthcoming discussion is that large payload fractions are desirable from the viewpoint of maximizing the amount of payload that is delivered. However, it is at the expense of much longer transit times for payload delivery. Large payloads also minimize the importance of minimizing the dry vehicle mass, because it becomes only a small fraction of the total mass to be accelerated.

The material below is copied from the monthly report, except as noted by material enclosed in ( )s.

We will be interested in the flow rate of payload from 300 kilometer orbit to geosynchronous orbit as a function of some parameter that can be readily understood and that can be closely related to other parameters of the system. A very useful parameter is a kilowatt of power into the ion thruster. This, together with the specific impulse at which the thruster is operated, will give us the propulsive force per kilowatt. We can also associate a mass of the ion thruster with each kilowatt of power input. Then the assumption is made that the dry weight of the vehicle is three times the mass of the ion thruster. Therefore we can find the acceleration of the empty vehicle by itself, and from there we can add the payload mass and the propellant mass and examine what happens with an increase in payload fraction from zero to a high value.

We will base the performance of the ion thruster on that projected for the 50 cm thruster on page 13 of NASA Technical Memorandum 100109, AIAA-87-1903, D.L.Galecki and N.J. Patterson. We find that the thrust per kilowatt of power consumed is 0.038 Newtons per kilowatt. The mass of the thruster per kilowatt of power input, usually known as the specific mass, has been obtained by referring to Table VI of the same report. There it is found that the ratio of mass to power consumed by the thrusters is 0.685 kg/kw.

Each kilowatt of power input to the thruster provides 0.038 Newtons of propulsive force and corresponds to a thruster mass of 0.685 kilograms. The self acceleration of the thruster is then  $0.038/0.685$  or  $0.055 \text{ m/s}^2$ .

The assumption was previously made that the rest of the vehicle, including the rectenna, power conditioning, structure, and propellant tanks, would have a mass twice as great, so that the acceleration of the dry vehicle would be  $0.055/3$  or  $0.0185 \text{ m/s}^2$ .

Procedure to calculate payload delivery rate.

1. Normalize the ratio of the dry mass of the vehicle to the power input as three times the ratio of the mass of the ion thruster to its power input which is  $0.68\text{kg/kW}$  so that the ratio of dry vehicle mass to power consumed by the ion thrusters is  $2 \text{ kg/kW}$ . Also the ratio of propulsive force to power is  $0.037 \text{ Newtons/kW}$ . The acceleration of the dry vehicle is then  $.0185 \text{ m/s}^2$ .
2. Find the mass of the propellant to return the empty vehicle from GEO to LEO. The amount of propellant is determined as  $M_0 - M$  from the equation

$$M_0 = M e^{U/v}, \text{ where} \quad (1)$$

$M_0$  = initial mass  
 $M$  = terminal mass  
 $U$  = velocity change between LEO and GEO  
assumed to be  $4600 \text{ m/s}$   
 $v$  = exhaust velocity of the thruster. For Xenon and  
an applied potential of 1500 volts to the ion thruster,  
the velocity  $v$  is  $40,000 \text{ m/s}$ .

Inserted comment: The propellant mass from (1) to bring the dry vehicle mass of 3 kg back to LEO is 0.36 kg.

3. Find the transit time between GEO and LEO for the empty vehicle plus the propellant carried aboard (from equation 3.7 in text). It is recognized that the propellant will be consumed during the journey so that its average mass will be approximately  $(M_0 - M)/2$ . This mass of .18 kg is then added to the dry vehicle mass of 3 kilograms and the average acceleration found. (At this point it is assumed that the rectenna is provided with full power density at all points between LEO and GEO. This is an unreal assumption except for the largest of microwave power transmission systems which would support a much larger transmitting antenna but the differences in the transit times between this ideal system and that achieved with an initial 2 square kilometer transmitting antenna with peak power of 500 megawatts output is not that great, perhaps 15% less).
4. Examine the vehicle and its payload as it arrives in GEO. It will have not only the payload aboard but residual propellant mass for the return trip of the empty vehicle to LEO. The mass  $M$  in equation (1) then becomes

$$M = M_{\text{payload}} + M_{\text{propellant for return trip}} \quad (2)$$

5. Calculate the  $M_0$  in LEO to deliver the  $M$  in expression (2) to GEO.

Again, the difference between  $M_0$  and  $M$  is the propellant.

6. Find the transit time between LEO and GEO (from equation 1.7). Again the average propellant mass between LEO and GEO is added to the mass of the vehicle and its payload to determine the average acceleration.
7. Divide the total payload delivered by the sum of the transit times up and down. This will give the time rate of payload delivery for each kilowatt of power into the ion thrusters. The unit of time to be selected is arbitrary but it is natural to think in terms of days so that the "day" unit is selected and delivery rate is in terms of kg/day.
8. Determine the payload fraction by dividing the arbitrarily selected payload by the total takeoff mass in LEO.

Payload delivery rate as a function of payload fraction.

Figure 1 shows the relationship between payload delivery rate and payload fraction. This graph was obtained by using the first seven steps in the foregoing procedure to find the rate of delivery corresponding to various payload units. The corresponding payload fraction, using step 8, was found for each of these cases. Each case is a point on the curve of figure 1. It is noted that the payload delivery rate is a strong function of the payload fraction.

Propellant fraction as a function of payload fraction.

The propellant fraction can be obtained by dividing the propellant used for a given payload mission by  $M_0$  at takeoff from LEO. It can then be plotted against the payload fraction. As figure 1 indicates this fraction varies from 0.195 for zero payload to about 0.1 for a payload fraction of 0.8.

Number of metric tons of payload delivered to geosynchronous orbit per year as a function of OTV power rating, system maturity, and payload fraction.

Table A represents a compilation of data obtained by assuming different payload fractions, power levels, and system maturity. The results range from 29.2 metric tons (1000 kilograms is one metric ton) for a 0.2 payload fraction, a 10,000 kilowatt vehicle and a single beam OTV system, to 30,360 metric tons for a 0.8 payload fraction, a 100,000 kilowatt vehicle, and a mature 4 beam, 4 OTV system. These payloads are for one year of operation.

Note to the reader if Table A in this appendix is compared with Table 3.3 in the regular text of the report. The difference between 30,000 metric tons delivered per year and 60,000 metric tons is in the size of the OTV, being rated at 200,000 kW of power into the thrusters rather than 100,000 as in Table A. Only an extremely ambitious program would justify a single 200,000 kw OTV or a convoy of smaller units adding up to 200,000 kw consumption.

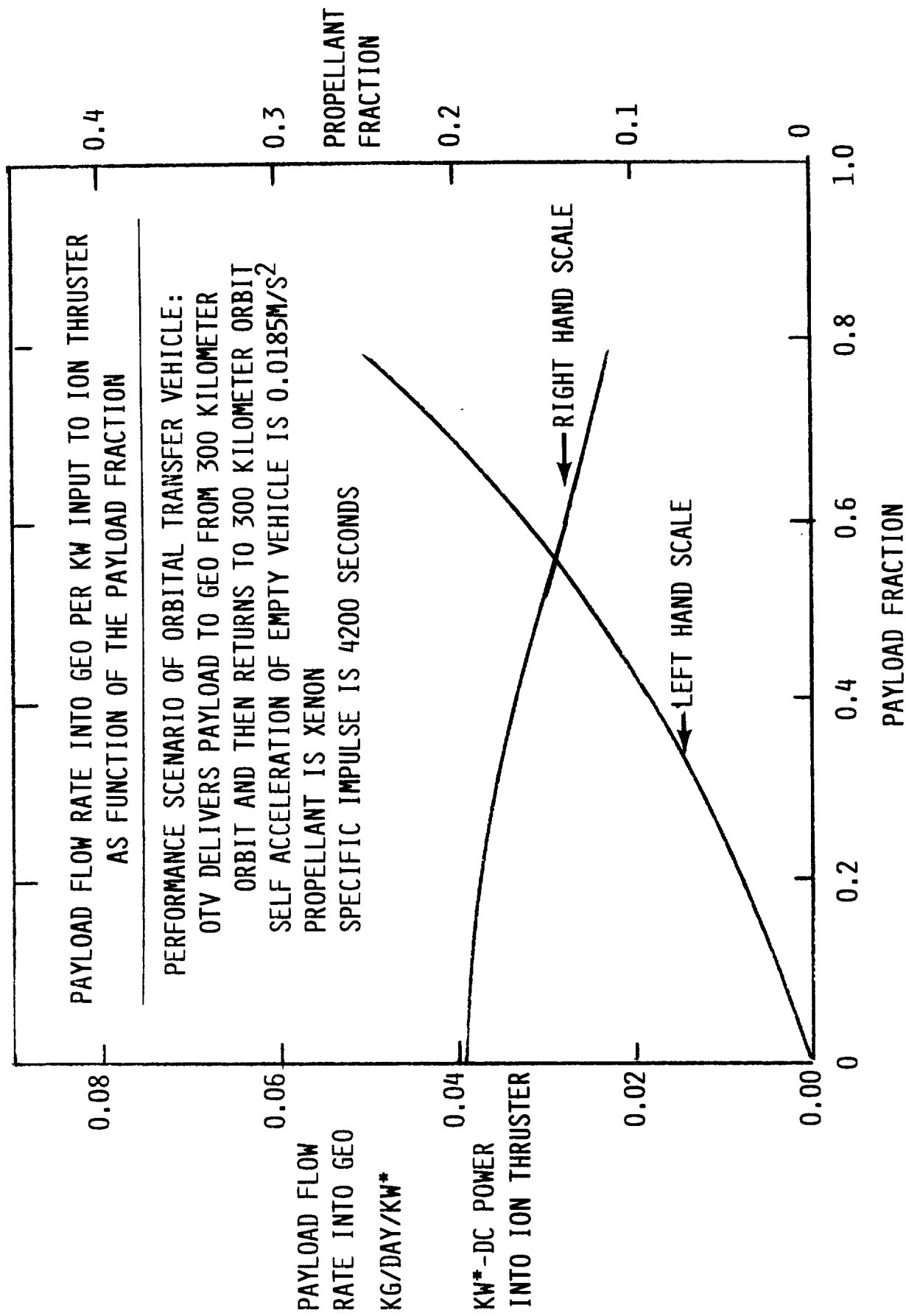


**TABLE A**  
**NUMBER OF METRIC TONS OF PAYLOAD DELIVERED TO GEOSYNCHRONOUS ORBIT PER YEAR  
 AS FUNCTION OF OTV POWER RATING, SYSTEM Maturity, AND PAYLOAD FRACTION**

NO. OF BEAMS AND OTV'S	1 BEAM - 1 OTV			2 BEAMS - 2 OTV'S			4 BEAMS - 4 OTV'S		
	1 BEAM - 4 OTV'S			4 BEAMS - 1 OTV					
	4 BEAMS - 4 OTV								
ION THRUSTER POWER	10,000 KW	100,000 KW	1,000,000 KW	10,000 KW	100,000 KW	1,000,000 KW	10,000 KW	100,000 KW	1,000,000 KW
PAYLOAD FRACTION	TONS	TONS	TONS	TONS	TONS	TONS	TONS	TONS	TONS
0.2	29.2	292	117	1170	467	4670			
0.3	47.5	475	190	1900	759	7590			
0.4	65.7	263	263	2630	1051	10510			
0.5	87.6	876	350	3500	1400	14000			
0.6	117	1170	467	4670	1868	18680			
0.7	150	1500	600	6000	2400	24000			
0.8	190	1900	759	7590	3036	30360			



## APPENDIX B

### MATHEMATICAL ANALYSIS OF BUS BAR MASS AND ELECTRICAL LOSSES IN OTV

For purposes of analysis it is assumed that the rectenna is rectangular as shown in Figure 1 with coordinates  $y$  and  $x$ , and that it is uniformly illuminated by the microwave beam, a condition that approximately exists when the rectenna intercepts less than 50% of the beam..

If the uniform DC power density taken for the rectenna is  $P_d$ , then the power collected from an element of the rectenna that is  $ky$  wide and  $dx$  long is  $P_d y dx$ . If the potential between the busses is  $V$  (also the potential applied to the electric thrusters) the resulting current flow is

$$dI = \frac{P_d y dx}{V} \quad (1)$$

The total current flowing in the conductor at distance  $x$  is then

$$I = \frac{\int_0^x P_d y dx}{V} = \frac{P_d y x}{V} \quad (2)$$

Let the conductance of the bus vary with distance  $x$  as  $k\sigma x$ , where  $\sigma$  is the conductivity of the metal used for the conductor, and  $k$  is a proportionality constant with dimension such that  $kx$  is the cross sectional area at distance  $x$ . The conductance  $\sigma$  is that of a unit cube of material. Then the electrical resistance,  $r$ , per unit length that corresponds to the conductance is :

$$r = 1/k\sigma x \quad (3)$$

The  $I^2 r$  losses that occur per unit length at distance  $x$  if found by combining equations (2) and (3) so that

$$d(I^2 r) = \frac{P_d^2 y^2 x^2 dx}{V^2 k \sigma x} \quad (4)$$

The total power,  $P_b$ , dissipated in a single bus of length  $L$  is then

$$P_b = \frac{\int_0^L P_d^2 y^2 x^2 dx}{V^2 k \sigma} = \frac{P_d^2 y^2 L^2}{2 k \sigma V^2} \quad (5)$$

The loss in both busses will be twice that given by equation (5)

From a practical point of view we would like to know the factor  $k$ , from which the mass and cross section of the physical conductor can be determined, as a function of the ratio of dissipated power to power collected by the rectenna, which will be denoted as  $\beta$

The ratio,  $\beta$ , is easily found because the power collected is simply  $P_d y L$ , from which

$$\beta = \frac{P_d y L}{V^2 \beta \sigma} \quad (6)$$

from which  $k = \frac{P_d y L}{V^2 k \sigma}$  (7)

Now we will want to know the corresponding mass of the conductors and compare that with the total mass of the rectenna, and eventually with the total mass of the vehicle.

The mass  $dM_c$  of the conductor per unit length at distance  $x$  is easily found by multiplying  $kx$  which is the cross section at distance  $x$  by the mass of the conductor material per unit cube,  $\alpha$

$$dM_c = k x \alpha dx$$

and  $M_c = \int_0^L k \alpha x dx = k \alpha L^2 / 2$  (8)

The total mass of the two conductors is twice that given by (8)

Now the mass of the rectenna (without the main conductors) is  $M_d y L$  where  $M_d$  is the rectenna mass per unit area.

Then the ratio,  $r_m$ , of the mass of the two conductors to the mass of the rectenna is

$$r_m = k \alpha L^2 / M_d y L = k \alpha L / M_d y \quad (9)$$

Substituting the value of  $k$  given in equation (7)

$$r_m = \frac{P_d L^2 \alpha}{\sigma V^2 M_d} \quad (10)$$

#### Discussion of the results of the analysis

Equation (10) indicates how the ratio of the mass of the conductors to the total mass of the rectenna varies as a function of the total area of the rectenna and the percentage of the rectenna power that is dissipated in the current carrying busses.

Quite clearly the ratio depends upon the size of the rectenna as given by  $L^2$  and depends inversely upon the square of the voltage rating of the electric thrusters to which the busses are connected. Therefore, for large rectennas it is very important to have the power collected at high voltage. Finally, as expected, the ratio  $r_m$  depends upon the electrical conductivity and the density of the conducting busses.

It might be interesting to apply some of the material developed above to the rectenna in the OTV scenario examined in section 3.6. For example, it might be of interest to know what the mass of the bus bars would be if, for example the electrical losses in the bus bars was held to 2% of the power output of the rectenna. To find the bus bar size equation (7) is used to determine the parameter  $k$  which will determine the cross section at any distance  $x$ . In equation (7)  $P_d$  is taken as  $400 \text{ w/m}^2$ ,  $y$  as 226 meters, and  $L$  as 226 meters to produce 20 megawatts of power. The bus voltage  $V$  is taken as 1500 volts.,  $\beta$ , the ratio of dissipated power to rectenna power output, is to be limited to 2%, and  $\sigma$  is  $0.36 \times 10^8$ . From (7) the computed value of  $k$  is  $1.23 \times 10^{-5}$ .

The largest bus bar section is when  $x = L$ , and the cross section is found to be  $27.6 \times 10^{-4}$  square meters. Now because the bar is linearly tapered between  $x = 0$  and  $x = L$ , the average cross section is  $13.8 \text{ cm}^2$ , or  $13.8 \times 10^{-4} \text{ m}^2$ . The total volume of the 226 meter long bus is then 0.312 cubic meters if aluminum is used. A cubic meter of aluminum has a mass of 2800 kilograms, so that the total mass of the two bus bars is 1,744 kilograms.

In the scenario the total mass of the rectenna was assumed to be 14,000 kilograms, so that the ratio of the bus mass to the rectenna mass is  $1,744/14,000$  or 12.5%.

The computed bus loss  $P_b$  is from (5) approximately 200,000 watts or 1% of the rectenna power output. The two busses account for 2% which is the value of  $\beta$  used in the calculation.

If we increased  $\beta$  to 5%, then the ratio of the mass of the bus bars to that of the rectenna would decrease to 5% also.

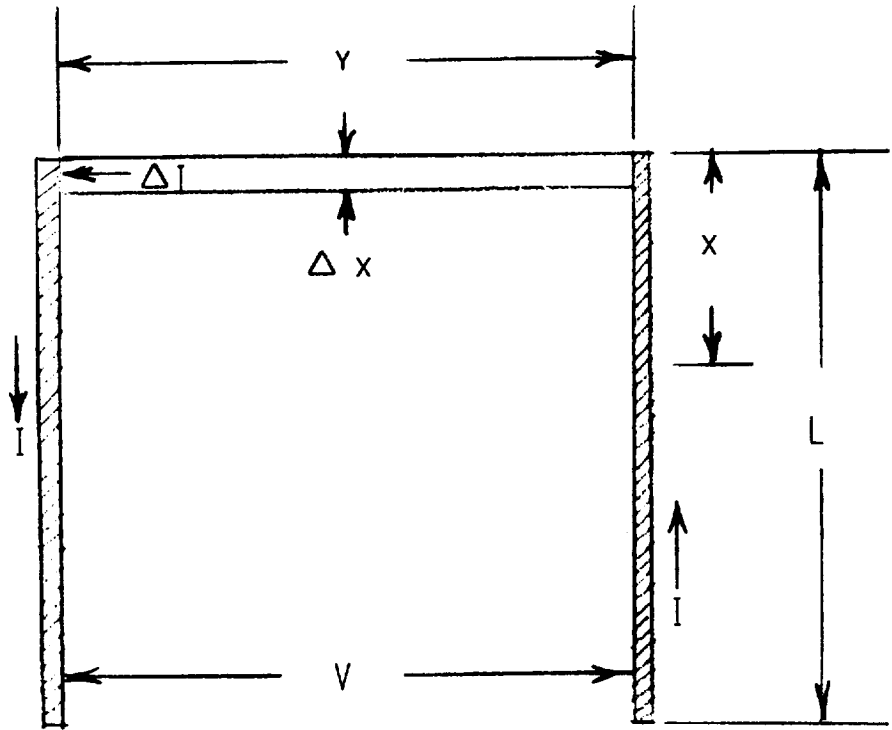


Figure 1. Schematic that defines the parameters used in the mathematical analysis of current flow in the two side bus bars that conduct the power to the electric propulsion engines.

DISTRIBUTION LIST FOR FINAL REPORT ON NASA 3-25066

	<u>No. of Copies</u>
Mr. Ronald Cull Mail Stop 301-5 NASA Lewis research Center 21000 Brookpark Rd. Cleveland OH, 44135	10
Mr. Ira Myers Mail Stop 301-5 NASA Lewis Research Center 21000 Brookpark Rd. Cleveland OH 44135	1
Mr. Jose Christian Mail Stop 301-2 NASA Lewis Research Center 31000 Brookpark Rd. Leveland, OH 44135	1
David Byers SPT-D1 NASA Lewis Research Center 21000 Brookpark Rd. Cleveland, OH 44135	1
Michael Patterson SPT-D1 NASA Lewis Research Center 21000 Brookpark Rd. Cleveland Oh, 44135	1
Vincent Rawlins SPT-D1 NASA Lewis Research Center 21000 Brookpark Rd. Cleveland, OH 44135	1
John Bozek Mail Stop 301-5 NASA Lewis Research Center 21000 Brookpark Rd. Cleveland OH 44135	1
David Criswell University of Houston SR-1 Room 504 Houston TX 77204-5505	1

Hubert P. Davis Davis Aerospace HCZ Box 296-0 Canyon Lake, TX 78133	1
R. Bryan Erb Canadian Space Agency NASA Johnson Space Center Houston, TX 77058	1
Penny Haldane Alaska Energy Authority Box 190869 Anchorage, AK 99519-0869	1
Professor Kai Chang Electrical Engineering Department Texas A&M University Zachry Bldg. College Station, Texas 77843	1
Henry Brandhorst NASA Lewis Research Center 21000 Brookpark Rd. Cleveland, OH 44135.	1
Dr. Ernst Stuhlinger 3106 Rowe Drive Huntsville, Alabama	1
Dr. Martin Hoffert Dept. of Applied Science New York University 26-36 Stuyvesant St. New York, NY 10003	1
Mr. Donald Reid Los Alamos National Laboratory Los Alamos, New Mexico	1
Dr. Peter Koert ARCO Power Technologies, Inc. 1250 Twenty-fourth Street, N.W. Washington, DC 20037	1
Dr. E. David Hinkley TRW Space and Technology Group R1/1062 One Space Park Redondo Beach, CA 90278	1

Mr. Richard Dickinson Jet Propulsion Laboratory 4800 Oak Grove Drive Pasadena CA, 91103	1
Mr. Richard Edgar 7 Blaisdell Road Chelmsford, MA 01824	1
Mr. E. Eugene Eves 40 Plain Road Westford, MA 01886	1
Mr Alan M. Brown Center for Space Power 223 Wisenbaker Engineering Research Center Texas A&M University College Station, TX 77843-3118	1
Frank Little Center for Space Power 223 Wisenbaker Engineering Research Center Texas A&M University College Station, TX 77843-3118	1
Mr. James McSpadden Electrical Engr.Dept Zachry Bldg. Texas A&M Univ. College Station, TX 77843	1
Prof. Joseph Hawkins Electrical Engineering Dept. Duckering Building University of Alaska Fairbanks, Alaska 99775	1
Dr. A. D. Patton Chairman, E.E. Department Zachry Building Texas A&M Univ. College Station, TX 77843	1
Dr. Nobuyuki KAYA Associate Professor Dept. of Computer and Systems Engr. Kobe University Rokkodai, Nada, Kobe 657,	1
Dr. Fred Koamanoff 1700 Montrose Ave. P.O.Box 2221 Garrett Park, MD 20896	1

Mr. Tom Rogers 1  
7404 Colshire Drive  
McLean, VA 22102

Mr. Robert Bowen 1  
Manager, New Products Center  
Raytheon Co.  
63 Second Ave.  
Burlington, MA 01803

Dr. John Osepchuk 1  
Raytheon Research Division  
131 Spring Street  
Lexington, MA 02173

Dr. Philip Cheney 1  
Vice President, Engineering  
Raytheon Co.  
141 Spring Street  
Lexington, MA 02173

Mr. Jerome Hanfling 1  
Box NNL  
Raytheon Equipment Division  
430 Boston Post Road  
Wayland, MA 01776

Mr. Brad Schupp 1  
Mail stop 91  
Raytheon Equipment Development Laboratories  
528 Boston Post Road  
Sudbury, MA 01776

Paul Rawlinson 1  
Mail Stop 123  
Raytheon Equipment Development Labs.  
528 Boston Post Rd.  
Sudbury, MA 01776

Mr. Owen Maynard 1  
55 Blue Springs Drive #705  
Waterloo, Ontario  
N2J 4T3 Canada,

Mr. Stephen Gluck 1  
Strategic Systems Directorate  
Raytheon Co.  
528 Boston Post Road  
Sudbury, MA 01776

Guy PIGNOLET 1  
C.N.E.S.  
2 Place Maurice Quentin  
75039 PARIS CEDEX 01, FRANCE

Dr. Peter Glaser Arthur D. Little, Inc. Acorn Park Cambridge MA 02140	1
Mr. Gregg Maryniak 6 Newell Road Hopewell, NJ 08525	1
Sargi Bharj David Sarnoff Research Center 201 Washington Road Princeton, N.J.	1
Gay Canough Extra Terrestrial Materials Box 67 Endictoo, NY 13761	1
Edmund Coomes U.S. Dept. of Energy 1000 Independence, MS ST-60 Washington DC 20585	1
David Criswell University of Houston SR-1 Room 504 Houston, TX 77204-5505	1
Hubert P. Davis Davis Aerospace HCZ Box 296-0 Canyon Lake, TX 78133	1
R. Bryan Erb Canadian Space Agency NASA Johnson Space Center Houston, TX 77058	1
Penny Haldane Alaska Energy Authority Box 190869 Anchorage, AK 99519-0869	1
James Johnson Electric Power Research Inst. 2000 L.St.NW, Suite 805 Washington DC 20036	1
Geoffrey Landis Sverdrup, Inc. 21000 Brookpark Rd. Cleveland, OH 44135	1

Ray Leonard Ad Astra, Ltd. Rt. 1, Box 92LL Sante Fe, NM 87501	1
Leik Myrabo Rensselaer Polytechnic Inst. 15 St. ME Troy, NY 12180	1
Glenn Olds Dept. of Natural Resources 400 Willoughby Juneau, AK 99801-1724	1
Gordon Woodcock Boeing Aerospace Box 240002, M/S JW 21 Huntsville, AL 35824-6402	1
Dickey Arndt Johnson Space Center Houston, TX 77508	1
Dr. Mario Grossi Submarine Signal Division, Raytheon 1847 W. Main Road Portsmouth, RI 02871-1087	1
Thomas Ruden Box T2SH5 Missile Systems Laboratory P.O.Box 1201 Tewksbury, MA 01876-0901	1
James Burke 165 Olivera Lane Sierra Madre, CA 91024	1
Jerry Grey AIAA One Lincoln Plaza 25-0 New York, NY 10023	1
Lyle Jenkins NASA Johnson Space Center Mail Code IC Houston, TX 77058	1
Dr. John Lewis Lunar and Planetary Laboratory Spacae Sci Bldg/Univ. of Arizona Tucson, AZ 85721	1

Bruce Mackenzie  
110 Van Norden Road  
Reading, MA 01867-1246

1





